

TMX-71407

A PHOTOMETRIC STUDY OF THE ORION OB 1 ASSOCIATION

III. SUBGROUP ANALYSES

(NASA-TM-X-71407) A PHOTOMETRIC STUDY OF
THE ORION OB 1 ASSOCIATION. 3: SUBGROUP
ANALYSES (NASA) 231 p HC A11/MF A01

N77-34062

CSSL 03A

Unclas
50336

G3/89

WAYNE H. WARREN, JR.
JAMES E. HESSER

OCTOBER 1977



GODDARD SPACE FLIGHT CENTER
GREENBELT, MARYLAND

For information concerning availability
of this document contact:

Technical Information & Administrative Support Division
Code 250
Goddard Space Flight Center
Greenbelt, Maryland 20771
(Telephone 301-982-4488)

"This paper presents the views of the author(s), and does not necessarily
reflect the views of the Goddard Space Flight Center, or NASA."

A PHOTOMETRIC STUDY OF THE ORION OB 1
ASSOCIATION. III. SUBGROUP ANALYSES

WAYNE H. WARREN JR.*

Laboratory for Astronomy and Solar Physics
NASA-Goddard Space Flight Center

and

JAMES E. HESSER

Cerro Tololo Inter-American Observatory[†]

* Visiting Astronomer, Kitt Peak National Observatory, which is operated by the Association of Universities for Research in Astronomy, Inc., under contract with the National Science Foundation. NAS-NRC Resident Research Associate,

[†] The Cerro Tololo Inter-American Observatory is supported by the National Science Foundation under contract NSF-C866.

Accepted by *Astrophysical Journal Supplement Series*

ABSTRACT

The four principal subgroups of the association are examined in detail using individual distances and reddening values determined for their B-type members from $uvby\beta$ data presented in the previous papers of this series (Warren and Hesser (1977a,b)). Subgroup 1a appears not to show a spread in age as suggested by a previous study; nor does it show a systematic distance increase with right ascension when fainter members are considered, although such a trend in declination indicates a possible connection of this subgroup with the λ Orionis clustering to the north. An eastwardly increase in distance is found for subgroup 1b, in agreement with previous studies, but the reddening law for the east Belt appears normal. The small subclusterings in the vicinity of the Orion Nebula appear not to differ in evolutionary state, but their ages are considerably greater than those of stars in the nebula and its associated cluster.

Both uniform differences and large individual discrepancies in the m_0 index, similar to those found in a study of the Upper Scorpius region of the association Sco OB 2, have been found for the young stars surrounding the Orion Nebula. They appear to be a result of several effects connected with line and/or continuum anomalies and mechanisms associated with local absorption. Several pre-main-sequence candidates are found among the late B- and A-type stars in the nebula region, and the lower main-sequence turn-up occurs at

approximately spectral type A0, beyond which the A- and F-type stars define a uniform sequence running parallel to the main sequence, but above it by about 1.3 mag. A clear gap in the F-star sequence is found in the range $0.21 \leq (b-y)_0 \leq 0.26$, indicating possible implications for the theory of convection in stellar envelopes of pre-main-sequence stars.

The distribution of reddened B stars in the northern and southern sections of the association is indicative of absorption by circumstellar remnant dust for stars near the pre-main-sequence turn-up. New age estimates for the association subgroups, made using intrinsic colors of their bluest main-sequence stars, are in substantial agreement with earlier determinations, but the accuracy can be improved by correcting for rotational-velocity effects if and when rotating models for higher mass stars become available.

Subject headings: clusters: associations--nebulae: Orion
Nebula - photometry - stars: early-type -
stars: evolution - stars: pre-main-sequence

I. INTRODUCTION

New photoelectric data on the uvby β and UBV systems have been presented for 526 stars in the vicinity of the young stellar association Orion OB 1 in Paper I of this series (Warren and Hesser 1977a), where we also established criteria for membership in the association based upon proper-motion, radial-velocity, and photometric data. The procedures adopted for analysis of the photometric data in terms of color excesses, absolute visual magnitudes, rotational-velocity effects and spectral types were discussed in Paper II (Warren and Hesser 1977b), where we also examined the photometry with regard to polarization and infrared excesses. We now turn our attention to the detailed analyses of the individual subgroups of the association, with respect to both their individual properties and the relationships among them.

Analyses of subgroups 1a (Northwest region), 1b (Belt region), 1c (outer Sword) and 1d (Orion-Nebula cluster) are presented in § II; these subassociations closely resemble those defined by Blaauw (1964) except for additional subdivisions into which we have divided the 1b, 1c and 1d subgroups (see Fig. 6 of Paper I). As in Paper II, our discussion of each subgroup is separated into sections for the early group (O- and B-type stars), the

intermediate group (\sim A0-A3) and the late group (A-F stars), a division which follows naturally from the procedures used to analyze the uvby β photometry (Strömgren 1966). An important feature of these discussions is the presentation of extensive summary tables for this investigation, containing our mean values of the original photometric data, plus the relevant intrinsic parameters derived from the reductions, such as intrinsic colors, color excesses, absolute visual magnitudes and related spectroscopic data. In § III we intercompare the distances and properties of the individual subgroups, while their ages are briefly discussed in § IV. Finally, in § V, we summarize the major conclusions of this study and discuss possibilities for future work on the association which might solve some of the problems encountered in the present work.

II. PHOTOMETRIC PROPERTIES OF INDIVIDUAL SUBGROUPS

The principal results of this investigation are contained in Tables 5-11 and their associated notes: for convenience of future reference we have grouped these tables in the Appendix and urge the reader to briefly examine them before proceeding with the detailed discussion following.

a) Subgroup 1a (Northwest region)

i) Previous Investigations

The 1a group is located to the west and north of δ Orionis, being the most dispersed and presumably the oldest in the Orion OB 1 association. It contains the bright stars η , ψ , and ω Orionis and extends westward to approximately 5 hours right ascension and northward to about +6 degrees declination in the present program.

Although this subgroup was not distinguished from the 1b group (Belt region) by Sharpless (1962), Blaauw (1964) found that its color-magnitude diagram shows a higher degree of evolution away from the top of the zero-age main sequence than that of the Belt.

The internal motions and MK spectral types of the brightest members were studied by Lesh (1968a), who found a significantly smaller mean distance modulus for 1a than for the Belt and Sword (1c) subgroups. The spectral types of the brightest B stars indicate a more advanced evolutionary

state and the internal motions show a rapid rate of expansion. The kinematic results of Lesh have been questioned by Steffey (1973) on the basis that an important condition for the use of Blaauw's method of finding expansion (which Lesh used) is not met by her results; namely, that the expansion rates must be nearly equal in two coordinates. [Lesh found expansion rates of $\mu_{\alpha} = 0!00074 \text{ deg}^{-1} \text{ year}^{-1} \pm 0!00027 \text{ (p.e.)}$, $\mu_{\delta} = 0!00029 \text{ deg}^{-1} \text{ year}^{-1} \pm 0!00049 \text{ (p.e.)}$]. Another problem with the derived expansion is that a systematic distance increase across a group can mimic expansion and Steffey finds just such an increase from west to east for the bright B stars used by Lesh. He also notes that the \underline{M}_V , $(\underline{U}-\underline{B})_0$ diagram indicates a large range of ages for the bright stars studied by Lesh, and even suggests that the 1a subgroup may consist of mostly peripheral members of the nearby 1b and λ Orionis groups. Considering the possible effects caused by rotation on the \underline{M}_V , $(\underline{U}-\underline{B})_0$ diagram, the latter argument may not be valid; nevertheless, Steffey's analysis suggests that we examine our data for any implications regarding the existence of the 1a subgroup.

ii) Distance Modulus

Tables 5a, b, c of the Appendix contain the intrinsic parameters for our program stars in the Northwest region. Figure 1 shows a plot of the \underline{m}_0 index against β for all stars listed in these tables. The diagram demonstrates the

well-known effect that the group classification (B, I, AF) depends primarily on the \underline{m}_1 index, and shows that the B-type stars define a fairly tight sequence. This correlation is expected for early-type stars due to the inclusion of the H δ line in the \underline{v} filter, but reference to the β , $\underline{W}(\text{H}\gamma)$ diagram (Fig. 4, Paper II) shows that the scatter is greater than that expected if the \underline{m}_1 index is dependent upon H δ strength alone.¹ This dispersion suggests that the \underline{m}_1 index is

¹The very high \underline{m}_0 index for M78B (WH503) may be a result of its high reddening and/or contamination from a nearby F-type optical companion which was included in the measurement.

sensitive to composition differences in early-type stars through its detection of metal lines in the $\lambda 4100 \text{ \AA}$ region. This is supported by the abnormally high indices usually found for Ap stars (Cameron 1967, Warren 1973), whose spectra contain many weak lines in this region. Evidence for abundance sensitivity of the \underline{m}_1 index has also been found for the B stars of the Sco-Cen association by Glaspey (1971b).

Figure 2 shows the corrected apparent magnitude \underline{V}_0 plotted against β for the B- and I-type stars in subgroup 1a. Stars exhibiting emission form an almost parallel sequence

to the left of the ZAMS line, while stars having peculiar spectra fall to the right of the ZAMS relation. The scatter about the ZAMS line drawn for a distance modulus of 7.8 mag (the mean found from all normal stars in Table 10, Paper I) is large and skewed for $\beta > 2.8$. This effect can be seen more clearly in Figure 3 where we plot the derived distance moduli against β . A trend in these diagrams can be caused by either a systematic error in the β , \underline{M}_v calibration or by a different mean distance for stars in a certain part of the dm , β plane. Since work on other groups has not revealed any systematic errors in the calibration (see Crawford 1973), we attribute the effect to the latter reason, i.e. a bias in the selection of program stars according to apparent magnitude. It is also important to note that an overpopulation of member stars below the 7.8-mag line occurs for $\beta < 2.7$; in fact, for all member stars in this range the mean distance modulus appears to be closer to 8.2. Even if there is an increase in distance from west to east in this subgroup (cf. Steffey 1973) it seems unlikely that all late B and I stars are located toward the west and that most earlier-type stars are in the eastern section, although this possibility must still be checked (see below) by correlating distance modulus with right ascension.

Crawford and Barnes (1966) previously discussed the observed scatter for the lb (Belt) stars in a \underline{V}_0 , β diagram similar to our Figure 2. Since the reddening

corrections are small and reasonably uniform for the 1a subgroup and since no abnormal reddening has been posited in this part of the association (Lee 1968), it seems unlikely that the scatter in \underline{V}_0 can be due to inappropriate reddening corrections. Since duplicity corrections have been applied in our derivation of intrinsic parameters, very little scatter in \underline{V}_0 can be attributed to such effects. Scatter is also ruled out because such a spread would also produce scatter in the β , \underline{c}_0 diagram shown in Figure 4. [The spread in ages suggested by Steffey (1973) in his argument for the non-existence of the 1a subgroup would also be evident here.] We therefore attribute this scatter, as did Crawford and Barnes for the 1b subgroup, to a distance spread among the 1a members.

Comparison of the top of the main sequence in Figures 2 and 4 also suggests that the mean distance (7.8 mag) to the subgroup, as given in Paper I (Table 10) and derived from the complete range of B-type stars, is too small. While the β , \underline{c}_0 diagram indicates that stars near the top of the main sequence are slightly evolved, the ZAMS line at 7.8 mag in the \underline{V}_0 , β diagram places these stars on the unevolved sequence, and also indicates that most member stars in the range $2.65 \leq \beta \leq 2.80$ lie about 0.5 mag below the ZAMS line. The mean distance has therefore been recalculated from the data of Table 5a using only non-peculiar (normal spectral types and no known emission) presumed members having β indices smaller than

2.8. The result is $\langle dm \rangle = 8.03 \pm 0.46$ mag (σ for one star, 60 stars).

iii) Mean Color Excess

The same stars used in the above calculation of the new mean distance to the 1a subgroup have been used to find the mean color excess, with the exception of two stars showing excesses higher than 0.15 mag in $\underline{E(b-y)}$. The average color excess is $\langle \underline{E(b-y)} \rangle = 0.040 \pm 0.025$ (σ , 58 stars). The variation in $\underline{E(b-y)}$ is higher than might be expected for a group having such small and apparently uniform foreground absorption. Color excess is plotted against distance modulus in Figure 5 and the diagram demonstrates the variation in reddening within the subgroup. These variations apparently occur locally in certain areas within the association, although most of the region, including the lines of sight to the background stars observed, is nearly clear.

€

iv) Distance Variations within the Subgroup

In Figures 6 and 7 we investigate the apparent increase in distance with right ascension found by Steffey (1973). Triangles represent the stars studied by Lesh (1968a) and examined by Steffey. The dense clustering between $5^{\text{h}} 20^{\text{m}}$ and $5^{\text{h}} 25^{\text{m}}$ in right ascension consists mostly of earlier-type members ($\beta < 2.8$) but these stars are spread rather evenly in declination. While no apparent distance trend

with right ascension is seen in Figure 6 where all program stars are considered, a possible systematic eastwardly increase in distance is seen for the stars studied by Lesh. The distribution looks rather even west of $5^{\text{h}} 20^{\text{m}}$, however, and the apparent general increase in distance based on the Lesh stars appears to be only a result of the particular stars used and/or random scatter due to the small number of stars used. The diagram indicates that a new expansion study based on the motions of all presumed members studied here should not be affected by systematic trends in distance.

Although no distance trend with declination appears in Figure 7 for the Lesh stars (also concluded by Steffey), when all presumed members in the present program are considered, a trend does appear in that the stars toward the northern part of the subgroup appear to be, on the average, more distant. This may be an indication that the northern part of the 1α subgroup does run smoothly into the λ Orionis clustering [see Penston et al. (1976) for a discussion], which is located at $\delta = +10^\circ$. Unfortunately, very few stars in the latter group have been observed photoelectrically or classified on the MK system.²

²Reddening and distances have been derived for the two brightest members of the group, ϕ^1 and λ Orionis, based

upon UBV photometry. Color excesses of $E(U-B) = 0.09$ and 0.08 mag, respectively, have been found using the modified Q method described in Paper II; these, combined with the absolute magnitudes of Walborn (1972) of -4.3 and -5.3 , yield a distance modulus of 8.3 for both stars, a value consistent with the trend in Figure 7.

The above discussion illustrates the difficulties encountered when trying to define a mean distance for the $1a$ subgroup: if the northern stars really should be excluded because of their possible connection with the λ Orionis group, then we over-estimate the mean distance by including them. If the later B-type stars are included then we under-estimate the mean distance because of selection effects. The new mean distance found earlier has been derived without considering possible λ Orionis group members since it would be extremely difficult, if not impossible, to separate them from $1a$ members. An obvious extension to the present work in the $1a$ subgroup would be to study B-type stars in the λ Orionis clustering and those extending southward to the $1a$ group, in order to see if there is a smooth "bridge" of B-type stars between these groups.

Finally, it is of interest to examine the consequence of a roughly spherical distribution on the spread in distance of the $1a$ subgroup. Figures 6 and 7 indicate an

average extent of about 11° in α and δ , corresponding at 400 pc to a distance of 80 pc. For a spherical group, this distance would result in a spread ~ 0.4 mag in distance modulus, as compared with our derived standard deviation of 0.46.

b) Subgroup lb (Belt Region)

i) Previous Investigations

The lb or so-called Belt subgroup is more condensed than la and extends from approximately $5^{\text{h}} 20^{\text{m}}$ to $5^{\text{h}} 40^{\text{m}}$ in right ascension and from -3° to 0° in declination (1900 coordinates).

Sahovskoy (1957) catalogued 470 stars over an area of about ten square degrees in the Belt region and showed that a space group of stars displaying a color-magnitude diagram similar to that of the Sword (lc) subgroup exists at a distance of about 450 pc. He suggested that both groups apparently belong to the larger Orion association. The UBV photoelectric studies of Sharpless (1952, 1954, 1962) included many stars in the Belt region and placed particular emphasis on the evolutionary differences between the Belt and Sword regions. The differences were detected by $H\gamma$ photometry, which indicated systematically weaker Balmer lines (higher luminosity) for a given color in the Belt stars.

Hardie, Heiser and Tolbert (1964) made the first systematic study of Henry Draper B-type stars in the Belt

region. A comparison of their UBV photometry with the calibration for the upper part of the Sco OB 2 association (Hardie and Crawford 1961) revealed no significant age differences between stars of the eastern and western ends of the group. An apparent increase in distance from west to east was attributed to an actual variation of from 7.9 to 8.4 mag with a mean of 8.2 for the middle group. This mean agrees well with the value of 8.3 found by Blaauw (1958) from comparing the H-R diagram of the Belt region with that of Upper Scorpius. As mentioned in § IIa the postulated distance spread was confirmed by Crawford and Barnes (1966). Upon elimination of probable non-members (on the basis of their positions in the β , $(\underline{U}-\underline{B})_0$ diagram) and the closer stars in the western group, the results of Crawford and Barnes give distance moduli of 8.1 ± 0.38 (rms), 8.1 ± 0.47 , and 8.6 ± 0.62 for the west, middle, and east groups, respectively.

From an analysis of extensive wide-band photometry throughout the association, Lee (1968) found no variations in the normal extinction ratio $\underline{E}(\underline{U}-\underline{V})/\underline{E}(\underline{B}-\underline{V})$ [in agreement with an earlier result of Sharpless (1954)], but did find anomalies in the total extinction in the Orion Nebula (subgroup 1d) and in the east Belt regions. His results for the east Belt suggest a ratio of total-to-selective absorption of $\underline{R} \sim 5.5$, but this must be considered uncertain for several reasons: (a) The monochromatic extinction

curves for NGC 2024 No. 1 (a highly reddened star located near ζ Ori in the east Belt) and for the other two stars used to determine \underline{R} in Lee's east Belt region, HD 37903 and HD 37140, are significantly different; (b) HD 37140, which has high weight in Lee's results, is actually located in the middle Belt region of Hardie, Heiser and Tolbert, implying abnormal reddening there as well; this star is also abnormal spectroscopically (Schild and Chaffee 1971; Schild and Cowley 1971) and may be a spectrum variable (Bernacca and Ciatti 1972). (A spectrum/color discrepancy of five subclasses is indicated by the photometry in Table 8a, although the $H\beta$ line strength agrees with the colors.)

Johnson (1968) also studied \underline{R} in the Belt region using the variable extinction method, finding $\underline{R} = 4.5 \pm 0.3$. This value must also be considered questionable because of the range in distance of the stars used. Walker (1962) has examined the apparent increase in \underline{R} with distance spread and finds that with $r = 500$ pc, $\Delta r = 200$ pc, $d(\underline{V}-\underline{M}_V)/dE(\underline{B}-\underline{V}) = \underline{R} + 2.9$. This distance spread is reasonable for the Belt region and, considering our \underline{V}_0 , \underline{M}_V diagrams of Paper I, may even be somewhat small. We shall return to this problem later when attempting a reddening analysis for the east Belt region.

ii) Distance Moduli for the B Stars

In an attempt to better define differences within the lb subgroup, the Belt region has been divided into three subdivisions corresponding approximately to those of Hardie, Heiser and Tolbert (1964). These regions, outlined in Figure 6 of Paper I, are centered roughly around the three high-luminosity Belt stars ζ , ϵ and δ Ori. In the following discussions the photometric data for the lb subgroup will be analyzed separately for the above subdivisions in certain respects such as mean distance and reddening, but will be combined in other diagrams since previous work has shown no appreciable differences in parameters such as age and composition. Our analysis will be based principally upon the B-type stars, since the present program does not contain enough I and AF stars to provide meaningful results. The photometric and related data for subgroup b are presented in Tables 6-8 in the Appendix.

The m_0 , β diagram for the stars of subgroup b is shown in Figure 8. A comparison with Figure 1 shows that while B stars of the la subgroup adhere closely to the Orion I and field-star sequences, those of the lb subgroup fall systematically below, especially in the mid B-star range. Although a closer comparison of these differences will be made in § III, where we compare the subgroups in detail, it should be noted here that systematically stronger Balmer lines in the Belt and Sword stars (Sharpless 1962) as

compared with those of subgroup a, probably do not account entirely for the systematic difference seen here.

The intermediate-group stars are seen to follow the ZAMS relation in Figure 8, except for a few having low β values.³ The AF-type non-members in Figure 8 fall along

³One of these, HDE 290799 (subdivision b2), has a variable β index and is also included in Table 7c for AF stars. The other, HDE 290497, has an uncertain group classification, as noted in Table 8b. The β indices of these two stars may be affected by axial rotation, but no $\underline{v}_e \sin \underline{i}$ data are available.

the standard Hyades sequence, but there is considerable scatter away from the sequence for presumed members. The direction is in most cases toward lower \underline{m}_0 , suggesting a lower metal abundance, but this cannot be substantiated because of a lack of $\underline{v}_e \sin \underline{i}$ data for these stars; a more detailed discussion will be given in § III where stars of all subgroups are compared.

The \underline{V}_0, β diagram for the B-type stars of subgroup b is shown in Figure 9. The systematic effect of late B stars falling above the ZAMS line seen in Figure 2 for subgroup a is not as pronounced in this diagram, although it does occur to a certain extent. Two possible reasons for this difference are readily apparent: (i) the la

subgroup is strung out toward the Sun and contains many probable members closer than its mean distance. This is not the case for subgroup b; (ii) fainter stars, mostly from the program of Hardie, Heiser and Tolbert (1964), have been observed in the Belt region; therefore, more late B stars are located near and below the ZAMS in the range $2.8 \leq \beta \leq 2.9$.

Additional differences become apparent when the V_0, β diagram is divided according to the symbols plotted, i.e. according to the subgroup divisions b1, b2, and b3. Most of the triangles form a parallel sequence about 0.6-0.8 mag below the ZAMS, while about half of the squares fall above the ZAMS. Filled circles follow the ZAMS closely except that, as for the triangles, quite a few mix with the squares for $\beta > 2.8$ mag. Assuming again (with good reason) that the spread in Figure 9 is primarily a result of distance dispersion along the line of sight, this immediately suggests a large overlapping of members of the three subdivisions. This superposition has previously been suggested for a few members of the 1a subgroup by Lesh (1968a) and appears to occur within the 1b subgroup as well. Such superposition is not unexpected and it is worth emphasizing that the purpose of attempting somewhat finer subdivision in the Belt region was only to examine the mean differences in east to west distance. Even this goal obviously becomes difficult to achieve quantitatively,

although we can easily see from the \underline{V}_0, β diagram, particularly for stars having $\beta < 2.8$ and considerable overlap notwithstanding, that a mean distance increase occurs across the Belt subgroup with the eastern stars lying generally farther away.

The disagreement between the mean distance to bl, as derived in Paper I, and that of Crawford and Barnes (1966) now becomes clear. Our distance (8.2 ± 0.61 mag) was derived by including all triangles in Figure 9, while their distance (8.6 ± 0.63) was determined after omission of the stars near the top of the main sequence.⁴ [These stars

⁴Our inclusion of the stars ζ Ori and σ Ori AB appears justified by the excellent agreement of their $\underline{M}_V(\beta)$ values with results based on MK types, particularly those of Walborn (1972) [see Paper II, Table 1].

were omitted only because their indices are outside the Upper Scorpius calibration which they used to obtain the distance.] Also, most stars having $\beta > 2.8$ were not included on their program and many of these are found to be closer than the mean distance. Upon comparing individual distances, most agree well except for several stars where we have slightly smaller values (0.1-0.3 mag). This disagreement may also be due to their use of the earlier Upper Scorpius $\beta, \underline{M}_V(\beta)$ calibration. Many of the

other stars having smaller distance moduli are again late B types ($\beta > 2.8$) and some observational selection may be present.

Figure 10 shows our derived distance moduli plotted against β for the B- and I-type stars of subgroup b. This diagram appears similar to Figure 3 for subgroup a. As expected from Figure 9, inclusion of stars to fainter limits in the Belt region results in a larger number of late B stars below the mean line, but the distribution is still noticeably skewed; we believe this to be due, at least in part, to observational selection effects. We therefore derive the final mean distances after omission of stars having $\beta > 2.80$; the results for subdivisions b1, b2, and b3 are, respectively: $\langle dm \rangle = 8.50 \pm 0.53$ (σ , 14 stars); and 8.15 ± 0.29 (24 stars); and 8.04 ± 0.55 (12 stars). These compare with 8.2 ± 0.61 (24 stars); 8.0 ± 0.40 (40 stars); and 8.0 ± 0.51 (22 stars) reported in Table 10 of Paper I, as derived from all normal B-type stars in the respective regions.

iii) Mean Color Excess from the B Stars

The mean color excesses⁵ calculated from the newly

⁵Because of the known patchy distribution of absorption in the Orion region, we have omitted a few stars in each subdivision which show considerably higher color excesses than the mean.

selected stars are: $\langle \underline{E}(\underline{b}-\underline{y}) \rangle = 0.091 \pm 0.084$ (σ , 14 stars); 0.057 ± 0.030 (23 stars); and 0.059 ± 0.049 (12 stars) for groups b1, b2, and b3, respectively. If we eliminate three east Belt stars suffering heavy absorption we obtain $\langle \underline{E}(\underline{b}-\underline{y}) \rangle = 0.051 \pm 0.022$ (11 stars) and the three subdivisions compare well.

iv) Distance Variations within Subgroup b

The β , c_0 diagram for the B-type stars of subgroup b is shown in Figure 11. Unlike the diagram for 1a (Fig. 4), in which most stars are located slightly above the main sequence, the present diagram shows very close adherence to the ZAMS for even the earliest types--only the supergiants are displaced upward. Such a systematic difference between the two subgroups can hardly be attributed to axial-rotation effects for the 1a stars and must therefore be associated with age differences between the a and b subgroups (stronger Balmer lines in 1b).

To investigate further the distance increase across the Belt region from west to east found by Hardie et al. (1964) and supported by Crawford and Barnes (1966), we show in Figures 12 plots of distance modulus against right ascension and declination. No significant trends appear with declination. In the dm , α diagram the apparent curvature can be seen as due to a small group of about a half-dozen more distant east Belt stars. If these more distant east

Belt stars happen to be associated with or behind the nebulosity located in the area, and if this material is causing variations in total absorption, then it is clear that the larger mean distance of the east Belt region would be accounted for. In this case we would expect all east Belt stars more distant than, say, 9.0 to exhibit higher than normal reddening. Only one of these stars HD 37903, shows a high color excess of 0.24--the others all have excesses ≤ 0.1 . Abnormal reddening of the amount suggested by Lee (1968) [$R(b-y) = 7.9$] therefore decreases their distances by only a few tenths of a magnitude and they remain at considerably greater distances than the mean. It seems a better possibility that if absorption in this region is abnormal due to local material, then it is abnormal on a non-uniform basis depending on the lines of sight to individual members.

A detailed investigation of anomalously high total absorption in the Orion association, i.e. an increase in the ratio of total-to-selective absorption \underline{R} , is very difficult due to the distance spread among the member stars. For the Belt region the standard deviation in distance modulus is about 0.5 mag, which by Walker's (1965) equation, gives a spurious increase in $\underline{R(B-V)}$, as determined from the variable extinction method, of 3.6.

In order to decrease the large spread in distance, a list of Belt region members having

$8.0 \leq (V_0 - M_V)[R(b-y) = 4.3] \leq 9.1$ has been compiled for purposes of examining the reddening diagrams. All stars, with the exception of HD 37776 [$E(b-y) = 0.059$], have been omitted on the bases of either spectral peculiarities and/or small distance moduli, i.e. there were no heavily reddened, more distant stars removed to satisfy the above criterion. Figure 13 shows the apparent distance modulus ($V - M_V$), plotted against the color excess $E(b-y)$, for the remaining sample of 47 stars. The stars included in this variable extinction diagram have a mean distance modulus of 8.39 ± 0.31 . The effect of the remaining spread in distance is indicated in the diagram by showing three lines for two different values of $R(b-y)$. The solid lines are drawn for a slope of 4.3 (equivalent to $R(B-V) = 3.0$) and for distances equal to the mean for these stars, and to $\pm \sigma$ (dm). The dashed lines are shown for the same distances and for a slope of $R(b-y) = 7.9$ [$R(B-V) = 5.5$]. While the small number of appreciably reddened stars in the Belt region makes any analysis of this diagram somewhat uncertain, the majority of points clearly show better agreement with the normal reddening law.⁶

⁶Although several east Belt stars having low color excesses fall along the lower dashed line, this is clearly a distance effect since the remaining bl members are located in the upper part of the populated region and two of the reddened stars fall in the normal region. Also, if the

zero point is moved to the average distance modulus of these stars, $\langle \underline{V}_0 - \underline{M}_V \rangle = 8.95$ ($\underline{R}=4.3$), the resulting slope of the best fitting line is approximately equal to that of the solid line. If we then move the zero point to $\langle \underline{V}_0 - \underline{M}_V \rangle = 8.61$ ($\underline{R}=7.9$), the resulting line through the low excess points has slope $\underline{R}(\underline{b}-\underline{y}) = 10$ and the open square is discordant. (The latter star is HD 37903 and is probably the exciting star of the nebula NGC 2023 near the Horsehead complex, hence it may display a high \underline{R} value due to local absorption by the nebula.)

To further strengthen the preceding arguments, we have computed residuals from the mean distance modulus of 8.39 by calculating new moduli using $\underline{R}(\underline{b}-\underline{y}) = 4.3$ and 7.9. A plot of these residuals against $\underline{E}(\underline{b}-\underline{y})$ should show no trend with color excess if the correct value of \underline{R} has been used. These diagrams, which were used by Crawford and Barnes (1970b) in their analysis of the Cepheus OB 3 association, are shown in Figures 14. The clear trend in the lower diagram shows that $\underline{R}(\underline{b}-\underline{y}) = 7.9$ is inappropriate for all subdivisions of the 1b subgroup. A possible exception is the open symbol HD 37903 (NGC 2023). If this star does have $\underline{R}(\underline{b}-\underline{y}) = 7.9$ as indicated, then its true distance modulus is 8.2 rather than 9.1 as given in Table 6a.

v) Analysis of the I- and AF-type Stars

Very little information can be obtained from the intermediate- and AF-group stars in subgroup b because few are included in the program and many of these are probable non-members.

Figure 15 shows a plot of the quantity $\underline{a}_0 - \underline{r}$ against \underline{a}_0 for the I-type stars. Since \underline{a}_0 is the temperature index for the I group and \underline{r} is dependent almost entirely on luminosity (Strömgren 1966 and Paper II), this is like a color-magnitude diagram. The zero-age main sequence has been calculated from the photometric data of Glaspey's (1971a) calibration for intermediate-group stars. Several of the filled circles above the ZAMS have no proper-motion data and may well be non-members.

The \underline{c}_0, β H-R-type diagram for AF-type stars in subgroup b is shown in Figure 16. Most of the stars located above the main sequence in this diagram are presumed non-members from independent considerations such as distances and proper motions. The positions of presumed members along and below the ZAMS is encouraging and indicates that the Belt region may contain member stars along the main sequence well into the A-star range. A more thorough study to fainter magnitude limits might prove very valuable in locating a lower main-sequence turn-up for subgroup b.

c) Subgroups lc and ld (Sword region)

i) Previous Investigations

In this section we combine discussions of the lc and ld subgroups since together they comprise the so-called "Sword" region and because they are treated together in most previous work. Important differences may exist between these subgroups with regard to the reddening law and to peculiarities of the stars embedded in the Orion Nebula, however, hence individual analyses of the photometry and diagrams are desirable in some respects. It is also necessary to treat the B- and later-type stars in these groups separately since very little useful information on distances can be obtained from I- and AF-type members due to their peculiarities and pre-main-sequence character.

The Orion lc subgroup extends from approximately $5^{\text{h}} 22^{\text{m}}$ to $5^{\text{h}} 50^{\text{m}}$ in right ascension and from $-8^{\circ} 30'$ to -3° in declination (1900 coordinates), covering an area of about 25 deg^2 surrounding the Orion Nebula. The ld subgroup contains stars within the geometrical boundaries of the nebula itself, plus those immediately surrounding the nebula but outside the main boundaries. The present program contains a total of 238 stars of all types in the lc subgroup, plus two bright stars outside the above limits which had previous four-color and β photometry and were included in the reductions for B-type stars in this region. The ld subgroup contains 28 program stars, mostly of B-type.

As with the Belt (1b) subgroup, the Sword region has been divided into several subdivisions in order to examine more closely any differences among the small clusterings of stars immediately surrounding the nebula. Included within the 1c subgroup are subdivisions c1-c4, which follow very closely Walker's (1969) groups 1, 2, 3, and 5, respectively. Subdivisions c1 and c4 also correspond to the "Upper Sword" and "1 Orionis" clusterings of Morgan and Lodén (1966). Subgroup 1d is subdivided into the "inner nebula," designated d, and the "outer nebula," designated d1 (see Fig. 6, Paper I). The reason for this segregation concerns the fact that almost all stars within the nebula are peculiar (and/or the reddening law is abnormal) and anomalous distances result from any photometric analysis (Johnson 1967). On the other hand, many of the early-type stars just outside the nebular boundaries appear reasonably normal and may be expected to yield reliable distances whose mean can be applied to the Trapezium region. This mean may then be used in an attempt to learn why the photometry for the Trapezium region gives anomalous distances.

Sharpless⁷ (1952, 1954) found a mean spectroscopic

⁷An excellent historical review of early work is given by Sharpless (1952).

nebula; from a more detailed study (1962) of the Belt and Sword subgroups, he found systematically stronger Balmer-line absorption for stars in the latter region via photoelectric measures of $H\gamma$. This result confirmed Morgan's (1956, 1958) qualitative estimates from the spectra of B-type members. The stronger Balmer lines in the Sword stars provide evidence that they have a lower mean age than do the stars of the Belt region. For the Sword stars, Sharpless found a lower main-sequence turn-up in the range $-0.05 \leq (B-V)_0 \leq +0.10$, confirming suggestions by Johnson (1957) and by Strand (1958) that the A0 stars in the nebula region have not yet reached the zero-age main sequence.

Strand (1958) obtained an astrometric distance modulus of 8.6 mag for the Orion-Nebula stars, while Johnson (1965) combined radial velocities and proper motions of 21 nebula-region stars and obtained a kinematic distance modulus of 7.9 mag.

Morgan and Lodén (1966) studied two small clusterings in the outer Sword region--the so-called "Upper Sword" and "1 Orionis" groups--by means of UBV photometry and MK spectral types. These clusterings correspond to our subdivisions c1 and c4, respectively. A distance modulus of 8.1 was derived for the latter group by fitting its main sequence to that of Upper Scorpius.

Walker (1969) studied a large number of stars in the vicinity of the Orion Nebula, including many faint

objects, using UBV photometry. His program was restricted to stars listed in the catalogue of Brun (1935) because its limits correspond closely to the region in front of the well-known dark cloud extending from $5^{\text{h}} 28^{\text{m}} \lesssim \alpha$ (1900) $\lesssim 5^{\text{h}} 33^{\text{m}}$, $-4^{\circ} 25' \gtrsim \delta$ (1900) $\gtrsim -6^{\circ} 30'$, which eliminates background objects at optical wavelengths. The two-color diagram for this area shows that for most stars the reddening is small and uniform at $\underline{E(B-V)} \approx 0.06$, but a number of individual stars display high local absorption. Many of the later-type stars also show ultraviolet excesses and lie well above the main sequence. Differences among the small clusterings of stars around the nebula were investigated by Walker, who found their c-m diagrams to be very similar after due allowance for differential reddening and duplicity. The overall c-m diagram for the area shows a well-defined main sequence to $(\underline{B-V})_0 = -0.09$, redward of which a somewhat broader parallel sequence rises above the ZAMS and extends out to where the RW Aurigae and T Tauri variables appear. This sequence contains a very noticeable gap in the range $0.3 \leq (\underline{B-V}) \leq 0.4$ which had not been found by Walker in his studies of other young clusters. Theoretical reasons for the existence of such gaps have recently been discussed by Böhm-Vitense and Canterna (1974) and a more detailed discussion will be given in § IIc.iv below.

Walker's c-m diagram for stars in the range $-0.20 \leq (\underline{B-V}) \leq -0.05$ (excluding known variables and binaries) yielded a true distance modulus of 8.37 ± 0.05 . This should be the best available distance to the nebula and to the stars embedded within it [if $\underline{R(B-V)} = 3.0$] since it is derived from mostly normal objects in the immediate vicinity.

Bernacca (1968) has discussed in detail several stars in the lc subgroup which display colors too blue for their spectra. He found that the so-called helium-weak and hydrogen-strong stars lie at the lower boundary of the main sequence in the upper and lower sections of the B-star c-m diagram, respectively (see also Fig. 20) while stars later than A0-A1 all lie one to two magnitudes above the ZAMS. Many of the stars showing spectrum/color discrepancies are apparently associated with bright nebulosity, as is the case with similar stars in Upper Scorpius.

The reddening law for the Orion-Nebula region has been the subject of numerous investigations and no clear picture has emerged as yet. Sharpless (1952) has reviewed earlier work in the ld subgroup which indicated an abnormal reddening law. His own observations revealed a ratio of total-to-selective absorption of as much as $\underline{R(B-V)} \sim 6$ for the nebula region. However, his diagrams revealed high R values in other parts of the association as well and they may be affected by the distance spread among the stars used, many of which lie outside the nebular boundaries.

Sharpless also found a smooth decrease in color excess outward from the Trapezium, a contradiction to earlier work which had suggested a transparent area near the center of the nebula.

Hallam (1959) found that large deviations from a linear $1/\lambda$ law of reddening appear to occur only for the stars immersed in emission nebulosity, while those outside the nebula exhibit more nearly normal reddening curves. Red companions, as suggested by Stebbins and Kron (1956), do not account for these departures and the contribution from the nebula is negligible at only a few per cent. Significant departures from the normal extinction law in the far ultraviolet have also been found for the Trapezium stars by Carruthers (1969).

Johnson (1968) found $\underline{R} = 5.0 \pm 0.3$ for the Sword region using the variable extinction method, in agreement with the value 4.8 found by Mendéz (1967); this work may also be affected by the large spread in distance.

Lee (1968) found no sign of abnormal extinction in the outer Sword (1c) subgroup, but obtained a value of $\underline{R} \geq 5.5$ for stars in the nebula on the basis of their steep infrared gradients. Red companions and/or circumstellar shells were found not to account for the observed excess infrared radiation.

On the other hand, Walker (1964) has reviewed the effects of anomalously bright visual absolute magnitudes for the Orion-Nebula stars on derived values of \underline{R} for that region. He finds that $\underline{M}_V[\underline{W}(\text{H}\gamma)]$ values do not support the $\underline{M}_V(\text{MK})$

results used by Johnson and Borgman (1963) to derive $\underline{R} = 7.4 \pm 0.3$ for the Trapezium region. Using the $\underline{M}_V(H\gamma)$ data, Walker derives values of \underline{R} closer to the normal value of 3.

Walker (1969) examined \underline{R} by differentially correcting the highly reddened objects to a uniform sequence in his c-m diagram. The uniform sequence was defined by the stars of small uniform reddening. This was done for $\underline{R(B-V)}$ values of 3.0 and 5.0 and a better fit was obtained for the former. For this reason Walker believes that the excess infrared radiation found by Johnson (1968) and by Lee (1968) is due to some other physical process(es). (Evidence of remnant circumstellar material which could cause infrared anomalies and high polarization was discussed as possible processes in Paper II.)

Schild and Chaffee (1971) have studied energy distributions of B stars in the Orion association, including several in the Sword region. Upon correcting the observed distribution for reddening, they found unsatisfactory fits to their models shortward of the Balmer jump for HD 36958 (KX Ori), 37061 (NU Ori), and 37356 when a normal reddening law was used.⁸

⁸The above stars are included in the present program and do not appear abnormal photometrically. Peculiarities do exist for these stars, however, in that the last two show higher than normal reddening and, more importantly, all

three are polarized. Although abnormal ultraviolet absorption does not affect R , these peculiarities do indicate a possible abnormal particle medium which could affect infrared fluxes and cause polarization.

Application of Whiteoak's (1966) abnormal law gave better agreement with their observations.

A normal reddening law as assumed by Penston (1973) in his discussion of UBVRIJHKL photometry of stars in the vicinity of the nebula, after concluding that other phenomena can account for the infrared emission. The average values of total absorption A_V obtained by Penston from visual and infrared excesses agree well with our results obtained using the normal value of $R(b-y) = 4.3$, except for stars in which a blue continuum is suspected. In a more recent paper, Penston, Hunter and O'Neill (1975) have examined the infrared excesses more closely using new photometry for fainter stars in the nebula cluster. They suggest that the reddening law may appear abnormal because excess emission in the infrared mimics a hole in the obscuration at these wavelengths. Their analysis of the color-excess ratios yields a wavelength dependence close to the normal curve (No. 15) of van de Hulst (1949). All c-m diagrams using infrared colors were found to give discordant distances because of the varying effects of infrared emission on these colors. An H-R diagram based

upon a normal reddening law yielded a mean distance modulus to the cluster of 8.0 ± 0.1 mag.

It is apparent that the question of abnormal reddening within the Orion Nebula is still not completely resolved, although evidence is quite strong now that these apparent anomalies occur only for stars within the main nebula or closely associated with nebulosity. Even for these stars, other hypotheses have been put forward to account for the anomalies, e.g. if we account for the infrared excesses by circumstellar phenomena, then the distance discrepancies can be explained by subluminescence of the nebula stars. Sharpless (1952) noted that a normal R for the Trapezium stars would require them to be subluminescent and Morgan (1956) has suggested that this is the case. He has estimated that in the spectral range B0-B3, the average difference in absolute magnitude between stars in the inner and outer groups is about 0.75. This possibility will be discussed in more detail in our discussion of the nebula stars in the following section.

ii) The Photometric Data and Distance Moduli
from the B Stars

Tables 9-11 present the photometric and related data for subgroups c and d. The results for the subdivisions of the lc group are listed separately in Tables 10 because individual distances and reddening will be derived

for these clusterings initially. We also wish to compare the c-m diagrams for these subdivisions.

Figure 17 shows the \underline{m}_0 , β diagram for the stars in subgroup c. Members of the subdivisions c1-c4 are also included. Comparison of this figure with similar diagrams for subgroups a (Fig. 1) and b (Fig. 8) shows that the B-star sequence corresponds more closely to that of the lb (Belt) region, i.e. most B-type stars fall below the mean relations for the Orion stars (solid line) and field stars (dashed line). There is an important difference for the late B stars, however, in that the lc sequence falls away from the mean Orion relation at approximately $\beta = 2.86$, corresponding to $(\underline{b}-\underline{y})_0 = -0.03$ [$(\underline{B}-\underline{V})_0$ of -0.09], the value found by Walker (1969) for the main-sequence turn-up of the lc subgroup.⁹ The adherence of the la and lb sequences to

⁹It will be seen shortly that this apparent turn-up for late B stars is not actually attributable to evolutionary effects, but may be a ramification of effects on the \underline{m}_0 index (see below).

the mean relation throughout the B-star range demonstrates that their PMS turn-up points are at least into the intermediate-group range and they they are older than the lc group.

The distributions for I-group stars are similar in the three subgroups except possibly for a larger number of I-type stars displaying low β values for their \underline{m}_0 indices in subgroup c. This cannot be stated positively on the basis of so few stars, however.

The larger number of field and presumed-member AF-type program stars in the lc subgroup allows a better discussion of composition differences between these groups and the Hyades standard relation (dashed line). Although the scatter is large, the A stars are seen to follow the Hyades relation. Most, but not all, of the high \underline{m}_0 stars are reddened objects. The gap in the late-group sequence found by Walker (1969) can be seen very clearly here. The F stars show systematically low \underline{m}_0 indices relative to the Hyades and do not show any apparent differences from the non-member stars. We will discuss the \underline{m}_0 indices in more detail when the photometric diagrams for the AF stars are presented in section (iv).

An unfortunate circumstance for analysis of stars in the lc and ld subgroups using uvby β photometry is that the lower main-sequence turn-up occurs near spectral type A0 where a transition from early to intermediate groups takes place.¹⁰ In Orion lc the problem is enhanced by the many

¹⁰As discussed in Paper II, results are more uncertain in this transition region because it is often difficult to

place stars into their correct groups and the different reduction procedures sometimes do not give entirely consistent results.

peculiarities associated with member stars at or near the turn-up point, making it particularly important to check for systematic effects along the late B-star sequence for subgroup c. These effects will be examined shortly as they have been for the other subgroups; however, we begin by comparing the subdivisions included within the outer Sword subgroup to see if any evolutionary differences are detectable. If not, we may then combine these subdivisions with each other and with the c subdivision in the ensuing analysis.

Figure 18 presents V_0 , c_0 color-magnitude diagrams for the subdivisions of the outer Sword region. Binaries corrected for duplicity have been indicated by open symbols primarily to discuss the diagram for subdivision c1. As mentioned previously, Morgan and Lodén (1966) found several B stars above the ZAMS in this clustering and suggested that its stars may be slightly more evolved than those in subdivision c4 (1 Ori group).¹¹ After corrections for duplicity, the

¹¹From left to right in their Fig. 4, these are HD 37017, 37016, 37040, 36883, and 36865. The first star is found slightly below the main sequence in our diagram and manifests the helium-strong spectral peculiarity (but not as

extreme as σ Ori E). Its smaller Balmer jump (higher T_{eff} , see Lester 1972) results in a lower than normal c_0 . The remaining stars are all binaries and require corrections of 0.5, 0.2, 0.3, and 0.2 mag, respectively, in the H-R diagram of Morgan and Lodén. These corrections result in a much narrower sequence, substantially in agreement with the ZAMS and with the sequence of subdivision c4.

only Morgan and Lodén star still well above the ZAMS is HD 36916, a peculiar luminosity class III object. The scatter in the diagram for subdivision c is undoubtedly a result of the distance spread among the stars far from the nebula, as will be demonstrated when the distance-independent β , c_0 diagram is constructed. No evolutionary differences are apparent for the different subdivisions and we conclude that they can therefore be combined in subsequent diagrams for the lc subgroup.

Following the procedure used for the other subgroups, we present in Figure 19 the \underline{V}_0 , β diagram for subgroup c. Although a spread in distance is apparent in this diagram, the systematic effects encountered for late B stars in subgroups a and b are not nearly as pronounced here. This is due to the inclusion of fainter program stars in the Sword region, a result of the more concentrated effort devoted to this area by previous workers from which our observing lists were drawn. It is probably also a result of there being

fewer stars strung out toward the Sun in this subgroup. Above a β value of 2.85, however, we do find an excess of stars above the ZAMS, hence our final distances will be derived using only stars having β indices below this value.

Final mean distances have been derived for the subdivisions of the 1c subgroup and for the entire group using the same procedure as used earlier for the 1a and 1b subgroups. All peculiar and/or emission stars, as well as probable and possible non-members, have been omitted, although the inclusion of the latter stars does not change the results appreciably. Due to the small number of B-type members in the subclusterings around the nebula, separate discussions of the stars omitted are in order. Table 10a and associated notes may be consulted for more details.

In subdivision c1, star 248 has been omitted because of its peculiar spectrum and uncertain photometric distance. Star 258 has a large β index. The remaining nine stars give $\langle dm \rangle = 8.02 \pm 0.40$ (σ , one star). (Although, as we shall see, within the precision of the determinations, all of the 1c subdivisions are at the same distance, the average distance modulus, uniform reddening, and complete absence of heavily reddened stars suggest that the c1 group is somewhat closer than the nebula and other subclusterings.)

Only star 277 has been omitted in subdivision c2, because it appears to lie beyond the clustering and may actually belong to the larger, more dispersed, c subdivision. The eight other stars yield $\langle dm \rangle = 8.45 \pm 0.49$ mag.

For subdivision c3 we have only six stars, three of which have β indices above 2.85. Exclusion of these three gives $\langle dm \rangle = 8.20 \pm 0.36$, while all six stars yield $\langle dm \rangle = 8.20 \pm 0.24$.

In subdivision c4 we have omitted star 245 because of its high β and star 246 because of peculiarities. The remaining eight stars give $\langle dm \rangle = 8.35 \pm 0.28$.

A total of 44 stars has been used to find a mean distance to the outer Sword region (subdivision c). The resulting value is $\langle dm \rangle = 8.16 \pm 0.49$. Taking all stars in subgroup c together we find $\langle dm \rangle = 8.21 \pm 0.42$ (78 stars).

Figure 20 shows the V_0, β diagram for the B-type stars in subgroup d (subdivisions d and d1). The V_0 values have been calculated using the normal value of $R(b-y) = 4.3$. Stars having color excesses appreciably higher than the foreground value of $\langle E(b-y) \rangle = 0.04$ are denoted by "r." The appearance of most stars below the 8.4-mag ZAMS line cannot be accounted for by a translation of the ZAMS to 8.6, the value found in some previous studies, since a vertical sliding fit would yield a value ~ 1 mag greater than 8.4. If we assume an emission effect of 0.03 in β , as estimated by Smith (1972b) for the later-type FMS stars of Orion lc, we obtain the dashed ZAMS line shown in the figure. A somewhat larger shift of 0.05 would bring the sequence of early B stars in subdivision d (inner nebula) into coincidence with the ZAMS; hence one way to account

for the appearance of the nebula stars below the main sequence in the \underline{V}_0, β diagram is to postulate a Balmer-line emission amounting to 0.05 in β . This hypothesis is consistent with the decreasing divergence of later B stars from the ZAMS line and with the considerably greater photometric distances obtained from $\underline{M}_V(\beta)$.

The possibility still exists, however, that the greater distances and positions below the ZAMS for these stars are caused by subluminescence of the nebula stars, as posited by Morgan (1958), and/or by a high value of \underline{R} , as proposed by Johnson (1968), Lee (1968), and others. Since these mechanisms will affect the parameter \underline{V}_0 and not β , while Balmer-line emission will affect β only, an effect on \underline{V}_0 can be checked by constructing a $\underline{V}_0, \underline{c}_0$ diagram for the stars, as shown in Figure 21. We again find a sequence of appreciably reddened stars well below the ZAMS line; in fact, all O and early B stars are located below the main sequence as they are in the \underline{V}_0, β diagram. Notice, however, that only reddened stars appear well below the line and that most of the stars near the line are unreddened.¹² The appearance of these stars below the

¹²The exceptions are star 278 (θ^1 Ori D) which is extremely peculiar and falls well above the main sequence in the β, \underline{c}_0 diagram (Fig. 25), star 308 (HD 37062A) which is

variable in \underline{V} , and star 243 (HD 36917) which is also very peculiar and a possible foreground object.

main sequence may be coupled with the reddening and/or with Balmer emission (both continuum and line since this occurs in both the \underline{V}_0, β and $\underline{V}_0, \underline{c}_0$ diagrams) and suggests that we should look for correlations between the β and \underline{c}_0 indices and color excess $\underline{E}(\underline{b}-\underline{y})$.

To investigate the possible existence of these correlations, new indices $\Delta\beta(\underline{V}_0)$ and $\Delta\underline{c}_0(\underline{V}_0)$ have been found by measuring the horizontal distances of stars from the ZAMS lines in the \underline{V}_0, β and $\underline{V}_0, \underline{c}_0$ diagrams. These indices should measure the amounts of Balmer-line and continuum emission, respectively, and are derived on the assumptions of a mean distance modulus of 8.4 mag and that the shifts are independent of \underline{V}_0 . In Figure 22 these indices are plotted against $\underline{E}(\underline{b}-\underline{y})$. The $\Delta\beta(\underline{V}_0)$ index appears independent of color excess, suggesting that the Balmer-line emission is approximately constant for all stars in the nebula region. On the other hand, the $\Delta\underline{c}_0(\underline{V}_0)$ index is seen to correlate quite well with $\underline{E}(\underline{b}-\underline{y})$, suggesting that the Balmer continuum emission is coupled with reddening. If the reason for the deviations of stars below the ZAMS were in \underline{V}_0 entirely (because of an inappropriate value of \underline{R} and/or subluminality), then both $\Delta\beta(\underline{V}_0)$ and $\Delta\underline{c}_0(\underline{V}_0)$

would be expected to correlate with color excess. These diagrams therefore suggest that either the normal reddening law is appropriate in this region and that the anomalous positions of the stars can be accounted for by emission mechanisms, or that the deviations in the β index are due to the nebula itself and are approximately constant throughout the region. If the β emission is constant, which it appears to be, then the scatter in the \underline{V}_0, β diagram still suggests that other causes may be partly responsible for the location of many stars below the ZAMS.

In order to further investigate possible deviations in \underline{V}_0 , we next employ the MK spectral types and their corresponding mean β and \underline{c}_0 values from the calibration of Warren (1976) to construct $\underline{V}_0, \beta[\text{MK}]$ and $\underline{V}_0, \underline{c}_0[\text{MK}]$ relations, Figures 23 and 24. A comparison of Figures 20 and 23 shows some of the discrepancies to have decreased, but many early B-type stars are still located well below the ZAMS. The unpolarized stars are in general closer to the line but still show a shift which now must be taken as vertical, i.e. there is a contributing effect in \underline{V}_0 which may be due either to high values of \underline{R} , to subluminality, or to a combination of the two. A comparison of Figure 24 with Figure 23 shows effects similar to those in the \underline{V}_0, β diagrams.

The fact that the unpolarized stars are rather uniformly distributed below the main sequence and that the polarized stars are widely scattered suggests that high \underline{R} values

produced by circumstellar material are causing the deviations in \underline{V}_0 . For the unpolarized stars a shift of 0.5-0.75 mag in \underline{V}_0 due to subluminality would bring the points into agreement with the ZAMS, but we must then account for the coincidence of many stars with the ZAMS in Figures 23 and 24. Of course the polarized stars could be subluminal also, with varying contributions due to abnormal \underline{R} being superimposed to cause the scatter.

Figure 25 shows the β , \underline{c}_0 diagram for the stars of subgroup d. Due to the combined effects of emission on the β and \underline{c}_0 indices, most stars appear closer to the ZAMS in this diagram. It is of course independent of distance and \underline{V}_0 , hence contributors to the \underline{V}_0 scatter in previous diagrams are not operative here.

In summary, the above diagrams show that there are effects on the β and \underline{c}_0 indices from Balmer-line and continuum emission for stars in the nebula, but that these effects do not account completely for the appearance of many stars below the main sequence. Although it is highly probable that the locations of many of the polarized stars are due to circumstellar shells displaying various abnormally high \underline{R} values, the effects of uniformly high \underline{R} and subluminality cannot be disentangled with the present data. Even if \underline{R} does turn out to be normal for the region in general, it appears almost certain that particular polarized stars display anomalously high ratios of total-to-selective

absorption due to local material. This suggestion may be investigated by the procurement of wavelength-dependent polarization data for stars in the nebula region, whence individual R values can be calculated from the expression given by Serkowski et al. (1975), if this equation turns out to be valid for absorption not interstellar in origin. The only nebula-region star for which these authors give data is star 307 (NU Ori). Their expression $R(\underline{B-V}) = 5.5 \lambda_{\max}$ yields 3.5, while a vertical translation to the ZAMS in Figure 20 gives $R(\underline{B-V}) = 3.6$.

A reddening analysis using the variable extinction method, as was done for the Belt region, would not be appropriate here due to the effects of emission on our derived absolute magnitudes for stars in the nebula.

A mean distance to subdivision dl has been found by omitting the three stars (WH 243, 321, and 349) showing serious discrepancies in the data. The remaining six stars, which are found near the ZAMS in Figures 20 and 21, yield a mean distance modulus of 8.42 ± 0.53 (one star). The larger error is due mainly to the polarized star No. 307 (NU Ori), for which a dm of 9.4 was derived. In § IIIId we will examine the lc and ld stars further in terms of physical effects (blue continuum emission, etc.) which may be degrading the photometric indices.

iii) Mean Color Excesses from the B Stars

Mean color excesses for subgroup c, including all subdivisions except c3, which is nearest to the nebula and contains highly reddened stars not representative of the foreground absorption, have been found using the same stars as used in the distance analysis. As in subgroups a and b, stars having $\underline{E}(b-y) > 0.10$ have been omitted. These means are given in Table 1, where all final distances and reddening values are summarized.

iv) Analysis of the I- and AF-type Stars

While subgroup c contains only twenty program stars in the I-group range, examination of their c-m diagram is worthwhile since the lower main-sequence turn-up is located near the early side of this group (at B9-A0).

The $\underline{a}_0 - \underline{r}_0$, \underline{a}_0 (c-m)-type diagram is shown in Figure 26. Insufficient stars are available to make a convincing case for the reality of any sequence in this figure, but there is a slight suggestion of a sequence of members above the ZAMS. However, many lie well above the ZAMS in the region occupied by field stars. Although these cannot be declared certain members, other considerations indicate that at least some of them are.¹³ The nine presumed members lying

¹³The five filled circles in this region are, from left to right, stars WH 190, 402, 391 (lower), 214 (upper), and

357. Star 190 is a suspected pre-main-sequence object showing variability, reddening, and high polarization (see note to Table 10b). Stars 214 and 402 are also reddened and appear to have abnormally low β indices, while star 357 (V586 Ori) is variable in all indices (but not polarized or reddened). Finally, star 391 is an approximately equal-component binary which has been corrected in V by 0.6 mag. Stars 190, 214, and 402 appear to be good candidates for extreme youth and may presently be in gravitationally contracting states.

closest to the ZAMS yield a mean distance modulus of 7.90 ± 0.41 mag (one star); elimination of two moderately reddened stars gives an average color excess of $\langle E(b-y) \rangle = 0.019 \pm 0.015$. These values are in reasonable agreement with those obtained from the B-type stars (see Table 1), but probably reflect the selection of program stars by apparent magnitude.

There are two indices which are indicators of effective temperature in the A- and F-star range, namely $(b-y)$ and β , but for a variety of reasons Crawford (1975b) has chosen the β index to be his independent parameter for the calibration of the $uvby\beta$ systems in terms of intrinsic colors and absolute magnitudes. Figure 27 shows the relation between β and $(b-y)_0$ for the program stars in subgroup c. The ZAMS relation for A-type stars is from the preliminary calibration

by Crawford (1973), while the relation for F-type stars ($\beta \leq 2.720$) is taken from the recently completed final calibration of Crawford (1975b).¹⁴ It is readily apparent

¹⁴This final relation differs little from the preliminary ZAMS relation (Crawford 1970) used in the reductions described in Papers I and II, but it seems preferable to use the final relation in the diagrams since the (b-y) color corresponding to a given β is redder by about 0.004 mag on the average due to blanketing corrections considered in the final calibration. Also, we have used the final calibration equations for the F stars in the derivation of intrinsic colors for the present study.

that the sequences in Figure 27 do not coincide exactly. For the A stars ($\beta > 2.720$) they nearly coincide but the ZAMS appears to define an upper envelope in both (b-y)₀ and β . The same is true for the F stars ($\beta \leq 2.720$) until we reach $\beta \leq 2.65$ [(b-y)₀ ≥ 0.30] where the observed sequence departs noticeably and rather uniformly from the ZAMS relation. The presumed members and field stars behave similarly, indicating that the deviations are not associated with the Orion lc stars alone; the reasons for their behavior are not clear at present.¹⁵

¹⁵As the field stars show the same deviations, it seems unlikely that the deviations are due to presumed ultraviolet excesses in the Orion lc members. For the late F-type stars ($\beta < 2.65$) the increasing deviations could be attributed to blanketing effects on the $(\underline{b-y})$ colors, except that blanketing corrections have been applied in the derivation of intrinsic colors. As seen in Crawford's (1975b) $(\underline{b-y})$, β diagrams (Figs. 1 and 2) the blanketing corrections appear to work well, although his Fig. 1 does show an excess of stars in the same sense as in Fig. 27. Although we cannot account for the divergence of the observed sequence from the ZAMS for $(\underline{b-y}) > 0.30$, we do not think that this phenomenon will affect the remaining analysis to any great extent. If the deviations are in $(\underline{b-y})_0$ rather than in β , the remaining diagrams will not be affected at all.

However, it should also be noted here that a large number of negative color excesses for F stars are found using the new calibration. A comparison was made between the new (Crawford 1975b) and preliminary (Crawford 1970) calibrations by calculating color excesses for normal F-type program stars using both: the new calibration gives systematically lower color excesses (with no exceptions) by 0.022 ± 0.008 (17 stars) in $\underline{E}(\underline{b-y})$. This

difference therefore accounts for many of the negative $E(\underline{b-y})$ values found for F stars in the summary tables. The systematic effect cannot be ascribed to peculiar Orion stars since most of the negative excesses obtained are for non-member field stars. Although we could have gone back to the older calibration, it has been suggested by D. L. Crawford (private communication) that the new calibration be retained for purposes of beginning checks on its accuracy.

We now wish to investigate abundance and luminosity differences among the AF stars in subgroup c by using the δ indices listed in Table 10c. Using the \underline{k} index as a measure of the strength of the Ca II K line, Hesser and Henry (1971) found what appears to be an overabundance of calcium in several Orion 1 A-type stars; however, Hesser, McClintock and Henry (1977) have shown the original measurements and analysis (which depended upon UBV instead of uvby colors) to be in error. Their latest results show no enhancement of K-line strength over that of solar neighborhood stars. Smith (1972a), on the other hand, found an upper envelope approximately 0.01 higher than the field-star value in the $[\underline{m}_1], (\underline{b-y})_0$ diagram for Orion 1c. Since Smith did not have β photometry and had to estimate $(\underline{b-y})_0$ using spectral types and use Strömgen's (1966) $[\underline{m}_1]$ index $\{m_1 + 0.18(\underline{b-y})\}$, we wish to examine the \underline{m}_0, β diagram to

see if the apparent metallicity enhancement persists when more accurate intrinsic indices are used.

Figure 28a shows the \underline{m}_0 , β diagram for the I and AF stars of subgroup c. (For purposes of discussing the indices we will refer to both I- and AF-type stars as A stars.) The distribution of A-type stars is rather uniform among presumed members and field stars but most members tend to fall above the Hyades (AF stars) and ZAMS (I stars) standard relations (lower \underline{m}_0 indices).

The deviations from the standard relations can be seen more clearly in Figure 28b. A significant number of members fall below the zero line, a result similar to that of Smith (1972a) except that the apparent envelope found here for the Orion 1c members is not as far to the metal-rich side of the standard relation as in his diagram.¹⁶

¹⁶This may be a result of his use of $[\underline{m}_1]$ rather than \underline{m}_0 , but is not considered a serious discrepancy in any case. The larger deviations for the intermediate (I)-group stars are partly due to our use of a ZAMS rather than Hyades standard relation [note the difference in diagram (a)], but it does appear that $\delta\underline{m}_0$ is more uniformly negative for I than for A and F stars. We note that as for the B-type stars, high \underline{m}_0 values (more negative $\delta\underline{m}_0$) seem in some way connected with reddening--this connection will be examined shortly.

Both field and presumed-member F-type stars deviate uniformly to the metal-poor side of the Hyades relation, indicating that both groups display less blanketing than the Hyades stars and are comparable to each other. If we presume no anomalies in the \underline{m}_0 indices for the F-type member-stars in diagram (b) and omit all stars with parentheses, plus the star with the largest $\delta\underline{m}_0$, we obtain an average $\delta\underline{m}_0$ of 0.021 ± 0.007 for the remaining seven stars. [It has been shown earlier that rotational velocity is unlikely to affect $\delta\underline{m}_0$ for B-type stars and Crawford and Barnes (1974) have indicated that this is also the case for the A-type stars in the α Persei cluster, which tend to have higher than average rotational velocities; however, Hartwick and Hesser (1974) have found a possible threshold effect in \underline{m}_1 for late-group stars in the sense that high rotational velocities tend to decrease \underline{m}_1 . The reddening effect on \underline{m}_0 should not be a problem here since all the stars used are unreddened.] This value is in good agreement with the result found for F stars in the Coma Cluster ($\langle\delta\underline{m}_1\rangle = 0.014$, Crawford and Barnes 1969) and with the value of $\delta\underline{m}_1 = 0.018$ implied for the Sun by the analysis of Crawford (1975b). If this result is representative of blanketing in most Orion 1c F-type stars, then these stars have metal abundances very similar to stars in the solar neighborhood.

We now discuss the c - m diagrams for the A- and F-type stars in Orion 1c starting with Figure 29, the distance dependent \underline{V}_0 , β diagram. Here the non-members (all foreground) are clearly separated from presumed members, but the sequence of members is widely scattered above the ZAMS relation. The mean observed sequence runs approximately parallel to the ZAMS at 1.0-1.2 mag above it; the separation may increase slightly for the F stars. Both the scatter (~ 0.75 mag) and direction of the Orion 1c sequence are similar in appearance to those in the \underline{V} , $(\underline{B}-\underline{V})$ diagram presented by Walker (1969). The diagram clearly supports Smith's (1972a) arguments for membership of his Am stars in the 1c subgroup (see also Hesser, McClintock and Henry 1977).

We should now be able to reduce the scatter in the observed sequence by use of the distance-independent \underline{c}_0 , β diagram, which is shown in Figure 30. Here we find confirmation of the displacement of the member sequence from the ZAMS, since several F-type field stars lie nearly on the latter relation, while all presumed Orion 1c members are found at approximately the same distance above it. This diagram also shows even more clearly that the Am presumed members follow the association sequence closely. As in the \underline{V}_0 , β diagram, the F-star sequence appears farther above the ZAMS than that of the A stars. Considering only members not showing obvious peculiarities, the average value of $\delta \underline{c}_0$ for the A-type stars is 0.088 ± 0.088

(20 stars), while the F-type members yield $\langle \delta c_0 \rangle = 0.118 \pm 0.040$ (10 stars). Since $\Delta M_V(\beta) = 11\delta c_0(\beta)$ (cf. Paper II), the mean value of δc_0 implies that the F-type stars in Orion 1c are an average of 1.3 mag above the zero-age main sequence.

Mean distance-modulus and color-excess values have also been calculated for the AF stars using mostly the same stars as above, i.e. known variables, peculiar stars and non-members have been omitted. Three stars having uncertain and/or variable V magnitudes, but which appear normal otherwise (WH 149, 198, and 230), were given half-weight in the $\langle dm \rangle$ calculation, while two more highly reddened stars (363, 365) plus stars having $E(b-y) < -0.010$, were eliminated from the $\langle E(b-y) \rangle$ calculation. The results are $\langle dm \rangle = 7.87 \pm 0.52$ mag (one star, 23 stars used) and $\langle E(b-y) \rangle = 0.015 \pm 0.023$ mag (one star, 17 stars used). These results are in satisfactory agreement with those obtained from the B- and I-type stars.

We conclude this section by discussing in detail the apparent gap (cf. Fig. 27) in the observed sequence for the late-group Orion stars.

Using a statistical method due to Aizenman, Demarque and Miller (1969), Böhm-Vitense and Canterna (1974) have recently searched for gaps in the main sequences of field-star and cluster diagrams. A gap is clearly present for field stars in the range $0.22 \leq (B-V) \leq 0.31$, but gaps are not as clearly defined for clusters. The cluster gaps do not always occur

(Pleiades); sometimes there are two apparent gaps (Praesepe); when the gaps do occur they are often located in different ranges of $(\underline{B-V})$. Böhm-Vitense and Canterna attribute the presence of main-sequence gaps to the abrupt onset of convection as T_{eff} decreases.

A gap in the color-magnitude diagram for Orion lc stars was first clearly seen by Walker (1969) and occurs in the F-star range $0.30 \leq (\underline{B-V}) \leq 0.40$; such a gap had not been found by Walker in his studies of other extremely young clusters. Figure 27 shows that the gap occurs between $(\underline{b-y})_0 = 0.21$ [$(\underline{B-V})_0 = 0.30$] and $(\underline{b-y})_0 = 0.26$ [$(\underline{B-V})_0 = 0.37$], corresponding to $2.72 \geq \beta \geq 2.68$ and to a main-sequence spectral-type range of F0-F4 [$\underline{M_V}(\text{ZAMS}, \beta) = 3.1 - 3.5$ mag]. The color range of this gap is considerably redward of the gaps for field stars and most clusters, but is similar to the Hyades gap. It is interesting that such a gap has been found at $(\underline{B-V})_0 \sim 0.40$ along the evolved main sequence of the old open cluster NGC 2477 by Hartwick, Hesser and McClure (1972).

According to Böhm-Vitense and Canterna, axial rotation produces a stabilizing effect against the onset of convection, thus clusters having high mean rotational velocities would be expected to show gaps at lower T_{eff} (redder colors). This suggestion and the fact that Orion lc stars on the late side of the Balmer maximum display rather high rotational velocities (Abt et al. 1970) may explain the gap occurrence 0.1 mag redward of the field-star gap.

d) Possible Effects of Blue Continuum Emission
on the 1c and 1d Results

i) B Stars

In Paper II we discussed briefly the effects that blue continuum emission might have on the reduction of our photometric indices; we now examine the (weak) evidence that some of the Orion B-type stars are affected by such emission. To begin we note that in the distance-independent β , c_0 diagram shown in Figure 31, the appearance of many BMS (below-main-sequence) stars suggests abnormally strong Balmer lines. A suspicion arises with this interpretation as the only cause for the BMS stars, however, because many of these objects have not been noted as displaying strong hydrogen lines and show higher-than-normal reddening and m_0 indices.

Glaspey (1971a,b) also found a discrepancy in the m_0 index between stars in the Upper Centaurus and younger Upper Scorpius subgroups of the Sco-Cen association. He found the change in m_0 not to be correlated with color excess $E(b-y)$, and considered the most likely cause of the discrepancies to be detection in the young Upper Scorpius stars of peculiarities such as those found by Garrison (1967).

Consequently, upon detection of an apparent trend in m_0 with color excess in Orion, it was considered useful to investigate possible causes for this dependence, even though the m_0 index is not used directly in the important aspects of our photometric analysis.

Figure 32 relates a quantity $\delta' \underline{m}_0$, as calculated by comparing each \underline{m}_0 index with the mean relation shown as a solid line in Figure 17, to the color excess $\underline{E}(\underline{b}-\underline{y})$ for all Orion 1 B-type members having spectra not known to be peculiar. These indices are obviously related, but the scatter is large. The line in Figure 32 is our eye fit to the points and implies that $\delta' \underline{m}_0 \sim 0.1 \underline{E}(\underline{b}-\underline{y})$. This in turn implies that $\underline{E}(\underline{m}_0) / \underline{E}(\underline{b}-\underline{y}) = -0.2$ rather than the normal slope of -0.3 . This difference is rather hard to accept, since the most recent determination of this slope by Crawford (1975a) from O stars (many of which are also heavily reddened) gives -0.32 . Also, the scatter suggests that an inappropriate reddening slope cannot account for the effect.

The apparent existence of two groups of reddened stars in Figure 32, one above the line and showing large \underline{m}_0 discrepancies, the other below the line and showing small \underline{m}_0 discrepancies, suggested that data for these stars be examined more closely. A detailed comparison does not clarify the situation: (a) All stars in both groups having polarization data are polarized; (b) Most of the discrepant stars are in the late B-star range, but several early B stars are also included; (c) The only apparent difference between the groups is that seven of the twelve stars showing large $\delta' \underline{m}_0$ indices lie below the main sequence ($\delta' \beta \leq -0.010$, where $\delta' \beta$ is found by comparing an observed β

to the mean Orion sequence for a given \underline{c}_0) while only one of seven stars in the small $\delta'm_0$ group is BMS, as can be seen in Figure 33, where we plot $\delta'\beta$ against $\delta'm_0$. We thus have some weak evidence that the BMS character of these stars may be coupled with \underline{m}_0 discrepancies.

Possible effects due to rotational velocity have been checked (Warren 1976, Fig. 5) and there appears to be no dependence of $\delta'm_0$ on axial rotation, in agreement with the results of Glaspey (1971a) for the Upper Scorpius region of the Scorpius-Centaurus association and of Crawford and Barnes (1974) for the A-type stars in the α Persei cluster.

Only the dependence of the \underline{m}_0 discrepancies on reddening, and the fact that many of the discrepant stars appear below the main sequence in the β, \underline{c}_0 diagram and are polarized, support a conclusion that large \underline{m}_0 discrepancies are attributable to blue continuum emission from these young Orion stars. Using the presently available data, it is difficult to see how this hypothesis can be tested. The δ' indices can only be found by using a parameter not affected by the continuum emission--we have no parameter since \underline{c}_0 is probably contaminated and very few MK types are available for these faint stars. One possible approach to this problem would be to use narrow-band colors in the red region of the spectrum, such as those used by Grasdalen et al. (1975) to detect blue continuum emission in members

of the Chamaeleon T association. These authors have found that the emission may extend out as far at 5500 \AA .

Another complication in the interpretation of BMS stars in the β , c_0 diagram is the possible presence of Balmer-line emission (cf. Paper II). For stars in NGC 2264, Strom, Strom and Yost (1971) have suggested an effect $\sim 0.1-0.2$ mag in c_0 due to blue continuum emission, while Smith (1972b) has suggested a change in $\beta \sim 0.03$ due to line emission for Orion stars. These effects very nearly cancel in the β , c_0 diagram, but must certainly complicate its interpretation and our calculation of δ' indices.

In conclusion, only the weak dependence of the m_0 discrepancies on $E(b-y)$ and the recognition that many of the discrepant stars appear below the main sequence and are polarized links the blue continuum emission process to these stars. Lacking MK spectral types for these faint stars and an index free of these effects, we do not see how the present data can be used to test further for the presence of blue continuum emission, and alternate approaches seem to be required.

ii) AF Stars

We have found an apparent dependence of the m_0 index on color excess for the B-type stars (see Fig. 32). This situation appears also for the I- and A-type stars in Figures 28, and the correlation is displayed in Figure 34.

As with the B-star relation, there is considerable scatter, but a correlation does seem to be present. It is in the same sense as for the B-type stars, i.e. higher reddening appears to correlate with higher \underline{m}_0 indices.

The occurrence of a blue continuum would seem not to be the cause of this effect since it would presumably brighten the \underline{V} magnitude and result in a decrease of \underline{m}_1 . On the other hand, a decrease in β , due possibly to Balmer-line emission, would cause \underline{m}_0 (standard, β) to decrease and would result in more negative $\delta\underline{m}_0$, hence the rather uniform weakening of the Balmer lines detected by Smith (1972a) for the stars in Orion lc could produce this \underline{m}_0 effect. Of course the dependence on color excess does not agree with this explanation unless the line emission depends on color excess also, a result which is contrary to Smith's findings and to our diagram for B-type stars (Fig. 22).

To investigate this problem further and to look for luminosity differences among the A and F stars, correlations among the indices $\delta\underline{m}_0$, $\delta\underline{c}_0$ and $\delta(\underline{u-b})_0$ have been examined. Crawford and Barnes (1970a) and Crawford (1975b) have found the $\delta\underline{m}_0$ index to be virtually free of luminosity effects, while the ultraviolet excess index $\delta(\underline{u-b})_0$ depends upon both luminosity and abundance differences. If this is the case, then $\delta(\underline{u-b})_0$ cannot be used to measure either parameter uniquely without first correcting for the effects of the

other. Since δm_0 measures only blanketing differences (except for the reddening problems encountered above) and δc_0 presumably measures only luminosity differences, $\delta(u-b)_0$ should correlate with both; δm_0 should not correlate with δc_0 .

Figures 35 show the relations among these indices. The solid line in diagram (a) is drawn with slope $\delta m_0 / \delta(u-b)_0 = 1/3$, the value found by Crawford and Barnes (1970a) for F-type stars in the open cluster NGC 752, thus indicating that the $(u-b)$ index is about three times as sensitive to abundance differences as is m_1 . Diagram (b) indicates little if any correlation between δm_0 and δc_0 , a result in agreement with that of Crawford (1975b). It should be noted, however, that two highly reddened stars (filled circles in lower right) showing large deviations in m_0 are located far above the ZAMS according to the δc_0 index. Diagram (c) shows the correlation between δc_0 and $\delta(u-b)_0$ and indicates a clear dependence of $(u-b)$ on luminosity differences. The line drawn has slope $\delta c_0 / \delta(u-b)_0 = -0.6$ and shows that $(u-b)$ is also more sensitive to luminosity differences than c_1 , by almost a factor of 2. The double dependence of $(u-b)$ makes its use unadvisable as an abundance or luminosity index for late-group stars, unless one is certain that one parameter or the other is constant.¹⁷

¹⁷Although we have encountered difficulties with the \underline{m}_0 index, it should be noted that the reddening effect cannot account for the seemingly high \underline{m}_0 envelope for the Orion 1c stars. A check of Smith's (1972a) and the present diagrams involving the metal index shows that the stars defining the apparent envelope are not highly reddened objects. A few of the stars in both diagrams are peculiar, however, and a more thorough study involving more stars of the intermediate and late groups in the Orion association would be worthwhile as a check on these results.

III. PROPERTIES OF THE ORION ASSOCIATION AND GALACTIC STRUCTURE IN THE ORION DIRECTION

In this section the subgroups of the Orion association are compared by combining some of the diagrams presented in the preceding section, for purposes of studying certain details of the photometric system employed and the Orion association itself. We then present several summary diagrams for all stars studied, in order to show an overall picture of the association in the color-magnitude diagram and with regard to Galactic structure in the Orion direction.

a) Comparison of Subgroups

i) The \underline{m}_0 Index

We begin our intercomparison of the subgroups by studying the detailed behavior of the \underline{m}_0 index, because systematic differences have been detected (cf. Figs. 1, 8, 17) between the subgroups in this index. Figure 36 shows the relation between \underline{m}_0 and $\underline{W}(\text{H}\gamma)$ for the same stars used in Paper II (Fig. 4) to demonstrate the good correlation between β and $\underline{W}(\text{H}\gamma)$. In spite of large scatter, a dependence of \underline{m}_0 on $\text{H}\delta$ line strength is apparent. The scatter cannot be attributed solely to reddening effects on \underline{m}_0 , nor can it be a result of plotting stars in different subgroups together. The rather uniform mixture of stars in the diagram indicates that the systematic differences between the a, b and c

subgroups in \underline{m}_1 is probably not attributable to systematic differences in the Balmer-line strengths alone.

The \underline{m}_0 , \underline{c}_0 diagrams for the a, b and c subgroups, Figure 37, are similar to the \underline{m}_0 , β relations shown earlier (cf. Figs. 1, 8, 17) implicating \underline{m}_0 rather than β or \underline{c}_0 as the source of subgroup differences detectable in these diagrams. Stars in the 1a subgroup adhere more closely to the field-star relation in Figure 37 than do the stars of the 1b and 1c groups, for which the field-star relation appears to define a lower envelope in \underline{m}_0 . As seen in the \underline{m}_0 , β diagrams, almost all heavily reddened stars lie along the top of the \underline{m}_0 sequence or deviate toward considerably larger \underline{m}_0 . The implications for a change in the slope $\underline{E}(\underline{m}_1)/\underline{E}(\underline{b-y})$, if the reddening corrections are at fault, have been discussed previously and this would seem not to be the case. Peculiarities in the properties of the continua of the reddened stars may then be causing these deviations, while the systematic differences between the sequences lead one to believe that age effects also play a role.

As mentioned earlier, the problem of systematic differences in the \underline{m}_0 index for two subgroups in the Scorpius-Centaurus association was discussed by Glaspey (1971a,b). To compare the situation in Sco-Cen with that in Orion, lists of B-type Sco-Cen subgroup members were compiled from Bertiau (1958), Garrison (1967), and Glaspey (1971a). These were reduced to intrinsic indices in the same way as

the Orion program stars after collecting uvby β photometry from Lindemann and Hauck (1973) and Glaspey, and UBV photometry from the catalogue of Mermilliod (1973) [with a few stars taken from Blanco et al. (1968)].¹⁸

¹⁸The intrinsic photometric indices have been compared with those of Glaspey, as a check on our reduction procedures, and the results are the same except that Glaspey's $(\underline{u}-\underline{b})_0$ values are somewhat smaller. This has been found to be due to his use of a slope $\underline{E}(\underline{u}-\underline{b})/\underline{E}(\underline{b}-\underline{y}) = 1.7$, rather than the slope 1.6 which results from our calculating $(\underline{u}-\underline{b})_0$ directly from the relation $\underline{c}_0 + 2\underline{m}_0 + 2(\underline{b}-\underline{y})_0$.

The \underline{m}_0 , \underline{c}_0 diagrams for the Centaurus and Upper Scorpius subgroups are shown in Figure 38, where we have again separated stars having color excesses considerably higher than the foreground mean. The different sequences in Sco-Cen appear essentially the same as for the Orion subgroups, the younger Upper Scorpius stars defining a noticeably higher locus in the \underline{m}_0 , \underline{c}_0 plane. The deviations from the mean relation for field stars do not appear as dependent upon color excess for the Upper Scorpius stars, however, and the very high \underline{m}_0 values seen in Figure 37(c) are not present here. Of course, the reddening in Upper Scorpius appears more uniform than in Orion 1c--only a few heavily reddened stars occur. The three most heavily reddened

stars are those with parentheses and, although the indices are uncertain, they do seem to display higher m_0 values. It seems likely that whatever is causing these systematic differences in the m_0 sequences among different subgroups is basically the same in the Orion and Sco-Cen associations.

The discussion by Glaspey (1971b), wherein he concludes that the systematic differences are not caused by errors in the photometry, reddening corrections, axial rotation, relative differences in H δ line strengths, or duplicity, is entirely appropriate to the situation in Orion. The only difference is that particular large discrepancies for Orion stars appear to be more dependent upon color excess than in Upper Scorpius. However, if Glaspey's conclusion that the systematic differences are due to spectral peculiarities of the type found by Garrison (1967) in Upper Scorpius stars is valid, then the situation in Orion indicates that these peculiarities are remarkably uniform in most stars of the lb and lc subgroups. Detailed spectral scans of selected stars in all three Orion subgroups and a close comparison between continuous energy distributions in the la and lb, c subgroups might resolve some of these puzzling photometric observations. Spectrophotometry of 60 stars in the association has recently been reported by Moreno (1974), but unfortunately only one star in the la subgroup was observed.

Another approach to examining the scatter in the \underline{m}_0 index is to use the \underline{c}_0 , $(\underline{u}-\underline{b})_0$ diagram. Since $(\underline{u}-\underline{b})_0$ is defined as $\underline{c}_0 + 2\underline{m}_0 + 2(\underline{b}-\underline{y})_0$, and since our \underline{c}_0 is determined from $(\underline{b}-\underline{y})$ only [as $-0.112 + 0.097(\underline{b}-\underline{y})_0$], any scatter in the \underline{c}_0 $(\underline{u}-\underline{b})_0$ relation is dependent only upon \underline{m}_0 .¹⁹ Figure 39 shows

¹⁹In other words, if one plots $(\underline{b}-\underline{y})_0$ against \underline{c}_0 , a perfect correlation is obtained because $(\underline{b}-\underline{y})_0$ is determined directly from \underline{c}_0 ; therefore, any scatter between \underline{c}_0 and $(\underline{u}-\underline{b})_0$ must be due to the \underline{m}_0 index. Of course, reddening effects are greater in the $(\underline{u}-\underline{b})_0$ index [$\underline{E}(\underline{u}-\underline{b})/\underline{E}(\underline{b}-\underline{y}) = 1.6$].

the relation between \underline{c}_0 and $(\underline{u}-\underline{b})_0$ for all B-type presumed members of the Orion association on the present program. The ZAMS relation appears to define the lower envelope for the Orion sequence, but the sequence turns away from the ZAMS at $(\underline{u}-\underline{b})_0 \sim 1.05$ ($\underline{c}_0 \sim 0.85$). Since this value corresponds to a $(\underline{b}-\underline{y})_0$ of -0.03 , the turn-up in the diagram is near to where the suspected lower main-sequence turn-up occurs for Orion 1c, leading one to suspect that this evolutionary turn-up is being detected in the \underline{m}_0 index. If this is the case, then the various sequences in diagrams involving \underline{m}_0 are indeed explainable by age differences.

However, uncertainties in the ZAMS relation for late B stars and/or a variable $\underline{E}(\underline{u}-\underline{b})/\underline{E}(\underline{b}-\underline{y})$ ratio could also be responsible. A partial check on the reliability of the ZAMS

relation may be made via a c_0 , $(u-b)_0$ diagram, Figure 40, for the reduced Sco-Cen data, in which the divergence for late B stars is also seen. A check of the relation derived by Warren (1976) for field stars shows that it too turns up slightly for the late B stars, hence the problem may be uncertainties in the ZAMS relation.

The other possibility mentioned above is an increase in the ratio $E(u-b)/E(b-y)$ as we go from early to later spectral types. The ratios used for the c_1 and $(b-y)$ indices in the present work (-0.20 and +0.30, respectively) yield a value of 1.60 for $(u-b)$. An observed ratio of 1.7 has been used previously for A- and F-type stars (Crawford 1970), while a recent study of O-type stars by Crawford (1975a) indicates a slope of 1.5. If this ratio does increase slightly through the B-type domain, then the trend for O stars to lie slightly below the line and for late B stars to move upward from the line, as is seen in the diagrams, would occur. These questions may be answered upon completion of the final calibration of the $uvby\beta$ systems for B-type stars now in preparation by Crawford.

Returning to Figure 39, we see that the distribution of reddened stars along the observed sequence is not uniform. Many more highly reddened objects occur among the later B stars, even though our observational program is complete for O and early B stars but may not be for heavily reddened late B stars because of their faintness. This distribution

is again suggestive of the picture presented earlier of a combination of intracluster and circumstellar reddening accounting for the color excesses in the association (mostly in the Sword region). If the reddening were entirely intracluster, one would expect a rather uniform distribution of reddened objects along the sequence. The clumping of reddened objects in the late B-star range as we approach the turn-up is probably a result of many of these stars still retaining their remnant dust shells as they approach or first arrive on the main sequence. [The distribution of reddened B-type stars will be displayed more clearly in the next section.]

ii) The β , c_0 Diagrams

Figures 41 show the β , c_0 relations for the 1a, 1b and 1c subgroups. These diagrams are the same as those presented earlier during the discussions for individual subgroups (Figs. 4, 11, 31) except that probable and possible non-members are now omitted.

Only a few differences can be seen among these diagrams. The relation for subgroup 1a indicates that stars near the top of the main sequence are slightly evolved and that members all along the sequence out to $c_0 \sim 0.7$ tend to lie slightly above the ZAMS rather than along or below it, as in subgroups 1b and 1c. Since we have found that this general effect is not attributable to axial rotation, the 1a stars presumably have generally greater ages.

Comparison of the lower end of the main sequence indicates that the turn-up does not occur for 1c in the photometric range of the B-type stars. If it occurs at $(\underline{B-V})_0 = -0.09$, as suggested by Walker's (1969) c-m diagram, it should be detectable in the β , \underline{c}_0 diagram, since the corresponding values of $(\underline{b-y})_0$ and \underline{c}_0 are approximately -0.06 and 0.6 , respectively. Although this discrepancy may be due to adverse effects on the β and \underline{c}_0 indices for stars above the turn-up, it seems unlikely that such effects would be so uniform. Another possibility is the previously discussed (Paper II) blueing of the $(\underline{B-V})$ indices for PMS stars that might cause the apparent turn-up to appear too blue in Walker's diagram. If the $(\underline{B-V})$ indices are too blue by only a few hundredths of a magnitude, the turn-up would not be seen in our diagrams, since the corresponding change in \underline{c}_0 is several tenths of a magnitude. This subject will be discussed again below when we examine the \underline{V}_0 , $(\underline{b-y})_0$ diagram for the whole association.

iii) The C-M Diagrams

In this section we present some summary diagrams displaying results obtained for the entire association. These diagrams are shown only to give an overall picture of the c-m diagram for the group, and the reddening and Galactic structure in the Orion direction, since detailed information about the association can only be obtained by treating the subgroups separately, as has been done in the preceding sections.

Although a large scatter due to distance spread has been demonstrated earlier for diagrams using \underline{V}_0 , this investigation would not be complete without illustrating the c-m diagram for all types of stars in the Orion association. This can only be accomplished by using the distant-dependent parameter \underline{V}_0 and the less sensitive effective temperature index $(\underline{b-y})_0$, since all other intrinsic indices change roles for stars belonging to different groups. The resulting c-m diagram is shown in Figure 42, where all stars having NM or NM? designations in the summary tables have been omitted. Several possible sources contribute to the scatter seen in the diagram for B-type stars. Comparison with similar diagrams presented earlier for individual subgroups shows that most of the scatter is due to a large distance spread among the subgroups. Additional, less pronounced, scatter is probably due to undetected and inadequately corrected binaries, uncertain reddening due to peculiarities in the photometric indices, and variability.

To continue the discussion of the lower main-sequence turn-up point begun in the last section, we see that the turn-up is not apparent in the B-star sequence of the \underline{V}_0 , $(\underline{b-y})_0$ diagram either, which ends at $(\underline{b-y})_0 \sim -0.02$ [$(\underline{B-V})_0 = -0.03$]. [In the inset we show the diagram for 1c and 1d only, since a turn-up is expected only in the region of the Orion Nebula.] All stars redder than this do lie above the ZAMS, however, indicating that the turn-up

lies at spectral type $\sim A0$, where we cross from the early to intermediate groups in the photometric analysis.²⁰

²⁰As we have seen earlier, peculiarities expected to be associated with the PMS stars are the same as those suspected of being responsible for discrepancies in the m_1 index. Since this index is the principal determinant of group membership, abnormally high values such as those found for many reddened and variable stars, would result in many B-type stars being classified as members of the I group. Adding to this problem is the fact that the m_1 index is used directly to determine intrinsic indices for I-group stars. This unfortunate characteristics of the $uvby\beta$ systems is quite detrimental to our study of the turn-up in Orion 1c, and is a principal reason for our attempt, mentioned in Paper II, to find an improved method for reducing the I-group stars (for details see Warren 1975).

On the other hand, the $V_0, (B-V)_0$ diagram (Walker 1969) shows a turn-up at $(\underline{B-V})_0 = -0.09$ [$(\underline{b-y})_0 = -0.06$]. This discrepancy could be partly due to uncertainties in the differential reddening corrections applied by Walker (individual reddening corrections were determined only on a differential basis for certain stars), or could be a result of blueing of the $(\underline{B-V})$ indices for stars near the

turn-up. Due to the position of the turn-up for Orion 1c, and to uncertainties in the photometric analysis in this range, the apparent difference between the $(\underline{B-V})_0$ and $(\underline{b-y})_0$ turn-ups can only be checked properly by considering a group whose turn-up is even earlier. An appropriate choice would be the extremely young cluster NGC 6611, for which Walker (1961) finds a pre-main-sequence turn-up at $(\underline{B-V})_0 = -0.17$. This is well into the B-type domain of the $\underline{uvby\beta}$ systems, where the photoelectric reduction procedure is more secure.

b) Reddening and Galactic Structure

i) Distribution of Reddened Stars

As an illustration of the distribution of reddened stars in the Orion association, Figure 43 shows histograms for B-type presumed members of the northern (1a and 1b) and southern (1c and 1d) regions. Only the B-type stars are considered here, because for these the sample should be reasonably complete. The distributions show a generally higher percentage of reddened stars along the entire B-star sequence in the Sword region, of course, but the significant difference between the regions is for stars fainter than $\underline{M_V} = -1$ mag. While the percentages of reddened stars in the range $-1 \rightarrow 0$ do not differ markedly, the lower graph shows that almost all B9-A0 ($0 \rightarrow +1$ mag) stars in the Sword region are reddened objects. If the reddening in the Sword region were mostly due to intracluster dust, we

would expect a generally higher percentage of reddened stars along the entire sequence, as we do find for stars brighter than -1 mag, but we would not expect the entire population of B-type stars fainter than $M_V = 0$ mag to consist of reddened objects. These distributions therefore suggest that as we approach the turn-up in the Sword region, many stars are reddened by local material, possibly because they still retain their remnant dust shells from the gravitational contraction phases of their evolution.

ii) Galactic Structure in the Orion Direction

This investigation, with its detailed information on distances and reddening in the direction of Orion OB 1 ($\langle l \rangle = 206^\circ$, $\langle b \rangle = -18^\circ$) adds one small piece to the larger puzzle of detailed structure in the so-called Orion Spiral Feature, at the inside of which our Sun is located. This feature was first delineated and described by Morgan, Sharpless and Osterbrock (1952) from their studies of spectroscopic parallaxes of H II regions in the anti-center direction.

A study of twenty-seven OB associations by Morgan, Whitford and Code (1953) revealed a bifurcation of the Local Arm at approximately $l = 100^\circ$, resulting in two apparent spurs which diverge from one another. The closer of these spurs descends to negative latitudes and contains the associations Lac OB 1, Per OB 2 (ζ Per group), and

Ori OB 1, while the more distant spur remains in the Galactic plane, curves away from the Sun, and includes such groups as Gem OB 1 and Mon OB 1. Beyond the ends of these spurs (Ori OB 1 and Mon OB 1), little is known. The apparent bending of the spurs, as outlined by their associations, suggests that they may converge toward one another again beyond $l = 210^\circ$. "Our" arm may virtually end beyond $l = 210^\circ$; or, if our Galaxy is indeed almost identical to the spiral NGC 1232 (Becker and Fenkart 1970), the Local Arm may extend all the way around to the opposite side of the Galactic center. Additionally, there is controversy over whether the Cygnus Arm connects through the Orion arm to Puppis-Vela or directly to the Carina Feature, thereby demoting Puppis-Vela and Orion to mere spurs rather than major spiral features (see Bok 1967; Becker and Fenkart 1970; and Bok, Hine and Miller 1970).

The end of the inner extension of the Orion Arm (or Spur) is shown quite well by the distribution in distance of stars on our program. This distribution is shown in Figure 48 for all B- and I-type stars. Since this diagram represents a projection onto the Galactic plane, it should be noted that the feature descends rather rapidly in Galactic latitude b , from -18° for the most concentrated part of subgroup 1a, to -21° for the southern portion of subgroup 1c. The general curvature in distance across the association can be seen clearly, a maximum mean distance being reached near

$l = 207^\circ - 209^\circ$, with a gentle curvature back toward the Sun being weakly indicated for higher longitudes.

The distribution of R associations, as depicted by Racine (1968), corresponds quite closely to that of OB associations. Some additional data are available for R associations beyond Orion OB 1, and these indicate that the inner spur may indeed curve upward and intersect the outer spur in the region of Mon OB 1, at a distance greater than 1 kpc. A wide gap between approximately 600 and 1200 pc still exists along the inner spur, however, hence it is impossible to shed further light on this problem at present (see Herbst 1975).

IV. AGES

a) Review of Previous Work

Age determinations for young clusters and associations are complicated by many factors (Larsson-Leander 1972, Stothers 1972, McNamara 1976) including large age spreads. One of our original goals in this study was to estimate ages for the Orion OB 1 subgroups by comparison of their distance-independent c-m diagrams for B-type stars [e.g. β , c_0 ; β , $(u-b)_0$] with theoretical isochrones such as those of Kelsall and Strömgren (1965), Iben (1966, 1967), and Stothers (1972). The above procedure was used by Glaspey (1971a) to estimate a nuclear age $\sim 12-16 \times 10^6$ years for the Upper Centaurus region of the Sco-Cen (Sco OB 2) association. As seen in Figures 41, the main sequences of the three Orion subgroups extend to the bluest stars with no evidence of a turnup.²¹ There is an indication of a turnoff for the la

²¹The definitions of turnup and turnoff used in the ensuing discussion are those of Stothers (1972).

subgroup, but its location is sufficiently uncertain that an age estimate cannot be reliably achieved. Consequently, we must seek alternate methods of estimating ages in Orion.

The kinematic age of subgroup la has been determined by Lesh (1968a) from proper motions derived as part of a larger study of expansion in the Gould Belt system (Lesh 1968b).

This expansion determination, which has been questioned by Steffey (1973) [see § IIa.i], yielded an age of 4.5×10^6 years \pm 30 percent (p.e.).

Stothers (1972) has estimated the age of subgroup 1a in two ways: (i) the observed spectral type of the main-sequence turnup, B0.5 Vnn (η Ori), compared to theoretical isochrones, yields 10×10^6 years; (ii) the blue and red post-main-sequence supergiants β and α Ori give 6.3×10^6 years and 7.9×10^6 years, respectively. These values must be considered uncertain because η Ori has a peculiar spectrum (it is classified nn with $\underline{v}_e \sin \underline{i} = 47 \text{ km s}^{-1}$, an obviously nearly pole-on case; see Lesh 1968a), and is a member of a multiple system; while α Ori is an uncertain member (Lesh 1968a, Schild 1970) and β Ori is not necessarily a member of 1a and was not included in the present program (it is far south of this subgroup).

Maeder (1972b) has used the intrinsic colors of the bluest stars in the 1a subgroup, corrected for rotational-velocity effects, to obtain a mean nuclear age of 6.2×10^6 years. He considers statistical effects due to varying numbers of stars near the top of the main sequence to be responsible for large overestimates of nuclear ages in clusters and associations. From studies of synthetic clusters based on Stothers' (1972) models, Maeder also finds that age estimates based on absolute magnitudes yield very uncertain values because of statistical fluctuations

and uncertainties in upper mass limits. He has therefore developed age estimates based on effective temperatures of stars near the evolutionary turnup, i.e. on the intrinsic colors of the hottest stars in a group. The resulting age estimates are found to give better agreement with kinematic methods. Maeder's technique will be discussed in more detail later in this section when we attempt to estimate ages for the Orion subgroups.

The relative ages of the subdivisions in subgroup 1b (Belt) have been discussed by Hardie, Heiser and Tolbert (1964), Crawford and Barnes (1966), and in § IIb. No significant differences appear to be present across the subgroup.

Blaauw (1961) estimated an age of $2.2-4.9 \times 10^6$ years for subgroup 1b from consideration of the origin of the runaway stars AE Aurigae, μ Columbae, and 53 Arietis. This estimate must be considered a lower limit if Blaauw's (1972) hypothesis of runaways originating from explosions in proto-stellar binary systems is correct.

Comparison of the c-m diagram for the Belt subsystem using the evolutionary calculations of von Hoerner (1957) resulted in an age estimate $\sim 5 \times 10^6$ years by Sharpless (1962), while Stothers (1972) obtained 5×10^6 years from the main-sequence turnup (09-09.5). The latter author did not use the supergiants in the Belt since they are not certain post-main-sequence objects.

Although many age estimates have been made for the Orion Nebula and its associated cluster, not much information is available for the more dispersed lc subgroup. Sharpless (1962) estimated an age $\sim 5 \times 10^5$ years from its c-m diagram, while Smith (1972a) estimates $2-3 \times 10^6$ years for its Am members. He also indicates an age spread²² $\sim 3 \times 10^6$ years

²²Evidence for the existence of large age spreads in young clusters has been accumulating at a rapid rate in recent years and it now seems fairly certain that star formation occurs over extended periods of time (see Iben 1972). Consequently, the discrepancies between nuclear and kinematic ages for young aggregates are to be expected, since the brightest stars in these groups may not have yet formed when expansion began or have not yet passed through their main-sequence lifetimes. On the other hand, one would naturally expect the expansion of a group to start during or before the formation of its brightest stars (Blaauw 1961, 1964; Stothers 1972) unless the fragmentation mechanism of van Albada (1968) is operative. In this case expansion would not occur until sometime after star formation begins, and fragmentation of a large group into smaller groups of multiple systems, such as the subclustering in Orion OB lc, would result in the onset of overall expansion.

for these stars (Smith 1972b).

In the Orion-Nebula region one must distinguish among the nebula itself, the Trapezium stars immersed within it, and the surrounding group known as the Trapezium or Orion-Nebula cluster, since their derived ages are different. From a relative proper-motion study of the Trapezium stars themselves Parenago (1953) derived an expansion age $\leq 10^4$ years. This value was later strengthened by studies of the gas dynamics of the nebula by Kahn and Menon (1961) and by Vandervoort (1964), which yielded ages $\sim 1-2 \times 10^4$ years.

An expansion age of 0.3×10^6 years was derived for the cluster by Strand (1958) from relative proper motions. Expansion was found by Parenago (1953, 1954) and by Strand, but the latter's results have been questioned by Vasilevskis (1962, 1971) as possibly due to changes in plate scale (see also van Altena and Monnier 1968 and Strand 1973); however, Cannell and Tanna (1974) have also found expansion, although it is a factor of 4 smaller than that derived by Strand. Fallon (1975) has recently determined new proper motions by the plate overlap method and has found weak evidence for contraction.

Allen, Poveda and Worley (1974) examined all visual observations of the Trapezium stars back to the early nineteenth century and found no evidence for expansion, except possibly for component E, even though the expansion determined by Parenago and by Strand should be detectable over this time scale. It has been found, however, that many of

the well-observed trapezia do have at least one component showing a significant transverse motion, indicating that many of these systems may be ejecting individual members occasionally.

Other age estimates for the Orion-Nebula cluster include those of: Johnson (1957), based upon the absence of main-sequence stars later than A0; Walker (1969), using his observed lower main-sequence turn-up of $(\underline{B}-\underline{V})_0 = -0.09$ and models of Iben (1965) and Ezer (1966), which yield 3×10^6 years; Maeder (1972b), using the method described earlier; and Penston et al. (1975) for individual members using \underline{V} and spectral types in conjunction with Iben's pre-main-sequence (PMS) models. The latter authors found an age spread from 2×10^5 years to 9×10^6 years, which they take as evidence for continuous star formation within the cluster.

The various age estimates for the Orion I subgroups are summarized in Table 2 for reference, along with a few determinations not discussed in detail above. Agreement among the results is seen to be rather poor, even when the same method is used by different workers. This is especially true for the older Ia and Ib subgroups and is probably a reflection of the difficulty in determining evolutionary turnup points in H-R diagrams, possibly as a result of the statistical uncertainties posited by Maeder (1972b).

Since turnoffs are not detectable in our β , c_0 diagrams for the Orion subgroups, we adopt the technique of Maeder (1972b) to make new age estimates for the 1b and 1c subgroups using the colors of their bluest stars. (Maeder has already done this for subgroups 1a and 1d.) These values can then be compared with the other estimates tabulated above.

Diagrams for correction of the observed color indices ($\underline{B-V}$) and ($\underline{B_2-V_1}$) of the Geneva photometric system have been presented by Maeder (1972a) and by Maeder and Peytremann (1970), respectively, based on theoretical models for uniformly rotating main-sequence stars presented in the latter paper. These corrections for rotation depend not only on $\underline{v_e} \sin \underline{i}$, but also on the mass of the particular star concerned--the corrections increase with decreasing mass.²³ In view of the

²³Individual corrections to the ($\underline{U-B}$)₀ indices of stars in Orion 1a and 1d were applied by Maeder (1972b) to obtain new age estimates based upon zero-rotation positions of their bluest main-sequence stars in the c-m diagram. However, all stars in these subgroups to which corrections were applied are earlier than spectral type B3, and have masses above $6M_{\odot}$. The models computed by Maeder and Peytremann, from which the correction diagrams were constructed, go up to only $5M_{\odot}$, hence it is unclear how Maeder applied corrections for the O-type stars which presumably have masses in excess of $15-20M_{\odot}$, or even for

stars as late as B3. Although the $(\underline{U}-\underline{B})_0$ changes of Maeder and Peytremann agree well with those of Hardorp and Strittmatter (1968a), even the latter authors' models go only to $8.1M_{\odot}$, equivalent to a main-sequence spectral type $\sim B1$.

unavailability of rotating models for more massive stars and of present uncertainties in masses for upper main-sequence stars (see Stothers 1972), it has been decided not to attempt correction of our intrinsic color indices for rotation, and thence not to derive corrected age estimates representative of our photometric data. We do wish, however, to find mean intrinsic indices for the bluest stars in the Orion subgroups, so that when models do become available, corrections can be applied to these indices to find rotation-corrected ages. It is also of interest to find preliminary age estimates (uncorrected for rotation) in order to compare these with both Maeder's corrected values and those of previous workers.

Following Maeder (1972b), we present in Table 3, intrinsic color indices for the bluest presumed-member stars in each subgroup of the Orion association, as derived in the present work. The final three columns give the values of $(\underline{U}-\underline{B})_0$ for the bluest star in each subgroup and the mean values for the three bluest and five bluest, respectively. Based on the rotational velocities given in column 5, age corrections due to rotational-velocity effects should be small or negligible for most subgroups, with the possible exception of Ia.²⁴

²⁴A comparison of the mean $(\underline{U-B})_0$ values for subgroup 1a with those of Maeder shows that the rotation corrections amount to several hundredths of a magnitude, hence our age value for this subgroup is almost certainly an overestimate. It appears that Maeder did not use θ^1 Ori A in his analysis of the 1d subgroup.

The decrease in age from subgroups 1a to 1d can easily be seen in Table 3 by the decrease in both the $(\underline{U-B})_0$ values for the bluest stars and for the means. If we use these values (uncorrected for rotation) in the diagrams of $(\underline{U-B})_0$, $\log(\text{age})$ presented by Maeder (1972b), the ages presented in Table 4 are obtained. The quantities N refer to the numbers of stars earlier than spectral type B3 [$(\underline{U-B})_0 < -0.70$; $(\underline{u-b})_0 < 0.30$]; the columns labeled 1, 2, 3 refer to the means determined from the bluest, three bluest, and five bluest stars, respectively.

Finally, the Orion 1b subgroup has often been compared to the Upper Scorpius complex of young stars with regard to age (Hardie, Heiser and Tolbert 1964; Crawford and Barnes 1966). Since the age of 20×10^6 years derived by Bertiau (1958) applied to an admixture of stars from all subgroups of the Scorpius-Centaurus association, Maeder and Martinet (unpublished) applied FK4 proper motions with precessional corrections to obtain a new expansion age of 4.7×10^6 years. The three age estimates from the bluest main-sequence

stars (Maeder 1972b) are 3.7, 4.1, and 5.2×10^6 years (mean 4.3×10^6 years), and compare very closely with our values in Table 4 for the Belt region of Orion 1. Considering the small corrections for rotation which are possibly needed, the 1b subgroup may be slightly younger than Upper Scorpius, but the results confirm that there is ample justification for considering the two regions to be comparable in age.

V. SUMMARY AND FUTURE WORK

This final section presents a summary of the principal results obtained from this investigation (including Papers I and II) and outlines some ideas and suggestions for future work designed to resolve some of the unanswered questions and difficulties encountered during the present study.

a) Summary of Results

This investigation provides a large collection of uniform photometric data on the standard uvby β systems for stars in the main body of the Orion OB 1 association. The program should be reasonably complete for B-type stars, but the visual-magnitude limits have excluded most of the later types, particularly in the northern part of the association. In Paper I complete compilations of UBV photometry and spectral types on the MK system have also been presented for comparison with the new data and to help in their interpretation. A cross-identification table, including coordinates and chart identifications, has been provided for the 526 stars on the program as a guide to future work in the region. A complete membership table has been compiled for the program stars (see Paper I) by evaluating proper-motion data qualitatively and by considering radial velocities and distance-modulus criteria. In Appendix Tables 5-11 of this paper we summarize the reduced photometry, color excesses, and absolute visual magnitudes for the program stars.

In Paper II the absolute visual magnitudes $\underline{M}_V(\beta)$ derived for B-type stars in the present work are found to be systematically brighter than those obtained from the $\underline{W}(\text{H}\gamma)$ calibration of Balona and Crampton (1974). For the Orion-Nebula stars, both calibrations yield systematically brighter absolute magnitudes with respect to MK types due to the degrading effects of line and possibly continuum emission on both indices. These effects are larger for the β index, however. For stars outside the nebula, comparison of the derived absolute magnitudes with those given by MK spectral types reveals that $\underline{M}_V(\beta)$ values show somewhat better agreement in most cases where $\underline{M}_V(\gamma)$ is significantly fainter than $\underline{M}_V(\beta)$. This result also holds for the MK calibration of Balona and Crampton (1974). The β , $\underline{M}_V(\beta)$ calibration used in the present work appears more appropriate for young stars near the ZAMS than does the two-dimensional β , $\underline{M}_V([\underline{u}-\underline{b}], \beta)$ calibration of Eggen (1974). This is probably due to the inclusion of older aggregates and wide binary systems in the latter's calibration data.

A new calibration of intrinsic $\underline{uvby}\beta$ indices for main-sequence B-type stars in terms of MK spectral types, mostly on the new \dagger system (Morgan and Keenan 1973), has been derived (Warren 1976). As expected, considerable overlap occurs in β among the MK types. Excellent agreement between the \underline{c}_0 values of the present calibration and those of Crawford (1973) for MK types earlier than B7 is found. The

break at spectral type B4 found by Balona and Crampton (1974) in their $\underline{W}(\text{Hy})$, MK-type calibration is clearly seen in the present photometric calibration.

The photometric indices of the $\underline{uvby\beta}$ systems appear affected by axial rotation. The reasonably good agreement with the $(\underline{v}_e \sin \underline{i})^2$ dependence predicted by Hardorp and Strittmatter (1968a,b) means that the effects do not become significant until velocities above 250-300 km s⁻¹ are reached. Probable rotational-velocity effects on MK spectral classification of late B stars, as suggested by the theoretical studies of Collins (1974), are also indicated by an analysis of the photometry (Warren 1976).

For the intermediate-group stars (\sim A0-A3), an attempt (Warren 1975 and Paper II) has been made to eliminate the use of the $[\underline{m}_1]$ index in calculating intrinsic colors and reddening, by employing both an iterative procedure similar to that used for the early group and the \underline{k} index of Henry (1969). The iterative technique has not been successful and the \underline{k} -index method gives little improvement over Strömgren's $[\underline{m}_1]$ relation, mostly because of variations in \underline{k} caused by abundance differences from star to star. The use of \underline{dk} improves the accuracy significantly, but the calculation of this displacement index requires that intrinsic colors be known. An iterative procedure may be successful in this respect but has not been attempted for the present program.

The β , c_0 diagram for subgroup 1a (Fig. 4) does not show the spread in age suggested by Steffey (1973), nor does a systematic distance increase with right ascension appear for this group when all presumed members are considered; such a trend may appear for the brighter stars studied by Lesh (1968a), however, thus indicating the need for a detailed proper-motion study to fainter magnitude limits to retest for expansion. A trend toward indreasing distance with declination is seen in Figure 7, which suggests a possible bridge of early-type stars between subgroup 1a and the λ Orionis clustering located at $\delta = +10^\circ$. At the present time there is no direct evidence to indicate the non-existence of the 1a subgroup, however. Although the reddening in subgroup 1a is small and uniform in most areas, regions of higher absorption occur within the subgroup (cf. Fig. 5).

A systematic distance increase across subgroup 1b (Belt region) is found in the present study, in agreement with the earlier results of Hardie, Heiser and Tolbert (1964) and Crawford and Barnes (1966). These distance determinations may be affected by stars of the more dispersed 1a subgroup being superimposed in front of and behind the 1b subgroup, as suggested by Lesh (1968a).

The reddening law for the 1b subgroup is indicated by Figures 13 and 14 to be normal, except possibly for stars deeply embedded in nebulosity, e.g. HD 37903 (NGC 2023); consequently, a normal value of $\underline{R}(\underline{b-y}) = 4.3 [= \underline{R}(\underline{B-V}) = 3.0]$ has been used in the present work.²⁵

²⁵The change in \underline{R} will not alter the mean distances presented in Table 1 significantly because few of the stars used are reddened objects; distances to individual reddened stars will of course be decreased, the change amounting to 0.2 mag in distance modulus for a star having $\underline{E}(\underline{b-y}) = 0.5$.

The small sub-clusterings in the vicinity of the Orion Nebula (subdivisions c1-c4), previously studied by Morgan and Lodén (1966) and by Walker (1969), are found in the present study (see Fig. 18) not to differ in evolutionary state after appropriate duplicity corrections have been applied; this is in agreement with Walker's analysis. The entire "outer Sword" region has therefore been treated as a single group in subsequent analyses.

Discrepancies in the \underline{m}_0 index similar to those detected in Upper Scorpius stars by Glaspey (1971a,b) have been found for the young stars in the Orion-Nebula region (subgroup 1c). These discrepancies are found to depend weakly upon color excess $\underline{E}(\underline{b-y})$, but the scatter is very large. No clear explanation has been found for these anomalies, but they appear to be coupled with the BMS character of these stars, and all discrepant stars are polarized. The discrepancies do not appear to be coupled with the β index (Fig. 33) and no dependence on rotational velocity is found.

Effects on the β and c_0 photometric indices for stars within the Orion Nebula are caused by Balmer lines and continuum emission, respectively, but these effects do not account completely for the appearance of many of these stars below the main sequence. The scatter in positions of the polarized stars suggests a possible circumstellar shell interpretation, but the effects of uniformly high R and subluminality cannot be separated with the present data.

In the intermediate-group range ($\sim A0-A3$), several stars in the nebula region are found to be good candidates for PMS objects (Fig. 26). The A- and F-type stars near the nebula fall rather uniformly along a sequence which is displaced upward from the ZAMS by about 0.09 mag in δc_0 for the A stars and 0.12 mag for the F stars (Fig. 30). This mean is not very significant for the A stars since the observed sequence converges toward the ZAMS for earlier types until meeting it near A0; for the F-star sequence, which runs roughly parallel to the ZAMS, the mean displacement in δc_0 corresponds to 1.3 mag.

A comparison of the preliminary calibration for determining reddening and intrinsic indices for F-type stars (Crawford 1970) with results from the recently completed final calibration (Crawford 1975b) shows a mean difference of 0.022 ± 0.008 (one star, 17 stars used), in the sense that the new calibration produces smaller values of $E(b-y)$. This systematic difference is not attributable to the peculiar

Orion lc stars since many of the objects used are non-member field stars. The results obtained from the newer calibration have been retained in the analysis, however, since the difference is not large and may serve as initial checks on the accuracy of the new calibration relations.

The F-type presumed members of Orion lc show an average displacement of 0.021 ± 0.007 (one star) in δm_0 from the standard Hyades relation (Fig. 28). This value checks closely with that for the Coma cluster derived by Crawford and Barnes (1969) [$\langle \delta m_1 \rangle = 0.014$] and with the value of 0.018 implied for the Sun by the analysis of Crawford (1975b) thus indicating that if the $\langle \delta m_0 \rangle$ value above is really representative of metal-line blanketing in these young Orion stars, then they have metal abundances similar to F- and G-type dwarfs in the solar neighborhood.

Correlation diagrams among the δm_0 , δc_0 , and $\delta(u-b)_0$ indices for A and F stars show that $\delta(u-b)_0$ is approximately three times more sensitive to abundance differences than is δm_0 and almost twice as sensitive to luminosity differences than is δc_0 . These results are in agreement with those found by Crawford and Barnes (1970a) for NGC 752. No correlation is found between δm_0 and δc_0 , however, showing that the m_1 index is virtually free of luminosity effects, as suggested by Crawford (1975b).

Stars of spectral class A in Orion lc appear to define a slightly higher upper envelope in the m_0 index, in

agreement with earlier results of Smith (1972a) using Strömgren's $[m_1]$ index (see Fig. 28b). This effect is not attributable to the apparent reddening effect on the m_0 indices since most of these stars are unreddened. A few of these stars are peculiar, however, and a more thorough study utilizing additional I- and A-group stars in the nebula region is necessary in order to confirm this effect. The c-m diagrams for A- and F-type stars in subgroup lc (Figs. 29, 30) support the contention of Smith (1972a) that the Am stars found by him are members of the Orion association (see also Hesser, McClintock and Henry 1977).

A clear gap in the F-star sequence for Orion lc is found in the range $0.21 \leq (b-y)_0 \leq 0.26$ [$0.30 \leq (B-V)_0 \leq 0.37$; $F0-F4$; $3.1 \leq M_V(\beta) \leq 3.5$]. This color range is redward of the field-star and most cluster gaps, but is similar to that of the Hyades cluster (cf. Böhm-Vitense and Canterna 1974).

A close comparison of subgroup sequences for B-type stars in the m_0, c_0 diagram (Fig. 37) reveals uniformly higher upper envelopes for the lb and lc stars. Although many large discrepancies appear coupled with reddening effects, the uniformly higher sequences suggest that the cause resides in some property of the continuum rather than in line absorption.

A similar comparison of the β, c_0 c-m-type diagrams for B-type stars in subgroups la, b, c shows that stars in la

tend to lie higher in the main-sequence band, apparently because of their generally greater ages. No apparent lower main-sequence turn-up toward the contraction stage is apparent in the B-star sequence for subgroup 1c. If the turn-up actually occurs at $(\underline{B-V})_0 = -0.09$, as implied by Walker's (1969) \underline{V} , $(\underline{B-V})$ diagram, then one would expect to see it in Figure 41. A blueing of the $(\underline{B-V})$ indices of only a few hundredths of a magnitude due to blue continuum emission could be causing this discrepancy, or it may be due to combined emission effects on the β and \underline{c}_0 indices.

An examination of the distributions of reddened B stars in the northern and southern sections of the association (Fig. 43) suggests that late B stars near the PMS turn-up retain their remnant dust shells from the contraction phase. This is indicated because almost all B-type stars in the 1c and 1d subgroups having $\underline{M}_V > 0$ mag are reddened objects, while this is not the case for late B stars in subgroups 1a and 1b or earlier B stars in either section.

Previous age determinations for the various subgroups of the Orion OB 1 association are summarized in Table 2. New age estimates based upon the bluest main-sequence stars in each subgroup (Table 3), are provided in Table 4 for subgroups 1b and 1c. Unlike Maeder's (1972b) estimates for 1a and 1d, we have not attempted to correct for the effects of axial rotation on the color indices due to the lack of rotating models for upper-main-sequence stars, hence the

values given in Table 4 are probably overestimates. The results for 1b and 1c should not be seriously affected, however, since Table 3 shows that the bluest stars in these subgroups do not display extremely high projected rotational velocities.

b) Future Work

During the course of this study, many areas have been encountered in which additional work is needed. These areas lie both in the general interpretation and analysis of uvby β photometry, as treated in Paper II and by Warren (1975), and in specific interpretation of the results obtained for the Orion OB 1 association, as attempted in this paper. In order to encourage further investigations of the Orion region, we briefly outline some of the latter areas below:

1. Good quality proper-motion data for late B- and A-type stars in subgroups a, b, and c would be useful for re-examining the question of expansion in subgroup a (see § IIa.iv) and to investigate possible expansion in the southern regions of the association, particularly with regard to the spherical 1c subgroup surrounding the Orion-Nebula cluster.

2. A photometric study of late B and A-F stars in the northern parts of the association may reveal lower main-sequence turn-up points to provide checks on the derived ages from evolutionary turnoffs, supergiants, and bluest stars.

0-2

3. In connection with supergiants in the 1a subgroup, Stothers (1972) has assumed membership of the B8 Ia star β Orionis in this subgroup to estimate its age. This star and its associated group of lower luminosity B-type stars are located far south of the 1a subgroup. No detailed study of this group has been made as yet and a photometric and/or spectroscopic study of its individual members is needed in order to place it within the overall picture of the association. Such a study would also be useful for the λ Orionis clustering located to the north of subgroup 1a, in order to investigate a possible smooth bridge of B-type stars which may connect the two groups.

4. Several types of \underline{m}_0 discrepancies exist for Orion association stars. For the B-type stars we have found apparently systematic differences among the observed sequences for the subgroups, e.g. the \underline{m}_0 envelopes for stars in the 1b and 1c subgroups are significantly greater than that for the 1a stars (Fig. 37). These differences may be caused by line absorption from numerous weak features in the $\lambda 4100\text{-}\overset{\circ}{\text{A}}$ region, in which case high resolution spectroscopy would be needed to study and compare the spectra. On the other hand, if these differences reside in the continuous energy distributions, it should be possible to detect them via accurate photoelectric spectrophotometric observations.

In addition, anomalously high m_0 values, which appear to be connected with reddening, are found for individual stars in all subgroups. These discrepancies do not appear to be a result of inadequate reddening corrections and may be due to continuous and/or line emission mechanisms, as suggested by the fact that all discrepant stars are polarized and many lie below the main sequence in various photometric diagrams.

5. Additional work on the late B-, A-, and F-type members of the southern part of the association may clarify the problem of blue continuum emission. One possible approach would involve narrow-band colors in the red region of the spectrum (as used by Grasdalen *et al.* 1975). The question of high R values and the existence of circumstellar shells around pre-main-sequence stars in the nebula region may be partly resolved through an analysis of multicolor polarization data such as those of Serkowski *et al.* (1975); however, the validity of their relation between the wavelength of maximum polarization and R must first be tested for stars suffering circumstellar and/or intracluster reddening, since their expression was derived for the interstellar case and different grain sizes may result in a change of their constant of proportionality.

6. Further observational work in the infrared is also necessary for interpretation of R values and circumstellar and/or intracluster dust absorption in the nebula region.

Data in the visual and near-infrared show that energy budgets are not balanced for many stars, i.e. more radiation is absorbed at optical wavelengths than is emitted in the near-infrared (Penston 1973). If R values are increased then these discrepancies also increase since more radiation must be absorbed in the visible region. Additional observations out to 20 μ and analysis of energy budgets may resolve this problem. Infrared observations are also important in regions just outside the nebular boundaries and to somewhat fainter magnitudes, because most of the ultraviolet excess stars found by Walker (1969, 1972) fall into this category and ultraviolet excess may be related to infrared excess.

Many of the unusual properties encountered for late B-, A-, and F-type stars in Orion may also be present for similar stars in other young clusters and associations. Detailed studies to fainter magnitude limits in the northern part of Orion OB 1, in the Sco-Cen association, and in young clusters such as NGC 2264, NGC 6611, and NGC 2362 should be undertaken.

ACKNOWLEDGMENTS

The authors wish to thank D. L. Crawford for sharing preliminary analyses of the B-star calibration data and for supplying the calibration for F-type stars prior to publication.

J.E.H. gratefully acknowledges the warm hospitality extended to him by D. E. Osterbrock and his colleagues at Lick Observatory during preparation of this paper.

W.H.W. expresses appreciation to Indiana University's Marshal H. Wrubel Computing Center for generous allotments of computer time. He is also indebted to the faculty of the Indiana University department of astronomy, and to Mr. and Mrs. W. H. Warren, Mr. and Mrs. J. R. Wills, Dr. J. M. Mead, and M. H. Warren for support during the course of this investigation. Assistance was provided by D. Owings, K. Robertson, L. Spencer, and M. H. Warren in proofreading the data tables.

The authors are grateful to M. H. Warren for her typing and assistance during the preparation of the manuscript.

REFERENCES

- Abt, H. A., Muncaster, G. W., and Thompson, L. A. 1970, A.J., 75, 1095.
- Aikman, G. C. L., and Goldberg, B. A. 1970, J. Roy. Astr. Soc. Canada, 68, 205.
- Aizenman, M. L., Demarque, P., and Miller, R. H. 1969, Ap.J., 155, 973.
- Allen, C., Poveda, A., and Worley, C. E. 1970, Rev. Mexicana Astr. and Ap., 1, 101.
- Andrews, P. J. 1968, Mem. R.A.S., 72, 35.
- Balona, L., and Crampton, D. 1974, M.N.R.A.S., 166, 203.
- Barry, D. C. 1970, Ap.J. Suppl., 19, 281.
- Batten, A. H. 1967, Pub. Dom. Ap. Obs. (Victoria), 13, 119.
- Becker, W., and Fenkart, R. 1970, in IAU Symposium No. 38, The Spiral Structure of Our Galaxy, ed. W. Becker and G. Contopoulos (Dordrecht: Reidel), p. 205.
- Bernacca, P. L. 1967, Contrib. Oss. Astrofis. Asiago, No. 195.
- _____. 1968, Contrib. Oss. Astrofis. Asiago, No. 202.
- Bernacca, P. L., and Ciatti, F. 1972, Astr. and Ap., 19, 482.
- Bernacca, P. L., and Molnar, M. R. 1972, Ap.J., 178, 189.
- Bertiau, F. C. 1958, Ap.J., 128, 533.
- Blaauw, A. 1956, Ap.J., 123, 408.
- _____. 1958, A.J., 63, 186.
- _____. 1961, Bull. Astr. Inst. Neth., 15, 265.
- _____. 1964, Ann. Rev. Astr. and Ap., 2, 236.
- _____. 1972, in IAU Colloquium No. 17, Stellar Ages, ed G. Cayrel de Strobel and A. M. Delplace (Meudon: Observatoire de Paris), Sec. XXII.

- Blanco, V. M., Demers, S., Douglass, G. G., and FitzGerald, M. P. 1968, Pub. U.S. Naval Obs., 2nd Ser., XXI.
- Böhm-Vitense, E., and Canterna, R. 1974, Ap.J., 194, 629.
- Bok, B. J. 1967, Am. Scientist, 55, 375.
- Bok, B. J., Hine, A. A., and Miller, E. W. 1970, in IAU Symposium No. 38, The Spiral Structure of Our Galaxy, ed. W. Becker and G. Contopoulos (Dordrecht: Reidel), p. 246.
- Breger, M. 1976, Ap.J., 204, 789.
- Brun, A. 1935, Pub. Obs. Lyon, 1, No. 12.
- Cameron, R. C. 1967, Georgetown Obs. Monograph No. 21.
- Cannell, W. D., and Ianna, P. A. 1974, Bull. AAS, 6, 439.
- Carruthers, G. R. 1969, Ap.J. (Letters), 157, L113.
- Ciatti, F., and Bernacca, P. L. 1971, Astr. and Ap., 11, 485.
- Collins, G. W. II 1974, Ap.J., 191, 157.
- Conti, P. A., and Alschuler, W. R. 1971, Ap.J., 170, 325.
- Crampton, D., and Byl, J. 1971, Pub. Dom. Ap. Obs. (Victoria), 13, 427.
- Crawford, D. L. 1958, Ap.J., 128, 185.
- _____. 1970, Stellar Rotation, ed. A. Slettebak (Dordrecht: Reidel), p. 93.
- _____. 1973, in IAU Symposium No. 54, Problems of Calibration of Absolute Magnitudes and Temperatures of Stars, ed. B. Hauck and B. E. Westerlund (Dordrecht: Reidel), p. 93.
- _____. 1975a, Pub. A.S.P., 87, 481.
- _____. 1975b, A.J., 80, 955.
- Crawford, D. L., and Barnes, J. V. 1966, A.J., 71, 610.
- _____. 1969, A.J., 74, 407.
- _____. 1970a, A.J., 75, 946.
- _____. 1970b, A.J., 75, 952.

- _____. 1974, A.J., 79, 687.
- Crawford, D. L., and Perry, C. L. 1966, A.J., 71, 206.
- Crawford, D. L., Barnes, J. V., and Perry, C. L. 1975, Pub. A.S.P., 87, 115.
- Duerbeck, H. W. 1975, Astr. and Ap. Suppl., 22, 19.
- Eggen, O. J. 1974, Ap.J., 188, 59.
- Ezer, D. 1966, Colloquium on Late-Type Stars, ed. M. Hack (Osservatorio Astronomico de Trieste), p. 357.
- Fallon, F. W. 1975, thesis, University of Florida.
- Faj, T., Honeycutt, R. K., and Warren, W. H. Jr. 1973, A.J., 78, 246.
- Garrison, R. F. 1967, Ap.J., 147, 1003.
- _____. 1973, in IAU Symposium No. 50, Spectral Classification and Multicolour Photometry, ed. Ch. Fehrenbach and B. E. Westerlund (Dordrecht: Reidel), p. 13.
- Glaspey, J. W. 1971a, thesis, University of Arizona.
- _____. 1971b, A.J., 76, 1041.
- Grasdalen, G., Joyce, R., Knacke, R. F., Strom, S. E., and Strom, K. M. 1975, A.J., 80, 117.
- Greenstein, J. L., and Wallerstein, G. 1958, Ap.J., 127, 237.
- Guetter, H. H. 1976, A.J., 81, 537.
- Hack, M. 1969, Ap. and Space Sci., 5, 403.
- Hall, D. S., and Garrison, L. M. Jr. 1969, Pub. A.S.P., 81, 771.
- Hallam, K. L. 1959, thesis, University of Wisconsin-Madison.
- Hardie, R. H., and Crawford, D. L. 1961, Ap.J., 133, 843.
- Hardie, R. H., Heiser, A. M., and Tolbert, C. R. 1964, Ap.J., 140, 1472.
- Hardorp, J., and Strittmatter, P. A. 1968a, Ap.J., 151, 1057.
- _____. 1968b, Ap.J., 153, 465.

- Hartwick, F. D. A., and Hesser, J. E. 1974, Ap.J., 192, 391.
- Hartwick, F. D. A., Hesser, J. E., and McClure, R. D. 1972, Ap.J., 174, 557.
- Heintz, W. D. 1974, A.J., 79, 397.
- Henry, R. C. 1969, Ap.J. Suppl., 18, 47.
- Henry, R. C., and Hesser, J. E. 1971, Ap.J. Suppl., 23, 421.
- Herbst, W. 1975, A.J., 80, 503.
- Hesser, J. E., and Henry, R. C. 1971, Ap.J. Suppl., 23, 453.
- Hesser, J. E., McClintock, W., and Henry, R. C. 1977, Ap.J., 213, 100.
- Hesser, J. E., Moreno, H., and Ugarte P, P. 1977, Ap.J., in press.
- Hesser, J. E., Walborn, N. R., and Ugarte P, P. 1976, Nature, 262, 116.
- Higgenbotham, N. A., and Lee, P. 1974, Astr. and Ap., 33, 277.
- Holden, F. 1972, Publ. Obs. Univ. Michigan, 12, 1.
- Hunger, K. 1974, Astr. and Ap., 32, 449.
- Iben, I. Jr. 1965, Ap.J., 141, 993.
- _____. 1966, Ap.J., 143, 483, 505, 516.
- _____. 1967, Ap.J., 147, 624, 650.
- _____. 1972, in IAU Colloquium No. 17, Stellar Ages, ed. G. Cayrel de Strobel and A. M. Delplace (Meudon: Observatoire de Paris), Sec. XI.
- Jaschek, C., Ferrer, L., and Jaschek, M. 1971, Catalogue and Bibliography of B-type Emission Stars, Obs. Astron. U. Nacional La Plata, Ser. Astron., Vol. 37.
- Jeffers, H. M., Bos, W. H. van den, and Greeby, F. M. 1963, Pub. Lick Obs., Vol. 21.
- Johnson, H. L. 1957, Ap.J., 126, 134.
- _____. 1963, Basic Astronomical Data, ed. K. Aa. Strand (Chicago: U. Chicago Press), p. 204.

- _____. 1967, Ap.J. (Letters), 150, L39.
- _____. 1968, in Nebulae and Interstellar Matter, ed. B. M. Middlehurst and L. H. Aller (Chicago: U. Chicago Press), p. 167.
- Johnson, H. L., and Borgman, J. 1963, Bull. Astr. Inst. Neth., 17, 115.
- Johnson, H. L., and Morgan, W. W. 1953, Ap.J., 117, 313.
- Johnson, H. M. 1965, Ap.J., 142, 964.
- Kahn, F. D., and Menon, T. K. 1961, Proc. Nat. Acad. Sci., 47, 1712.
- Kaufmann, J. P., and Hunger, K. 1972, Mitt. der Astr. Gesellschaft, Nr. 31, 185.
- Kelsall, T., and Strömberg, B. 1965, Vistas Astr., 8, 159.
- Kemp, J. C., and Herman, L. C. 1977, Ap.J., in press.
- Klinglesmith, D. A., Hunger, K., Bless, R. C., and Millis, R. L. 1970, Ap.J., 159, 513.
- Kukarkin, B. V., Kholopov, P. N., Pskovsky, Yu. P., Efremov, Yu. N., Kukarkina, N. P., Kurochkin, N. E., Medvedeva, G. I., Perova, N. B., Fedorovich, V. P., and Frolov, M. S. 1971, General Catalogue of Variable Stars, 3rd edition (Moscow: Publishing House of the Academy of Sciences of the U.S.S.R.).
- Larsson-Leander, G. 1972, in IAU Colloquium No. 17, Stellar Ages, ed. G. Cayrel de Strobel and A. M. Delplace (Meudon: Observatoire de Paris), Sec. II.
- Lee, T. A. 1968, Ap.J., 152, 913.
- Lesh, J. R. 1968a, Ap.J., 152, 905.
- _____. 1968b, Ap.J. Suppl., 17, 371.
- Lester, J. B. 1972, Ap.J., 178, 743.
- Lindemann, E., and Hauck, B. 1973, Astr. and Ap. Suppl., 11, 119.
- Maeder, A. 1972a, in IAU Colloquium No. 17, Stellar Ages, ed. G. Cayrel de Strobel and A. M. Delplace (Meudon: Observatoire de Paris), Sec. VII.

- _____. 1972b, in IAU Colloquium No. 17, Stellar Ages, ed. G. Cayrel de Strobel and A. M. Delpierre (Meudon: Observatoire de Paris), Sec. XXIV.
- Maeder, A., and Peytremann, E. 1970, Astr. and Ap., 7, 120.
- McAlister, H. A. 1976, Pub. A.S.P., 88, 957.
- McNamara, B. J. 1976, A.J., 81, 845.
- Meisel, D. D. 1968, A.J., 73, 350.
- Méndez, M. E. 1967, Bol. Obs. Tonantzintla y Tacubaya, 4, 91.
- Mermilliod, J.-Cl. 1973, Centre de Données Stellaires, Inform. Bull. No. 4, p. 20.
- Molnar, M. R. 1972, Ap.J., 175, 453.
- Moreno, H. 1974, Publ. Dep. Astr. Univ. Chile, 2, 143.
- Morgan, W. W. 1956, A.J., 61, 358.
- _____. 1958, Trans. I.A.U., 10, 576.
- Morgan, W. W., and Keenan, P. C. 1973, Ann. Rev. Astr. and Ap., 11, 29.
- Morgan, W. W., and Lodén, K. 1966, Vistas Astr., 8, 83.
- Morgan, W. W., Sharpless, S., and Osterbrock, D. 1952, A.J., 57, 3.
- Morgan, W. W., Whitford, A. E., and Code, A. D. 1953, Ap.J., 118, 318.
- Murphy, R. E. 1969, A.J., 74, 1082.
- Nissen, P. E. 1976, Astr. and Ap., 50, 343.
- Norris, J. 1971, Ap. J. Suppl., 23, 213.
- Odell, A. P. 1974, Ap.J., 194, 645.
- Parenago, P. P. 1953, Astr. J.U.S.S.R., 30, 249 (English Transl. Astr. Newsletter, No. 74, 20).
- _____. 1954, Trudy Sternberg Astr. Inst., Vol. 25.

- Penston, M. V. 1973, Ap.J., 183, 505.
- Penston, M. V., Allen, D. A., and Lloyd, C. 1976, Observatory, 96, 22.
- Penston, M. V., Hunter, J. K., and O'Neill, A. 1975, M.N.R.A.S., 171, 219.
- Popper, D. M., and Plavec, M. 1976, Ap.J., 205, 462.
- Racine, R. 1968, A.J., 73, 233.
- Rosendhal, J. D. 1973, Ap.J., 186, 909.
- Sahovskoy, N. M. 1957, Bull. Stalinabad Ap. Obs., No. 20, 3.
- Schild, R. E. 1970, A.J., 161, 855.
- Schild, R. E., and Chaffee, F. 1971, Ap.J., 169, 529.
- Schild, R. E., and Cowley, A. P. 1971, Astr. and Ap., 14, 66.
- Serkowski, K., Mathewson, D. S., and Ford, V. L. 1975, Ap.J., 196, 261.
- Sharpless, S. 1952, Ap.J., 116, 251.
- _____. 1954, Ap.J., 119, 200.
- _____. 1962, Ap.J., 136, 767.
- _____. 1974, A.J., 79, 1073.
- Smith, M. A. 1972a, Ap.J., 175, 765.
- _____. 1972b, Ap.J., 176, 617.
- Stebbins, J., and Kron, G. E. 1956, Ap.J., 123, 440.
- Steffey, P. C. 1973, Pub. A.S.P., 85, 520.
- Stothers, R. 1972, Ap.J., 175, 431.
- Strand, K. Aa. 1958, Ap.J., 128, 14.
- _____. 1973, Ap.J., 179, 147.
- Strom, K. M., Strom, S. E., and Yost, J. 1971, Ap.J., 165, 479.
- Strom, K. M., Strom, S. E., Carrasco, L., and Vrba, F. J. 1975, Ap.J., 196, 489.
- Strömberg, B. 1966, Ann. Rev. Astr. and Ap., 4, 433.

- Taviev, E. I., Frantrman, Yu. L., and Yungelson, L. R. 1970, Nauchn. Informatsii No. 16, 83.
- Turner, B. E. 1973, Sci. Am., 228, 51.
- Vaerewyck, E. G., and Beardsley, W. R. 1973, Ap.J., 182, 121.
- van Albada, T. S. 1968, Bull. Astr. Inst. Neth., 20, 57.
- van Altena, W. F., and Monnier, R. C. 1968, A.J., 73, 649.
- van de Hulst, H. C. 1949, Rech. Astr. Obs. Utrecht, 11, Part 2, 1.
- Vandervoort, P. O. 1964, Ap.J., 139, 869.
- Vasilevskis, S. 1962, A.J., 67, 699.
- _____. 1971, Ap.J., 167, 537.
- von Hoerner, S. 1957, Z. Ap., 42, 273.
- Wackerling, L. R. 1970, Mem. R.A.S., 73, 153.
- Walborn, N. R. 1972, A.J., 77, 312.
- _____. 1974, Ap.J. (Letters), 191, L95.
- Walborn, N. R., and Hesser, J. E. 1976, Ap.J. (Letters), 205, L87.
- Walker, G. A. H. 1962, Observatory, 82, 52.
- _____. 1964, Ap.J., 140, 1613.
- _____. 1965, Ap.J., 141, 660.
- Walker, M. F. 1961, Ap. J., 133, 438.
- _____. 1969, Ap.J., 155, 447.
- _____. 1972, Ap.J., 175, 89.
- Walker, R. L. Jr. 1969, Pub. U.S. Naval Obs., 2nd ser., Vol. XXII, Part I.
- Warren, W. H. Jr. 1973, A.J., 78, 192.
- _____. 1975, thesis, Indiana University-Bloomington.
- _____. 1976, M.N.R.A.S., 174, 111.

Warren, W. H. Jr., and Hesser, J. E. 1977a, Ap.J. Suppl.,
34, (Paper I).

_____. 1977b, Ap.J. Suppl., 34, (Paper II).

Whiteoak, J. B. 1966, Ap.J., 144, 305.

Worley, C. E. 1971, Pub. U.S. Naval Obs., 2nd ser., Vol. XXII,
Part II.

_____. 1972, Pub. U.S. Naval Obs., 2nd. ser., Vol. XXII,
Part IV.

WAYNE H. WARREN JR.: Laboratory for Solar Physics and
Astrophysics, Code 681, NASA-Goddard Space Flight Center,
Greenbelt, MD 20771.

JAMES E. HESSER: Observatorio Inter-Americano de Cerro
Tololo, Casilla 63-D, La Serena, CHILE.

TABLE 1
FINAL DISTANCES AND REDDENING FOR ORION OB 1 SUBGROUPS*

Subgroup	Subdivision	$\langle \underline{V}_0 - \underline{M}_V \rangle$	σ (one star)	distance (pc)	n	$\langle \underline{E}(b-y) \rangle$	σ (one star)	n
a		8.03	0.46	404	60	0.040	0.025	58
	b1	8.50	0.53	501	14	0.091 [†]	0.084	14
	b2	8.15	0.29	427	24	0.057	0.030	23
	b3	8.04	0.55	406	14	0.059	0.049	12
c		8.21	0.42	439	78	0.031	0.013	54
	c1	8.02	0.40	402	9	0.037	0.007	9
	c2	8.45	0.49	490	8	0.040	0.022	4
	c3	8.20	0.36	437	3	-	-	-
	c4	8.35	0.28	468	8	0.027	0.009	8
	c	8.16	0.49	429	44	0.030	0.014	32
	d1	8.42	0.53	483	6	-	-	-

*These results are from analysis of the B-type stars only.

[†]Elimination of three stars (WH 473, 490, 494) suffering heavy absorption yields 0.051 ± 0.022 .

TABLE 2

ESTIMATED AGES FOR ORION OB 1 SUBGROUPS

Subgroup	Age (10^6 years)	Ref.	Method
1a	4.5	1	Expansion
	10	2	Turnup
	12	12	
	28	13	
	6.2	3	Bluest m.-s. stars
	6.3	2	Supergiant (β Ori)
	7.9:	2	(α Ori)
1b	5	2	Turnup
	\sim 5	5	
	8	12	
	34	13	
	2.2-4.9	4	Runaways AE Aur, μ Col, 53 Ari
1c	\sim 0.5	5	Turnup
	2 -3	6	Am stars
1d Cluster	0.3	9	Expansion
	<3	2	Turnup
	4 :	12	
	5.4	13	
	3	10	PMS turn-up
	0.2-9	11	
	1 -10	14	
<0.5	3	Bluest m.-s. stars	
Trapezium	\leq 0.01	7	Expansion
Nebula	\sim 0.01-0.02	8	Gas dynamics

REFERENCES.--(1) Lesh 1968b; (2) Stothers 1972; (3) Maeder 1972b; (4) Blaauw 1961; (5) Sharpless 1962; (6) Smith 1972a; (7) Parenago 1953; (8) Kahn and Menon 1961, Vandervoort 1964; (9) Strand 1958; (10) H. L. Johnson 1957, M. F. Walker 1969; (11) Penston, Hunter and O'Neill 1975; (12) Blaauw 1964; (13) Tsviev, Frantrman and Yungelson 1970; (14) McNamara 1976.

TABLE 3

INTRINSIC COLORS OF THE BLUEST MAIN-SEQUENCE STARS IN EACH ORION SUBGROUP

Star	HD	Name	MK type(s)	$\frac{v_e \sin i}{(\text{km s}^{-1})}$	$(\underline{b}-\underline{y})_0$	$(\underline{B}-\underline{V})_0$	\underline{c}_0	$(\underline{u}-\underline{b})_0$	$(\underline{U}-\underline{B})_0$	1	$\langle \frac{(\underline{U}-\underline{B})_0}{2} \rangle$	3
Subgroup 1a												
21	34989	HR 1763	B1V	53	-0.118	-0.267	-0.024	-0.080	-0.988			
27	35149A	23 Ori	B1V,B1Vn	290	-0.111	-0.256	0.249	0.002	-0.947			
37	35411AB	η Ori	B0.5Vnn,B1V	47	-0.118	-0.270	-0.022	-0.080	-0.997			
38	35439	25 Ori	B1Vn,B1V:pe	327	-0.112	-0.257	0.041	-0.028	-0.951			
49	35715AB	ψ Ori	B1V,B2IV	143	-0.113	-0.263	0.029	-0.032	-0.970	-0.997	-0.985	-0.971
Subgroup 1b*												
159	36591AB	HR 1861	B1V,B1IV,B1.5III	20	-0.117	-0.268	-0.011	-0.064	-0.991			
184	36695	VV Ori	B1V,B1.5III	156	-0.114	-0.262	0.016	-0.065	-0.969			
415	37468AB	σ Ori	O9.5V	94	-0.125	-0.288	-0.090	-0.209	-1.063			
458	37744	HR 1950	B1V,B1.5V	35	-0.112	-0.253	0.038	-0.019	-0.936			
465	37776	IC 432	B2V,B4V	145	-0.112	-0.254	0.044	0.056	-0.937	-1.063	-1.008	-0.979
Subgroup 1c												
147	36512	ν Ori	B0V	17	-0.125	-0.299	-0.096	-0.216	-1.105			
265	36959B	HR 1886	B1V	26	-0.113	-0.253	0.028	-0.020	-0.936			
266	36960A	HR 1887	B0V,B0.5V	32	-0.122	-0.283	-0.059	-0.147	-1.045			
295	37018AB	42 Ori	B1V,B1III	69	-0.117	-0.267	-0.015	-0.070	-0.987			
374	37303	HR 1918	B1V,B1.5V	260	-0.115	-0.262	0.015	-0.045	-0.966	-1.105	-1.046	-1.008
Subgroup 1d												
279	37020CE	θ^1 Ori	O8Vn,B0.5Vp	93	-0.125:	-0.297	-0.090:	-0.152:	-1.098			
280	37022AF	θ^1 Ori	O7V	123	-0.135	-0.323	-0.201	-0.278	-1.193			
292	37023B	θ^1 Ori	B0.5Vp	92	-0.126:	-0.295	-0.107:	-0.163:	-1.092			
296	37041A	θ^2 Ori	O9V,O9.5V	183	-0.129	-0.296	-0.137	-0.236	-1.093			
297	37042B	θ^2 Ori	B0.5V,B1V	10	-0.126	-0.288	-0.104	-0.185	-1.062	-1.193	-1.128	-1.108

*Star No. 414 (σ Ori) is bluer than 465 but has been omitted--it is a helium-rich variable star (period $\sim 1.19^d$) with peculiar photometric properties (Walborn and Hesser 1976; Hesser, Walborn and Ugarte 1976; Hesser, Moreno and Ugarte 1977).

TABLE 4

ORION-SUBGROUP AGES (UNCORRECTED FOR ROTATION)
FROM THE BLUEST STARS

Subgroup	N	Age (10^6 years)			Mean
		1	2	3	
1a	19	7.9	7.9	7.9	7.9
1b	13	3.5	5.6	6.3	5.1
1c	22	1.6	4.0	5.6	3.7
1d	12	<0.5	<0.5	<0.5	<0.5

APPENDIX

RESULTS OF THE PHOTOMETRIC ANALYSES

The Appendix contains the tables in which the principal photometric data of this investigation are summarized. Each table contains the data for one subgroup of the Orion OB 1 association and is subdivided into three parts (a,b,c) for the B-, I- and AF-type stars, since the photometric parameters derived vary according to group.²⁶ The information

²⁶There are three stars (WH 21, 440, 507) in Table 1 of Paper I which are not included in a subgroup because they are quite far from the main body of the association; they are included in the present tables with the subgroups nearest to them (a, c, and c, respectively).

presented in the tables follows:

Column

- | | | |
|---|----------|--|
| 1 | Star | Number assigned in present study, as used on the charts and called WH in the data tables of Paper I. |
| 2 | ID | HD number if one exists; otherwise the BD or π (Parenago 1954) numbers are used. |
| 3 | <u>V</u> | <u>V</u> magnitude as listed in Table 2 of Paper I, rounded to the nearest hundredth except when |

Column

a 5 is present in the thousandths column.
Colons indicate uncertain values.

- 4-8 uvby β The mean observed photoelectric uvby β indices used in the present analysis, as taken from the individual measures in Table 17 of Paper I. The (u-b) index is computed from the four-color photometry via the relation $\underline{c}_1 + 2[\underline{m}_1 + (\underline{b-y})]$.
- 9 $\delta\beta$ Index measuring the distance of a B-type star from the zero-age main sequence, computed by comparing the expected β (ZAMS) value for the derived intrinsic index \underline{c}_0 with the measured β : $\beta(\underline{c}_0) - \beta(\text{observed})$.
- 10 \underline{V}_0 Intrinsic V magnitude assuming a ratio of total-to-selective absorption of $\underline{A}_V/\underline{E}(\underline{b-y}) \equiv \underline{R} = 4.3[\underline{V}_0 = \underline{V} - 4.3\underline{E}(\underline{b-y})]$. As discussed in the text, this value of \underline{R} may not be valid for certain areas. The \underline{V}_0 data have been corrected for duplicity when considered necessary and these corrections are described in the table notes. In these cases, \underline{V}_0 values are reported only to a tenth of a magnitude.

Column

11-14	<p>Intrinsic indices of the four-color system, as determined from the observed indices and $\underline{E}(\underline{b-y})$ using the relations given in Paper II.</p>
15	<p>$\underline{E}(\underline{b-y})$ Computed color excess $\underline{E}(\underline{b-y}) \approx 0.7\underline{E}(\underline{B-V})$.</p>
16	<p>$\underline{E}(\underline{U-B})$ Color excess computed from the <u>UBV</u> photometry given in Table 2 of Paper I. The expression used, $(\underline{U-B}) = 1.242(\underline{U-B}) - 0.894(\underline{B-V})$, is valid only for B-type stars and is discussed in more detail in Paper II. Since $\underline{E}(\underline{U-B}) \approx 0.7\underline{E}(\underline{B-V})$, these values are expected to compare favorably with $\underline{E}(\underline{b-y})$. Poor agreement indicates anomalies in a star's energy distribution or in the photometry; colons indicate uncertainties in the $(\underline{B-V})$ and/or $(\underline{U-B})$ indices used.</p>
17	<p>\underline{M}_V Absolute visual magnitude as determined from the photometric parameters (see Paper II). In cases where the β index is considered abnormal or affected by emission, the $(\underline{b-y})_0$ color has been used to derive $\underline{M}_V(\beta)_{ZAMS}$. This procedure can only be used for the B-type stars since the calculation of intrinsic colors for I and AF stars requires β. In all cases where β has not been used directly to find $\underline{M}_V(\beta)$, as with</p>

Column

- the $(\underline{b}-\underline{y})_0$ method described above, details are given in the notes.
- 18 dm Distance modulus $(\underline{V}_0 - \underline{M}_V) = 5 \log (r/10)$, where r is in parsecs.
- 19 Sp The photometric spectral type as determined from \underline{c}_0 in the case of B-type stars (Warren 1976) or from β for AF-type stars (Barry 1970). No calibration exists for intermediate (I)-group stars, hence this heading is omitted in sub-tables b.
- 20 Spectrum Spectroscopic types from Table 2 of Paper I; in most cases all types are included. For additional details and information on peculiar stars, the notes to the above table should be consulted. OP denotes objective-prism types.
- 21 Notes An asterisk indicates a note at the end of the table. Presumed or suspected non-membership is also indicated in this column.

The tables "b" and "c" for I- and AF-type stars differ from tables "a" in that no $\underline{E}(\underline{U}-\underline{B})$ is derived and several additional parameters are listed. In tables "b" for I-group stars they are as follows:

Column

- 9 \underline{r} A measure for I-group stars analogous to the $\delta\beta$ index for B stars: $\underline{r} = 0.35\underline{c}_1 - (\beta - 2.565) - 0.07(\underline{b}-\underline{y})$.
- 15 \underline{a}_0 Intrinsic temperature parameter:
 $\underline{a}_0 = 0.80\underline{r} + 2\underline{m}_1 - 0.358 + 0.36(\underline{b}-\underline{y})$.
- 16 $\delta\underline{m}_0$ Index measuring the difference between the standard \underline{m}_0 for the same \underline{a}_0 , as defined by the I-group calibration of Glaspey (1971a), and \underline{m}_0 for the star: $\delta\underline{m}_0 = \underline{m}_0(\text{ZAMS}) - \underline{m}_0(\text{star})$.
- 17 $\delta\underline{c}_0$ Difference between the observed \underline{c}_0 and $\underline{c}_0[\underline{a}_0]$ from the calibration:
 $\delta\underline{c}_0 = \underline{c}_0(\text{star}) - \underline{c}_0(\text{ZAMS})$.
- 18 $\delta(\underline{u}-\underline{b})_0$ The ultraviolet excess:
 $\delta(\underline{u}-\underline{b})_0 = (\underline{u}-\underline{b})_0[\text{ZAMS}] - (\underline{u}-\underline{b})_0[\text{star}]$.

The above indices are also discussed in Paper II, § IV. The δ indices are defined similarly for the AF-type stars except that \underline{m}_0 is compared to the standard value for the Hyades (Crawford and Perry 1966, Crawford and Barnes 1974, Crawford 1975b). For the A and F stars the standard values are those for a star of the same β rather than for the same \underline{a}_0 as with the I group. Additional details concerning the derivation of these indices may be found in Paper II and its references.

TABLE 5a
DATA FOR B-TYPE STARS, SUBGROUP a

(1) Star	(2) ID	(3) V	(4) (b-g)	(5) m ₁	(6) c ₁	(7) (u-b)	(8) β	(9) δ _B	(10) V ₀	(11) (b-g) ₀	(12) m ₀	(13) c ₀	(14) (u-b) ₀	(15) E(b-g)	(16) E(U-B)	(17) M _V	(18) dm	(19) Sp	(20) Spectrum	(21) Note
1	32686	6.045	-0.055	0.101	0.457	0.549	2.685	0.043	5.97	-0.072	0.106	0.454	0.222	0.017	0.020	-1.3	7.3	B6	B5 IV	
2	32867	7.51	-0.044	0.096	0.517	0.621	2.726	0.017	7.42	-0.066	0.103	0.513	0.585	0.022		-0.4	7.9	B6	B8	
3	38884	7.66	0.007	0.143	0.997	1.297			7.54	-0.020	0.151	0.992	1.254	0.027		+1.2	6.3	A0	B9	*, NM?
4	293815	10.09	0.159	0.103	0.935	1.459			9.28	-0.029	0.159	0.897	1.158	0.188	0.177	+1.0	8.3	B9	B9V	*
6	33038	7.61	-0.006	0.847	0.845	1.007	2.778	0.054	7.48	-0.035	0.096	0.839	0.961	0.029		+0.3	7.2	B8	B9	NM?
7	33056	8.88	-0.004	0.118	0.872	1.100			8.76	-0.032	0.126	0.866	1.055	0.028		+0.9	7.9	B9	B9	
8	33647AB	6.675	-0.028	0.114	0.678	0.850	2.771	0.003	7.1	-0.051	0.121	0.673	0.814	0.023	0.018	+0.2	6.9	B7	B8V, B9Vn	*
9	33765	8.895	-0.007	0.080	0.301	0.447	2.682	0.009	8.54	-0.088	0.104	0.285	0.317	0.081		-1.4	9.9	B3	B8	NM?
10	33900	8.71	0.039	0.109	0.771	1.067	2.808	-0.011	8.35	-0.043	0.134	0.755	0.936	0.082		+0.7	7.7	B8	B9	
11	34098	8.77	-0.031	0.072	0.102	0.184	2.637	0.005	8.44	-0.108	0.095	0.087	0.061	0.077		-2.6	11.0	B2	B8	*, NM
12	34179	8.035	0.016	0.075	0.549	0.731	2.687	0.060	7.69	-0.064	0.099	0.533	0.603	0.080	0.061	-1.2	(8.9)	B6	B8V	*, NM?
13	34307AB	7.89	0.051	0.101	0.758	1.062	2.808	-0.017	8.1	-0.044	0.130	0.739	0.910	0.095		+0.7	7.4	B8	B8	*
14	34280AB	7.76	0.081	0.121	0.987	1.391	2.897	-0.009	7.9	-0.022	0.152	0.966	1.226	0.103		+1.2	6.7	B9	B9	*
15	34317	6.41	-0.005	0.159	1.130	1.438	2.876			-0.02					-0.018	+1.1	(5.2)		B8-5V, AOV	*, NM
16	34510	8.075	0.017	0.091	0.623	0.839	2.737	0.024	8.39	-0.057	0.113	0.608	0.721	0.074		-0.2	8.6	B7	B9	
17	34511	7.38	-0.034	0.078	0.263	0.351	2.675	0.008	7.14	-0.092	0.095	0.251	0.259	0.058	0.052	-1.5	8.7	B3	B5V	
18	34748	6.33	-0.019	0.080	0.150	0.272	2.639	0.014	6.1	-0.103	0.105	0.133	0.138	0.084	0.082	-2.5	8.6	B2	B1-5Vn	*
19	34929	8.41	0.003	0.107	0.668	0.888	2.770	0.000	8.17	-0.052	0.124	0.657	0.800	0.055	0.051	+0.2	7.9	B7	B8	
20	34959	6.59	-0.019	0.079	0.552	0.672	2.598	0.151	6.40	-0.063	0.092	0.543	0.601	0.044	0.035			B7	B5Vp	*
21	34989	5.79	-0.017	0.060	-0.004	0.082	2.611	0.009	5.36	-0.118	0.090	-0.024	-0.080	0.101	0.100	-3.6	9.0	B1	B1V	*
22	35008	7.12	-0.023	0.108	0.721	0.891	2.781	0.003	7.02	-0.047	0.115	0.716	0.853	0.024	-0.013	+0.4	6.7	B8	B9	
23	35007A	5.68	-0.047	0.100	0.287	0.393	2.682	0.008	5.50	-0.089	0.113	0.279	0.326	0.042	0.044	-1.4	6.9	B3	B3V	
24	35039	4.73	-0.067	0.082	0.168	0.198	2.624	0.036	4.58	-0.100	0.092	0.161	0.145	0.033	0.039	-3.1	7.7	B2	B2 IV-V	
25	35079	7.07	0.021	0.089	0.369	0.589	2.713	-0.008	6.62	-0.082	0.120	0.348	0.424	0.103	0.094	-0.7	7.3	B3	B3V	
26	35148B	7.18	-0.028	0.073	0.321	0.411	2.678	0.019	6.93	-0.086	0.090	0.309	0.318	0.058	0.052	-1.4	8.4	B3	B3V	
27	35149A	5.00	-0.043	0.067	0.063	0.111	2.619	0.016	4.70	-0.111	0.087	0.049	0.002	0.068	0.075	-3.3	8.0	B1	B1V, B1 Vn	
28	35135AB	8.36	0.020	0.107	0.805	1.059	2.834	-0.022	8.4	-0.039	0.125	0.793	0.965	0.059	0.045	+0.9	7.5	B8	B9	*
29	35177	8.17	-0.023	0.102	0.546	0.704	2.748	-0.000	7.99	-0.064	0.114	0.538	0.639	0.041		-0.1	8.1	B6	B9	
30	35194	8.35	-0.035	0.100	0.769	0.899	2.781	0.021	8.32	-0.042	0.102	0.768	0.889	0.007	-0.002	+0.4	8.0	B8	B9	
31	35203A	7.99	-0.017	0.094	0.488	0.642	2.731	0.003	7.76	-0.070	0.110	0.477	0.558	0.053	0.032	-0.4	8.1	B6	B6V	
32	35258	8.81	0.003	0.119	0.959	1.203	2.880	0.003	8.70	-0.023	0.127	0.954	1.161	0.026	0.021	+1.1	7.5	B9	B8	
33	35298	7.90	-0.046	0.091	0.369	0.459	2.709	-0.002	7.75	-0.081	0.101	0.362	0.403	0.035	0.024	-0.8	8.5	B4	B3Vn, B9V	*
34	35299	5.69	-0.095	0.092	0.050	0.044	2.631	0.003	5.62	-0.111	0.097	0.047	0.018	0.016	0.019	-2.8	8.4	B1	B1V, B1.5V	
35	35305	8.42	-0.035	0.121	0.633	0.805	2.775	-0.010	8.34	-0.055	0.127	0.629	0.773	0.020	0.016	+0.3	8.0	B7	B6-7IV-V	
36	35407	6.32	-0.058	0.105	0.314	0.408	2.681	0.016	6.20	-0.086	0.113	0.308	0.363	0.028	0.018	-1.4	7.6	B3	B4 IVn, B5V	
37	35411AB	3.35	-0.058	0.071	-0.010	0.016	2.606	0.014	3.9	-0.118	0.089	-0.022	-0.080	0.060	0.073	-3.9	(7.8)	B1	B0.5Vnn, B1V	*
38	35439	4.945	-0.080	0.068	0.047	0.023	2.574	0.059	4.81	-0.112	0.078	0.041	-0.028	0.032	0.035	-2.7	7.5	B1	B1 Vn, B1V:pe	*
39	35454	8.73	-0.019	0.135	0.866	1.098	2.837	0.006	8.68	-0.032	0.139	0.863	1.077	0.013	0.002	+0.9	(7.7)	B9	B9	
40	35456AB	6.94	0.000	0.096	0.496	0.688	2.706	0.030	6.64	-0.069	0.117	0.482	0.577	0.069	0.074	-0.8	7.5	B6	B5-6Vw	
41	35501AB	7.43	-0.004	0.095	0.601	0.783	2.738	0.020	7.4	-0.059	0.111	0.590	0.695	0.055	0.047	-0.2	7.6	B7	B8V	*

TABLE 5a (CONTINUED)

(1) Star	(2) ID	(3) V	(4) (b-y)	(5) m ₁	(6) c ₁	(7) (u-b)	(8) β	(9) δβ	(10) V ₀	(11) (b-y) ₀	(12) m ₀	(13) c ₀	(14) (u-b) ₀	(15) E(b-y)	(16) E(U-B)	(17) M _V	(18) dm	(19) Sp	(20) Spectrum	(21) Note
42	35502A	7.35	0.010	0.107	0.335	0.569	2.718	-0.020	6.94	-0.085	0.136	0.316	0.416	0.095	0.096	-0.76	7.75	B3	B5V	
43	35548AB	6.57	-0.007	0.119	0.884	1.108	2.793	0.058	7.2	-0.031	0.126	0.879	1.070	0.024	0.006	+0.5	6.7	B9	B9p Hg-S1	*, NM?
44	35575	6.44	-0.072	0.108	0.205	0.277	2.667	0.003	6.33	-0.097	0.115	0.200	0.238	0.025	0.024	-1.7	8.0	B2	B3V	
45	35588	6.16	-0.082	0.112	0.186	0.246	2.659	0.007	6.2	-0.098	0.117	0.183	0.220	0.016	0.017	-1.9	8.1	B2	B2.5V, B3V	*
46	35612	8.33	-0.010	0.099	0.679	0.857	2.775	-0.002	8.16	-0.051	0.111	0.671	0.792	0.041	0.014	+0.3	7.9	B7	B9	
47	35657A	8.33	0.025	0.161	1.088	1.460	2.913	0.005	8.18	-0.011	0.172	1.081	1.402	0.036	0.027	+1.3	6.9	A0	B9	*
48	35673AB	6.52	0.016	0.112	0.802	1.058	2.803	0.008	6.5	-0.039	0.129	0.791	0.970	0.055	0.046	+0.6	5.9	B8	B9V	*, NM?
49	35715AB	4.59	-0.087	0.075	0.034	0.010	2.627	0.004	4.8	-0.113	0.083	0.029	-0.032	0.026	0.035	-3.0	7.8	B1	B1V, B2IV	*
50	35716	8.52	-0.014	0.107	0.751	0.937	2.809	-0.015	8.39	-0.044	0.116	0.745	0.889	0.030	0.006	+0.7	7.7	B8	B9	
51	35730	7.20	-0.061	0.090	0.304	0.362	2.680	0.015	7.08	-0.087	0.098	0.299	0.320	0.026	0.032	-1.4	8.5	B3	B3V, B5IV	
52	35731	9.30	0.007	0.142	0.939	1.237	2.898	-0.024	9.16	-0.026	0.152	0.932	1.185	0.033	0.015	+1.2	7.9	B9	A0	
53	35762	6.74	-0.064	0.091	0.210	0.264	2.671	-0.000	6.60	-0.096	0.101	0.204	0.212	0.032	0.024	-1.6	8.2	B2	B2V	
54	35777	6.62	-0.064	0.096	0.205	0.269	2.658	0.012	6.48	-0.097	0.106	0.198	0.217	0.033	0.029	-2.0	8.4	B2	B2V	
56	35791	8.90	-0.006	0.115	0.917	1.135	2.877	-0.011	8.81	-0.027	0.121	0.913	1.101	0.021	-0.001	+1.1	7.7	B9	B9	
57	35792	7.22	-0.060	0.103	0.329	0.415	2.699	0.001	7.11	-0.085	0.110	0.324	0.376	0.025	0.024	-1.0	8.1	B3	B3V, B5V	
58	35807	9.22	0.051	0.132	0.910	1.276	2.850	0.007	8.88	-0.029	0.156	0.894	1.148	0.080	0.075	+1.0	7.9	B9	A0	
60	35834AB	7.70	0.003	0.107	0.635	0.855	2.759	0.005	7.45	-0.056	0.125	0.623	0.761	0.059	0.051	+0.1	7.4	B7	B8V	
65	35881	7.81	-0.038	0.102	0.522	0.650	2.714	0.029	7.69	-0.066	0.110	0.516	0.605	0.028	0.036	-0.7	8.4	B6	B6V	
66	35882	7.82	-0.007	0.096	0.479	0.657	2.740	-0.008	7.55	-0.071	0.115	0.466	0.555	0.064	0.053	-0.2	7.7	B6	B6V	
67	35899	7.52	-0.056	0.109	0.322	0.428	2.692	0.006	7.40	-0.085	0.118	0.316	0.381	0.029	0.032	-1.1	8.5	B3	B5V	
69	35912	6.40	-0.080	0.104	0.210	0.258	2.669	0.003	6.33	-0.096	0.109	0.207	0.233	0.016	0.017	-1.7	8.0	B2	B2V	
71	35910	7.58	-0.033	0.096	0.440	0.566	2.712	0.011	7.40	-0.074	0.108	0.432	0.500	0.041	0.040	-0.7	8.1	B5	B6V	
72	35926AB	8.34	-0.037	0.126	0.628	0.806	2.766	-0.002	8.26	-0.055	0.132	0.624	0.777	0.018	0.023	+0.2	8.1	B7	B7IV:	
74	35948	8.37	0.023	0.140	0.966	1.292	2.874	0.010	8.17	-0.023	0.154	0.957	1.218	0.046	0.058	+1.1	(7.0)	B9	B8, A0	
75	35970	8.85	-0.004	0.122	0.871	1.107	2.843	0.001	8.73	-0.032	0.130	0.865	1.062	0.028	0.017	+1.0	7.8	B9	B8	
78	36012	7.34	-0.044	0.096	0.420	0.524	2.621	0.097	7.20	-0.076	0.106	0.414	0.473	0.032	0.043	-0.6	(7.8)	B5	B5Vne	*
79	36013A	6.90	-0.061	0.095	0.351	0.419	2.671	0.033	6.81	-0.082	0.101	0.347	0.385	0.021	0.027	-1.6	8.4	B3	B1.5V, B3V:n	
80	36032	9.16	0.001	0.119	0.843	1.083	2.835	-0.004	9.01	-0.035	0.130	0.836	1.026	0.036	0.017	+0.9	8.1	B8	B8	
86	36075	8.68	-0.007	0.105	0.872	1.068	2.813	0.032	8.57	-0.032	0.112	0.867	1.028	0.025	0.002	+0.7	7.8	B9	B9	
90	36115	8.21	0.045	0.093	0.543	0.819	2.730	0.014	7.74	-0.065	0.126	0.521	0.642	0.110		-0.4	8.1	B6	B8	
91	36133A	7.12	-0.063	0.100	0.296	0.370	2.679	0.014	7.02	-0.088	0.107	0.291	0.330	0.025	0.053	-1.4	8.4	B3	B2V, B5V	
92	36118	8.88	-0.004	0.133	0.892	1.150	2.819	0.035	8.77	-0.030	0.141	0.887	1.108	0.026	0.028	+0.8	8.0	B9	A0	
100	36165	8.14	-0.051	0.119	0.567	0.703	2.746	0.007	8.10	-0.061	0.122	0.565	0.687	0.010	0.015	-0.1	8.2	B7	B7V	
101	36166	5.78	-0.088	0.094	0.099	0.111	2.641	0.003	5.70	-0.107	0.100	0.095	0.081	0.019	0.022	-2.5	8.2	B2	B1.5V, B2V	
102	36176	8.67	-0.023	0.125	0.762	0.966	2.803	-0.005	8.59	-0.042	0.131	0.758	0.935	0.019	0.025	+0.6	8.0	B8	A0	
103	36219AB	7.65	-0.006	0.099	0.680	0.866	2.798	-0.025	8.2	-0.051	0.112	0.671	0.794	0.045	0.024	+0.6	7.6	B7	B7, B9	*
111	36267AB	4.20	-0.075	0.134	0.413	0.531	2.724	-0.006	4.4	-0.076	0.134	0.413	0.529	0.001	0.004	-0.5	4.9	B5	B5V, B5IV	*, NM
114	36310ABC	7.94	0.040	0.098	0.448	0.724	2.732	-0.011	8.2	-0.075	0.132	0.425	0.540	0.115	0.098	-0.3	8.5	B5	B6V	*
120	36340	7.98	-0.050	0.087	0.135	0.209	2.642	0.009	7.74	-0.104	0.103	0.124	0.123	0.054	0.044	-2.4	10.2	B2	B2V	NM?
123	36351AB	5.46	-0.078	0.089	0.120	0.142	2.634	0.014	5.6	-0.105	0.097	0.115	0.099	0.027	0.035	-2.7	8.3	B2	B1.5V	*

TABLE 5a (CONCLUDED)

(1) Star	(2) ID	(3) V	(4) [b-y]	(5) m ₁	(6) c ₁	(7) [u-b]	(8) β	(9) δβ	(10) V ₀	(11) [b-y] ₀	(12) m ₀	(13) c ₀	(14) (u-b) ₀	(15) E[b-y]	(16) E(U-B)	(17) M _V	(18) dm	(19) Sp	(20) Spectrum	(21) Note
130	36392	7 ^m 54	-0 ^m 060	0 ^m 105	0 ^m 335	0 ^m 425	2 ^m 688	0 ^m 013	7 ^m 44	-0 ^m 084	0 ^m 112	0 ^m 330	0 ^m 387	0 ^m 024	0 ^m 039	-1.2	8 ^m 7	B3	B3V	
136	36429A	7.56	-0.036	0.091	0.329	0.439	2.684	0.015	7.35	-0.085	0.106	0.319	0.361	0.049	0.029	-1.3	8.6	B3	B5V	
139	36471	8.68	0.099	0.080	0.689	1.047	2.778	-0.007	8.03	-0.052	0.125	0.659	0.805	0.151		+0.3	7.7	B7	B8V	
156	36549	8.57	-0.038	0.119	0.648	0.810	2.766	0.002	8.50	-0.053	0.124	0.645	0.785	0.015	0.025	+0.2	8.3	B7	B6Vwp	
167	36627	7.58	-0.038	0.098	0.456	0.576	2.708	0.019	7.43	-0.072	0.108	0.449	0.521	0.034	0.035	-0.8	8.2	B5	B6V	
175	36645	8.64	0.014	0.124	0.915	1.191	2.849	0.014	8.46	-0.028	0.137	0.907	1.124	0.042	0.030	+1.0	(7.5)	B9	B9	
193	36741	6.59	-0.081	0.097	0.160	0.192	2.648	0.011	6.50	-0.101	0.103	0.156	0.160	0.020	0.028	-2.2	8.7	B2	B2V	
199	36776	8.53	-0.021	0.102	0.602	0.764	2.761	-0.002	8.37	-0.058	0.113	0.595	0.704	0.037	0.017	+0.1	8.3	B7	B8	
209	36810	8.63	0.003	0.132	0.884	1.154	2.870	-0.020	8.48	-0.031	0.142	0.877	1.100	0.034	0.017	+1.1	7.4	B9	B9	
219	36824	6.70	-0.059	0.090	0.242	0.304	2.667	0.012	6.56	-0.093	0.100	0.235	0.249	0.034	0.045	-1.7	8.3	B2	B3V	
234	36897	8.31	0.111	0.087	0.771	1.167	2.755	0.037	7.64	-0.044	0.134	0.740	0.919	0.155		0.0	7.6	B8	B8	*
353	37234ABC	7.74	0.035	0.136	0.704	1.046	2.816	-0.039	7.6	-0.049	0.161	0.687	0.911	0.084	0.081	+0.4	7.2	B8	B9	*
377	37342B	8.01	-0.044	0.091	0.451	0.545	2.712	0.014	7.89	-0.073	0.100	0.445	0.499	0.029	0.017	-0.7	8.6	B5	B5V	*
378	37330A	7.47	-0.024	0.091	0.458	0.592	2.641	0.086	7.26	-0.072	0.106	0.448	0.514	0.048	0.032	-0.4	7.7	B5	B5V, B6V	*
413	37467	7.895	-0.035	0.120	0.672	0.842	2.751	0.022	7.83	-0.051	0.125	0.669	0.816	0.016	0.010	0.0	7.9	B7	B7IV-V	
421	37490	4.54	-0.016	0.060	0.184	0.272	2.560	0.102	4.18	-0.100	0.085	0.167	0.138	0.084	0.100	-3.5	(8.0)	B2	B2IIIe	*
433	37591	8.01	-0.021	0.126	0.779	0.989	2.825	-0.020	7.92	-0.041	0.132	0.775	0.957	0.020	0.008	+0.8	7.1	B8	B9	
435	37592	8.35	-0.037	0.127	0.817	0.997	2.805	0.017	8.35	-0.037	0.127	0.817	0.997	-0.000	0.019	+0.7	7.7	B8	A0	
436	37606	6.905	-0.013	0.092	0.753	0.911	2.744	0.050	6.77	-0.044	0.101	0.747	0.862	0.031	0.009	-0.1	6.9	B8	B8V	*
482	37958	6.67	-0.005	0.101	0.956	1.148	2.766	0.116	6.59	-0.024	0.107	0.952	1.118	0.019	-0.013	+0.2	(6.4)	B9	B8	*
484	38022	8.15	0.026	0.132	0.990	1.306	2.853	0.040	7.95	-0.021	0.146	0.981	1.231	0.047		+1.0	6.9	B9	B9	*, NM?
486	38048	9.29	0.086	0.154	0.891	1.371	2.867	-0.022	8.78	-0.032	0.189	0.867	1.182	0.118	0.119	+1.1	7.7	B9	B9	
489	38098	6.75	0.008	0.089	0.892	1.086	2.699	0.154	6.58	-0.030	0.100	0.884	1.025	0.038		-1.0	(7.6)	B9	B8	*
496	38270AB	7.53	0.029	0.127	0.912	1.224	2.849	0.011	7.5	-0.029	0.144	0.900	1.132	0.058	0.054	+1.0	6.5	B9	B9	*, NM?
499	38311	8.71	0.030	0.154	0.954	1.322	2.886	-0.007	8.48	-0.024	0.170	0.943	1.235	0.054	0.054	+1.2	7.3	B9	A0	
502	38563C	10.43	0.500	-0.055	0.492	1.382	2.698	0.012	7.94	-0.079	0.119	0.376	0.455	0.579	0.540	-1.0	8.9	B4	B5	NM?
503	38563AB	10.59	0.916	-0.070	0.210	1.902	2.589	0.037	6.15	-0.115	0.239	0.004	0.252	1.031	0.939	-3.0	(9.1)	B1	B1V, B2II-III	*, NM?
504	38650	7.66	-0.010	0.113	0.881	1.087	2.796	0.053	7.57	-0.031	0.119	0.877	1.053	0.021		+0.6	7.0	B9	B9	*, NM?
510	38856	7.24	-0.060	0.117	0.428	0.542	2.716	0.005	7.17	-0.075	0.121	0.425	0.518	0.015		-0.6	7.8	B5	B8, B3III	
511	38900	7.81	-0.026	0.122	0.872	1.064	2.803	0.044	7.79	-0.032	0.124	0.871	1.055	0.006		+0.6	7.2	B9	B9	NM?
512	38912	9.48	0.178	0.078	0.768	1.280	2.835	-0.049	8.52	-0.046	0.145	0.723	0.922	0.224		+0.5	8.0	B8	B8	*
513	38946	9.86	0.155	0.075	0.837	1.297	2.766	0.048	9.02	-0.038	0.133	0.798	0.987	0.193		+0.2	8.8	B8	B9	NM?
515	39082	7.44	-0.025	0.199	0.881	1.229	2.869	-0.018	7.41	-0.031	0.201	0.880	1.220	0.006		+1.1	6.3	B9	B9	*, NM?
516	39103	9.12	0.032	0.122	0.784	1.092	2.813	-0.010	8.81	-0.041	0.144	0.769	0.975	0.073		+0.7	8.1	B8	B8	
523	39557	8.93	0.337	0.016	0.630	1.336	2.616	0.134	7.21	-0.062	0.136	0.550	0.697	0.399		0.0	7.2	B7	B8ne	*
525	39773AB	6.80	0.010	0.112	0.621	0.865	2.758	0.003	6.6	-0.057	0.132	0.608	0.758	0.067		+0.1	6.5	B7	B9	*

NOTES TO TABLE 5a

In most cases duplicity corrections have been made using separations and magnitude differences given in the IDS catalogue (Jeffers et al., 1963). Where newer data have been used, details and references are reported in these notes.

- 3,4 $\underline{M}_V(\beta)_{\text{ZAMS}}$ determined from $(\underline{b-y})_0$.
- 8 \underline{V}_0 corrected by 0.5 for duplicity.
- 11 This star appears to lie well beyond the association and displays a spectrum/color discrepancy. The HD, AGK2 and SAO catalogues all give B8. The identification has been checked and appears correct. An MK classification is needed.
- 12 The intrinsic UBV colors derived are $(\underline{B-V})_0 = -0.14$, $(\underline{U-B})_0 = -0.51$, consistent with the photometric spectral type of B6 (Johnson 1963). The large $\delta\beta$ index suggests an evolved field star situated about 1 mag above the ZAMS. Since both spectrum/color and color/hydrogen-line-strength discrepancies are present, this star should be re-examined spectroscopically.
- 13 \underline{V}_0 corrected by 0.6 for duplicity.
- 14 \underline{V}_0 corrected by 0.6 for duplicity (separation 0!64, Δm 0.3, Worley 1972).
- 15 The measured index $\underline{c}_1 = 1.130$ is outside the calibration range for B stars. A normal β has been assumed and used to derive $\underline{M}_V(\beta)$ and $(\underline{b-y})_0$, from which

NOTES TO TABLE 5a (CONTINUED)

- $\underline{E}(\underline{b-y})$ has been calculated. An extrapolation of the calibration gives $\underline{E}(\underline{b-y}) = 0.00$, $\underline{M}_V(\beta) = +1.0$, in good agreement. This star is a definite evolved foreground object, as indicated by the membership table (in Paper I) and the computed distance modulus. It should be noted that the star is suspected of displaying emission at H α (Crawford, Barnes and Perry 1975), but β appears normal for the spectral type.
- 18 \underline{V}_0 corrected by 0.1 [spectroscopic binary (SB)].
- 20 The spectrum/color discrepancy indicates that the four-color indices are affected by the spectral peculiarities associated with this shell star. The $\delta\beta$ value confirms the strong emission found in the spectrum. The emission is also seen clearly in the photometric H α index of Andrews (1968) [see Fig. 2 of Paper II].
- 21 Star is located far north of the 1a subgroup boundaries used in the present work, but is included in Table 5a because it is closest to the 1a subgroup. It is not used in deriving mean values for the subgroup, however.
- 28 \underline{V}_0 corrected by 0.3 for duplicity (separation 0^h52, Δm 1.3, Worley 1972). The β index may be affected by the secondary, but the $(\underline{b-y})_0$ value gives $\underline{M}_V(\beta)_{ZAMS} = +0.7$, increasing the distance modulus by only 0.2.

NOTES TO TABLE 5a (CONTINUED)

- 33 The β and \underline{c}_0 spectral type of B4 supports the assignment of the B3 Vw type by Ciatti and Bernacca (1971).
- 37 η Orionis. \underline{V}_0 corrected by 0.8 for multiplicity (separation 1"5, Δm 0.9, R. L. Walker Jr. 1969; SB3 system--see discussion by Lesh 1968a). Star listed in the catalogues of Jaschek, Ferrer and Jaschek (1971) and Wackerling (1970) as Be but $\delta\beta$ does not indicate photometrically detectable emission. A discussion of speckle interferometric observations and the distance of the system is given by McAlister (1976).
- 38 25 Orionis. The $\delta\beta$ index shows emission-- $\underline{M}_V(\beta)_{ZAMS}$ determined from $(\underline{b}-\underline{y})_0$.
- 41 \underline{V}_0 corrected by 0.2 for duplicity (separation 2"95, Δm 1.8, Worley 1972).
- 43 \underline{V}_0 corrected by 0.7 for duplicity (separation 0"12, Δm 0.0, Worley 1971; separation 0"11, Δm 0.0, Worley 1972). The $(\underline{b}-\underline{y})_0$ color yields $\underline{M}_V(\beta)_{ZAMS} = +1.0$, but the Balmer-line strength (at least H β) appears weaker than B9 and gives the $\underline{M}_V(\beta)$ reported. The radial velocity and distance modulus taken together strongly suggest non-membership.
- 45 \underline{V}_0 corrected by 0.1 (SB).
- 47 This star is a borderline case between B- and I- (intermediate group) types. The I reduction gives comparable results to those reported in this table.

NOTES TO TABLE 5a (CONTINUED)

- 48 \underline{V}_0 corrected by 0.2 for duplicity. The distance modulus suggests a foreground star, but no radial velocity is available and the proper motions are not definitive.
- 49 ψ Orionis. \underline{V}_0 corrected by 0.4 for a magnitude difference between the spectroscopic components of 1.0 (Batten 1967).
- 78 The $\delta\beta$ index supports the Be classification. $\underline{M}_V(\beta)_{ZAMS}$ is determined from $(\underline{b}-\underline{y})_0$ since the uvby photometry appears normal.
- 103 \underline{V}_0 corrected by 0.7 for duplicity (separation 0"27, Δm 0.0, Holden 1972).
- 111 32 Orionis. \underline{V}_0 corrected by 0.2 for duplicity. This star is a definite foreground object and is a member of Blaauw's Cassiopeia-Taurus group (Blaauw 1956) and Eggen's Pleiades group (Eggen 1974).
- 114 \underline{V}_0 corrected by 0.7 for duplicity (separation 0"16, Δm 0.0, Worley 1971).
- 123 33 Orionis. \underline{V}_0 corrected by 0.3 for duplicity (separation 1"87, Δm 1.3, Worley 1971).
- 234 This star should be reobserved. The high $\delta\beta$ index could be due to emission, yet the photometry agrees with the HD type; also, the color excess is high for such a small distance modulus.

NOTES TO TABLE 5a (CONTINUED)

353 V_0 corrected by 0.3 for multiplicity. Because of the large negative $\delta\beta$ index, probably due to contamination from the other components, the intrinsic color $(\underline{b}-\underline{y})_0$ has been used to derive $\underline{M}_V(\beta)_{ZAMS}$.

377,
378 The $\delta\beta$ value clearly shows emission effects while the four-color photometry agrees with the MK spectral type. $\underline{M}_V(\beta)_{ZAMS}$ is derived from $(b-y)_0$. These stars comprise the visual binary system IDS150-67AB--component B is 377. Meisel (1968) gives a spectral type of B8 V:(e)nn for B (noting that H β appears to be in emission) and B5 V for A while other available types are normal for both stars (see Table 2 of Paper I). The $\delta\beta$ index for component B appears not to show a large emission effect while A does. Meisel also derives $\underline{M}_V = -0.4$ for his component B using a Δm of 0.66 on the basis that this is a physical system; however, our photometry suggests that the two stars are very similar and that component B is considerably farther away.

421 ω Orionis. The β index is strongly affected by line emission and $(\underline{b}-\underline{y})_0$ calibration is not strictly applicable for MK class III. The absolute visual magnitude given is therefore the value appropriate for spectral type B2 III and is determined from a mean of the MK calibrations discussed in Paper II.

NOTES TO TABLE 5a (CONTINUED)

- The agreement of the c_0 photometric temperature subclass and the slightly high $E(b-y)$ suggest a small amount of local visual absorption. Nebulosity is visible on the Palomar Sky Survey prints.
- 436 The $\delta\beta$ index suggests a possible field star but the proper motions are not definitive. For the present we assume membership.
- 482 The β index appears affected by emission but no further information is available for this star. The $(b-y)_0$ index implies $M_V(\beta)_{ZAMS} = +1.1$, which gives $dm = 5.5$, so the star may be an evolved foreground object. The m_0 index is low for this c_0 , however, and is more consistent with the observed β index. An MK type is needed.
- 484 Both the $\delta\beta$ index and proper motions suggest that this is a foreground field star.
- 489 The β index implies emission; $(b-y)_0$ gives $M_V(\beta)_{ZAMS} = +1.0$, placing the star 2 mag closer in distance modulus. Again m_0 is low for the c_0 value and more consistent with the observed β . The proper motions are not definitive--an MK type is needed.
- 496 V_0 corrected by 0.2 for duplicity. The distance modulus and proper motions suggest a foreground field star. MK type and radial velocity needed.

NOTES TO TABLE 5a (CONTINUED)

503 M 78B. The photometric indices appear affected by the nearby F-type optical companion which is 1.5 mag fainter and 2".1 distant. This is most clearly seen in the high \underline{m}_0 index, although the \underline{c}_0 index appears little affected and yields the correct spectral type. The β index may be similarly contaminated by the companion, hence the $(\underline{b}-\underline{y})_0$ color has been used to determine $\underline{M}_V(\beta)_{\text{ZAMS}}$. The resulting \underline{M}_V , as read from the calibration curve, is actually slightly fainter than -3.0 and the dm has therefore been rounded down to 9.1. Stars 502 and 503 are associated with the reflection nebula NGC 2068 (M 78) and are discussed by Sharpless (1952), Lee (1968), and more recently by Strom *et al.* (1975). The latter authors have found a number of infrared objects in the area, indicating this to be a region of current star formation. This nebula appears to be located beyond the Ia subgroup and should probably be considered apart from it physically. Lee suggests from near-infrared observations that the ratio of total-to-selective absorption is approximately normal for the two brighter stars discussed here.

504 The $\delta\beta$ index suggests a foreground field star, although there may be an emission problem. The available proper motions are not discordant with membership.

NOTES TO TABLE 5a (CONCLUDED)

- 512 Further observations are needed. The high β index suggests strong hydrogen lines or anomalous colors, but since the colors check with the HD type, $\underline{M}_V(\beta)_{ZAMS}$ is derived from $(\underline{b}-\underline{y})_0$.
- 515 The photometry indicates that this may be an Ap star having an abnormally high \underline{m}_1 index. It may be a foreground object, but the proper-motion data are not definitive and no other information exists. An MK spectral type is needed.
- 523 This star may be a more extreme example of the situation found for ω Orionis (421). Strong emission affects the β index while the four-color parameters appear normal for the spectral type. The distance modulus is rather low, yet the star is heavily reddened, possibly by local material. $\underline{M}_V(\beta)$ is derived from $(\underline{b}-\underline{y})_0$.
- 525 \underline{V}_0 corrected by 0.1 for duplicity.

TABLE 5b
DATA FOR I-TYPE STARS, SUBGROUP a

(1) Star	(2) ID	(3) V	(4) (b-y)	(5) m ₁	(6) c ₁	(7) (u-b)	(8) β	(9) r	(10) V _o	(11) (b-y) _o	(12) m _o	(13) c _o	(14) (u-b) _o	(15) α _o	(16) δm _o	(17) δc _o	(18) δ(u-b) _o	(19) E(b-y)	(20) M _V	(21) dm	(22) Spectrum	(23) Note
5	33023	8 ^m 31	0 ^m 071	0 ^m 183	0 ^m 995	1 ^m 503	2 ^m 876	0 ^m 032	8 ^m 20	0 ^m 047	0 ^m 190	0 ^m 990	1 ^m 464	0 ^m 059	0 ^m 009	0 ^m 033	-0 ^m 000	0 ^m 024	+1 ^m 3	6 ^m 9	B9	
55	35793	9.79	0.067	0.164	1.002	1.464	2.919	-0.008	9.52	0.003	0.183	0.989	1.361	-0.012	-0.011	0.018	-0.037	0.064	+1.6	7.9	A0	
59	294103	9.76	0.074	0.160	0.994	1.462	2.889	0.019	9.51	0.016	0.177	0.982	1.369	0.004	0.004	0.003	-0.004	0.058	+1.2	8.3	A2	
64	290469	9.795	0.070	0.194	0.974	1.502	2.903	-0.002	9.68	0.043	0.202	0.969	1.458	0.054	-0.005	0.007	-0.001	0.027	+1.9	7.8	A2	
73	290470	9.77	0.052	0.184	0.989	1.461	2.906	0.002	9.65	0.026	0.192	0.984	1.419	0.030	-0.001	0.011	0.011	0.026	+1.7	8.0	A2	
85	36057AB	8.71	0.051	0.189	0.957	1.437	2.894	0.002	8.9	0.035	0.194	0.954	1.411	0.040	-0.000	-0.014	0.027	0.016	+1.7	7.2	A0	*

85 V_o corrected by 0.3 for duplicity.

TABLE 5c
DATA FOR A- AND F-TYPE STARS, SUBGROUP a

(1) Star	(2) ID	(3) V	(4) (b-y)	(5) m ₁	(6) c ₁	(7) (u-b)	(8) β	(9) V _o	(10) (b-y) _o	(11) m _o	(12) c _o	(13) (u-b) _o	(14) δm _o	(15) δc _o	(16) δ(u-b) _o	(17) E(b-y)	(18) M _V	(19) dm	(20) Sp	(21) Spectrum	(22) Note	
505	38662A	9 ^m 35	0 ^m 053	0 ^m 187	1 ^m 033	1 ^m 513															B9	
514	39033	7.90	0.078	0.217	0.973	1.563	2.874	7.86	0.065	0.221	0.970	1.543	-0.014	0.052	-0.073	0.013	+1.9	6.0	A5	B9	*,NM	
524	39572	8.43	0.119	0.229	0.863	1.559	2.844	8.35	0.101	0.234	0.859	1.531	-0.026	0.002	-0.060	0.018	+2.4	5.9	A7	B9	*,NM	

514, 524 Classified as A-type on basis of high m₁ index. The large negative δm_o values suggest metallic-line spectra and MK classifications are desirable. Proper motions for these stars suggest non-membership, in addition to the distance moduli above.

TABLE 6a
DATA FOR B-TYPE STARS, SUBDIVISION b1

(1) Star	(2) ID	(3) V	(4) (b-y)	(5) m ₁	(6) c ₁	(7) (u-b)	(8) B	(9) δB	(10) V ₀	(11) (b-y) ₀	(12) m ₀	(13) c ₀	(14) (u-b) ₀	(15) E(b-y)	(16) E(U-B)	(17) M _V	(18) dm	(19) Sp	(20) Spectrum	(21) Note
407	294271B	7.91	-0.037	0.107	0.411	0.551	2.726	-0.010	7.74	-0.077	0.119	0.403	0.487	0.040	0.037	-0.4	8.2	B5	B5V	
408	294272A	7.85	0.002	0.135	0.855	1.129	2.828	0.008	7.69	-0.034	0.146	0.848	1.072	0.036		+0.9	6.8	B9	B8V	
414	37479E	6.68:	-0.069	0.099	0.039	0.099	2.598	0.033	6.49:	-0.113	0.112	0.030	0.029	0.044	0.044	-1.9	(8.4)	B1	B0.5V, B2Vp	*
415	37468AB	3.80:	-0.084	0.053	-0.082	-0.144	2.605	-0.002	4.1 :	-0.125	0.065	-0.090	-0.209	0.041	0.034	-3.9	(8.0)	B0	O9.5V	*
424	37524	8.745	-0.016	0.133	0.804	1.038	2.833	-0.018	8.65	-0.038	0.140	0.800	1.002	0.022	0.020	+0.9	7.7	B8	B9V, B9.5V	
425	37525	8.08	-0.022	0.099	0.345	0.499	2.699	0.003	7.81	-0.084	0.118	0.333	0.400	0.062	0.065	-1.0	8.8	B3	B5V, B6V	
426	37545	9.305	0.009	0.129	0.894	1.170	2.849	0.005	9.14	-0.030	0.141	0.886	1.108	0.039	0.018	+1.0	8.1	B9	B9.5V	
434	37577	9.28	0.009	0.156	0.991	1.321	2.911	-0.016	9.15	-0.020	0.165	0.985	1.274	0.029	0.062	+1.3	7.8	A0	B9, A0V, A3:V	
438	37633	9.03:	0.053	0.145	0.464:	0.860	2.743	-0.018:	8.49:	-0.073:	0.183:	0.439:	0.658:	0.126:	0.114	-0.2	(8.6)	B5	B9.5p Eu-Si	*
441	37641	7.57	-0.021	0.117	0.618	0.810	2.784	-0.022	7.41	-0.057	0.128	0.611	0.753	0.036	0.038	+0.1	7.5	B7	B6V, B7V	*
446	37674	7.675	0.003	0.088	0.265	0.447	2.665	0.017	7.27	-0.092	0.117	0.246	0.295	0.095	0.077:	-1.8	9.0	B3	B3Vn, B3-5Vn, B5:Vn	
447	37686	9.23	0.016	0.142	0.966	1.282	2.862	0.023	9.06	-0.023	0.154	0.958	1.220	0.039	0.040	+1.1	8.0	B9	B9Vn	
449	290813	11.00	0.358	0.061	0.922	1.760	2.863	-0.029	9.31	-0.034	0.179	0.844	1.133	0.392	0.408	+1.1	8.2	B8	B8, A0	
450	37699	7.625	-0.057	0.113	0.253	0.365	2.685	-0.003	7.47	-0.092	0.124	0.246	0.309	0.035	0.051	-1.3	8.8	B3	B4V	
458	37744	6.22	-0.077	0.073	0.045	0.037	2.629	0.004	6.06	-0.112	0.084	0.038	-0.019	0.035	0.030	-2.9	9.0	B1	B1V, B1.5V	
460	37742AB	1.76	-0.061	0.033	-0.121	-0.177	2.564	0.024	1.8	-0.129	0.053	-0.135	-0.286	0.068	0.071	-6.1	7.9	O9	O9.5Ib+BOIII	*
463	37756	4.93	-0.095	0.098	0.098	0.104	2.632	0.012	5.1	-0.107	0.102	0.096	0.085	0.012	0.012	-2.8	7.9	B2	B2IV-V, B3V, B3III	*
465	37776	6.98	-0.053	0.100	0.056	0.150	2.632	0.002	6.73	-0.112	0.118	0.044	0.056	0.059	0.077	-2.8	9.5	B1	B2V, B4V	*
466	294304	10.04	0.248	0.032:	0.657	1.217	2.721	0.038	8.73	-0.058	0.124:	0.596	0.727:	0.306		+0.1	8.6	B7	B8Ve	*
469	37806	7.96:	0.056	0.100	0.801:	1.113:	2.695	0.112:	7.54:	-0.040:	0.129:	0.782:	0.959:	0.096:	0.090	(+0.7)	(6.8)	B8	B9pe	*
472	37886	9.00	0.002	0.110	0.672	0.896	2.780	-0.009	8.77	-0.052	0.126	0.661	0.810	0.054	0.047	+0.3	8.4	B7	B9V	
473	37903	7.83	0.127	0.057	0.099	0.467	2.645	-0.010	6.81	-0.111	0.128	0.051	0.086	0.238	0.245	-2.3	9.1	B1	B1.5V, B2V	*
481	37927	8.44	-0.012	0.110	0.506	0.702	2.740	-0.001	8.20	-0.068	0.127	0.495	0.612	0.056	0.040	-0.2	8.4	B6	B6V	
490	38087	8.29	0.143	0.053	0.327	0.719	2.700	-0.010	7.30	-0.089	0.123	0.281	0.348	0.232	0.216	-0.9	8.2	B3	B5V	
494	38165	8.81:	0.187	0.078	0.551	1.081	2.747	-0.007	7.72:	-0.067	0.154	0.500	0.674	0.254	0.275:	-0.1	(7.8)	B6	B7IV-V	
500	38352	9.16	0.071	0.129	1.003	1.403	2.873	0.022	8.76	-0.020	0.156	0.985	1.257	0.091	0.083	+1.1	7.6	B9	A0	

NOTES TO TABLE 6a

414 HR 1932 = σ Ori E. This star has been demonstrated to be a member of the multiple system σ Ori by Greenstein and Wallerstein (1958). A fine abundance analysis by Klinglesmith et al. (1970) has shown an atmospheric enrichment of helium (hydrogen deficiency) and the star has since become the prototype for group II He stars (Kaufmann and Hunger 1972). These peculiarities can be seen clearly by comparing the detailed spectral scans of σ Ori E and the normal B3 V standard ϵ Her presented by Faj \ddot{a} , Honeycutt and Warren (1973). The Balmer lines are weak compared to a standard of similar spectral type and the height of the Balmer jump is considerably reduced due to the increased flux below 3800 \AA . These features show clearly in the photometry--the β index is low, resulting in a large positive $\delta\beta$ value; the c_1 index is low and indicative of a higher T_{eff} than that given by the B2 spectral type. The absolute magnitudes derived from both β and $(\underline{b-y})_0$ are not acceptable [β gives -4.2 mag, $(\underline{b-y})_0$ gives -2.8 mag]. We therefore adopt the value of \underline{M}_V derived by Higgenbotham and Lee (1974) from both MK and corrected $\underline{W}(\text{H}\gamma)$ values. Hunger (1974) and Walborn (1974) have recently found σ Ori E to display a variable spectrum; and spectroscopic, spectrophotometric and photometric

NOTES TO TABLE 6a (CONTINUED)

observations (Walborn and Hesser 1976; Hesser, Walborn and Ugarte 1976) have detected a period of 1.19^d in several parameters. Kemp and Herman (1977) have discussed variable linear polarization that is phase locked with the light variations and Hesser, Moreno and Ugarte (1977) have shown that the complex double minimum light curve is stable over three seasons.

415 HR 1931 = σ Ori AB(CD?). It is uncertain which components were included in the observations since they have been obtained from the literature. Component B is certainly included and a correction of 0.36 has been applied (separation $0.23''$, Δm 1.0, Heintz 1974). After the reddening correction, this results in $\underline{V}_0 = 3.99$ for A only. The probable inclusion of components C and D at angular distances of $11.1''$ and $12.8''$, respectively (IDS), and having a combined magnitude $\underline{V} = 6.53$, as calculated from the individual magnitudes given by Odell (1974), results in an additional correction of 0.1 mag and a final corrected $\underline{V}_0 = 4.09$ for component A. As indicated by the photometric spectral type, the colors are more indicative of a B0 star (also possibly due to contamination from the B2 V and A2 V companions D and C, respectively), hence $\underline{M}_V(\beta)$ may be a bit faint (see MK absolute-magnitude comparison in Table 1,

NOTES TO TABLE 6a (CONTINUED)

Paper II). This is also suggested by the disagreement of distance moduli for 414 and 415, which form a physical pair; on the other hand, our resulting distance modulus of $(\underline{V}_0 - \underline{M}_V) = 8.0$ agrees with that determined by Heintz (1974) from the system's dynamical parallax, as obtained from a detailed orbital analysis of AB.

- 438 The four-color indices indicate an earlier temperature subclass, in agreement with the peculiar classification. This results in a large $\underline{E}(\underline{b}-\underline{y})$ value, a negative $\delta\beta$ index, and an overcorrection in calculation of the intrinsic indices.
- 441 An anomalous H β strength is indicated by the large negative $\delta\beta$ index; therefore $(\underline{b}-\underline{y})_0$ has been used to derive $\underline{M}_V(\beta)_{\text{ZAMS}}$ and the distance modulus.
- 460 HR 1948/9 = ζ Ori AB. \underline{V}_0 corrected by 0.2 for duplicity (separation 2".62, Δm 2.0, Worley 1971) and by 0.1 for SB.
- 463 \underline{V}_0 corrected by 0.3 for SB (Δm 1.1, Batten 1967).
- 465 IC 432. Nissen (1976) has found a strongly variable \underline{I} (4026) helium index, the mean of which corresponds to atmospheric helium enrichment. He also notes that Hunger (private communication) has observed spectrum variability similar to that displayed by σ Ori E.

NOTES TO TABLE 6a (CONCLUDED)

- 466 The emission is evident in β , hence $(\underline{b}-\underline{y})_0$ has been used to derive $\underline{M}_V(\beta)_{ZAMS}$. The high color excess is not surprising since this star is located in a heavily obscured region immediately south of the "Horsehead" Nebula.
- 469 The spectral peculiarities and emission (see notes to Table 2 of Paper I) make the intrinsic indices highly uncertain since the colors are too blue and β is abnormal. $(\underline{b}-\underline{y})_0$ used to derive $\underline{M}_V(\beta)_{ZAMS}$.
- 473 NGC 2023. Located in an obscured region northeast of the "Horsehead." Nebulosity surrounds stars in the area and appears locally concentrated about this one.

TABLE 6b
DATA FOR I-TYPE STARS, SUBDIVISION b1

(1) Star	(2) ID	(3) V	(4) (b-y)	(5) m ₁	(6) c ₁	(7) (u-b)	(8) B	(9) r	(10) V ₀	(11) (b-y) ₀	(12) m ₀	(13) c ₀	(14) (u-b) ₀	(15) a ₀	(16) δm ₀	(17) δc ₀	(18) δ(u-b) ₀	(19) E(b-y)	(20) M _V	(21) dm	(22) Spectrum	(23) Note
373	294275	9 ^m .41	0 ^m .044	0 ^m .161	1 ^m .034	1 ^m .444	2 ^m .879	0 ^m .045	9 ^m .29	0 ^m .016	0 ^m .170	1 ^m .028	1 ^m .399	0 ^m .016	0 ^m .017	0 ^m .050	-0 ^m .003	0 ^m .028	+0 ^m .8	8 ^m .5	A1V	
376	37333	8.53	0.030	0.182	0.896	1.320	2.884	-0.008	8.49	0.022	0.184	0.894	1.307	0.011	-0.000	-0.086	0.080	0.008	+1.7	6.8	AOV	
464	37789	8.80	0.051	0.192	1.047	1.533	2.892	0.036	8.77	0.045	0.194	1.046	1.524	0.073	0.009	0.103	-0.052	0.006	+1.3	7.4	B9,A1,A2	*

464 A recent spectral type by Guetter (1976) of A3 V strengthens the intermediate-group assignment.

TABLE 6c
DATA FOR A- AND F-TYPE STARS, SUBDIVISION b1

(1) Star	(2) ID	(3) V	(4) (b-y)	(5) m ₁	(6) c ₁	(7) (u-b)	(8) B	(9) V ₀	(10) (b-y) ₀	(11) m ₀	(12) c ₀	(13) (u-b) ₀	(14) δm ₀	(15) δc ₀	(16) δ(u-b) ₀	(17) E(b-y)	(18) M _V	(19) dm	(20) Sp	(21) Spectrum	(22) Note
359	294270	10 ^m .88	0 ^m .383	0 ^m .102	0 ^m .412	1 ^m .382	2 ^m .604	10 ^m .67	0 ^m .335	0 ^m .116	0 ^m .402	1 ^m .305	0 ^m .095	0 ^m .094	0 ^m .191	0 ^m .048	(+3 ^m .5) (7 ^m .2)	G1	G0		
385	294269	10.68	0.527	0.276	0.360	1.966	2.573													G0	
405	294273	10.68	0.151	0.188	0.838	1.516	2.850	10.45	0.097	0.204	0.827	1.430	0.004	-0.043	0.042	0.054	(+2.7) (7.7)	A6	A3		
430	37564	8.49	0.139	0.175	1.042	1.670	2.823	8.31	0.097	0.187	1.034	1.604	0.019	0.207	-0.124	0.042	+0.9	7.4	A8	A5:III:	NM?
437	294299	11.48	0.394	0.056	1.263	2.163	2.848													F2	*
442	294298	10.80	0.515	0.239	0.290	1.798	2.578														G0,G3
448	294307	10.44	0.350	0.152	0.438	1.442	2.638	10.31	0.322	0.161	0.432	1.397	0.018	0.056	-0.008	0.028	+3.4	6.9	F8	F8,G0	NM?
453	294301	11.06	0.284	0.113	0.586	1.380	2.709	10.82	0.228	0.130	0.575	1.291	0.044	0.008	0.092	0.056	(+3.1) (7.7)	F3	A5,F3:		*
455	294297	10.12	0.366	0.144	0.385	1.405	2.634	9.95	0.327	0.156	0.377	1.343	0.026	0.009	0.055	0.039	+3.9	6.0	F8	G0	NM
468	37805	7.53	0.158	0.203	0.744	1.466	2.770	7.59	0.171	0.199	0.747	1.487	-0.007	0.027	-0.037	-0.013	+2.6	5.0	F0	A5	NM
474	37904AB	6.43	0.199	0.179	0.697	1.453	2.726	6.47	0.209	0.176	0.699	1.469	0.001	0.081	-0.062	-0.010	+2.4	4.1	F3	A7:V:	*,NM
478	294303	11.03	0.334	0.119	0.544	1.450	2.676	10.73	0.266	0.140	0.530	1.341	0.030	0.063	0.008	0.068	(+2.8) (7.9)	F5	F2,F8		
480	294302	11.45	0.355	0.182	0.458	1.532	2.556													F8	

437 The high c₁ value places this star outside the range of the calibration. It appears to be a reddened background giant.

453 The status of this star is uncertain. Although the low value of m₁ suggests a B-type star, the photometry would imply a B6 type at a distance modulus of 10.3, having a reddening of E(b-y) = 0.35 and a high m₀ index of 0.22. Due to the assigned spectral types of A5 and F3, we have preferred to classify it as an F star at the approximate distance of the nearby program stars and having normal reddening for its distance.

474 V₀ corrected by 0.4 for duplicity.

TABLE 7a
DATA FOR B-TYPE STARS, SUBDIVISION b2

(1) Star	(2) ID	(3) V	(4) $(b-y)$	(5) m_1	(6) c_1	(7) $(u-b)$	(8) β	(9) $\delta\beta$	(10) V_0	(11) $(b-y)_0$	(12) m_0	(13) c_0	(14) $(u-b)_0$	(15) $E\{b-y\}$	(16) $E(U-B)$	(17) M_V	(18) dm	(19) Sp	(20) Spectrum	(21) Note
118	36341	8.35	0.005	0.112	0.591	0.825	2.776	-0.020	8.07	-0.060	0.131	0.578	0.721	0.065	0.059	+0.3	7.8	B7	B9	
121	36352	9.20	0.015	0.149	0.991	1.319	2.925	-0.030	9.05	-0.021	0.160	0.984	1.262	0.036	0.030	+1.2	7.8	B9	B9	*
132	36393	8.48	-0.020	0.095	0.499	0.649	2.744	-0.007	8.27	-0.069	0.110	0.489	0.571	0.049	0.029	-0.1	8.4	B6	B8, B9	
138	36444	8.98	0.007	0.107	0.835	1.063	2.799	0.028	8.80	-0.036	0.120	0.826	0.994	0.043	0.031	+0.6	8.2	B8	B9V	
145	36502	9.23	0.016	0.105	0.918	1.160	2.846	0.018	9.04	-0.028	0.118	0.909	1.090	0.044	0.021	+1.0	8.1	B9	B9, 5V	
148	36526	8.31	-0.034	0.110	0.345	0.497	2.703	-0.001	8.10	-0.083	0.125	0.335	0.418	0.049	0.047	(-0.9)	(9.0)	B3	B9p S1-Sr, B6-7IV-Vw	*
159	36591AB	5.34	-0.073	0.077	-0.002	0.006	2.612	0.011	5.15	-0.117	0.090	-0.011	-0.064	0.044	0.054	-3.6	8.7	B1	B1V, B1 IV, B1.5 III	
160	36592	9.05	0.015	0.112	0.854	1.108	2.821	0.014	8.84	-0.034	0.127	0.844	1.029	0.049	0.039	+0.8	8.0	B8	B8V	
161	36590	9.35	-0.015	0.142	0.871	1.125	2.847	-0.002	9.28	-0.032	0.147	0.868	1.098	0.017	0.026	+1.0	8.3	B9	B9V	
164	36617	8.44	0.018	0.141	0.950	1.268	2.899	-0.021	8.26	-0.025	0.154	0.941	1.200	0.043	0.013	+1.2	(7.0)	B9	B9, 5V	
170	36628	7.98	-0.007	0.115	0.834	1.050	2.816	0.011	7.86	-0.036	0.124	0.828	1.004	0.029	0.022	+0.8	7.1	B8	B9V, B9, 5V	
173	36646AB	6.54	-0.036	0.100	0.278	0.406	2.689	-0.002	6.6	-0.090	0.116	0.267	0.319	0.054	0.057	-1.2	7.8	B3	B2, 5V, B3V, B4Vn	*
179	36684AB	8.65	0.003	0.133	0.930	1.202	2.849	0.022	9.3	-0.026	0.142	0.924	1.155	0.029	0.032	+1.0	8.3	B9	B9V, AOV	*
184	36695	5.345	-0.067	0.060	0.025	0.011	2.623	0.005	5.3	-0.114	0.074	0.016	-0.065	0.047	0.055	-3.1	8.4	B1	B1V, B1.5 III	*
197	36781	8.52	0.052	0.086	0.466	0.742	2.731	-0.006	7.98	-0.073	0.124	0.441	0.542	0.125	0.106	-0.4	8.3	B5	B5V, B5 IV-V, B6V	
202	36779A	6.23	-0.068	0.093	0.133	0.183	2.647	0.004	6.07	-0.104	0.104	0.126	0.126	0.036	0.041	-2.3	8.3	B2	B2, 5V, B3V	
210	36826	8.22	0.054	0.084	0.378	0.654	2.685	0.020	7.64	-0.082	0.125	0.351	0.437	0.136	0.123	-0.8	8.4	B4	B5Vn, B5-6Vn	*
211	36827	6.69	-0.067	0.101	0.207	0.275	2.657	0.013	6.56	-0.096	0.110	0.201	0.228	0.029	0.027	-2.0	8.5	B2	B5	
213	36825	8.655	0.016	0.139	0.891	1.201	2.875	-0.023	8.46	-0.030	0.153	0.882	1.127	0.046	0.062	+1.1	7.3	B9	AOV	
222	290666	9.81	0.067	0.118	1.005	1.375	2.896	-0.000	9.43	-0.020	0.144	0.988	1.236	0.087	0.078	+1.2	8.2	A0	B8, A1V	
241	36915	8.015	0.022	0.107	0.618	0.876	2.754	0.006	7.67	-0.058	0.131	0.602	0.749	0.080	0.075	0.0	7.7	B7	B8V, B9V	
256	36954	6.97	-0.044	0.107	0.282	0.408	2.698	-0.009	6.9	-0.090	0.121	0.273	0.335	0.046	0.063	-1.0	7.9	B3	B3V	*
257	290665	9.44	0.037	0.207	0.829	1.317	2.854	-0.033	9.13	-0.037	0.229	0.814	1.199	0.074	0.099	+1.0	(8.1)	B8	Ap Cr-Eu-(Sr)	*
267	36980AB	8.99	0.034	0.117	0.947	1.249	2.841	0.034	8.73	-0.025	0.135	0.935	1.154	0.059	0.058	+1.0	(7.8)	B9	B9, 5V, AOV, AOV IV	NM?
294	290684	9.56	0.056	0.149	0.999	1.409	2.906	-0.012	9.23	-0.021	0.172	0.984	1.287	0.077	0.139	+1.3	(8.0)	B9	A1V, A2V	*
310	37076A	8.06	-0.024	0.107	0.567	0.733	2.734	0.018	7.90	-0.062	0.118	0.559	0.673	0.038	0.028	-0.3	(8.2)	B7	B8V, B9V	
311	290671B	8.95	0.001	0.129	0.909	1.169	2.850	0.011	8.83	-0.028	0.138	0.903	1.122	0.029	0.029	+1.0	7.8	B9	A2-, B9, 5V	
318	37113	8.65	0.022	0.132	0.852	1.160	2.848	-0.015	8.41	-0.034	0.149	0.841	1.070	0.056	0.065	+1.0	7.4	B8	B9V, B9, 5V, AOV	
324	37112	8.02	-0.012	0.094	0.473	0.637	2.733	-0.003	7.76	-0.071	0.112	0.461	0.542	0.059	0.046	-0.3	8.1	B6	B6V, B7V	
328	37128A	1.69	-0.032	0.026	-0.090	-0.102	2.545	0.052	1.28	-0.127	0.054	-0.109	-0.253	0.095	0.088	-7.0	8.3	O9	B0 Ia	*
334	37149	8.035	-0.016	0.087	0.463	0.605	2.683	0.045	7.79	-0.072	0.104	0.452	0.515	0.056	0.113	-1.3	9.1	B6	B6Vnn, B7V, B8V	*, NM?
341	37173	7.86	-0.010	0.105	0.392	0.582	2.713	-0.002	7.56	-0.079	0.126	0.378	0.471	0.069	0.079	-0.7	8.2	B4	B5V, B6V	
342	37187	8.135	0.016	0.121	0.755	1.029	2.804	-0.011	7.88	-0.044	0.139	0.743	0.933	0.060	0.050	+0.6	7.2	B8	B9V	
354	37235	8.17	-0.032	0.106	0.544	0.692	2.734	0.014	8.03	-0.064	0.116	0.538	0.641	0.032	0.022	-0.3	8.3	B6	B8V, B7V-AOV, B7V	*
358	37272	7.91	-0.048	0.109	0.397	0.519	2.729	-0.016	7.78	-0.078	0.118	0.391	0.471	0.030	0.037	-0.4	8.2	B4	B5V, B6Ve	*
372	37321AB	7.11	-0.035	0.120	0.404	0.574	2.741	-0.027	7.3	-0.078	0.133	0.395	0.506	0.043	0.054	-0.6	7.9	B5	B3V, B4V	*
379	37332	7.61	-0.051	0.104	0.391	0.497	2.730	-0.018	7.49	-0.079	0.112	0.385	0.453	0.028	0.027	-0.4	7.9	B4	B5V, B5 IV-V	
383	37344	8.75	-0.024	0.141	0.872	1.106	2.857	-0.010	8.72	-0.032	0.143	0.870	1.094	0.008	0.014	+1.0	7.7	B9	B8V, B9V	
388	37370AB	7.46	-0.001	0.103	0.512	0.716	2.738	0.002	7.9	-0.068	0.123	0.499	0.609	0.067	0.071	-0.2	8.1	B6	B6V	*
393	37371CD	7.95	0.068	0.127	0.819	1.209	2.797	0.017	8.2	-0.039	0.159	0.798	1.038	0.107	0.126	+0.6	7.6	B8	B9, AOV+A1 III	*
397	37397	6.84	-0.071	0.114	0.200	0.286	2.662	0.007	6.73	-0.097	0.122	0.195	0.244	0.026	0.039	-1.8	8.6	B2	B2V, B3V	
404	37427AB	8.62	0.012	0.098	0.660	0.880	2.758	0.010	8.4	-0.053	0.118	0.647	0.776	0.065	0.053	+0.1	8.3	B7	B8V	*
445	290798	10.39	0.276	0.095	1.101	1.843	2.838	0.074	9.14	-0.015	0.182	1.043	1.378	0.291	0.279	(+0.9)	(8.2)	B9	A1, A2	*, NM?
457	290787	10.14	0.446	0.033	0.639	1.597	2.760	-0.012	7.95	-0.064	0.186	0.537	0.781	0.510	0.492	+0.1	7.8	B6	B8, A0	

NOTES TO TABLE 7a

- 121 The H β line strength appears anomalous and places this star 0.2 mag below the ZAMS according to the intrinsic colors. The $(\underline{b-y})_0$ color has been used to derive $\underline{M}_V(\beta)_{\text{ZAMS}}$, but this changes the distance modulus by only 0.2 mag.
- 148 As expected from the peculiar and He-weak classifications, this star appears much earlier photometrically than spectroscopically. Using the \underline{Q} -method of Johnson and Morgan (1953), Bernacca and Ciatti (1972) have determined \underline{S}_Q as B4. The latter authors have provided the B6-7IV-Vw classification and note that the star may display a variable spectrum. As can be seen in the table, the H β line strength is perfectly normal for the photometric colors. The significant problem in the present work is whether these He-weak stars have luminosities corresponding to their colors or to their spectral types. Evidence has been presented (Bernacca and Molnar 1972) that the energy distributions of most He-weak stars are normal and this view is supported for HD 36526 by the agreement of the intrinsic-color and β indices and by the derived $\underline{E}(\underline{b-y})$. The He-weak stars supposedly do, however, have systematically lower luminosities than do 'normal' stars having similar colors (Garrison 1973) and this is supported by the unexpectedly large distance modulus derived for

NOTES TO TABLE 7a (CONTINUED)

- HD 36526, for which Nissen (1976) finds the helium abundance to be about a factor 2 lower than in normal field stars. The above discussion suggests that the color excess be employed but that the mean distance to the group should be used to derive \underline{M}_V .
- 173 \underline{V}_0 corrected by 0.3 for duplicity (separation 1"5, Δm 1.3, R. L. Walker Jr. 1969).
- 179 \underline{V}_0 corrected by 0.75 for duplicity.
- 184 VV Ori. This multiple system is described in a note to Table 2 of Paper I. The fact that the secondary spectrum has been seen and that a tertiary component is present leads us to a correction of 0.2 in \underline{V}_0 . The photometry does not appear to show any peculiarities. For a detailed study of this system see Duerbeck (1975).
- 210 There may be a rotational-velocity effect on β , but no $\underline{v}_e \sin i$ is available. From $(\underline{b}-\underline{y})_0$ we obtain $\underline{M}_V(\beta)_{ZAMS} = -0.8$, which places the star at dm 8.4. The β index corresponds to a spectral subclass slightly earlier than B3, hence we have chosen to use the intrinsic color in this case. Crawford and Barnes (1966) declare this star a non-member on the basis of its position in their β , $(\underline{U}-\underline{B})_0$ diagram, but the seemingly evolved nature of the star may be caused by an anomalous β index, as mentioned above.
- 256 \underline{V}_0 corrected by 0.1 for SB.

NOTES TO TABLE 7a (CONTINUED)

- 257 Photometry supports Ap classification, the photometric colors being too blue for both temperature class and β index. We assume that a redistribution of flux gives the excessively blue colors and that the β index yields the appropriate absolute magnitude, as discussed in Paper II; i.e. the normal procedure of the photometry determining the reddening and β defining the absolute magnitude is used here.
- 294 This star has also been reduced by the method for I-group stars because of its high β index. The method gives comparable results: $\underline{E(b-y)} = 0.066$, $\underline{M_V} = +1.2$.
- 328 ϵ Ori. A small amount of emission may be present at $H\beta$. Emission has been found at $H\alpha$ by Rosendhal (1973) and the β index gives $\underline{M_V}(\beta) = -7.5$, 0.5 brighter than the MK calibrations discussed in Paper II. The presence of emission here is also suspected because the $\underline{M_V}(\beta)$ and $\underline{M_V}(\text{MK})$ calibrations agree well for supergiants in the association. We therefore use the most recent MK value of Walborn (1972) in the table.
- 334 This star is a possible non-member on the basis of its large $\delta\beta$ index, and was categorized as such by Crawford and Barnes (1966). Previous spectral classification work (see references cited in Table 2, Paper II) has revealed no reported emission to account for the low β value, but the high rotational velocity of 395 km s^{-1}

NOTES TO TABLE 7a (CONTINUED)

(Sharpless 1974) may be the cause. The difference between spectroscopic and photometric classification has been cited by Bernacca and Ciatti (1972) to be three spectral subclasses and the four-color results agree approximately. The $[\underline{u}-\underline{b}]$, β calibration of Eggen (1974), as discussed in Paper II, gives $\underline{M}_V = -2.4$, evidently much too bright, while the $(\underline{b}-\underline{y})_0$, $\underline{W}(\text{H}\gamma)$ calibration yields $\underline{M}_V = -0.9$, in fair agreement with $\underline{M}_V(\beta)$. Crampton and Byl (1971) derive an average distance modulus of 8.6 using Balmer line and UBV photometry plus MK type. The proper-motion data are not definitive (code b), while the radial velocity is somewhat low and is also coded b in Table 11 of Paper I.

- 354 Noted as a spectrum variable by Bernacca and Ciatti (1972) but the present photometry does not display any outstanding peculiarities. The radial velocity (Crampton and Byl 1971) supports membership.
- 358 Bernacca and Ciatti (1972) report an H β emission core and one would expect from this and the photometrically earlier spectral type a positive $\delta\beta$ index. The H β line may be anomalously strong but does not appear to have varied between the observations of Crawford and Barnes (1966) and that of the present investigation (see Table 17 of Paper I).

NOTES TO TABLE 7a (CONTINUED)

- 372 Molnar (1972) notes from variations of the He line strengths that this star appears to have changed its spectral type. Old objective-prism plates show B8, in agreement with the HD catalogue, but the photometric and spectroscopic classifications agree here. \underline{V}_0 has been corrected by 0.4 for duplicity (separation 0".77, Δm 0.8, Worley 1972); the β index appears affected by the presence of the cooler secondary, hence $(\underline{b}-\underline{y})_0$ has been used to derive $\underline{M}_V(\beta)_{ZAMS}$.
- 388 \underline{V}_0 corrected by 0.7 for duplicity. The higher than average reddening for this star and for 393 is not surprising since both are imbedded in or behind nebulosity clearly visible on the National Geographic-Palomar Sky Survey print of the region.
- 393 \underline{V}_0 corrected by 0.7 for duplicity. The average \underline{V} magnitude from Table 2 of Paper I is 7.95. Sharpless (1962) measured the two components separately and found $\underline{V} = 8.83$ and 8.66 for the east (D) and west (C) components, respectively. The difference 0.17 implies a correction to \underline{V} which yields 8.62, in good agreement with the individual \underline{V} measured for the primary.
- 404 \underline{V}_0 corrected by 0.1 for duplicity.
- 445 The intrinsic parameters are uncertain because \underline{c}_1 is near the upper limit of the calibration range. The photometry indicates that this is an evolved star,

NOTES TO TABLE 7a (CONCLUDED)

possibly of luminosity class III or IV. The only proper motion available is compatible with membership.

TABLE 7b
DATA FOR I-TYPE STARS, SUBDIVISION b2

(1) Star	(2) ID	(3) V	(4) (b-y)	(5) m ₁	(6) c ₁	(7) (u-b)	(8) β	(9) r	(10) V ₀	(11) (b-y) ₀	(12) m ₀	(13) c ₀	(14) (u-b) ₀	(15) a ₀	(16) δm ₀	(17) δc ₀	(18) δ(u-b) ₀	(19) E(b-y)	(20) M _v	(21) dm	(22) Spectrum	(23) Note
189	290603	10 ^m 18	0 ^m 058	0 ^m 177	0 ^m 972	1 ^m 442	2 ^m 912	-0 ^m 011	10 ^m 00	0 ^m 016	0 ^m 190	0 ^m 964	1 ^m 374	0 ^m 008	-0 ^m 007	-0 ^m 017	0 ^m 005	0 ^m 042	+1 ^m 7	8 ^m 3	A2Vn	
203	290605	10.12:	0.071	0.194	0.936	1.466	2.910	-0.022	9.97:	0.037	0.204	0.929	1.411	0.038	-0.011	-0.040	0.025	0.034	+2.1	(7.9)	A0,A1	
247	36955	9.46	0.057	0.198	0.848	1.358	2.866	-0.008	9.45	0.054	0.199	0.847	1.353	0.052	-0.002	-0.115	0.102	0.003	+2.0	7.5	A0,A1,A2	*
333	290677	10.01	0.117	0.179	0.905	1.497	2.863	0.011	9.75	0.057	0.197	0.893	1.402	0.051	-0.000	-0.070	0.051	0.060	+1.6	8.1	B9,A0,A5V	*
343	37172	8.30	0.068	0.156	1.010	1.458	2.887	0.027	8.06	0.012	0.173	0.999	1.368	-0.000	0.007	0.023	-0.015	0.056	+1.0	7.0	A3V	
355	290672	10.17	0.085	0.168	1.015	1.521	2.875	0.039	9.96	0.037	0.183	1.005	1.444	0.040	0.011	0.037	-0.005	0.048	+1.1	8.9	A0,A2	
361	37284	8.98	0.057	0.169	0.949	1.401	2.900	-0.007	8.78	0.012	0.183	0.940	1.328	-0.005	-0.005	-0.033	0.015	0.045	+1.6	7.2	A1III-IV	*
452	290799	10.63	0.117	0.164	0.841	1.403	2.832:	0.019	10.36:	0.053:	0.183:	0.828:	1.301:	0.027:	0.007:	-0.145:	0.127:	0.064:	(+1.3)	(9.0)	A0	*

247 Star is also included in Table 7c for A- and F-type stars because its classification as to type is uncertain. The c₁ index is considerably lower than expected from β for both groups. Further observations and an MK type are desirable.

333 See note for 247. The new MK type is from Guetter (1976) and clarifies the situation

361 A new MK type by Guetter (1976) of A2 V is more in agreement with the observed r value.

452 See note for 247.

TABLE 7c
DATA FOR A- AND F-TYPE STARS, SUBDIVISION b2

(1) Star	(2) ID	(3) V	(4) (b-y)	(5) m ₁	(6) c ₁	(7) (u-b)	(8) β	(9) V ₀	(10) (b-y) ₀	(11) m ₀	(12) c ₀	(13) (u-b) ₀	(14) δm ₀	(15) δc ₀	(16) δ(u-b) ₀	(17) E(b-y)	(18) M _v	(19) dm	(20) Sp	(21) Spectrum	(22) Note
174	290617	9 ^m 30:	0 ^m 167	0 ^m 164	0 ^m 951	1 ^m 613	2 ^m 795	9 ^m 14:	0 ^m 128	0 ^m 176	0 ^m 943	1 ^m 551	0 ^m 025	0 ^m 173	-0 ^m 083	0 ^m 039	+1 ^m 3	(7 ^m 8)	A9 A5	NM?	
208	36811A	7.08	0.088	0.196	0.971	1.539	2.883	6.94	0.057	0.205	0.965	1.490	0.001	0.029	-0.020	0.031	+2.0	4.9	A4	A1m,A3V	*,NM
223	36863	8.28	0.150	0.208	0.976	1.692	2.820	8.11	0.110	0.220	0.968	1.628	-0.014	0.148	-0.150	0.040	+1.4	6.7	A8	A0,A1,A2	*,NM?
247	36955	9.46	0.057	0.198	0.848	1.358	2.866	9.56	0.080	0.191	0.853	1.395	0.016	-0.049	0.075	-0.023	+2.7	6.7	A5	A0,A1,A2	*
333	290677	10.01	0.117	0.179	0.905	1.497	2.863	9.84	0.078	0.191	0.897	1.435	0.017	0.001	0.036	0.039	+2.3	7.5	A5	B9,A0,A5V	*
394	290750	9.86	0.113	0.194	0.891	1.505	2.860	9.73	0.083	0.203	0.885	1.457	0.005	-0.005	0.014	0.030	+2.4	7.3	A6	A5III	
432	290743	10.60	0.176	0.227	0.742	1.548	2.794	10.52	0.155	0.233	0.738	1.515	-0.033	-0.030	-0.047	0.021	+2.9	7.6	A9	B8,B9,A5	*
452	290799	10.63	0.117	0.164	0.841	1.403	2.832:	10.59:	0.107:	0.167:	0.839:	1.387:	0.040:	-0.003:	0.091:	0.010:	(+2.5)	(8.1)	A7	A0	*

208 The δm₀ index does not support the Am classification of Schild and Cowley (1971). The star is undoubtedly a foreground object, as previously suggested by Crampton and Byl (1971), and their radial velocity also supports this conclusion.

223 Considered by Sharpless (1962) and by Lee (1968) to be a reddened B star, but the high m₁ index indicates the A type, in fact, the δm₀ index suggests a possible metallic-line spectrum.

247 This star is also included in Table 7b for I stars, due to the uncertainty in determining its type. The large negative E(b-y) suggests that the type is earlier but, if so, the m₁ index is anomalously high.

333 May be a member of the I group and is also included in Table 7b.

432 The high m₁ index suggests that the A type is probably correct. When reduced as a B-type star, the color excess is quite high [E(b-y) = 0.22] and an unlikely value of 0.29 is derived for m₀.

452 The β index indicates an A type, but this star is included in Table 7b for I stars because of the low m₀ index and the reported spectral type.

TABLE 8a
DATA FOR B-TYPE STARS, SUBDIVISION b3

(1) Star	(2) ID	(3) V	(4) (b-y)	(5) m ₁	(6) c ₁	(7) (u-b)	(8) B	(9) δB	(10) V ₀	(11) (b-y) ₀	(12) m ₀	(13) c ₀	(14) (u-b) ₀	(15) E(b-y)	(16) E(u-B)	(17) M _V	(18) dm	(19) Sp	(20) Spectrum	(21) Note
61	35836	8.92	-0.030	0.175	0.961	1.251	2.884	0.003	8.95	-0.023	0.173	0.962	1.263	-0.007	0.018	+1.2	7.8	B9	B9,A2	*
63	35867A	8.14	-0.019	0.113	0.785	0.973	2.783	0.024	8.05	-0.040	0.119	0.781	0.939	0.021	0.010	+0.4	7.7	B8	B9	
76	35971	6.67	-0.028	0.125	0.844	1.038	2.830	0.004	6.64	-0.034	0.127	0.843	1.028	0.006	0.004	+0.9	5.8	B8	B9	NM
77	35972	8.83	0.087	0.091	0.715	1.071	2.717	0.060	8.24	-0.049	0.132	0.688	0.853	0.136	0.128	-0.6	8.9	B8	B8,A0	*,NM?
84	36046	8.07	-0.020	0.088	0.414	0.550	2.721	-0.005	7.82	-0.077	0.105	0.403	0.459	0.057	0.046	-0.5	8.4	B5	B7V	*
97	36139	6.88	0.035	0.155	1.080	1.460	2.872	0.082	6.68	-0.012	0.169	1.071	1.385	0.047	-0.016	+1.1	5.6	A0	B8,A0	*,NM
107	290517	9.00	-0.010	0.111	0.781	0.983	2.799	0.006	8.88	-0.041	0.120	0.775	0.934	0.031	0.025	+0.6	8.3	B8	B9,A0	
108	290516	9.47	-0.007	0.133	0.917	1.169	2.867	-0.001	9.38	-0.027	0.139	0.913	1.136	0.020	0.061	+1.1	8.3	B9	B9,A0	
112	290515	9.29	0.012	0.151	0.976	1.302	2.902	-0.013	9.14	-0.022	0.161	0.969	1.248	0.034	0.048	+1.3	7.9	B9	B9,A0	
115	36312	8.14	-0.012	0.100	0.673	0.849	2.795	-0.023	7.97	-0.051	0.112	0.665	0.786	0.039	0.025	+0.5	7.4	B7	B8	
117	36313AB	8.21	-0.016	0.124	0.571	0.787	2.772	-0.019	8.5	-0.061	0.138	0.562	0.714	0.045	0.034	+0.3	8.2	B7	B9p(S1)	*
129	290492AB	9.27	0.084	0.133	0.931	1.365	2.851	0.013	9.1	-0.028	0.167	0.909	1.186	0.112	0.112	+1.0	8.1	B9	A0	*
140	36485C	6.86	-0.063	0.118	0.185	0.295	2.663	0.001	6.70	-0.099	0.129	0.178	-0.238	0.036	0.028	-1.8	8.5	B2	B2V,B2IV-V	
141	36486A	2.225	-0.081	0.060	-0.126	-0.168	2.568	0.020	2.2	-0.129	0.074	-0.136	-0.245	0.048	0.061	-5.9	8.1	O8	O9.5II	*
144	-0 984	8.435	-0.045	0.134	0.518	0.696	2.741	0.002	8.34	-0.066	0.140	0.514	0.662	0.021		-0.2	8.5	B6	B9	
163	36605	7.96	0.081	0.092	0.817	1.163	2.762	0.050	7.44	-0.039	0.128	0.793	0.971	0.120	0.120	+0.1	7.3	B8	B8V	*,NM?
176	36668	8.07	-0.043	0.119	0.592	0.744	2.730	0.028	8.00	-0.059	0.124	0.589	0.719	0.016	0.007	-0.4	8.4	B7	B6Vwp	*
194	36726A	8.84	0.043	0.164	0.975	1.389	2.922	-0.036	8.56	-0.023	0.184	0.962	1.284	0.066	0.057 (+1.4)	(7.2)	B9	A0	*	
200	290556	9.56	0.119	0.087	0.677	1.089	2.746	0.022	8.82	-0.054	0.139	0.642	0.813	0.173	0.161	-0.1	(8.9)	B7	B9,A2	
201	36760	7.63	-0.039	0.108	0.575	0.713	2.767	-0.013	7.54	-0.061	0.114	0.571	0.678	0.022	0.016	+0.2	7.3	B7	B7V	
221	36841	8.60	0.071	0.071	0.547	0.831	2.742	0.002	8.01	-0.066	0.112	0.520	0.613	0.137	0.113	-0.2	8.2	B6	B6Vn,B7V	
240	36898AB	7.09	-0.020	0.109	0.546	0.724	2.747	0.001	6.90	-0.064	0.122	0.537	0.654	0.044	0.035	-0.1	(7.0)	B6	B6V,B7V	
255	36935	7.515	-0.042	0.096	0.441	0.549	2.716	0.008	7.38	-0.074	0.106	0.435	0.498	0.032	0.023	-0.6	8.0	B5	B5Vn,B6Vn,B7V	
274	37015	8.33	-0.023	0.133	0.869	1.089	2.846	-0.001	8.30	-0.032	0.136	0.867	1.075	0.009	0.009	+1.0	7.3	B9	B9,A0	
293	37037	8.50	0.037	0.104	0.736	1.018	2.797	-0.012	8.14	-0.046	0.129	0.719	0.885	0.083	0.070	+0.6	7.6	B8	B9V	
332	37140	8.55	0.105	0.079	0.407	0.775	2.711	-0.002	7.76	-0.080	0.135	0.370	0.479	0.185	0.184	-0.7	8.5	B4	B8p,B8III,B9.5IV-V	*

ORIGINAL PAGE IS
OF POOR QUALITY

NOTES TO TABLE 8a

- 61 The (b-y) index is several hundredths of a magnitude bluer than expected from the measured (B-V) of Hardie, Heiser and Tolbert (1964) and suggests variability, as is also indicated by the negative E(b-y). Since the distance modulus suggests possible membership, further observations should be made.
- 77 According to $\delta\beta$ this star is located about 1 mag above the ZAMS and may be a background field star. The only proper motion available is inconclusive regarding membership and a spectrogram would be useful to check for emission.
- 84 Nissen (1976) finds this star to be helium poor, as indicated here by the discrepancy between photometric and MK spectral types.
- 97 This star is a borderline case between the B and I groups and is included in both Tables 8a and 8b. The $\delta\beta$ index suggests an evolved field star, although this index is uncertain because of the high c₀ index. However, both the distance modulus and proper motions support this conclusion.
- 117 V₀ corrected by 0.5 for duplicity. The low $\delta\beta$ index may be due to the companion and/or to the peculiar spectral type.
- 129 V₀ corrected by 0.3 for duplicity.

NOTES TO TABLE 8a (CONTINUED)

- 141 δ Orionis A. \underline{V}_0 corrected by 0.2 (SB) on the basis that a trace of the secondary spectrum has been observed (Batten 1967).
- 163 The $\delta\beta$ index suggests that this is an evolved field star and a closer examination of the spectrum would be desirable. This conclusion was also reached by Crawford and Barnes (1966) from their β , $(\underline{U}-\underline{B})_0$ diagram.
- 176 The spectrum has been studied by Ciatti and Bernacca (1971), who made the MK classification given. Our β value corresponds to B6, in agreement with their evaluation of the Balmer-line strengths. Numerous weak absorption features are seen in the range $\lambda\lambda 3889-4482$ which are not present in standards, but no corresponding increase in the \underline{m}_1 index appears present. The low color excess may result from spectral peculiarities, however. Both the radial velocity given by Ciatti and Bernacca ($\rho = +18 \text{ km s}^{-1}$) and the available proper motions support membership.
- 194 Also included in Table 8b for I-group stars-- classification uncertain.
- 332 This star displays a large spectrum/color discrepancy which is in agreement with that determined by Bernacca and Ciatti (1972) from the UBV colors. However, the Balmer line strengths, noted by these authors to be

NOTES TO TABLE 8a (CONCLUDED)

indicative of a type near A0 V, are seen from our photometry to be in agreement with the color, at least for H β . Helium lines are absent from the spectrum and Bernacca and Ciatti suggest possible spectral variability. The high color excess agrees well with that of Lee (1968) and is not surprising in light of the fact that nebulosity is seen in this region on the Palomar Sky Survey prints. The distance of course depends upon whether the true absolute magnitude corresponds to the photometric colors or to the spectral type, if either.

TABLE 8b
DATA FOR I-TYPE STARS, SUBDIVISION b3

(1) Star	(2) ID	(3) V	(4) (b-y)	(5) m ₁	(6) c ₁	(7) (u-b)	(8) β	(9) r	(10) V ₀	(11) (b-y) ₀	(12) m ₀	(13) c ₀	(14) (u-b) ₀	(15) a ₀	(16) δm ₀	(17) δc ₀	(18) δ(u-b) ₀	(19) E(b-y)	(20) M _V	(21) dm	(22) Spectrum	(23) Note
83	36056	8 ^m 885	0 ^m 027	0 ^m 176	0 ^m 985	1 ^m 391	2 ^m 921	-0 ^m 013	8 ^m 77	0 ^m 001	0 ^m 184	0 ^m 980	1 ^m 350	-0 ^m 007	-0 ^m 007	0 ^m 008	-0 ^m 010	0 ^m 026	+1 ^m 7	7 ^m 1	A0	
88	290497	9.48	0.100	0.170	0.902	1.442	2.834	0.040	9.30	0.057	0.183	0.893	1.374	0.050	0.014	-0.070	0.078	0.043	+1.1	8.2	A2	*
96	36117	7.97	0.059	0.164	0.980	1.426	2.877	0.027	7.81	0.021	0.175	0.972	1.365	0.013	0.009	-0.007	0.026	0.038	+1.4	6.7	A0	NM?
97	36139	6.88	0.035	0.155	1.080	1.460	2.872	0.059	6.79	0.013	0.162	1.076	1.425	0.019	0.026	0.099	-0.019	0.022	+0.5	6.3	B8,A0	*,NM
116	290490	9.93	0.038	0.180	0.987	1.423	2.903	0.005	9.84	0.018	0.186	0.983	1.392	0.020	0.002	0.007	0.014	0.020	+1.5	8.3	B9,A1,A2	
194	36726A	8.84	0.043	0.164	0.975	1.389	2.922	-0.019	8.62	-0.008	0.179	0.965	1.308	-0.030	-0.005	-0.010	0.030	0.051	(+1.6)	(7.0)	AOV	*
323	37111	8.81	-0.001	0.180	0.940	1.298	2.895	-0.001	8.85	0.008	0.177	0.942	1.312	0.001	0.003	-0.035	0.045	-0.009	+1.5	7.3	A1V	

88 It is uncertain that this is an I-group star. The low β suggests an A type, but m₁ is too low and the HDE spectral type indicates I. Also, when the star is reduced as A, E(b-y) turns out to be zero and the δm₀ and δc₀ values are quite large. The M_V(β) value is then +2.2, giving (V₀-M_V) = 7.3.

97 Also reduced as B-type star--see note to Table 8a.

194 Also included in Table 8a. This star looks anomalous in both groups because of its high β. The δ indices have been obtained from (b-y)₀ rather than from a₀, because a₀ is abnormally blue for the intermediate group.

TABLE 8c
DATA FOR A- AND F-TYPE STARS, SUBDIVISION b3

(1) Star	(2) ID	(3) V	(4) (b-y)	(5) m ₁	(6) c ₁	(7) (u-b)	(8) β	(9) V ₀	(10) (b-y) ₀	(11) m ₀	(12) c ₀	(13) (u-b) ₀	(14) δm ₀	(15) δc ₀	(16) δ(u-b) ₀	(17) E(b-y)	(18) M _V	(19) dm	(20) Sp	(21) Spectrum	(22) Note
131	290491	10 ^m 22	0 ^m 183	0 ^m 173	0 ^m 933	1 ^m 645	2 ^m 825	9 ^m 90	0 ^m 108	0 ^m 195	0 ^m 918	1 ^m 526	0 ^m 011	0 ^m 087	-0 ^m 046	0 ^m 075	+1 ^m 8	8 ^m 2	A8	AO,A1	
188	36694	9.09	0.136	0.216	0.827	1.531	2.831	9.00	0.115	0.222	0.823	1.498	-0.015	-0.018	-0.019	0.021	+2.6	6.4	A7	A0	NM?
235	290636	9.55	0.117	0.168	0.993	1.563	2.819	9.49	0.103	0.172	0.990	1.541	0.034	0.172	-0.064	0.014	+1.2	8.3	A8	A2,A5	NM?

ORIGINAL PAGE IS
OF POOR QUALITY

TABLE 9a
DATA FOR B-TYPE STARS, SUBDIVISION c

(1) Star	(2) ID	(3) V	(4) [b-y]	(5) m ₁	(6) c ₁	(7) (u-b)	(8) β	(9) δB	(10) V ₀	(11) (b-y) ₀	(12) m ₀	(13) c ₀	(14) [u-b] ₀	(15) E(b-y)	(16) E(U-R)	(17) M _v	(18) dm	(19) Sp	(20) Spectrum	(21) Note
70	35901	9 ^m 03	-0 ^m 007	0 ^m 149	0 ^m 1917:	1 ^m 201:	2 ^m 790	0 ^m 076:	8 ^m 94:	-0 ^m 027:	0 ^m 155:	0 ^m 913:	1 ^m 168:	0 ^m 020:	0 ^m 008	+0 ^m 5	(8 ^m 5)	B9	A0, B8-9(OP)	*, NM
87	36058AB	6.39	0.003	0.143	1.028	1.320	2.833	0.074	6.9	-0.017	0.149	1.024	1.289	0.020	0.002	+0.9	6.0	A0	AOVn	*, NM
89	36120	7.97	-0.016	0.117	0.631	0.833	2.769	-0.005	7.80	-0.056	0.129	0.623	0.770	0.040	0.048	+0.2	7.6	B7	B8, B9	
99	36151	6.68	-0.036	0.096	0.387	0.507	2.701	0.010	6.50	-0.079	0.109	0.378	0.438	0.043	0.036	-0.9	7.4	B4	B5V	
109	36234	8.65	-0.022	0.109	0.631	0.805	2.774	-0.010	8.50	-0.055	0.119	0.624	0.752	0.033	0.034	+0.3	8.2	B7	B8, A0, B8-9(OP)	
113	36285	6.33	-0.086	0.094	0.119	0.135	2.646	0.003	6.25	-0.105	0.100	0.115	0.105	0.019	0.026	-2.3	8.6	B2	B1.5V, B2IV-V	
124	294166	10.315	0.16	0.14	0.87	1.47	2.954	-0.125	9.48	-0.04	0.20	0.83	1.16	0.20	0.157	+0.8	8.7	B8	A2Vn	*
125	294180	10.82	0.351	0.106	0.923	1.837			9.16	-0.034	0.221	0.846	1.221	0.385	0.380	(+0.9)	(8.1)	B9	B8, A1, A2	*
128	36366A	8.18	0.036	0.154	0.922	1.302	2.885	-0.021	7.91	-0.028	0.173	0.909	1.200	0.064	0.054	+1.2	6.7	B9	B9	
134	36411	9.71	0.045	0.159	1.031	1.439	2.888	0.018	9.44	-0.017	0.178	1.019	1.340	0.062	0.068	+1.2	8.3	A0	B8, A0, B8-9(OP)	
137	36430	6.22	-0.086	0.110	0.203	0.251	2.671	-0.001	6.18	-0.097	0.113	0.201	0.234	0.011	0.020	-1.6	7.8	B2	B2V	
143	36487	7.79	-0.047	0.110	0.462	0.588	2.723	0.006	7.68	-0.072	0.117	0.457	0.549	0.025	0.029	-0.5	8.2	B6	B5V	
146	36513	9.49	-0.002	0.163	0.929	1.251	2.875	-0.004	9.39	-0.026	0.170	0.924	1.212	0.024	0.040	+1.1	8.3	B9	A0, B8-9(OP)	
147	36512	4.61	-0.112	0.061	-0.093	-0.195	2.596	0.005	4.56	-0.125	0.065	-0.096	-0.216	0.013	0.029	-4.3	8.9	O9	BOV	
151	36540	8.16:	0.080	0.066	0.393	0.685	2.711	-0.004	7.47:	-0.081	0.114	0.361	0.427	0.161	0.160	-0.7	(8.2)	B4	B7III:	*
152	36550B	9.35	-0.003	0.173	0.977	1.317	2.917	-0.026	9.27	-0.022	0.179	0.973	1.287	0.019	0.032	+1.3	7.9	B9	A0, B8-9(OP)	*
153	36541	7.68	-0.026	0.107	0.557	0.719	2.746	0.004	7.52	-0.063	0.118	0.550	0.660	0.037	0.024	-0.1	7.6	B7	B6V, B8V	
155	36560A	8.26	-0.025	0.099	0.634	0.782	2.751	0.014	8.13	-0.055	0.108	0.628	0.734	0.030	0.020	0.0	8.2	B7	A0, B8-9(OP)	
157	36559	8.81	-0.007	0.122	0.815	1.045	2.832	-0.013	8.68	-0.038	0.131	0.809	0.996	0.031	0.021	+0.9	7.8	B8	B8, B9	
162	294216	11.31	0.306	0.046	1.016:	1.720:			9.89:	-0.024:	0.145:	0.950:	1.192:	0.330:		(+1.1)	(8.7)	B9	A0, A3	*
166	36607	9.20	-0.015	0.129	0.899	1.127	2.863	-0.005	9.14	-0.029	0.133	0.896	1.104	0.014	0.008	+1.1	8.1	B9	B9, A0, B8-9(OP)	
169	36630B	9.53	0.01	0.22	0.96	1.42	2.921	-0.038	9.39	-0.02	0.23	0.95	1.37	0.03		+1.1	8.3	B9	B9V	*
171	36629	7.66	0.067	0.067	0.138	0.406	2.657	-0.011	6.92	-0.106	0.119	0.103	0.129	0.173	0.172	-2.0	8.9	B2	B2V	
177	36655	8.61	-0.015	0.121	0.773	0.985	2.802	-0.000	8.50	-0.042	0.129	0.768	0.943	0.027	0.023	+0.6	7.9	B8	B8, B9	
182	36670	8.95	0.002	0.161	0.956	1.282	2.891	-0.009	8.84	-0.024	0.169	0.951	1.241	0.026	0.020	+1.2	7.6	B9	A0, B8-9(OP)	
187	36697	8.64	0.047	0.147	0.959	1.347	2.868	0.011	8.33	-0.024	0.168	0.945	1.233	0.071	0.070	+1.1	7.2	B9	A0, B8-9(OP)	
206	36783	9.50	-0.007	0.162	0.892	1.202	2.886	-0.032	9.40	-0.030	0.169	0.887	1.165	0.023	0.036	+1.2	8.2	B9	B8, A0, B8-9(OP)	
218	36813	8.55	0.068	0.117	0.727	1.097	2.792	-0.011	8.06	-0.048	0.152	0.704	0.912	0.116	0.118	+0.5	7.6	B8	B8, B9	
231	36867	9.29	-0.016	0.151	0.915	1.185	2.889	-0.023	9.24	-0.027	0.154	0.913	1.167	0.011	0.029	+1.2	8.0	B9	A0, B8-9(OP)	
273	37001	8.88	-0.027	0.131	0.781	0.989	2.818	-0.012	8.82	-0.040	0.135	0.778	0.967	0.013	0.023	+0.8	8.0	B8	B8, A0, B8-9(OP)	
275	294248	9.87	0.150	0.080	1.020	1.480	2.798	0.097	9.14	-0.020	0.131	0.986	1.208	0.170	0.106	(+0.6)	(8.6)	A0	A4Vn	*
302	37055AB	6.41	-0.050	0.106	0.308	0.420	2.704	-0.009	6.25	-0.087	0.117	0.301	0.361	0.037	0.038	-0.9	7.1	B3	B3V, B3IV	
312	37056	8.37	-0.018	0.118	0.640	0.840	2.757	0.009	8.22	-0.055	0.129	0.633	0.781	0.037	0.031	+0.1	8.2	B7	B8	
313	37057	9.29	0.010	0.132	0.878	1.162	2.854	-0.008	9.11	-0.032	0.144	0.870	1.095	0.042	0.038	+1.0	8.1	B9	A0, B8-9(OP)	
331	37131	8.32	-0.012	0.094	0.570	0.734	2.727	0.025	8.11	-0.062	0.109	0.560	0.655	0.050	0.089	-0.4	8.5	B7	B9, B8-9(OP)	
340	37151	7.39:	-0.033	0.113	0.619	0.779	2.777	-0.014	7.29:	-0.056	0.120	0.614	0.742	0.023	0.025	+0.3	(7.0)	B7	B8V	
346	37210	8.125	-0.046:	0.147:	0.570:	0.772:	2.789	-0.035:	8.06:	-0.061:	0.151:	0.567:	0.748:	0.015:	0.037	(+0.5)	(7.6)	B7	B9IV-Vp	*
350	37209AB	5.72	-0.082	0.072	0.054	0.034	2.623	0.012	5.60	-0.111	0.081	0.048	-0.013	0.029	0.024	-3.1	8.7	B1	B1V, B2IV	
352	294253	9.68	0.023	0.133	0.926	1.238	2.904	-0.037	9.46	-0.027	0.148	0.916	1.158	0.050	0.019:	+1.0	8.5	B9	A0, B8-9(OP)	*
362	37273	9.92	0.130	0.116	0.953	1.445	2.849	0.021	9.25	-0.027	0.163	0.922	1.195	0.157	0.124	+1.0	8.3	B9	A2, B8-9(OP)	
367	-4 1193	11.29	0.503:	-0.009:	0.874:	1.862:	2.774:	0.031:	8.95:	-0.042:	0.154:	0.765:	0.991:	0.545:	0.525	(+0.3)	(8.6)	B8	A0	
374	37303	6.05	-0.090	0.077	0.020	-0.006	2.616	0.012	5.94	-0.115	0.084	0.015	-0.045	0.025	0.031	-3.4	9.4	B1	B1V, B1.5V	
380	37322	9.80	0.037	0.157	1.017	1.405	2.914	-0.012	9.56	-0.018	0.174	1.006	1.316	0.055	0.058	+1.3	8.2	A0	A0, B8-9(OP)	*
381	37334	7.17:	-0.069	0.096	0.192	0.246	2.656	0.010	7.04:	-0.098	0.105	0.186	0.200	0.029	0.037	-2.0	(9.1)	B2	B1.5V	
390	37356	6.20	0.023	0.073	0.126	0.318	2.624	0.021	5.64	-0.106	0.112	0.100	0.111	0.129	0.138	-3.1	8.7	B2	B1.5V, B2IV, B2IV-V	

TABLE 9a (CONCLUDED)

(1) Star	(2) ID	(3) V	(4) $(b-y)$	(5) m_1	(6) c_1	(7) $(u-b)$	(8) β	(9) $\delta\beta$	(10) V_0	(11) $(b-y)_0$	(12) m_0	(13) c_0	(14) $(u-b)_0$	(15) $E(b-y)$	(16) $E(U-B)$	(17) M_V	(18) dm	(19) Sp	(20) Spectrum	(21) Note
392	37373	8.32	-0.042	0.120	0.644	0.800	2.763	0.004	8.27	-0.054	0.124	0.642	0.781	0.012	-0.001	+0.1	8.1	B7	B9	
395	37390	9.42	0.140	0.110	0.788	1.288	2.794	0.002	8.63	-0.043	0.165	0.751	0.995	0.183	0.153	+0.5	(8.1)	B8	AO, B8-9(OP)	
398	π 2632	11.83	0.598	0.035	1.105	2.371	2.816	0.075	9.17	-0.021	0.221	0.981	1.381	0.619	0.571	+0.7	(8.5)	B9	A1	*
401	π 2652	11.44	0.663	-0.028	0.737	2.007	2.755	0.004	8.34	-0.058	0.188	0.593	0.853	0.721	0.724	0.0	8.3	B7	B9	
406	37428AB	8.68	0.104	0.108	0.714	1.138	2.794	-0.018	8.02	-0.050	0.154	0.683	0.892	0.154	0.148	+0.5	7.5	B7	AO, B8-9(OP)	
412	-6 1273	10.25	0.263	0.048	0.733	1.355	2.806	-0.033	8.90	-0.051	0.142	0.670	0.853	0.314	0.274	+0.7	(8.2)	B7	B9, B8-9(OP)	
416	37469	9.62	0.174	0.093	0.913	1.447	2.817	0.030	8.74	-0.031	0.155	0.872	1.118	0.205	0.170	+0.8	8.0	B9	B9, AO, B8-9(OP)	
417	37470	8.235	0.072	0.088	0.682	1.002	2.787	-0.017	7.70	-0.052	0.125	0.657	0.803	0.124	0.085	+0.4	7.3	B7	B8p (S1)	*
419	37481A	5.96	-0.088	0.086	0.074	0.070	2.636	0.003	5.87	-0.109	0.092	0.070	0.036	0.021	0.009	-2.6	(8.5)	B1	B1V, B1.5IV	
422	37480	9.21	0.000	0.149	0.970	1.268	2.887	0.001	9.11	-0.022	0.156	0.966	1.232	0.022	0.023	+1.2	7.9	B9	B9, AO, B8-9(OP)	
423	37492	7.09	-0.026	0.125	0.590	0.788	2.734	0.023	6.94	-0.059	0.135	0.583	0.735	0.033		-0.3	7.2	B7	B9	
427	37526	7.61	-0.046	0.116	0.428	0.568	2.723	-0.003	7.48	-0.075	0.125	0.422	0.522	0.029	0.019	-0.5	8.0	B5	B3V	
428	37547	9.30	-0.012	0.141	0.953	1.211	2.870	0.012	9.25	-0.024	0.145	0.951	1.192	0.012	0.000	+1.1	(8.1)	B9	B9, AO	
440	37635	6.495	-0.047	0.106	0.494	0.612	2.714	0.023	6.40	-0.068	0.112	0.490	0.578	0.021	0.016	-0.7	7.1	B6	B7V	*
443	37642	8.06	-0.059	0.127	0.332	0.468	2.703	-0.003	7.95	-0.084	0.135	0.327	0.428	0.025	0.021	-0.9	8.8	B3	B9Vp (S1)	*
444	37663	9.18	0.005	0.139	0.931	1.219	2.884	-0.013	9.04	-0.026	0.148	0.925	1.169	0.031	0.004	+1.2	7.9	B9	AO, B8-9(OP)	
454	37687	7.04	0.063	0.092	0.486	0.796	2.682	0.048	6.46	-0.071	0.132	0.459	0.581	0.134	0.133	-1.4	7.8	B6	B6V	*, NM?
456	37700	8.01	-0.032	0.110	0.485	0.641	2.730	0.004	7.84	-0.070	0.121	0.477	0.581	0.038	0.024	-0.4	(8.2)	B6	B5V, B6V	
461	37745	9.19	0.019	0.139	0.973	1.289	2.865	0.022	9.01	-0.022	0.151	0.965	1.223	0.041	0.035	+1.1	7.9	B9	AO, B8-9(OP)	
462	π 2946	12.01	0.496	-0.028	0.898	1.834	2.746	0.065	9.71	-0.039	0.133	0.791	0.978	0.535		(+0.1)	(9.6)	B8	AO	*, NM?
471	37807	7.91	-0.048	0.106	0.317	0.433	2.701	-0.004	7.74	-0.086	0.117	0.309	0.372	0.038	0.057	-0.9	8.7	B3	B2V	
476	37888	9.21	0.040	0.125	1.024	1.354	2.849	0.055	8.96	-0.018	0.142	1.012	1.262	0.058	0.034	+1.0	8.0	AO	AO, B8-9(OP)	*
477	37889	7.67	-0.028	0.097	0.213	0.351	2.678	-0.008	7.38	-0.097	0.118	0.199	0.241	0.069	0.054	-1.4	8.8	B2	B2V	
479	37887	7.71	-0.001	0.135	0.919	1.187	2.865	0.001	7.60	-0.027	0.143	0.914	1.145	0.026	0.018	+1.1	6.5	B9	AOV	NM?
485	38023	8.84	0.256	0.060	0.306	0.938	2.677	0.002	7.34	-0.093	0.165	0.236	0.380	0.349		-1.5	(8.8)	B2	B4V	*
487	38051	8.49	0.333	-0.005	0.335	0.991	2.673	0.010	6.66	-0.092	0.122	0.250	0.312	0.425	0.391	-1.5	8.2	B3	B3, B8	*
491	38088	9.68	0.13	0.10	1.00	1.46	2.859	0.030	9.03	-0.02	0.15	0.97	1.22	0.15	0.127	+1.0	8.0	B9	AOV	
493	38120	9.07	0.046	0.127	0.965	1.311	2.766	0.116	8.77	-0.024	0.148	0.951	1.199	0.070	0.046	(+1.1)	(7.7)	B9	AO, B8-9(OP)	*
495	38239	9.22	0.034	0.155	1.015	1.393	2.915	-0.014	8.99	-0.019	0.171	1.004	1.309	0.053	0.040	+1.3	7.7	AO	AO	
501	38531	8.13	0.220	0.064	1.024	1.592	2.781	0.111	7.09	-0.021	0.136	0.976	1.206	0.241		(+1.2)	(5.9)	B9	B9	*, NM?
506	38755	7.69	-0.045	0.103	0.491	0.607	2.723	0.014	7.59	-0.069	0.110	0.486	0.569	0.024	0.027	-0.5	8.1	B6	B5V, B6V	
507	38771	2.07	-0.036	0.026	-0.084	-0.104	2.564	0.035	1.68	-0.126	0.053	-0.102	-0.248	0.090	0.088	(-6.1)	(7.8)	O9	BO, 5Ia	*
508	38800	8.48	0.034	0.107	0.813	1.095	2.774	0.040	8.17	-0.039	0.129	0.798	0.979	0.073		+0.3	7.9	B8	B8	NM?
509	38824A	7.285	-0.041	0.117	0.403	0.555	2.711	0.003	7.13	-0.078	0.128	0.396	0.496	0.037		-0.7	7.9	B5	B9	
517	39230	9.405	0.169	0.083	0.995	1.499	2.811	0.073	8.58	-0.023	0.141	0.957	1.192	0.192		+0.7	7.9	B9	B9	NM
518	39254	9.52	0.228	0.116	0.523	1.211	2.755	-0.024	8.23	-0.071	0.206	0.463	0.733	0.299		0.0	8.2	B6	B9	*
519	39291	5.35	-0.094	0.096	0.104	0.108	2.641	0.004	5.30	-0.106	0.100	0.102	0.089	0.012	0.021	-2.5	7.8	B2	B2V, B2 IV-V	
520	39376A	7.91	-0.050	0.132	0.612	0.776	2.757	0.005	7.88	-0.057	0.134	0.611	0.765	0.007		+0.1	7.8	B7	B9	
521	39419	9.125	0.060	0.130	0.743	1.123	2.794	-0.008	8.67	-0.046	0.162	0.722	0.953	0.106		+0.5	8.1	B8	B9	
522	39540	8.87	-0.010	0.155	0.942	1.232	2.893	-0.016	8.81	-0.025	0.159	0.939	1.208	0.015		+1.2	7.6	B9	B9	
526	39777	6.56	-0.080	0.077	0.108	0.102	2.650	-0.004	6.45	-0.106	0.085	0.103	0.060	0.026	0.024	-2.2	8.6	B2	B1.5V, B2V	

NOTES TO TABLE 9a

- 70 Probably an evolved field star but should be checked for emission.
- 87 V_0 corrected by 0.6 for duplicity. This is an evolved foreground field star.
- 124 The β index is far above normal values and hence outside the calibration. It depends upon only a single observation and should be remeasured. $\underline{M}_V(\beta)_{ZAMS}$ is determined from $(\underline{b}-\underline{y})_0$.
- 125 Classified as a B-type star in terms of $[\underline{u}-\underline{b}]$ and $[\underline{m}_1]$, in spite of the high value of \underline{m}_0 derived. $\underline{M}_V(\beta)_{ZAMS}$ is determined from $(\underline{b}-\underline{y})_0$ -- β observations are desirable.
- 151 Classified as He-weak (Bernacca 1967, 1968; Hack 1969) but according to Bernacca (1967) it is not a typical He-weak star because of other peculiarities (see note to Table 2, Paper I). His suggestion that its location near an obscured region may result in a high color excess is supported by the derived $\underline{E}(\underline{b}-\underline{y})$, which agrees well with previous $\underline{E}(\underline{B}-\underline{V})$ values obtained by Sharpless (1962) and Lee (1968). The four-color and β results agree well and show a spectrum/color discrepancy of the same order as do the He-weak stars.
- 152 The intrinsic color $(\underline{b}-\underline{y})_0$ gives $\underline{M}_V(\beta)_{ZAMS} = +1.2$.
- 162 Additional observations should be obtained for this star to check the reddening and distance modulus. The intrinsic color $(\underline{b}-\underline{y})_0$ has been used to derive $\underline{M}_V(\beta)_{ZAMS}$,

NOTES TO TABLE 9a (CONTINUED)

but the color excess and spectral type suggest a young object which may lie well above the ZAMS.

169 See note for 124.

275 The MK type of Smith (1972a) suggests that this star should be reduced as A-type, but the photometry (primarily the low m_1 index) indicates that the calibration for B-type stars should be used. Of course, the disagreement of the four-color and β results points to photometric peculiarities and neither reduction may be valid. The $(\underline{b-y})_0$ color yields $\underline{M}_V(\beta)_{ZAMS} = +1.2$ and $dm = 7.9$, but the star is almost certainly located above the ZAMS. The m_1 index may be severely affected by the problems discussed in the text.

346 The spectrum is peculiar in that the Si II doublet $\lambda\lambda 4128-30$ is very strong (Bernacca 1967). The usual spectrum/color discrepancy is seen, but in this case β is indicative of a later type (about B8). The $(\underline{b-y})_0$ index gives $\underline{M}_V(\beta)_{ZAMS} = 0.0$, hence the distance modulus may be as great as 8.1.

352 The β index is anomalously high, possibly due to strong hydrogen lines; $(\underline{b-y})_0$ has been used to derive $\underline{M}_V(\beta)_{ZAMS}$.

380 Reduced as an intermediate-group star also. The results check closely [$\underline{E}(\underline{b-y}) = 0.047$, $\underline{M}_V = +1.3$]. Classified as B-type because of low m_1 .

NOTES TO TABLE 9a (CONTINUED)

- 398 Spectroscopic and further photometric observations are needed to decide on the status of this star. It may be either an evolved interloper or a pre-main-sequence star.
- 417 The usual spectrum/color discrepancy is absent here, probably because the peculiarity is marginal. The $(\underline{b-y})_0$ index gives $\underline{M}_V(\beta)_{ZAMS} = +0.3$, not a significant difference from the value derived from β .
- 440 This star is outside the boundaries of our observing region and is not assigned to a subgroup. Data are included in Table 9a since the star is located nearest to subgroup c. Results are not used in the formation of means for this subgroup, however.
- 443 Found to be helium poor by Nissen (1976). The large spectrum/color discrepancy is similar to those seen for other helium-weak stars.
- 454 The large $\delta\beta$ index suggests an evolved field star, as concluded previously by Crawford and Barnes (1966). The high color excess for this distance and the uncertain MK class suggest the possibility of a peculiar spectrum, however.
- 462 Both the four-color and β values are from single observations and should be rechecked. This could be a background star since it is located at some distance from the nebula. The $\underline{M}_V(\beta)$ value has been

NOTES TO TABLE 9a (CONTINUED)

used here--the $(\underline{b}-\underline{y})_0$ index gives $\underline{M}_V(\beta)_{ZAMS} = +0.7$, placing the star somewhat closer.

- 476 The β observation may be low, causing $\delta\beta$ to be too large. An observation by Crawford (1958), using a narrower band H β filter, gives 2.884. While β observations on the "old" system have not been incorporated into the present work, they very often check well with measures made on the currently used system. Further observations are needed for this star.
- 485 Very little information is available for this star. Nebulosity can be seen around it on the Palomar Sky Survey prints, so the high color excess is not surprising. The disagreement of the spectral types with the photometry is not understood. The \underline{m}_0 index is also abnormally high for β and \underline{c}_0 .
- 487 Our β index (from a single observation) appears bad (2.628); therefore the value as measured by Crawford (1958) on the old β system, has been used in the reductions.
- 493 The $\delta\beta$ index is certainly indicative of emission and β should be rechecked. The $(\underline{b}-\underline{y})_0$ index has been used to derive $\underline{M}_V(\beta)_{ZAMS}$ here since the photometric spectral type agrees.
- 501 Same comments as for 493.

NOTES TO TABLE 9a (CONCLUDED)

507 κ Orionis. See note for 440.

518 . The high \underline{m}_0 index indicates possible spectral peculiarities, reddening effects, and/or blue continuum emission.

TABLE 9b
DATA FOR I-TYPE STARS, SUBDIVISION c

(1) Star	(2) ID	(3) V	(4) (b-y)	(5) m ₁	(6) c ₁	(7) (u-b)	(8) β	(9) r	(10) V ₀	(11) (b-y) ₀	(12) m ₀	(13) c ₀	(14) (u-b) ₀	(15) a ₀	(16) δm ₀	(17) δc ₀	(18) δ(u-b) ₀	(19) E(b-y)	(20) M _V	(21) dm	(22) Spectrum	(23) Note
68	35885	9. ^m 67	0. ^m 042	0. ^m 183	0. ^m 956	1. ^m 406	2. ^m 909	-0. ^m 012	9. ^m 56	0. ^m 018	0. ^m 190	0. ^m 951	1. ^m 367	0. ^m 013	-0. ^m 005	-0. ^m 028	0. ^m 025	0. ^m 024	(+1. ^m 8)	(7. ^m 8)	A0	
106	36203	9.18	0.057	0.206	0.957	1.483	2.897	-0.001	9.17	0.053	0.207	0.956	1.477	0.074	-0.004	0.015	-0.006	0.004	+2.0	7.2	A3Vs	
119	36324	9.02	0.035	0.165	1.096	1.496	2.894	0.052	8.93	0.013	0.172	1.092	1.461	0.026	0.018	0.118	-0.035	0.022	+0.8	8.2	A0	*,NM?
122	36342	7.53	0.053	0.188	1.034	1.516	2.878	0.045	7.51	0.048	0.190	1.033	1.508	0.073	0.013	0.091	-0.036	0.005	+1.2	6.3	A0,A2	*,NM
150	36527	9.49	0.08	0.17	1.05	1.55	2.864	0.063	9.34	0.045	0.180	1.043	1.494	0.061	0.019	0.087	-0.029	0.035	+0.8	8.5	A1Vn	*,NM?
214	294202	10.19	0.20	0.13	0.93	1.59	2.821	0.056	9.57	0.054	0.174	0.901	1.357	0.018	0.013	-0.076	0.045	0.146	+0.7	8.9	A3Vn	*
229	36866	9.29	0.050	0.186	1.045	1.517	2.866	0.061	9.30	0.052	0.185	1.045	1.520	0.081	0.019	0.115	-0.052	-0.002	+0.9	8.4	A2V	*,NM?
322	37091	9.80	0.056	0.173	0.954	1.412	2.909	-0.014	9.61	0.011	0.186	0.945	1.340	-0.003	-0.008	-0.029	0.006	0.045	+1.7	7.9	A3V	
357	37258	9.62	0.084	0.156	0.962	1.442	2.833	0.063	9.44	0.042	0.169	0.954	1.375	0.034	0.024	-0.017	0.059	0.042	(+0.6)	(8.8)	A2V	
375	37304	10.16	0.079	0.204	0.926	1.492	2.900	-0.016	10.06	0.054	0.211	0.921	1.453	0.065	-0.011	-0.031	0.016	0.025	+2.2	(7.9)	A3V	
386	-6 1266	10.87	0.212	0.175	0.933	1.707	2.872	0.005	10.30	0.080	0.215	0.907	1.495	0.072	-0.012	-0.037	-0.024	0.132	(+1.9)	(8.4)	A2	
391	37357AB	8.865	0.058	0.159	0.976	1.410	2.856	0.047	9.3	0.026	0.169	0.970	1.359	0.018	-0.018	-0.007	0.042	0.032	+0.8	8.5	A0	*
399	37412	9.79	0.030	0.200	0.939	1.399	2.924	-0.032	9.76	0.023	0.202	0.938	1.388	0.027	-0.012	-0.036	0.039	0.007	+2.2	7.5	A0,A1	
400	37410	6.86	0.041	0.194	0.975	1.445	2.899	0.004	6.83	0.036	0.196	0.974	1.437	0.048	0.000	0.009	0.013	0.005	+1.7	5.1	A1,A2	NM
402	37411	9.79	0.110	0.149	1.010	1.528	2.870	0.041	9.43	0.026	0.174	0.993	1.394	0.012	0.010	0.013	-0.004	0.084	+0.9	8.6	B9V	
411	37455	9.57	0.071	0.161	1.039	1.503	2.904	0.020	9.31	0.011	0.179	1.027	1.407	0.005	0.003	0.047	-0.036	0.060	+1.2	8.1	A3V	NM?

119 The large δc₀ and r values suggest that this is an evolved field star. The available proper motions are quite large and support non-membership.

122 This star is a definite non-member, as shown by δc₀, r, dm, and its proper motions.

150 Another possible field star. No other data available.

214 The β index appears much too low for the spectral type and may be adversely affected by rotation. The color excess does agree closely with that determined by Smith (1972a) from the (b-y)₀ color and MK type [E(b-y) = 0.16]. Hallam (1959) finds that a best fit to the ultraviolet flux distribution is obtained at B8 V, but our colors agree with the A3 V type and the ultraviolet excess δ(u-b)₀ is small.

229 A K-line index is available from Hesser, McClintock and Henry (1977), the measured h of 0.363 gives (b-y)₀ = 0.04, using the relation (b-y)₀ = 0.216h - 0.036 derived by Warren (1975).

391 V₀ corrected by 0.6 for duplicity.

ORIGINAL PAGE IS
OF POOR QUALITY

TABLE 9c
DATA FOR A- AND F-TYPE STARS, SUBDIVISION c

(1) Star	(2) ID	(3) V	(4) (b-y)	(5) m ₁	(6) c ₁	(7) (u-b)	(8) β	(9) V ₀	(10) (b-y) ₀	(11) m ₀	(12) c ₀	(13) (u-b) ₀	(14) δm ₀	(15) δc ₀	(16) δ(u-b) ₀	(17) E(b-y)	(18) M _V	(19) dm	(20) Sp	(21) Spectrum	(22) Note	
62	35868	9 ^m .64	0 ^m .17	0 ^m .19	0 ^m .84	1 ^m .56	2 ^m .781	9 ^m .56	0 ^m .152	0 ^m .195	0 ^m .836	1 ^m .532	0 ^m .002	0 ^m .094	-0 ^m .071	0 ^m .018	+2 ^m .0	7 ^m .6	F0	A9IV	NM?	
81	36017AB	7.52	0.163	0.146	0.980	1.598	2.765	7.46	0.147	0.151	0.977	1.573	0.039	0.267	-0.127	0.016	+0.7	6.8	F1	A3	NM?	
82	36016	9.02	0.169	0.180	0.752	1.450	2.788	8.96	0.154	0.184	0.749	1.426	0.015	-0.007	0.038	0.015	+2.8	6.2	F0	A0,A2	NM?	
93	294175	9.85	0.355	0.178	0.478	1.544														F5,F8,GO		
94	π 106	11.62	0.256	0.185	0.960	1.842														A1		
95	36119	9.59	0.325	0.132	0.464	1.378															F8,F9,G5	
98	294171	11.21	0.452	0.092	1.156	2.244															A2,A3,A5	
104	294170	10.26	0.196	0.190	0.764	1.536															A8,F0	
105	36202	9.51	0.263	0.150	0.592	1.418															F3,F5,F8,GO	
110	36235	9.45	0.333	0.162	0.352	1.342															F8,F9	
126	36363	9.53	0.324	0.171	0.530	1.520															F3,F6,GO	
127	36364	9.51	0.320	0.146	0.569	1.501															F5,F8,G5	
133	-6 1205	10.79	0.264	0.154	0.606	1.442															A5,A8	
135	36412	9.47	0.506	0.138	0.982	2.270	2.726	8.12	0.193	0.232	0.919	1.769	-0.055	0.301	-0.363	0.313	(+0.7)	(7.5)	F3	F8		
142	294219	10.25	0.103	0.208	0.907	1.529	2.851	10.19	0.089	0.212	0.904	1.507	-0.004	0.032	0.035	0.014	+2.1	8.1	A6	A8IV		
149	-7 1108	9.91	0.21	0.18	0.77	1.55	2.749	9.81	0.186	0.187	0.765	1.511	-0.004	0.087	-0.078	0.024	+2.2	(7.6)	F1	A6m		
154	-5 1284	10.42	0.190	0.222	0.740	1.564															A5	
158	-6 1214	9.46	0.268	0.142	0.508	1.328															F2	
165	36606	8.755	0.080	0.198	0.949	1.505	2.875	8.69	0.065	0.202	0.946	1.481	0.004	0.026	-0.012	0.015	+2.1	6.6	A5	A4Vn	NM?	
168	294225	10.04	0.14	0.20	0.79	1.47	2.756	10.19	0.177	0.189	0.797	1.529	-0.003	0.105	-0.090	-0.037	+2.0	8.2	F1	A8V	*	
172	-6 1217A	8.85	0.355	0.177	0.343	1.407	2.618	8.85	0.355	0.177	0.343	1.406	0.018	0.007	0.039	0.000	+4.2	4.6	GO	F8IV-V	NM	
178	-5 1288	10.64	0.273	0.163	0.507	1.379	2.658	10.73	0.292	0.157	0.511	1.409	0.014	0.087	-0.053	-0.019	(+2.8)	(8.0)	F6	F2,F3	NM?(u)	
180	36671	8.71	0.201	0.204	0.714	1.524	2.770	8.60	0.176	0.211	0.709	1.484	-0.019	-0.011	-0.034	0.025	+2.9	(5.7)	F0	A2m	NM	
181	-6 1219	10.21	0.291	0.159	0.568	1.468	2.660	10.20	0.288	0.160	0.567	1.463	0.011	0.137	-0.108	0.003	+2.2	8.0	F6	F6IV		
183	π 1158	10.94	0.382	0.153	0.304	1.374	2.553														GO	NM
185	π 1179	11.47	0.346	0.165	0.373	1.395	2.601	11.53	0.360	0.161	0.376	1.417	0.054	0.074	0.091	-0.014	(+3.8)	(7.8)	G1	F8		
186	36712	9.80	0.065	0.205	0.959	1.499	2.866	9.82	0.071	0.203	0.960	1.508	0.004	0.058	-0.038	-0.006	+1.9	8.0	A5	A3Vn		
191	-5 1290	10.68	0.416	0.171	0.343	1.517	2.543														G1,G2	
192	36714	9.65	0.280	0.148	0.420	1.276															F5,F8	
198	-5 1293	10.74	0.275	0.152	0.602	1.456	2.665	10.75	0.277	0.151	0.602	1.460	0.019	0.162	-0.109	-0.002	+1.9	(8.9)	F6	F3IV		
204	-5 1295	8.805	0.308	0.165	0.437	1.383	2.660	8.76	0.297	0.168	0.435	1.366	0.003	0.005	-0.011	0.011	+3.6	5.1	F6	F6V,F7IV	NM	
205	-5 1296	10.12	0.256	0.211	0.742	1.676	2.746	9.86	0.196	0.229	0.730	1.580	-0.046	0.057	-0.148	0.060	(+2.5)	(7.4)	F1	A3m		
207	-7 1118	9.97	0.253	0.186	0.634	1.512															F0,F2	
220	-6 1228	9.825	0.201	0.192	0.637	1.423															A5	
230	π 1513	10.54	0.134	0.187	0.836	1.478	2.817	10.49	0.123	0.190	0.834	1.460	0.015	0.020	0.018	0.011	+2.4	(8.1)	A8	A3		
336	-6 1249	10.43	0.236	0.148	0.678	1.446															F0,F2	
337	-6 1248	10.35	0.290	0.202	0.507	1.491															F3,F4	
345	37188	8.64	0.159	0.208	0.791	1.525	2.774	8.66	0.164	0.207	0.792	1.533	-0.012	0.064	-0.079	-0.005	+2.3	6.4	F0	F1IV	NM	
351	-6 1256	10.27	0.204	0.183	0.672	1.446															A8,F0	
356	-5 1339	9.585	0.356	0.152	0.427	1.443	2.609	9.55	0.348	0.154	0.425	1.430	0.051	0.107	0.048	0.008	(+3.2)	(6.3)	GO	F8	NM?	
360	π 2494	10.77	0.573	0.269	0.253	1.937	2.529														GO,G2	
363	π 2500	11.31	0.238	0.181	0.805	1.643	2.811	10.86	0.135	0.212	0.784	1.478	-0.007	-0.018	-0.002	0.103	+2.7	8.1	A8	A3,A5		
364	-6 1259	10.66	0.248	0.186	1.230	2.098															A1e,A5eII-III	
365	294286	10.96	0.140	0.222	0.858	1.582	2.788	10.99	0.147	0.220	0.859	1.593	-0.021	0.103	-0.129	-0.007	(+1.9)	(9.1)	F0	A2,A5,F0		
366	π 2515	12.05	0.398	0.151	1.011	2.109	2.805	10.88	0.125	0.233	0.956	1.672	-0.029	0.166	-0.199	0.273	+1.3	9.6	A9	AO		

TABLE 9c (CONCLUDED)

(1) Star	(2) ID	(3) V	(4) $[b-y]$	(5) m_1	(6) c_1	(7) $(u-b)$	(8) β	(9) V_0	(10) $(b-y)_0$	(11) m_0	(12) c_0	(13) $(u-b)_0$	(14) δm_0	(15) δc_0	(16) $\delta(u-b)_0$	(17) $E(b-y)$	(18) M_V	(19) dm	(20) Sp	(21) Spectrum	(22) Note
368	-5 1341	11 ^m 17:	0 ^m 294	0 ^m 153	0 ^m 456	1 ^m 350	2 ^m 648	11 ^m 21:	0 ^m 304	0 ^m 150	0 ^m 458	1 ^m 366	0 ^m 025	0 ^m 062	0 ^m 003	-0 ^m 010	+3 ^m 1	(8 ^m 1)	F7	F3,F4	
369	π 2526	11.97	0.762	0.108	0.958	2.698	2.726	9.58	0.205	0.275	0.847	1.807	-0.098	0.229	-0.401	0.557	+1.2	8.3	F3	A7:	
370	-6 1261	10.79	0.248	0.167	0.512	1.342	2.663	10.95	0.285	0.156	0.519	1.401	0.015	0.083	-0.049	-0.037	+2.8	8.2	F6	F0,F2	
371	-6 1260	10:675	0.306	0.184	0.421	1.401														F5	
382	294296	9.94	0.396	0.188	0.369	1.537	2.578													G0,G8	NM
384	-6 1263	10.52	0.200	0.201	0.660	1.462														A3	
387	37372	9.50	0.202	0.130	0.863	1.527	2.843	9.05	0.097	0.162	0.842	1.359	0.046	-0.013	0.112	0.105	+2.5	6.5	A7	A8V	NM?
389	294295	10.51	0.142	0.217	0.842	1.560														A0	
396	-6 1269	8.36	0.284	0.169	0.415	1.321	2.665	8.39	0.291	0.167	0.416	1.333	0.003	-0.024	0.018	-0.007	+3.9	4.5	F6	F6	NM
403	37413	9.62	0.127	0.186	0.896	1.522	2.837	9.50	0.100	0.194	0.891	1.479	0.014	0.044	-0.005	0.027	+2.1	7.4	A7	A6Vn	NM?
409	294291	10.67	0.238	0.169	0.572	1.386														A8,FO	
410	37444	7.65	0.170	0.241	0.849	1.671	2.776	7.61	0.160	0.244	0.847	1.656	-0.049	0.115	-0.199	0.010	+1.8	5.8	FO	A2,A4	*,NM
418	π 2700B	10.555	0.340	0.130	0.488	1.428														F5	
420	-6 1276	10.36	0.235	0.153	0.618	1.394														A8	
429	37527	8.68	0.052	0.205	0.974	1.488	2.879	8.71	0.059	0.203	0.975	1.499	0.003	0.047	-0.030	-0.007	+1.9	6.8	A5	A0V	*,NM?
431	-5 1352	10.45	0.450	0.113	0.929	2.055	2.816	9.04	0.123	0.211	0.864	1.532	-0.006	0.052	-0.055	0.327	+2.2	6.9	A8	A8	NM?
439	-5 1354	10.50	0.323	0.160	0.394	1.360														F3,F4	
451	-5 1356	10.44	0.475	0.116	1.028	2.210														A2,A5	
459	294319	10.26:	0.080	0.210	0.910	1.490	2.853	10.28:	0.086	0.208	0.911	1.500	-0.000	0.035	-0.028	-0.006	+2.1	8.2	A6	A2V	
467	294326	10.10	0.200	0.180	0.940	1.700	2.795	9.81	0.132	0.200	0.926	1.592	0.001	0.156	-0.124	0.068	+1.4	8.4	A9	A7V	NM?
470	294316	9.36	0.358	0.176	0.366	1.434	2.594	9.42	0.372	0.172	0.369	1.456	0.052	0.081	0.080	-0.014	+3.8	5.6	G2	G0	NM?
475	37874	9.67	0.190	0.180	0.870	1.610	2.831	9.33	0.111	0.204	0.854	1.483	0.003	0.013	-0.004	0.079	+2.4	6.9	A7	A1m	
483	-5 1365	10.12	0.150	0.200	0.850	1.550	2.799	10.065	0.137	0.204	0.847	1.530	-0.002	0.069	-0.059	0.013	+2.1	8.0	A9	A5m	
488	38052	9.55	0.123	0.192	0.904	1.534	2.855	9.39	0.086	0.203	0.897	1.475	0.005	0.017	-0.003	0.037	+2.2	7.1	A6	A7Vs	
492	38109	9.455	0.188	0.225	0.787	1.613	2.766	9.39	0.174	0.229	0.784	1.590	-0.039	0.072	-0.143	0.014	+2.2	7.2	FO	F2IVs	
497	-5 1377	9.78	0.314	0.131	1.145	2.035	2.841	8.77	0.077	0.202	1.098	1.657	0.006	0.246	-0.185	0.237	+0.5	8.3	A7	A4,II-III	
498	38274	10.235	0.199	0.158	0.704	1.418	2.774	10.11	0.169	0.167	0.698	1.371	0.027	-0.030	0.084	0.030	+3.0	7.1	FO	A8Vs	

168 The β value is inconsistent with the four-color photometry, which is from Smith (1972a); β should be rechecked. The observed $[b-y]$ is also not consistent with $(B-V)$, since the average $(B-V)$ is +0.28 and indicates a $[b-y]$ of +0.20. Star may be variable.

410 Since the photometry appears otherwise normal, the δm_0 index indicates a possible metallic-line spectrum for this foreground star.

429 The MK spectral type may not apply to this star. Smith (1972a) reports $(b-y) = 0.00$, $m_1 = 0.15$, $c_1 = 0.94$ and gives a y magnitude of 9.28. We obtain $y = 8.68$, in good agreement with the V magnitude of 8.67 reported by Sharpless (1962), hence either the star is highly variable or Smith's photometry is for a different star. It is not known if the MK type also applies to the different star.

TABLE 10a
DATA FOR B-TYPE STARS, SUBDIVISIONS c1,2,3,4

(1) Star	(2) ID	(3) V	(4) (b-y)	(5) m ₁	(6) c ₁	(7) (u-b)	(8) β	(9) δβ	(10) V ₀	(11) (b-y) ₀	(12) m ₀	(13) c ₀	(14) (u-b) ₀	(15) E(b-y)	(16) E(U-B)	(17) M _V	(18) dm	(19) Sp	(20) Spectrum	(21) Note
Subdivision c1																				
224	36842	8 ^m 13	-0 ^m 034	0 ^m 095	0 ^m 494	0 ^m 616	2 ^m 725	0 ^m 012	7 ^m 98	-0 ^m 069	0 ^m 105	0 ^m 487	0 ^m 560	0 ^m 035	0 ^m 034	-0 ^m 05	8 ^m 4	B6	B6V, B7V, B7-8V	*
227	36865AB	7.43	-0.019	0.111	0.560	0.744	2.756	-0.005	7.4	-0.063	0.124	0.551	0.674	0.044	0.039	0.0	7.4	B7	B8V	*
236	36883AB	7.25	-0.023	0.110	0.479	0.653	2.741	-0.009	7.4	-0.070	0.124	0.470	0.577	0.047	0.042	-0.2	7.6	B6	B5V, B6V, B7IV	*
248	36916	6.745	-0.068	0.116	0.486	0.582	2.705	0.032	6.74	-0.069	0.116	0.486	0.581	0.001	0.015: (-0.8)	(7.6)	B6	B8 III:p	*, NM?	
249	36936	7.57	-0.044	0.100	0.397	0.509	2.707	0.006	7.5	-0.078	0.110	0.390	0.454	0.034	0.026	-0.8	8.3	B4	B5V	*
258	36957	8.85	0.035	0.147	0.952	1.316	2.891	-0.014	8.59	-0.025	0.165	0.940	1.220	0.060	0.050	+1.2	7.4	B9	A1V	
276	36998	8.99	-0.010	0.129	0.836	1.074	2.832	-0.003	8.88	-0.035	0.137	0.831	1.033	0.025	0.032	+0.9	8.0	B8	B9V	
284	37016AB	6.24	-0.060	0.100	0.255	0.335	2.688	-0.006	6.6	-0.092	0.110	0.249	0.284	0.032	0.031	-1.2	7.8	B3	B2.5V, B3V, B2IV	*
285	37017	6.55	-0.057	0.104	0.158	0.252	2.641	0.016	6.36	-0.102	0.117	0.149	0.181	0.045	0.062	-2.0	8.4	B2	B1.5V, B2Vp, B2IV	*
303	37040AB	6.31	-0.056	0.096	0.245	0.325	2.677	0.003	6.3	-0.093	0.107	0.238	0.266	0.037	0.047	-1.5	7.8	B2	B2IV, B2.5V, B3V+B7V	*
335	37129	7.15	-0.065	0.104	0.219	0.297	2.677	-0.004	7.02	-0.095	0.113	0.213	0.248	0.030	0.032	-1.5	8.5	B2	B2V, B2Vp	*
Subdivision c2																				
251	36938	8.87	0.064	0.105	0.742	1.080	2.815	-0.030	8.40	-0.046	0.138	0.720	0.904	0.110	0.103	+0.5	7.9	B8	B8	*
260	36958A	7.34	-0.016	0.090	0.303	0.451	2.692	0.000	7.03	-0.088	0.112	0.289	0.336	0.072	0.069	-1.1	8.2	B3	B2IV, B3V	
277	294264	9.52	0.283	0.004	0.213	0.787	2.657	-0.003	7.87	-0.103	0.120	0.136	0.170	0.386	0.390	-2.0	9.8	B2	B3Vn	*
286	294262A	9.80	0.172	0.070	0.736	1.220	2.783	-0.005	8.86	-0.049	0.136	0.692	0.867	0.221	0.212	+0.4	8.5	B8	A0	
287	294263B	10.09	0.200	0.152	0.820	1.524	2.817	-0.009	9.06	-0.041	0.224	0.772	1.138	0.241	0.256	+0.2	8.8	B8	A0	*
295	37018AB	4.59	-0.080	0.079	-0.008	-0.010	2.617	0.005	4.5	-0.117	0.090	-0.015	-0.070	0.037	0.051	-3.4	7.9	B1	B1V, B2 III	*
304	37058	7.32	-0.070	0.105	0.160	0.230	2.654	0.003	7.19	-0.101	0.114	0.154	0.180	0.031	0.054	-2.1	9.3	B2	B2Vp	*
305	37059	9.08	-0.018	0.132	0.784	1.012	2.815	-0.008	8.98	-0.040	0.139	0.780	0.976	0.022	0.042	+0.8	8.2	B8	B8	
329	37130	9.97	0.130	0.090	0.803	1.243	2.788	0.014	9.23	-0.041	0.141	0.769	0.969	0.171	0.154	+0.5	8.8	B8	B8, B8-9(OP)	
Subdivision c3																				
233	π 1539	10.73	0.535	0.062	0.708	1.902	2.776	-0.018	8.17	-0.059	0.240	0.589	0.952	0.594	0.555	+0.1	8.1	B7	B8V	*
237	36899	9.59:	0.010	0.169	0.988	1.346	2.884	0.010	9.46:	-0.021	0.178	0.982	1.297	0.031	0.130:	+1.2	(8.3)	B9	B9V, B9-A0Vp	
262	-5 1310	10.46	0.413	0.068	0.837	1.799	2.809	-0.015	8.50	-0.043	0.205	0.746	1.069	0.456	0.438	+0.6	7.9	B8	B9	
269	36981	7.83	-0.053	0.105	0.382	0.486	2.701	0.009	7.72	-0.079	0.113	0.377	0.444	0.026	0.031	-0.9	8.6	B4	B1.5V, B3-5V, B5V	
288	37019	9.35	0.017	0.147	1.006	1.334	2.867	0.033	9.20	-0.019	0.158	0.999	1.276	0.036	0.034:	+1.1	8.1	A0	A0-1V, A0IV	
306	37060	9.35	0.007	0.142	0.959	1.257	2.858	0.025	9.22	-0.024	0.151	0.953	1.208	0.031	0.024	+1.0	8.2	B9	A0V	
Subdivision c4																				
245	36919B	9.32	-0.005	0.140	0.926	1.196	2.868	0.002	9.22	-0.027	0.146	0.922	1.161	0.022	0.015	+1.1	8.1	B9	B9V	
246	36918A	8.37	-0.042	0.108	0.457	0.589	2.717	0.011	8.24	-0.072	0.117	0.451	0.541	0.030	0.111	(-0.6)	(8.8)	B6	B8 III	*, NM?
264	π 1740	8.80	-0.021	0.110	0.769	0.947	2.790	0.011	8.71	-0.042	0.116	0.765	0.914	0.021	0.004	+0.5	8.2	B8	B9V	
265	36959B	5.68	-0.091	0.083	0.032	0.016	2.626	0.005	5.58	-0.113	0.090	0.028	-0.020	0.022	0.023	-3.0	8.6	B1	B1V	
266	36960A	4.78	-0.105	0.073	-0.056	-0.120	2.598	0.013	4.71	-0.122	0.078	-0.059	-0.147	0.017	0.026	-3.6	8.4	B0	B0V, B0.5V, B0.5Ve	*
271	36983	9.195	-0.008	0.130	0.849	1.093	2.840	-0.006	9.08	-0.034	0.138	0.844	1.051	0.026	0.023	+0.9	8.1	B8	B9.5V	
281	36999	8.48:	-0.040	0.113	0.531	0.677	2.762	-0.017	8.37:	-0.065	0.120	0.526	0.637	0.025	0.009	+0.1	(8.2)	B6	B7V	
282	37000	7.45	-0.046	0.088	0.267	0.351	2.673	0.012	7.3	-0.091	0.101	0.258	0.279	0.045	0.036	-1.6	8.9	B3	B3V, B5V	*
283	37025	7.16:	-0.056	0.104	0.334	0.430	2.688	0.013	7.04:	-0.084	0.112	0.328	0.385	0.028	0.036	-1.2	(8.3)	B3	B3V	
301	37043AB	2.77	-0.095	0.063	-0.120	-0.184	2.578	0.013	2.8	-0.128	0.073	-0.127	-0.237	0.033	0.044	-5.3	8.1	O9	O9 III	*

NOTES TO TABLE 10a

- 224 Bernacca (1968) notes stronger hydrogen lines than in standard (19 Tau), a weak Ca II K line, and a broad, washed-out appearance of the helium lines $\lambda\lambda 4026, 4471$. Photometry appears normal.
- 227 \underline{V}_0 corrected by 0.2 for duplicity.
- 233 The $\delta\beta$ index indicates an anomalously strong H β line. Strong hydrogen lines have been noted for several stars in the nebula region by H. M. Johnson (1965). The intrinsic $(\underline{b}-\underline{y})_0$ color has been used to derive $\underline{M}_V(\beta)_{ZAMS}$. The high index may be a result of a strong H δ line and/or high color excess.
- 236 \underline{V}_0 corrected by 0.3 for duplicity.
- 246 Morgan and Lodén (1966) note as a possible background star. The $(\underline{b}-\underline{y})_0$ color gives $\underline{M}_V(\beta)_{ZAMS} = -0.4$ and still places this star behind most others in the group. Garrison (1967) discusses the spectrum/color discrepancy, which shows up in our photometry via the B6 photometric type. Molnar (1972) finds the star to be of the weak helium type and derives $T_{\text{eff}} = 15600 \pm 600$ K, $\log g = 3.6 \pm 0.2$. Glaspey (1971a) finds that these stars lie on the main sequence in the $\beta, (\underline{u}-\underline{b})_0$ diagram, thus indicating normal luminosities; however, this would be expected if $\delta\beta$ is positive, as found here, and the $(\underline{u}-\underline{b})$ color is decreased due to back-warming effects from metal line blocking (Bernacca and Molnar 1972).

NOTES TO TABLE 10a (CONTINUED)

In fact, just such an effect is indicated here by the high color excess $E(U-B)$ determined from the UBV colors. The problem does not appear to be present in $(b-y)$ and a definite advantage in using the four-color system for the analysis of these stars is indicated.

248 Hack (1969) places this star ~ 1.5 above the main sequence which yields $\underline{M}_V = -1.8$. She states, however, that the \underline{M}_V , $H\gamma$ relation of Petrie gives ≈ -0.5 , in reasonable agreement with the $\underline{M}_V(\beta)$ found here. The $\delta\beta$ value found here places the star only 0.5 above the ZAMS. The absence of He lines in the spectrum (Bernacca 1968) explains the HD classification of B9. The rotational velocity of 100 km s^{-1} (Hack 1969) makes it unlikely that rotation is affecting the β index, hence the Balmer lines must be somewhat weak for the color. Hack also discusses some fairly strong unidentified absorption lines in the spectrum, mostly in the range $\lambda\lambda 3900-4600 \text{ \AA}$, but the \underline{m}_1 index appears normal for the color. She places the star among the typical silicon stars, but the photometry indicates that additional peculiarities may exist. The intrinsic color gives $\underline{M}_V(\beta)_{\text{ZAMS}} = -0.3$ and places the star at a less likely distance of 7.1 (assuming membership); the reddening value appears too low, however, and indicates that the colors are also affected somewhat by the

NOTES TO TABLE 10a (CONTINUED)

spectral peculiarities. The available proper motions are consistent and are outside the range for membership.

249 V_0 corrected by 0.1 (SB).

251 The H β line strength appears high for the intrinsic colors of this star. Since the c_0 spectral type is in agreement, $(\underline{b-y})_0$ has been used to derive $\underline{M_V}(\beta)_{\text{ZAMS}}$.

266 The high $\delta\beta$ index indicates possible emission and the resulting $\underline{M_V}(\beta)$ value (-4.2) has not been used. The $(\underline{b-y})_0$ result of -3.6 agrees well with $\underline{M_V}(\text{H}\gamma) = -3.7$, as derived from the calibration of Balona and Crampton (1974), hence this value is listed in the table. The spectrum may be composite (Murphy 1969), indicating a corrected distance modulus of 8.5 or 8.6, but no correction has been applied here.

277 The $\underline{M_V}(\beta)$ value derived here agrees well with that expected from the MK type and there is no reason to suspect intrinsic peculiarities in the stellar energy distribution, since the colors agree well with β . It appears that this star lies beyond the small clustering around 42 Orionis and that the heavy nebulosity in the region is producing the high color excess. This star also displays high polarization (2.6%) which is probably produced by aligned dust grains in the line of sight. The interpretation that both the reddening and polarization are produced by material in the

NOTES TO TABLE 10a (CONTINUED)

nebulous region surrounding the group is strengthened by the fact that all stars in the group having higher-than-normal $E(\underline{b-y})$ values show polarization, e.g. stars 251, 260, 277, 286, 287, 329. This star is omitted in the calculation of the mean distance to subgroup c2.

- 282 V_0 corrected by 0.1 (SB).
- 284 V_0 corrected by 0.5 for duplicity.
- 285 The spectrum displays exceedingly strong He I lines, similar in strength to those of σ Ori E (Morgan and Lodén 1966). An abundance analysis by Lester (1972) shows a He abundance higher than normal B stars by a factor of two but lower than that of σ Ori E. The derived effective temperature is 21000 K, as compared with 18600 K for the comparison star HD 37016 (No. 284). The difference in intrinsic colors reflects the higher temperature of this star. Due to anomalously weak Balmer lines, as indicated by $\delta\beta$, $(\underline{b-y})_0$ has been used to derive $\underline{M}_V(\beta)_{ZAMS}$. The β index gives -2.5 and a large distance modulus of 8.9.
- 287 The \underline{m}_0 index is very high and suggests spectral peculiarities.
- 295 42 Orionis. V_0 corrected by 0.1 for duplicity.

NOTES TO TABLE 10a (CONCLUDED)

- 301 1 Orionis AB. \underline{V}_0 has been corrected by 0.2 for a magnitude difference between the spectroscopic components of 1.99 (Batten 1967). According to Conti and Alschuler (1971) the spectral type of the spectroscopic secondary is B0 or later since He II $\lambda 4541$ does not appear in the spectrum.
- 303 \underline{V}_0 corrected by 0.2 for duplicity (the actual correction of 0.16 rounds \underline{V}_0 to 6.3).
- 304 V359 Orionis. This star has been noted as peculiar (see note to Table 2 of Paper I) and magnetic, but this has not been confirmed by other workers. The photometry indicates no abnormalities in color or H β line strength. The low reddening for this distance might be explained by its proximity to the very hot star 295 (also unreddened) which may have cleared local nebulous material by radiation pressure. These "holes" seem present in the Orion Nebula itself (see photograph in Turner 1973) and this phenomenon may be responsible for the lower reddening of the Trapezium stars relative to the less luminous objects immersed in the nebula.
- 335 The spectrum was suggested to have weak He lines by Sharpless (1952) but Molnar (1972) and Norris (1971) find that the star is a normal early B type. The photometry sustains the findings of the latter authors.

TABLE 10b
DATA FOR I-TYPE STARS, SUBDIVISIONS c1,2,3,4

(1) Star	(2) ID	(3) V	(4) (b-y)	(5) m ₁	(6) c ₁	(7) (u-b)	(8) β	(9) r	(10) V ₀	(11) (b-y) ₀	(12) m ₀	(13) c ₀	(14) (u-b) ₀	(15) a ₀	(16) δm ₀	(17) δc ₀	(18) δ(u-b) ₀	(19) E(b-y)	(20) M _V	(21) dm	(22) Spectrum	(23) Note
Subdivision c3																						
190	294224	11.39	0.532	0.074	0.911	2.123	2.829	0.018	9.49	0.091	0.206	0.823	1.418	-0.004	-0.028	-0.150	-0.074	0.441	(+1.42)	(8.23)	AOV,B6V	*
261	-5 1309	10.92	0.298	0.148	1.041	1.933	2.908	0.000	9.92	0.066	0.218	0.995	1.561	0.046	-0.023	0.029	-0.115	0.232	+1.8	8.2	AO,A2	
315	-5 1328	9.88	0.031	0.180	0.957	1.379	2.893	0.005	9.83	0.020	0.183	0.955	1.361	0.017	0.003	-0.023	0.037	0.011	+1.5	8.3	AOV	*
Subdivision c4																						
316	37078	9.42	0.037	0.189	1.005	1.457	2.892	0.022	9.41	0.035	0.190	1.005	1.453	0.051	0.007	0.041	0.000	0.002	+1.4	8.0	A2V	*

- 190 This star is extremely interesting and should be studied further. Although it lies far from the nebula, it seems to be at about the same distance as other members of the association and the reddening is abnormally high. The polarization is also one of the highest in the area (4.21%) surveyed by Breger (1976). The β index appears affected by incipient emission, hence the uncertainty in M_V, however, the star is categorized as intermediate type due to the spectral type and low [m₁] index. Detailed spectroscopy, spectrophotometry and infrared photometry would aid greatly in resolving the nature of this (peculiar?) object.
- 315 V566 Orionis. Abt, Muncaster and Thompson (1970) note broad H I lines and sharp Ca II H and K, Ca I and Mg II and suggest that this may be a shell star. We see no evidence of emission in the photometry, however.
- 316 A K-line index is available from Hesser, McClintock and Henry (1977). Using the relation (b-y)₀ = 0.216 - 0.036 from Warren (1975), the measured k of 0.376 gives (b-y)₀ = 0.04

TABLE 10c
DATA FOR A- AND F-TYPE STARS, SUBDIVISIONS c1,2,3,4

(1) Star	(2) ID	(3) V	(4) {b-y}	(5) m ₁	(6) c ₁	(7) {u-b}	(8) β	(9) V ₀	(10) {b-y} ₀	(11) m ₀	(12) c ₀	(13) {u-b} ₀	(14) δm ₀	(15) δc ₀	(16) δ{u-b} ₀	(17) E{b-y}	(18) M _v	(19) dm	(20) Sp	(21) Spectrum	(22) Note
Subdivision c1																					
212	π 1357	11 ^m .70	0 ^m .388	0 ^m .150	0 ^m .353	1 ^m .429	2 ^m .585													F8, G0	
232	294261	9.62	0.370	0.169	0.430	1.508	2.622	9.52	0.346	0.176	0.425	1.470	0.015	0.081	-0.039	0.024	+3.3	6.2	F9	F9V	*, NM
250	294257	9.80	0.315	0.152	0.474	1.408	2.632	9.83	0.321	0.150	0.475	1.418	0.032	0.111	-0.015	-0.006	+2.8	7.0	F8	F6V, F7IV	*, NM
259	36937	9.64	0.173	0.164	0.836	1.510	2.777	9.56	0.154	0.170	0.832	1.479	0.026	0.098	-0.022	0.019	+2.0	7.6	F0	A5Vn, A7V	
319	294256	11.04	0.408	0.175	0.394	1.560	2.581													F2, F8	
325	π 2267	11.38	0.388	0.156	0.391	1.479	2.571													F8	
Subdivision c2																					
225	36843	6.82	0.082	0.198	1.024	1.584	2.832	6.86	0.091	0.195	1.026	1.599	0.012	0.184	-0.121	-0.009	+1.0	5.8	A7	A3, A7 IV-V	NM
268	36958B	11.07	0.430	0.251	0.301	1.663	2.553													G5IV-V	
314	37077A	9.26	0.144	0.188	0.989	1.653	2.760	5.30	0.154	0.185	0.991	1.668	0.003	0.291	-0.226	-0.010	+0.5	4.8	F1	gP0	NM
330	294266	10.46	0.270	0.146	0.548	1.380	2.653	10.55	0.290	0.140	0.552	1.412	0.033	0.143	-0.050	-0.020	+2.2	8.4	F7	A7, F0	
Subdivision c3																					
195	294223	10.40	0.346	0.151	0.469	1.463	2.615	10.37	0.340	0.153	0.468	1.453	0.045	0.138	0.002	0.006	(+2.8)	(7.6)	G0	F6IV	
196	36742	9.68	0.241	0.161	0.647	1.451	2.678	9.77	0.261	0.155	0.651	1.482	0.015	0.177	-0.133	-0.020	+1.6	8.2	F5	F1 IV, F2 IV-V	
215	-5 1298	10.61	0.313	0.156	0.486	1.424	2.636	10.64	0.318	0.154	0.487	1.432	0.026	0.115	-0.039	-0.005	+2.8	7.9	F8	F7IV	
228	294265	10.26	0.164	0.169	0.907	1.573	2.810	10.08	0.121	0.182	0.898	1.504	0.023	0.098	-0.029	0.043	+1.8	8.3	A8	A7V, A8Vn	
289	-5 1317	9.87	0.469	0.178	0.400	1.694	2.568													F8-G0III-IV, V	
290	π 1955	10.91	0.747	0.167	0.304	2.132	2.575													G0-2III	
338	37142	9.38	0.316	0.148	0.456	1.384	2.618	9.45	0.332	0.143	0.459	1.410	0.052	0.123	0.035	-0.016	+2.9	6.5	G0	F4IV	NM
347	37208	9.19	0.169	0.168	0.829	1.503	2.753	9.21	0.174	0.167	0.830	1.511	0.019	0.144	-0.074	-0.005	+1.7	7.5	F1	A7Vn	NM?
Subdivision c4																					
239	-6 1230G	10.27	0.375	0.123	0.317	1.313	2.584	10.0	0.33	0.13	0.31	1.25				0.04	(+4.0)	(6.0)		F8V	*, NM?
244	π 1626	11.23	0.425	0.176	0.375	1.577	2.512													G2 IV, GOV	
253	π 1657	11.49	0.344	0.122	0.393	1.325	2.611	11.45	0.334	0.125	0.391	1.308	0.078	0.069	0.162	0.010	+3.6	7.8	G0	F5V	
254	π 1662	10.72	0.402	0.137	0.403	1.481	2.567													G0IV	
272	π 1789	10.50	0.331	0.168	0.409	1.407	2.615	10.58	0.349	0.163	0.413	1.436	0.039	0.089	0.030	-0.018	(+3.4)	(7.2)	G0	F6V	
299	-5 1322	9.78	0.082	0.213	0.930	1.520	2.850	9.80	0.087	0.211	0.931	1.528	-0.003	0.061	-0.056	-0.005	+1.9	7.9	A6	A6Vn	
300	-5 1321	9.74	0.244	0.166	0.692	1.512	2.679	9.80	0.259	0.162	0.695	1.536	0.008	0.218	-0.186	-0.015	(+1.1)	(8.7)	F5	F2IV, F3IV	
317	37102	8.99	0.291	0.160	0.390	1.292	2.648	9.07	0.309	0.155	0.394	1.320	0.020	-0.002	0.049	-0.018	+3.9	5.2	F7	F5V	NM

232 The derived distance modulus supports the suggestion of Morgan and Lodén (1966) and M. F. Walker (1969) that this is a foreground star.

239 Declared a foreground star by Morgan and Lodén (1966) and possible foreground by M. F. Walker (1969). Although the spectrum is normal, the β index appears too low by ~0.05 and is below the calibration limit of 2.590. We have therefore used the spectral type and MK, {b-y}₀ relation of Barry (1970) to find the intrinsic parameters. Unless this star is more than 2 mag above the ZAMS, it is a foreground field star. The proper motions agree with this conclusion; however, in addition to the low β, the photometric values of m₀ and c₀ do not agree with the spectral type at all. The F8 V type predicts m₀(Hyades) = +0.18, c₀(ZAMS) = 0.37. This star should be reobserved in order to check the photometry and for a possible mis-identification in the present work.

250 Same comments as for 232.

ORIGINAL PAGE IS
OF POOR QUALITY

TABLE 11a
DATA FOR B-TYPE STARS, SUBGROUP d

(1) Star	(2) ID	(3) V	(4) (b-y)	(5) m ₁	(6) c ₁	(7) (u-b)	(8) B	(9) δβ	(10) V ₀	(11) {b-y} ₀	(12) m ₀	(13) c ₀	(14) (u-b) ₀	(15) E(b-y)	(16) E(U-B)	(17) M _V	(18) d _m	(19) Sp	(20) Spectrum	(21) Note
Subdivision d																				
263	π 1685	10.17	0.098	0.131	0.922	1.380	2.858	0.000	9.62	-0.029	0.169	0.897	1.177	0.127	0.134	+1.0	(8.6)	B9	A0V	*
270	36982	8.45	0.140	0.012	0.147	0.451	2.635	0.010	7.39	-0.106	0.086	0.098	0.057	0.246	0.242	-2.3	9.7	B2	B1.5Vp	*
278	37021D	7.95	0.191	0.045	0.250	0.722	2.615	0.053	6.71	-0.097	0.131	0.192	0.261	0.288	0.318	(-1.6)	(8.3)	B2	B0V	*
279	37020GE	6.73	0.093	0.028	-0.046	0.196	2.584	0.019	5.79	-0.125	0.093	-0.090	-0.152	0.218	0.225	-4.0	(9.8)	B0	B0.5V	
280	37022AF	5.13	0.064	0.037	-0.161	0.041	2.553	0.007	4.28	-0.135	0.097	-0.201	-0.278	0.199	0.238	-6.4	10.7		O7V	
291	-5 1318	9.66	0.267	0.019	0.154	0.726	2.710	-0.069	8.05	-0.108	0.132	0.079	0.126	0.375	0.347	-2.4	(10.4)	B1	B0Vp	*
292	37023B	6.69	0.126	0.023	-0.057	0.241	2.610	-0.012	5.61	-0.126	0.099	-0.107	-0.163	0.252	0.275	-4.2	(9.8)	O9	B0.5Vp	
296	37041A	5.06	0.016	0.036	-0.108	-0.004	2.592	-0.005	4.7	-0.129	0.080	-0.137	-0.236	0.145	0.151	-4.7	9.4	O8	O9V, O9.5V, O9.5Vep	*
297	37042B	6.40	-0.004	0.049	-0.080	0.010	2.599	-0.000	5.88	-0.126	0.086	-0.104	-0.185	0.122	0.139	-4.2	10.1	O9	B0.5V, B0.5Vp, B1V	
298	-5 1326B	9.54	0.017	0.155	1.006	1.350	3.024	-0.124	9.39	-0.019	0.166	0.999	1.292	0.036	0.039	+1.2	(8.2)	A0	A0V	*
308	37062A	8.22	0.053	0.090	0.358	0.644	2.683	0.018	7.64	-0.084	0.131	0.331	0.425	0.137	0.151	-0.9	(8.5)	B3	B3-4V, B5V	
Subdivision d1																				
243	36917	7.99	0.121	0.093	1.079	1.507	2.811	0.103	7.41	-0.014	0.133	1.052	1.291	0.135	0.127	(+1.3)	(6.1)	A0	A0V	*
252	36939	9.00	-0.003	0.117	0.726	0.954	2.760	0.025	8.81	-0.046	0.130	0.717	0.885	0.043	0.042	+0.5	8.3	B8	B9V	*
307	37061	6.825	0.254	0.013	-0.048	0.486	2.610	-0.018	5.18	-0.128	0.128	-0.124	-0.125	0.382	0.395	-4.2	9.4	O9	B0.5V, B1V	*
321	π 2248	11.30	0.502	-0.027	0.194	1.144	2.672	-0.033	8.67	-0.109	0.156	0.072	0.167	0.611	0.602	(-2.5)	(11.2)	B1	B4V	*
326	37114	9.02	-0.010	0.136	0.870	1.122	2.842	0.002	8.93	-0.032	0.143	0.866	1.087	0.022	0.023	+1.0	8.0	B9	B8V, B9V	
327	37115AB	7.08	-0.039	0.112	0.357	0.503	2.572	0.133	7.3	-0.082	0.125	0.348	0.434	0.043	0.069	-0.8	8.1	B3	B4Veδ, B5ne, B6V	*
339	37150	6.56	-0.082	0.093	0.149	0.171	2.651	0.005	6.48	-0.102	0.099	0.145	0.139	0.020	0.029	-2.2	8.6	B2	B2V, B3V, B3IV	
344	37174	9.21	-0.015	0.131	0.886	1.118	2.878	-0.026	9.14	-0.030	0.136	0.883	1.093	0.015	0.015	+1.0	(8.1)	B9	B9V	
349	π 2425	10.66	0.578	-0.042	0.269	1.341	2.647	0.006	7.73	-0.103	0.162	0.133	0.252	0.681	0.644	-2.3	10.0	B2	B6V	*

NOTES TO TABLE 11a

Since the β indices in general appear adversely affected by nebulosity, the intrinsic colors $(\underline{b-y})_0$ will be used to predict absolute visual magnitudes for stars in subgroup d. When $|\delta\beta|$ values are small, these absolute magnitudes will of course agree with those determined from β . Since many of the nebula stars are near the top of the main sequence where the slope of the β , $\underline{M}_V(\beta)$ relation is large, small changes in β correspond to much larger changes in $\underline{M}_V(\beta)$ and, in view of the problems with nebulosity, it is safest to assume that all stars are on the ZAMS. The only star for which this assumption may not be valid is $-5^\circ 1326B$, since the photometry appears quite normal for $\pi 1685$. This assumption is of course invalid for all stars if they are subluminous and are located below the ZAMS; evidence for systematically fainter absolute magnitudes for stars in the inner nebula has been found by Morgan (1956).

243

V372 Orionis. The circumstances here are very peculiar in that the high reddening indicates possible membership while the low distance modulus and large $\delta\beta$ suggest a foreground field star. If the β index is used to predict $\underline{M}_V(\beta)$ [$(\underline{b-y})_0$ has been used in the table], we still obtain $\underline{M}_V(\beta) = +0.7$ and a dm of 6.7. Assuming a membership distance modulus of 8.4, this star would be located ~ 2 mag above the ZAMS. Although

NOTES TO TABLE 11a (CONTINUED)

used as a member by Vaerewyck and Beardsley (1973), we must still consider membership tentative. However, the star is polarized (0.84%) and Penston (1973) suggests the presence of a blue continuum, which makes it somewhat surprising that our c_0 value agrees with the MK spectral type.

- 252 The intrinsic index $(\underline{b-y})_0$ has been used to derive $\underline{M}_V(\beta)_{ZAMS}$, since β appears affected by incipient emission. The low reddening and distance modulus place the star slightly closer than the distance at which heavy absorption begins, as with star 298. The proper motions and radial velocity support membership.
- 263 Abt, Muncaster and Thompson (1970) suggest that the spectrum may be composite, but no correction to \underline{V}_0 has been applied.
- 270 LP Orionis. The hydrogen lines are found to be abnormally strong (Sharpless 1952) and Balmer cores appear redshifted (H. M. Johnson 1965). The large distance modulus is typical for many stars in the nebula and may be due to subluminality, a high ratio of total-to-selective absorption, or adverse effects of nebulosity on the photometry. The derived absolute magnitudes and distances for these stars are nevertheless reported in the table because it

NOTES TO TABLE 11a (CONTINUED)

may be possible to use these values to help disentangle the above effects. These problems are explored further in the text. This star is used as a cluster member in the relative proper-motion study of Vaerewyck and Beardsley (1973).

278 BM Orionis. Either an Algol (Kurkarkin et al. 1971)- or β Lyrae (Walker 1969)-type variable, this star has been studied extensively by Hall and Garrison (1969) and by Popper and Plavec (1976). The latter authors find a normal B3 V primary component and a secondary which appears to be a pre-main-sequence late A-type (best estimate A7 IV or V) star lying ~ 2 mag above the main sequence. The present four-color and β observations were all made outside eclipse, but they are obviously affected by nebulosity and/or the peculiar nature of the object. This appears especially so for β ; sky measures were taken on four sides about this star, as they were for all stars within the nebula.

291 Although used as a non-member reference by Vaerewyck and Beardsley (1973), we consider it here to be a possible member. The available proper motions indicate membership according to our criteria and the measured radial velocity (Johnson 1965) is close to the mean for nebula cluster stars ($+36 \text{ km s}^{-1}$). The high color excess would appear to indicate larger optical depth than for other nebula stars. The derived absolute magnitude is considerably fainter than expected for B0 V and corresponds to spectral type

NOTES TO TABLE 11a (CONTINUED)

- B2 V on Walborn's (1972) scale. Johnson has also noted broad Balmer lines in the spectrum, as is characteristic of many of the stars associated with the nebula.
- 296 θ^2 Orionis A. A careful examination of spectral tracings by Aikman and Goldberg (1974) has revealed profile asymmetries from which Δm is estimated to be 1.5; V_0 has therefore been corrected by 0.24 mag.
- 298 Although the β index is completely out of order and the measured four-color indices are variable, the photometric colors agree well with the reported MK type. The low reddening and derived distance modulus place the star on the near side of the nebula, yet very possibly a member of the cluster (there is no evidence to indicate otherwise). The star is also located in the region southeast of the shock front near θ^2 Ori A, an area in which the absorption appears lower, even at distances greater than 8.2 mag.
- 307 NU Orionis. The β index places this star below the ZAMS and appears affected by nebulosity, hence $(\underline{b}-\underline{y})_0$ is used for $\underline{M}_V(\beta)_{\text{ZAMS}}$. The star also appears considerably bluer photometrically than the spectral types indicate, i.e. incipient emission may be affecting the \underline{c}_1 index. The measured polarization is high (1.37%, Breger 1976; 1.54% variable, Serkowski *et al.* 1975) and the wavelength of maximum polarization λ_{max}

NOTES TO TABLE 11a (CONCLUDED)

is 6400 \AA . Using $R = 5.5 \lambda_{\text{max}}$ (Serkowski *et al.* 1975) gives $R(\underline{b-y}) = 5.0$, $V_0 = 4.9$, $dm = 9.1$.

- 321 The low \underline{m}_1 index and agreement of $\underline{E}(\underline{b-y})$ and $\underline{E}(\underline{U-B})$ indicate a B-type star, but the photometry is clearly adversely affected and makes analysis difficult. The absolute magnitude has been derived from $(\underline{b-y})_0$, but the assumed position on the main sequence may be incorrect. The measured polarization is very high (3.13%), in agreement with the high color excess. The recent spectral type of Penston *et al.* (1975), now included in the table, confirms the assumed B-star status.
- 327 V_0 corrected by 0.4 for duplicity and suspected SB2. Spectrum displays double He I and Mg II lines not attributable to the emission (Abt, Muncaster and Thompson 1970). The intrinsic color $(\underline{b-y})_0$ has been used to derive $\underline{M}_V(\beta)_{\text{ZAMS}}$. The \underline{c}_1 index appears a bit low for the spectral types reported and may be affected by continuum emission.
- 349 The B-type (see Table 2, Paper I) has been assumed here due to the low \underline{m}_1 index and agreement of $\underline{E}(\underline{b-y})$ and $\underline{E}(\underline{U-B})$. Like 321, this star appears to be behind much absorbing material and displays high polarization (3.47%). The spectral type in the present table is by McNamara (1976) and agrees with the B-type assumed.

TABLE 11b
DATA FOR I-TYPE STARS, SUBDIVISION d1

(1) Star	(2) ID	(3) V	(4) (b-y)	(5) m ₁	(6) c ₁	(7) (u-b)	(8) β	(9) r	(10) V ₀	(11) (b-y) ₀	(12) m ₀	(13) c ₀	(14) (u-b) ₀	(15) a ₀	(16) δm ₀	(17) δc ₀	(18) δ(u-b) ₀	(19) E(b-y)	(20) M _V	(21) dm	(22) Spectrum	(23) Note
242	-5 1306	10 ^m 26:	0 ^m 396	0 ^m 097	1 ^m 075	2 ^m 061	2 ^m 808	0 ^m 106	3 ^m 97:	0 ^m 096	0 ^m 187	1 ^m 015	1 ^m 580	0 ^m 063	0 ^m 013	0 ^m 061	-0 ^m 113	0 ^m 300	+0 ^m 1	(8 ^m 9)	A2,A6-7V	

TABLE 11c
DATA FOR A- AND F-TYPE STARS, SUBDIVISION d1

(1) Star	(2) ID	(3) V	(4) (b-y)	(5) m ₁	(6) c ₁	(7) (u-b)	(8) β	(9) V ₀	(10) (b-y) ₀	(11) m ₀	(12) c ₀	(13) (u-b) ₀	(14) δm ₀	(15) δc ₀	(16) δ(u-b) ₀	(17) E(b-y)	(18) M _V	(19) dm	(20) Sp	(21) Spectrum	(22) Note
216	-5 1297	10 ^m 31	0 ^m 365	0 ^m 187	0 ^m 377:	1 ^m 481:	2 ^m 661	10 ^m 08:	0 ^m 311:	0 ^m 203:	0 ^m 366:	1 ^m 395:	-0 ^m 032:	-0 ^m 066:	-0 ^m 040:	0 ^m 054:	(+4 ^m 4)	(5 ^m 7)	F6	F8III-IV, F5IV	
217	-5 1299	10.23:	0.389	0.151	0.455	1.535	2.601	10.10:	0.357	0.160	0.449	1.484	0.054	0.147	0.024	0.032	+3.0	(7.1)	G1	F6IV-V, F7IV	*, NM?
226	π 1455	10.92	0.447	0.177	0.339	1.587	2.497												G0-IIV		
238	π 1575	11.08	0.306	0.154	0.409	1.329	2.669	10.99:	0.285	0.160	0.405	1.296	0.010	-0.043	0.053	0.021	+4.1	6.9	F5	F0-2III-V	NM?
309	-5 1324	9.91:	0.370:	0.182	0.740:	1.844:	2.696:	9.39:	0.249:	0.218:	0.716:	1.650:	-0.049:	0.198:	-0.284:	0.121:	(+1.4)	(8.0)	F4	F2III-IV	*
320	-5 1329	10.30:	0.317:	0.148	1.268:	2.198:	2.794:													B8-A3Vp, A3Vea *	
348	-5 1337	10.715	0.155	0.183	0.799:	1.475:	2.769	10.76:	0.165:	0.180:	0.801:	1.490:	0.011:	0.083:	-0.041:	-0.010:	(+2.1)	(8.6)	F0	A9IV-F0IV	

All A- and F-type program stars in this region appear peculiar, hence the derived absolute magnitudes and distance moduli are practically meaningless. The alternate technique of finding M_V (ZAMS) from (b-y)₀, as used for B-type stars in this region, has not been attempted here since all these stars which are members are known to lie well above the ZAMS. For additional information on some of these stars, consult the notes to Table 2 of Paper I.

- 217 Used as a non-member by Vaerewyck and Beardsley (1973). Our collected proper-motion data from four sources are not definitive (Table 8, Paper I), but variability and assigned spectral types suggest possible membership. The four-color data (Table 17, Paper I) are quite consistent from three sources, however, so the variability in V may be strictly due to the nebula.
- 309 NV Orionis. See note to Table 2 of Paper I for additional spectral types and peculiarities. Considering the variability of the indices, our derived color excess is in reasonably good agreement with the value of 0.07 found by Smith (1972a) from his assigned spectral type
- 320 T Orionis. See note to Table 2 of Paper I Listed as A-type only on basis of A3 Vea classification. The c₁ index is well above the upper limit for the A-star calibration, hence no reduction has been attempted.

FIGURE CAPTIONS

FIG. 1.— Relation between m_0 and β for B-, I-, and AF-type stars in subgroup a. Emission and peculiar stars are designated by the letters "e" and "p," respectively. The solid line for B stars is a mean relation derived from an eye fit to all Orion 1 B-type program stars and will be useful for detecting differences in m_0 among the subgroups. The dashed line for B stars is a field-star sequence derived from dwarfs having known MK types, as described by Warren (1976, Table I). The solid line for intermediate (I)-group stars (near $\beta \sim 2.9$ and $m_0 \sim 0.18$) is the ZAMS relation of Glaspey (1971a), while the dashed line for AF stars is the standard Hyades sequence of Crawford and Perry (1966).

FIG. 2.— V_0, β diagram for B-type stars in subgroup a, omitting suspected non-members. Open symbols are emission and/or peculiar stars; parentheses indicate uncertain indices. The dashed and solid lines show the ZAMS at distance moduli of 7.8 and 8.0 mag, respectively. The uneven distribution of points with respect to these lines for stars having $\beta > 2.8$ suggests observational selection

effects and these stars have been omitted in the final distance calculation.

- FIG. 3.— Relation between distance modulus and β for B- and I-type stars of subgroup a. Emission and peculiar stars are omitted and non-members indicated by open symbols. The trend in this diagram for $\beta > 2.8$ is interpreted as due to observational selection.
- FIG. 4.— The β , c_0 diagram for the B-type stars of subgroup a. This diagram is independent of distance and does not show the scatter seen in Fig. 2 where the V_0 parameter is used. The deviation of the early B-star locus above the ZAMS (for a distance modulus of 7.8) is attributed to evolutionary effects.
- FIG. 5.— Color excess $E(b-y)$ plotted against distance modulus ($V_0 - M_V$) for subgroup Ia stars. Open symbols indicate probable or possible non-members. The large vertical spread for members indicates variable reddening within the subgroup.
- FIG. 6.— Diagram of distance modulus versus right ascension for B and I stars of subgroup Ia. Open symbols denote probable and possible non-members, while triangles represent stars studied by Lesh (1968a) and Steffey (1973).
- FIG. 7.— Diagram of distance modulus versus declination for B and I stars of subgroup Ia. Symbols are

the same as in Fig. 6. A trend toward increasing distance with δ indicates that the 1a subgroup may run smoothly into the λ Orionis clustering.

FIG. 8.— Relation between \underline{m}_0 and β for B-, I-, and AF-type stars in subgroup b. Symbols and mean relations are the same as in Fig. 1.

FIG. 9.— \underline{V}_0 , β diagram for B-type stars in subgroup b; non-members are omitted. Open symbols represent peculiar and/or emission stars; uncertain and/or variable indices are indicated by parentheses.

FIG. 10.— Relation between distance modulus and β for B- and I-type stars of subgroup b. Emission and peculiar stars are omitted and non-members indicated by open symbols. Parentheses denote variable and/or uncertain indices. The excess of nearer stars for $\beta > 2.8$ is interpreted as due to observational selection.

FIG. 11.— The β , \underline{c}_0 diagram for B-type stars in subgroup b. The many stars below the ZAMS indicate abnormally strong hydrogen lines.

FIG. 12.— Diagrams of distance modulus against equatorial coordinates for program stars in the 1b subgroup. Open symbols represent probable or possible non-members. See text for discussion.

FIG. 13.— Variable extinction diagram for members of the Belt subgroup. The open square represents HD

37903, which is embedded in the nebula NGC 2023 near the Horsehead complex. This appears to be the only program star exhibiting a higher-than-normal ratio of total-to-selective absorption. See text for discussion.

FIG. 14.— A plot against $E(\underline{b-y})$ of the residuals from the mean distance modulus of 8.39 for individual moduli obtained by setting $R(\underline{b-y}) = 4.3$ and 7.9; see text for discussion.

FIG. 15.— The $\underline{a_0} - r$, $\underline{a_0}$ (c-m)-type diagram for stars of the intermediate group in subgroup b. Open symbols represent non-members, while parentheses denote uncertain photometry.

FIG. 16.— The $\underline{c_0}$, β c-m diagram for AF-type stars in subgroup b. Open symbols denote probable or possible non-members, while parentheses indicate uncertain photometry. The line is the standard preliminary ZAMS relation (Crawford and Perry 1966 or Crawford and Barnes 1974). Most non-members fall well above the ZAMS, while most presumed members are located along or below same.

FIG. 17.— Relation between $\underline{m_0}$ and β for B-, I-, and AF-type stars in subgroup c. Symbols and mean relations are the same as in Fig. 1.

FIG. 18.— A comparison of the c-m diagrams for the subdivisions of subgroup c. Open symbols represent

binaries corrected for duplicity, while uncertain and/or variable indices are indicated by parentheses. ZAMS relations for subdivisions c, c1, c2, c3 and c4 are drawn for distance moduli of 8.1, 8.0, 8.45, 8.2 and 8.4, respectively. Scatter due to distance spread is very apparent in the outer region (c) but greatly reduced for the small clusterings (c1-c4) near the nebula. No evolutionary differences are seen in these diagrams.

FIG. 19.— V_0 , β diagram for B-type stars in subgroup c.

Probable and possible non-members are omitted; open symbols indicate peculiar and/or emission stars, while parentheses denote variable and/or uncertain indices. The ZAMS relation is drawn for a distance modulus of 8.1.

FIG. 20.— V_0 , β diagram for B-type stars in subgroup d.

Open symbols represent peculiar and/or emission stars; variable and/or uncertain indices are denoted by parentheses, and appreciably reddened stars are shown by the letter "r." The ZAMS is drawn for a distance modulus of 8.4; the dashed line shows the effect of 0.03 mag emission on the β index (see text).

FIG. 21.— V_0 , c_0 diagram for B-type stars in subgroup d.

Open symbols represent peculiar and/or emission stars; variable and/or uncertain indices are

denoted by parentheses, and stars having appreciably higher color excesses than the foreground value of $E(\underline{b-y}) = 0.04$ are shown by the letter "r." The ZAMS is drawn for a distance modulus of 8.4.

FIG. 22.— The $\Delta\beta(\underline{V}_0)$ and $\Delta c_0(\underline{V}_0)$ indices (as defined in the text) are plotted against color excess $E(\underline{b-y})$ for members of the 1d subgroup. Open symbols and parentheses denote peculiar and/or emission and variable and/or uncertain indices, respectively.

FIG. 23.— The \underline{V}_0 , β [MK] diagram for B-type stars in subgroup d. Symbols are the same as in Fig. 20 except that "p" now denotes that a star is polarized. [All stars in this diagram have polarization data.] Stars having more than one MK temperature subclass are displayed by connected symbols.

FIG. 24.— The \underline{V}_0 , c_0 [MK] diagram for B-type stars in subgroup d. Symbols are the same as in Fig. 23.

FIG. 25.— The β , c_0 diagram for B-type stars in subgroup d; symbols are the same as in Fig. 20. The solid line is the ZAMS as used in previous β , c_0 diagrams.

FIG. 26.— The $\underline{a}_0 - r$, \underline{a}_0 (c-m)-type diagram for stars of the intermediate group in subgroup c. Open symbols represent possible and probable non-members, while parentheses denote uncertain and/or variable

photometric indices. The ZAMS was found from the data of Glaspey (1971a).

FIG. 27.— Relation between the two temperature-sensitive indices β and $(\underline{b-y})_0$ for the A- and F-type stars of subgroup c. The ZAMS relation for the A stars is from a preliminary calibration of Crawford (1970), while that for the F stars is from the final calibration (Crawford 1975b). Parentheses indicate uncertain and/or variable indices.

FIG. 28.— (a) The \underline{m}_0 , β diagram for I and AF stars of subgroup c. Parentheses indicate uncertain photometry, while "m" denotes an Am star as classified by Smith (1972a). The ZAMS relation for the I group is that of Glaspey (1971a).

FIG. 28.— (b) Relationship between the blanketing parameter $\underline{m}_0 = \underline{m}_0(\text{standard}, \beta) - \underline{m}_0(\text{observed}, \beta)$ and β for the same stars as in (a). The deviations of some F-type stars in the upper diagram are not identical to those plotted in (b) because the final standard (Hyades) relation is plotted in (a) while the preliminary relation was used in calculating the $\delta\underline{m}_0$ values plotted in (b). The differences are very small, however.

FIG. 29.— The \underline{V}_0 , β diagram for A- and F-type stars in subgroup c. The line is the ZAMS relation at the mean distance of 8.2 found from the B-star

analysis. As before, parentheses denote uncertain photometry.

FIG. 30.— The \underline{c}_0 , β c-m diagram for the A- and F-type stars in subgroup c. The ZAMS relation for the A stars ($\beta > 2.720$) is from the preliminary calibration of Crawford (1970), while that for the F stars ($\beta \leq 2.720$) is from the final calibration of Crawford (1975b).

FIG. 31.— The β , \underline{c}_0 diagram for B-type stars in subgroup c. This diagram is very similar to its counterpart for subgroup b (Fig. 11) and shows many stars located below the ZAMS. This effect is often a result of abnormally strong hydrogen lines but may also be connected with blue continuum emission from these young objects (see text for discussion).

FIG. 32.— Relation between $\delta' \underline{m}_0$ ($= \underline{m}_0 - \underline{m}_0(\underline{c}_0)$, see text) and color excess $\underline{E}(\underline{b}-\underline{y})$ for B-type program stars having spectra not known to be peculiar. See text for discussion.

FIG. 33.— Diagram of $\delta' \beta$, $\delta' \underline{m}_0$ indices, as defined in the text. This diagram shows the relative independence of these indices, even though both are derived from \underline{c}_0 indices which may be affected by continuum emission (a possible slight trend from upper left to lower right may be due to a weak dependence of $\delta' \underline{m}_0$ on the H δ line strength).

FIG. 34.— Relation between $\delta \underline{m}_0$ [= \underline{m}_0 (std.) - \underline{m}_0 (obs.)] and the color excess $\underline{E}(\underline{b}-\underline{y})$ for I- and AF-type stars in Orion lc. As in previous diagrams, parentheses indicate uncertain photometric indices.

FIG. 35.— (a) Correlation between the blanketing index $\delta \underline{m}_0$ and the uv excess index $\delta(\underline{u}-\underline{b})_0$. Symbols are the same as in Fig. 29. (b) Relation between $\delta \underline{m}_0$ and the luminosity index $\delta \underline{c}_0$. Little, if any, correlation is present, thus indicating that $\delta \underline{m}_0$ is not strongly affected by luminosity differences. (c) Correlation between $\delta \underline{c}_0$ and $\delta(\underline{u}-\underline{b})_0$. Luminosity effects on the $\delta(\underline{u}-\underline{b})_0$ index are evident and the $(\underline{u}-\underline{b})$ index is more sensitive to luminosity changes than is \underline{c}_1 .

FIG. 36.— Relation between \underline{m}_0 and the equivalent width of H γ on the Victoria system for B-type stars. Bars denote stars having $\underline{E}(\underline{b}-\underline{y}) \geq 0.10$.

FIG. 37.— The \underline{m}_0 , \underline{c}_0 diagrams for B-type stars in subgroups a, b, and c. The solid lines represent the field-star relation given in Table I of Warren (1976). Parentheses again denote uncertain and/or variable indices.

FIG. 38.— Relations between the intrinsic indices \underline{m}_0 and \underline{c}_0 for B-type members of the Centaurus and Upper Scorpius subgroups of the Sco-Cen association. Parentheses indicate stars whose indices have been

reported as uncertain, while the letters "e" and "p" denote emission and peculiar stars, respectively. The field-star relations are shown for reference.

FIG. 39.— The \underline{c}_0 , $(\underline{u-b})_0$ diagram for all B-type presumed members of Orion OB 1 on the present program. Parentheses indicate uncertain and/or variable indices. The line is Crawford's preliminary ZAMS relation.

FIG. 40.— The \underline{c}_0 , $(\underline{u-b})_0$ relation for B-type presumed members of the Sco-Cen association. Parentheses indicate uncertainty in the indices, while the letters "e" and "p" denote emission and peculiar stars, respectively. The line is Crawford's preliminary ZAMS relation.

FIG. 41.— The β , \underline{c}_0 diagrams for subgroups a, b and c. Probable and possible non-members are excluded here. Open symbols refer to emission and/or peculiar stars, while parentheses denote uncertain and/or variable indices.

FIG. 42.— \underline{V}_0 , $(\underline{b-y})_0$ color-magnitude diagram for all program stars in the association not designated NM or NM? in the summary tables. Open symbols denote variable and/or uncertain indices. The line is the ZAMS for a distance modulus of 8.3. The inset

shows the same relation for subgroups 1c and 1d only. The ZAMS line is drawn for 8.4 here.

FIG. 43.— Histograms for the distributions of unreddened and reddened stars in the northern (upper diagram) and southern (lower diagram) regions of Orion OB 1. Only presumed B-type members are included. Solid bars represent stars having $E(b-y) < 0.1$, while dashed bars represent reddened stars [$E(b-y) \geq 0.1$].

FIG. 44.— The distribution of Orion OB 1 B- and I-type stars in distance and Galactic longitude, as projected onto the Galactic plane. Open symbols denote stars designated as probable or possible non-members in the summary tables, while parentheses indicate uncertain distances.

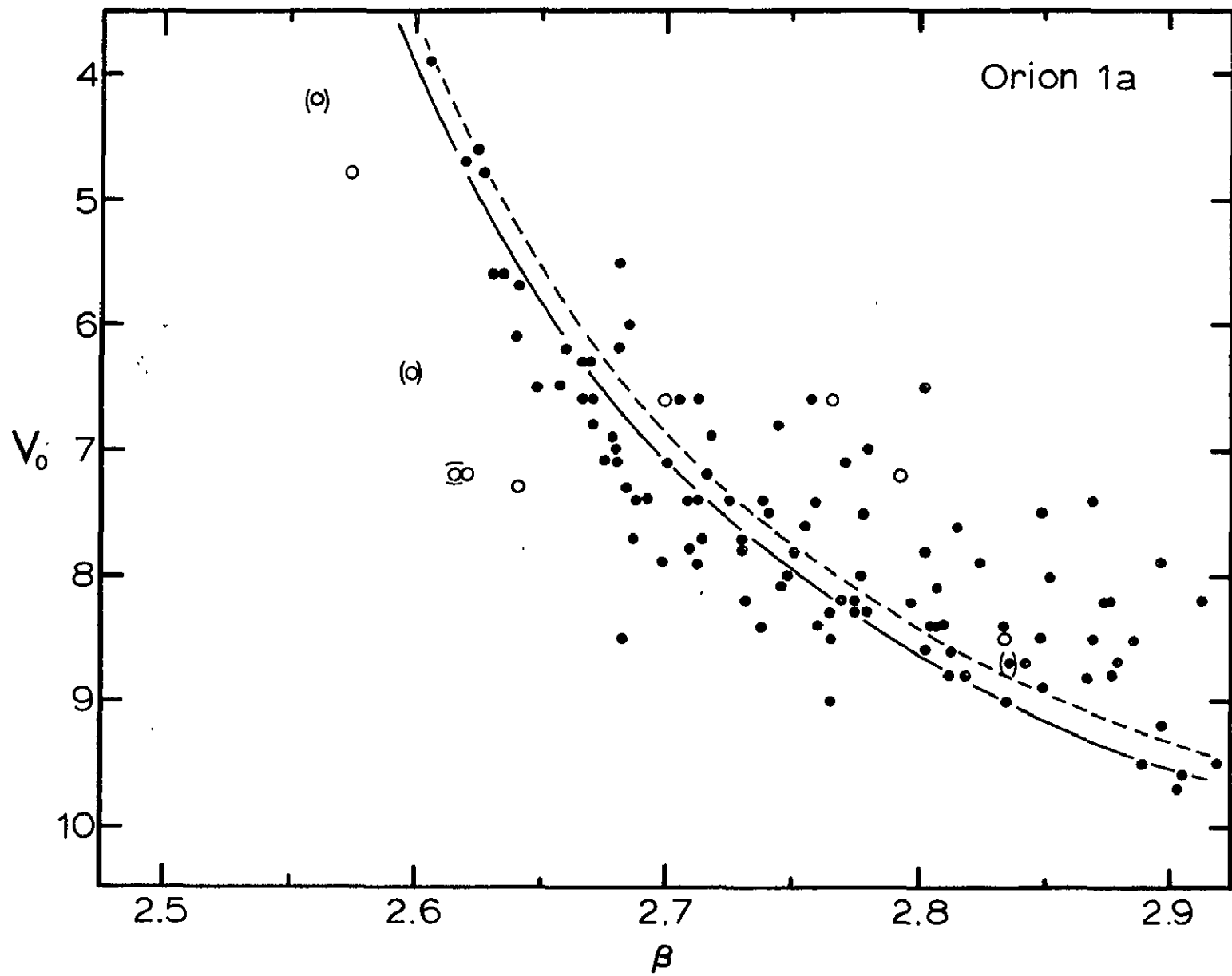


Figure 2

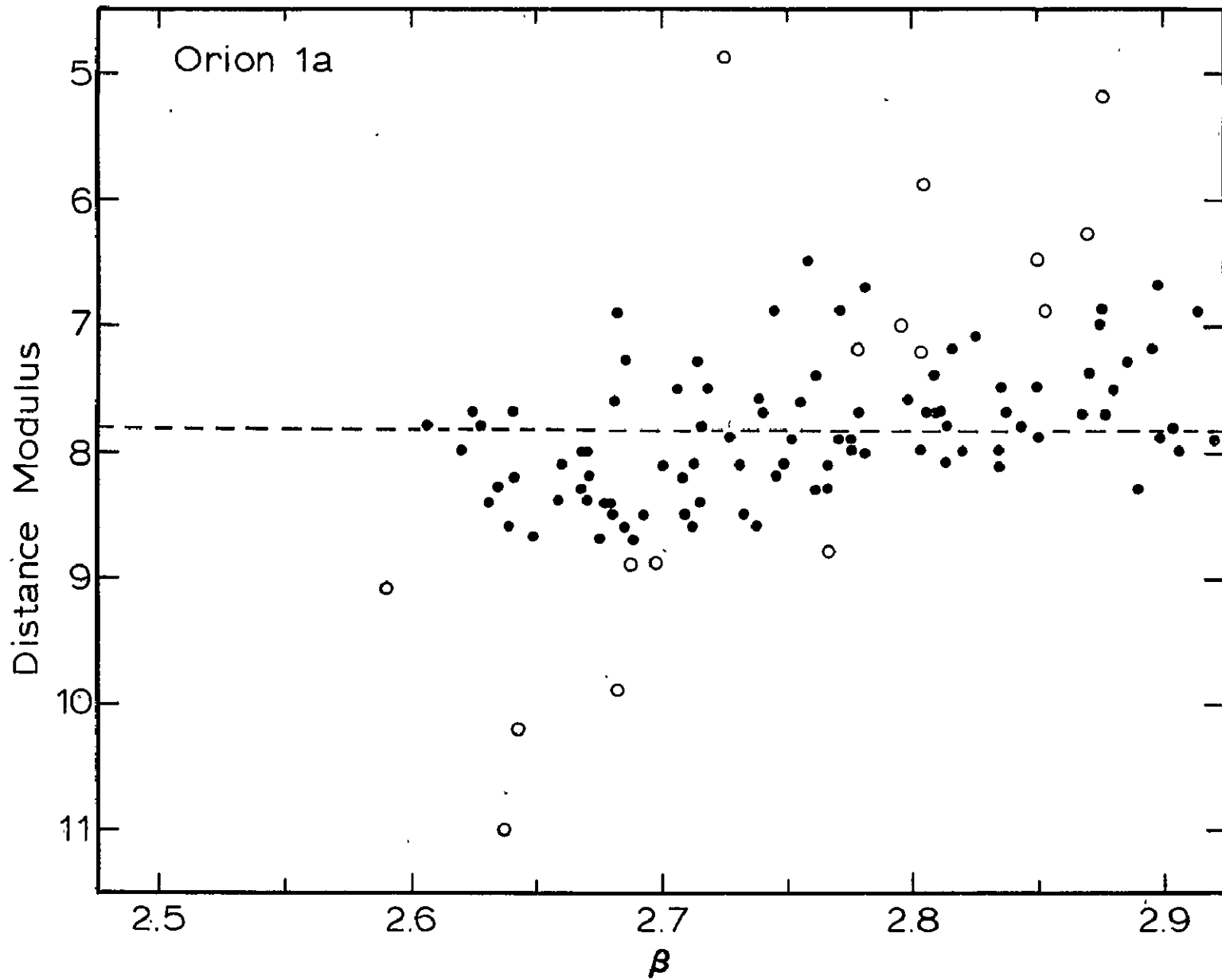


Figure 3

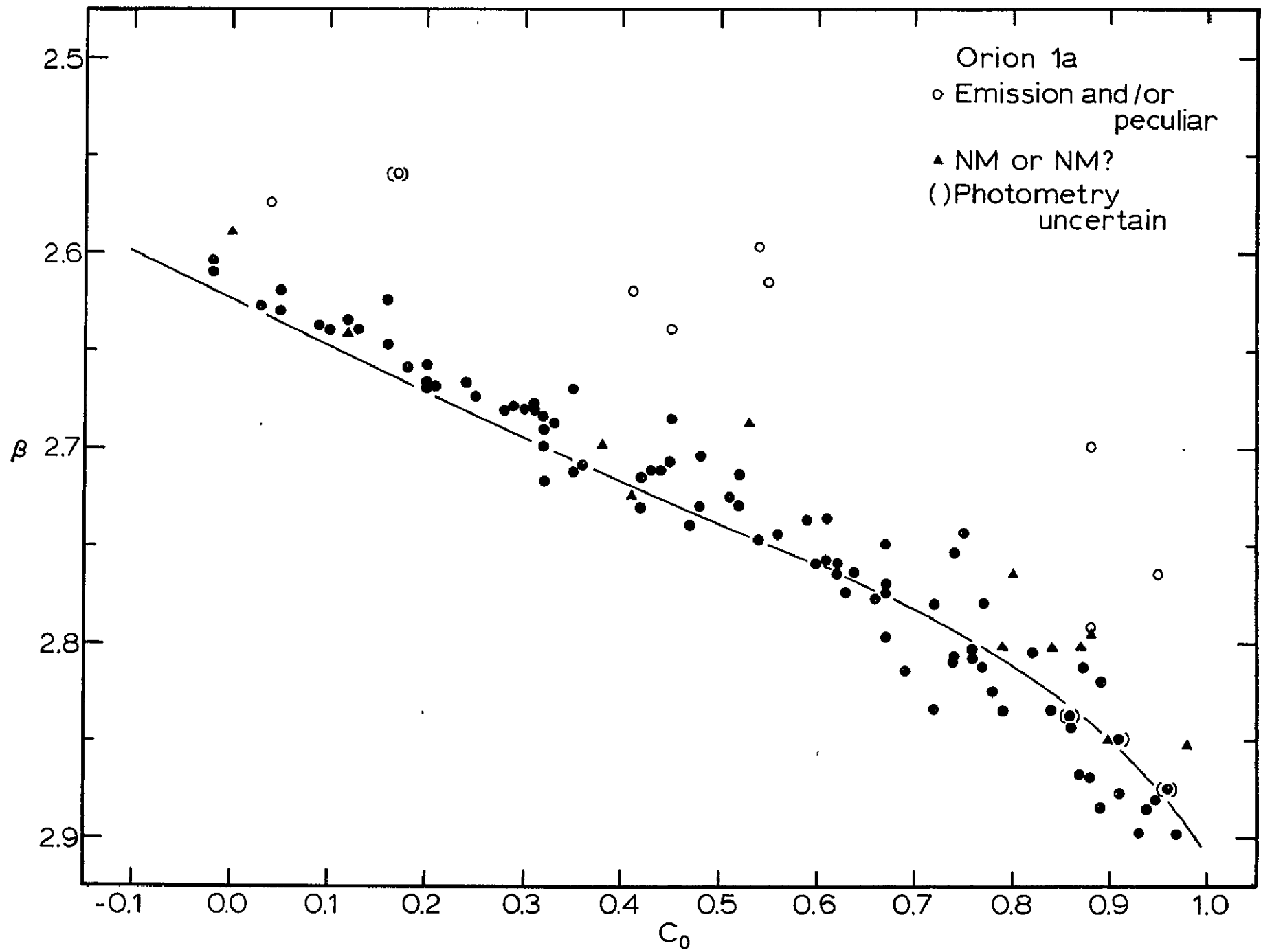


Figure 4

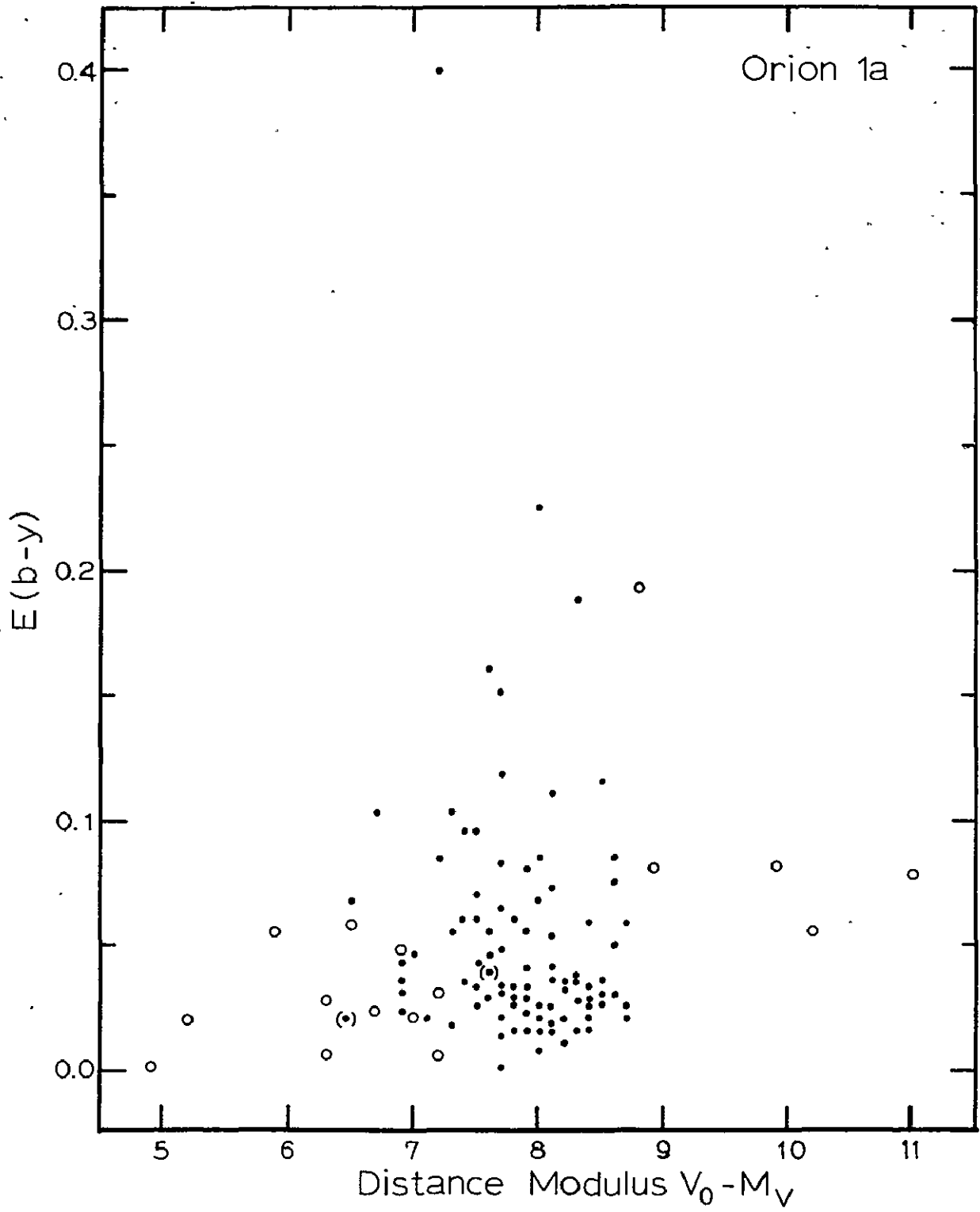
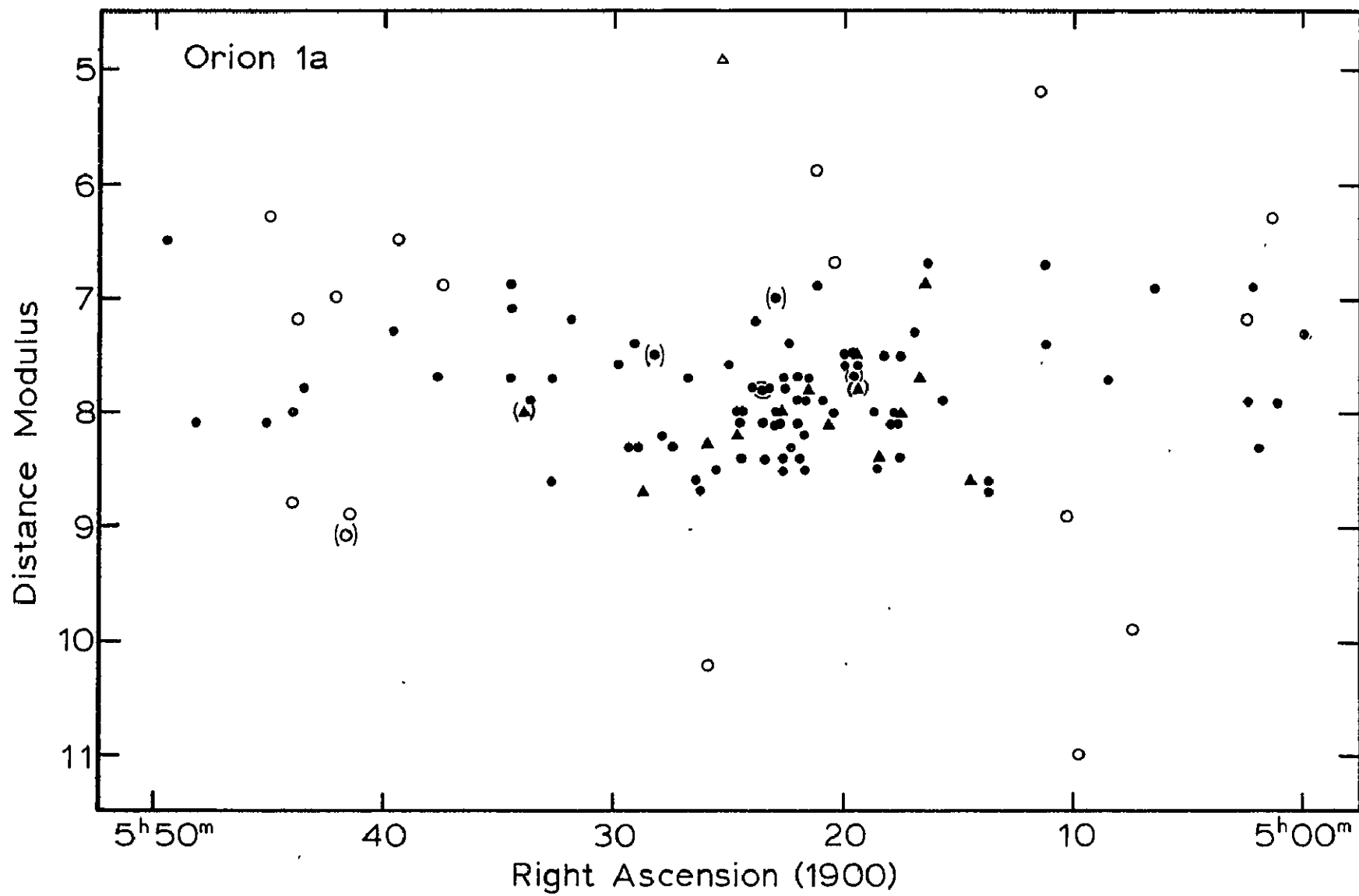


Figure 5



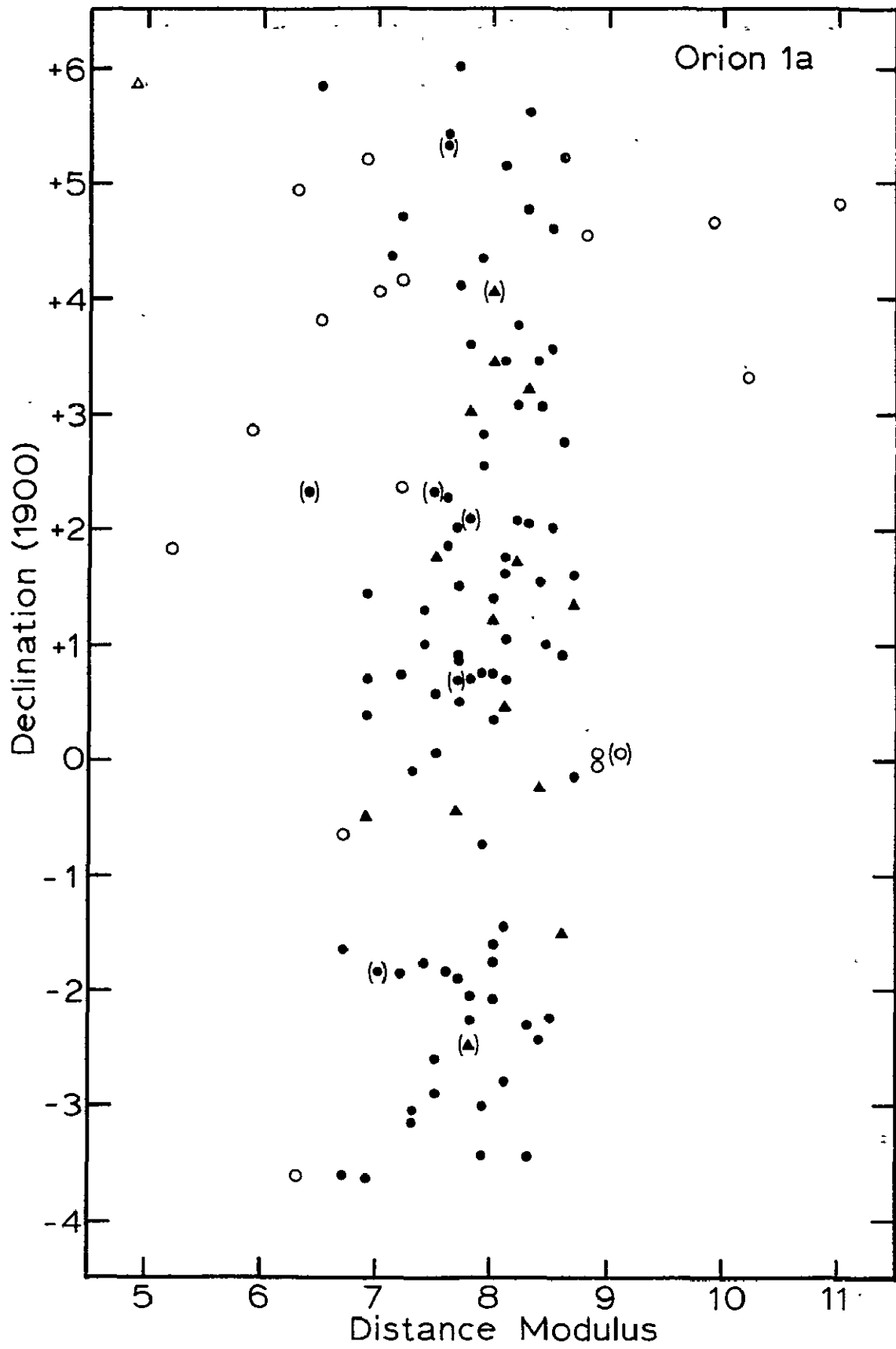


Figure 7

0-3

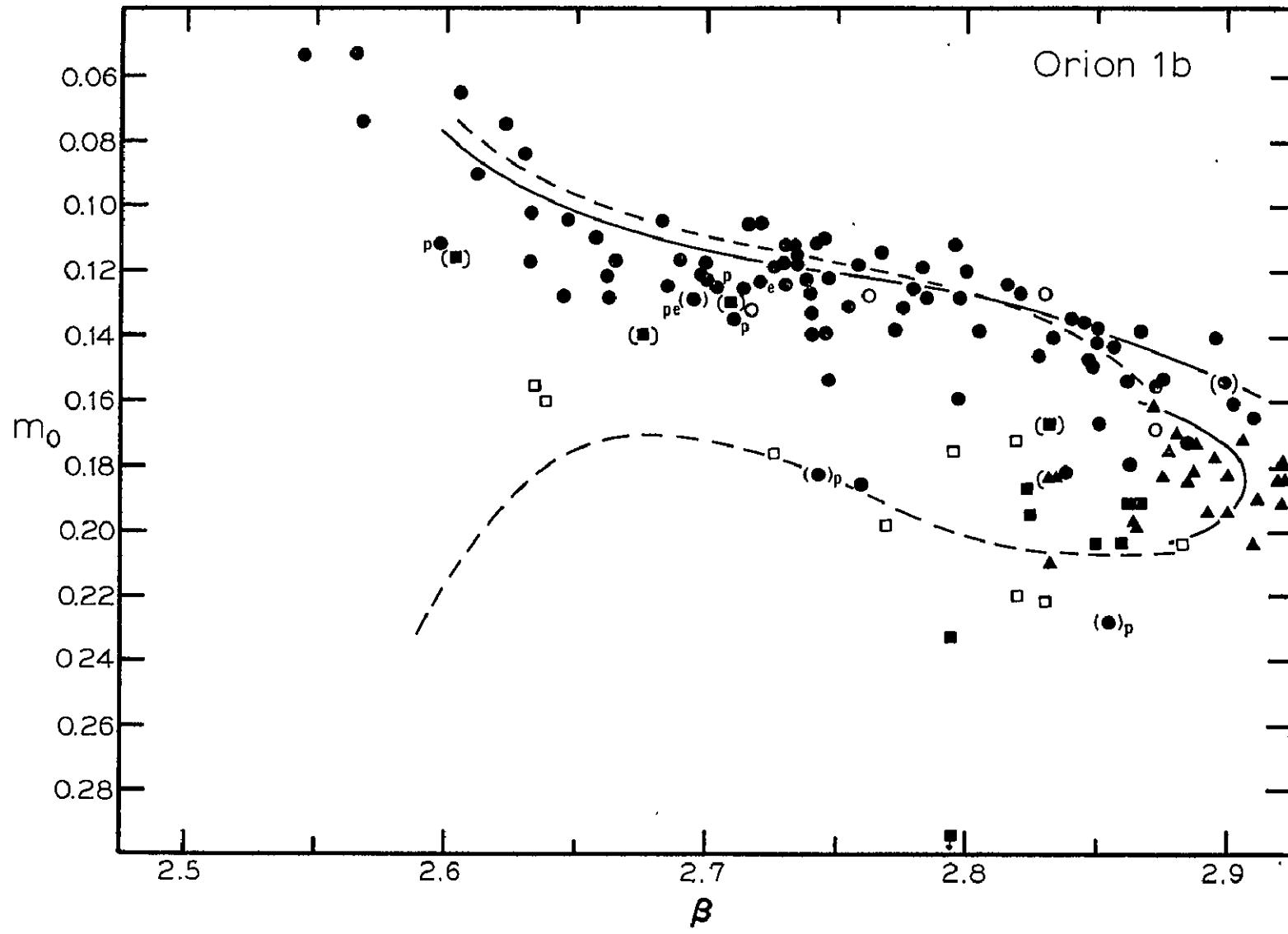


Figure 8

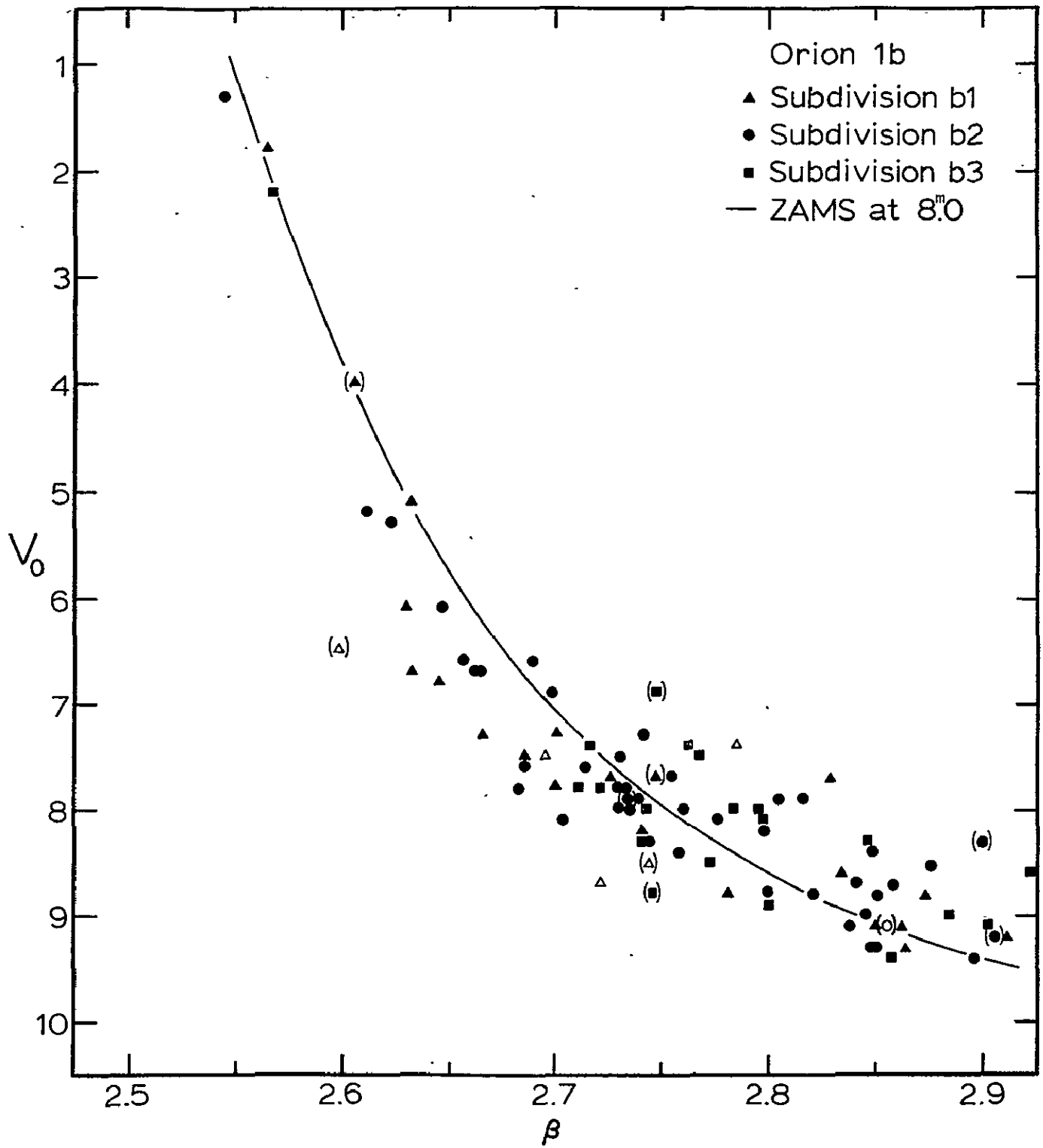
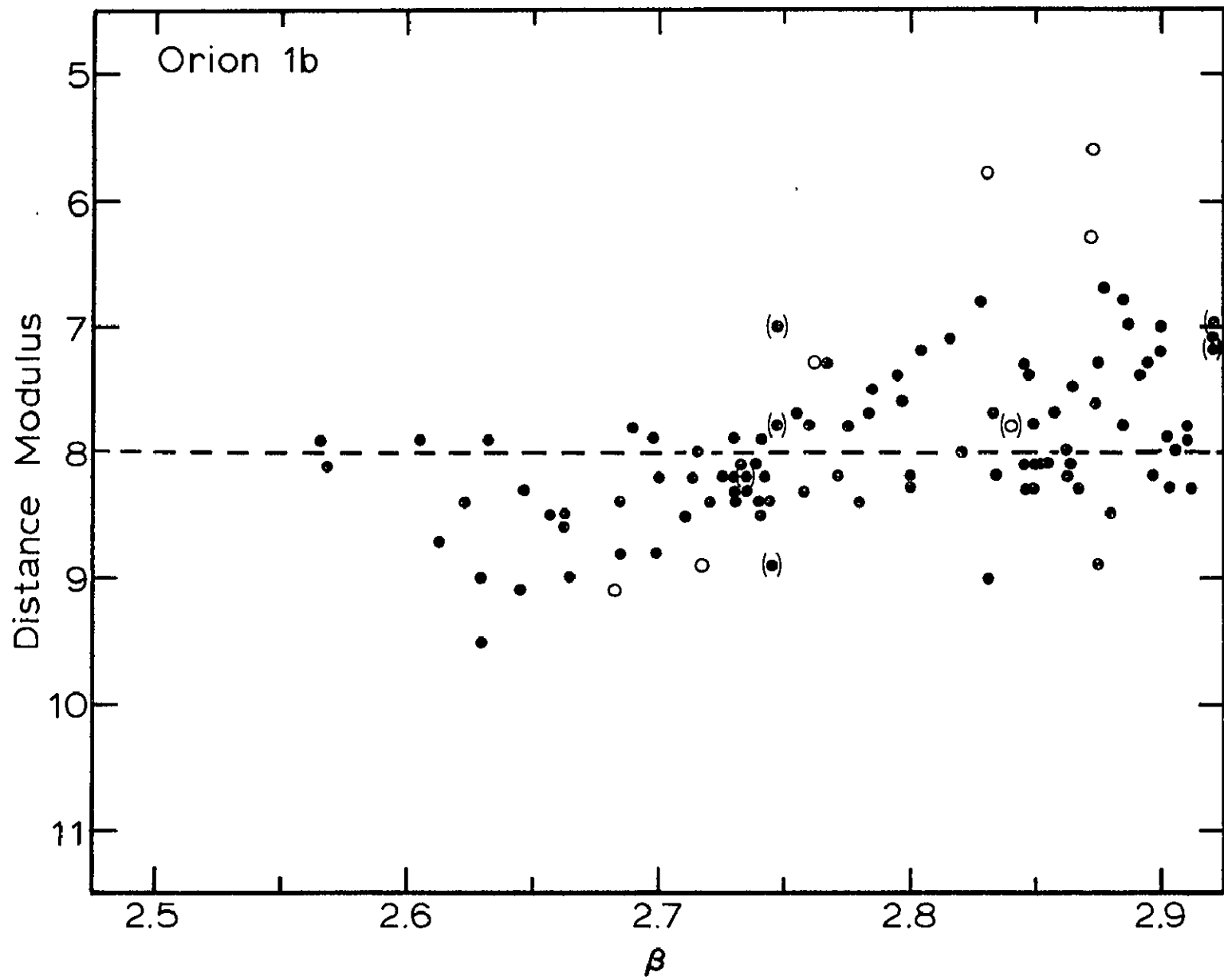


Figure 9





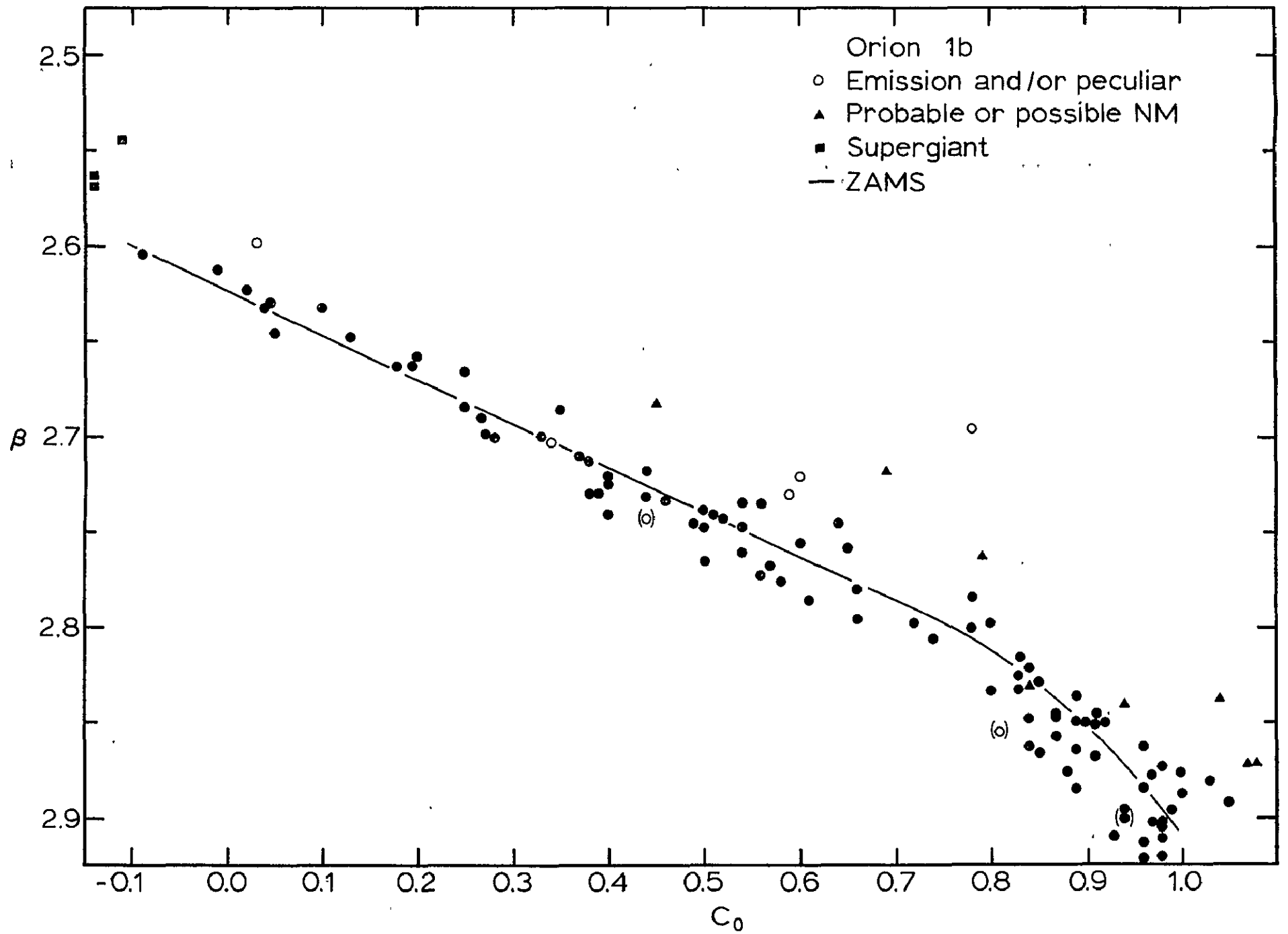


Figure 11

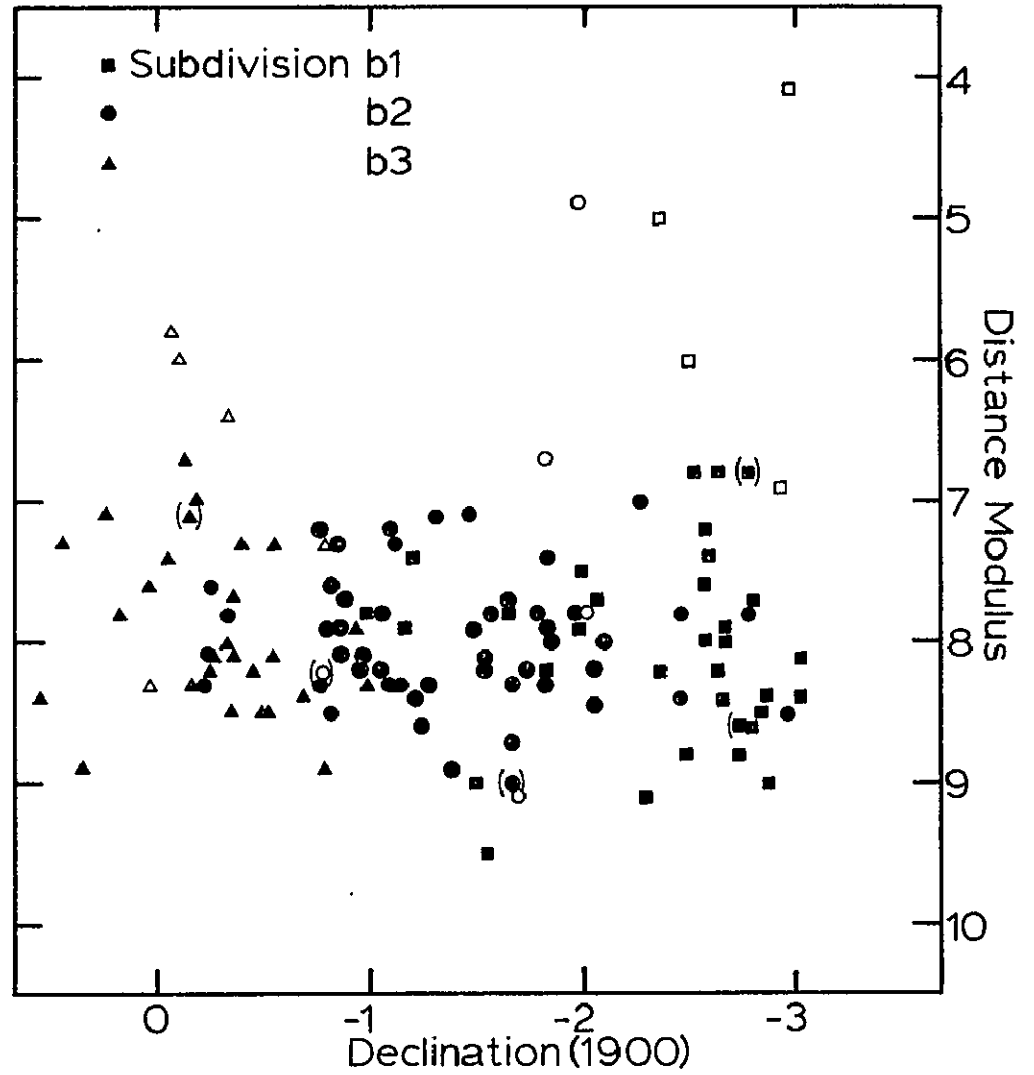
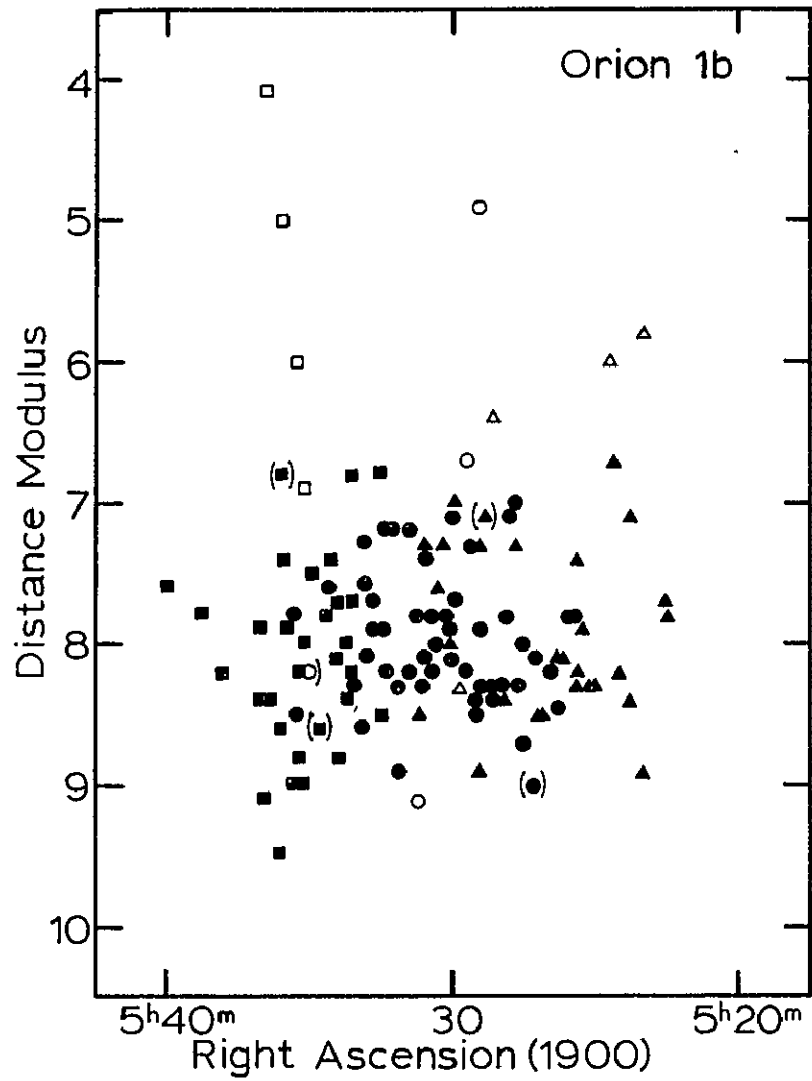


Figure 12

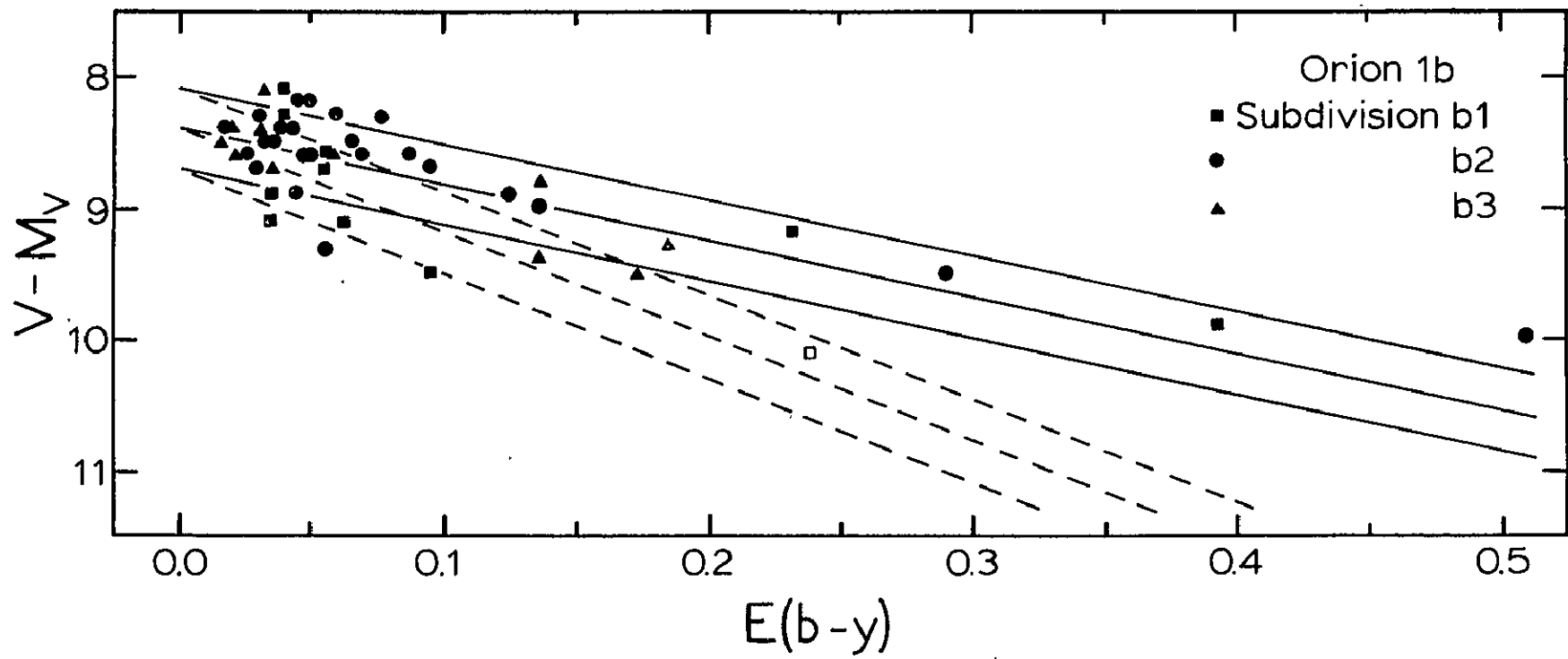


Figure 13

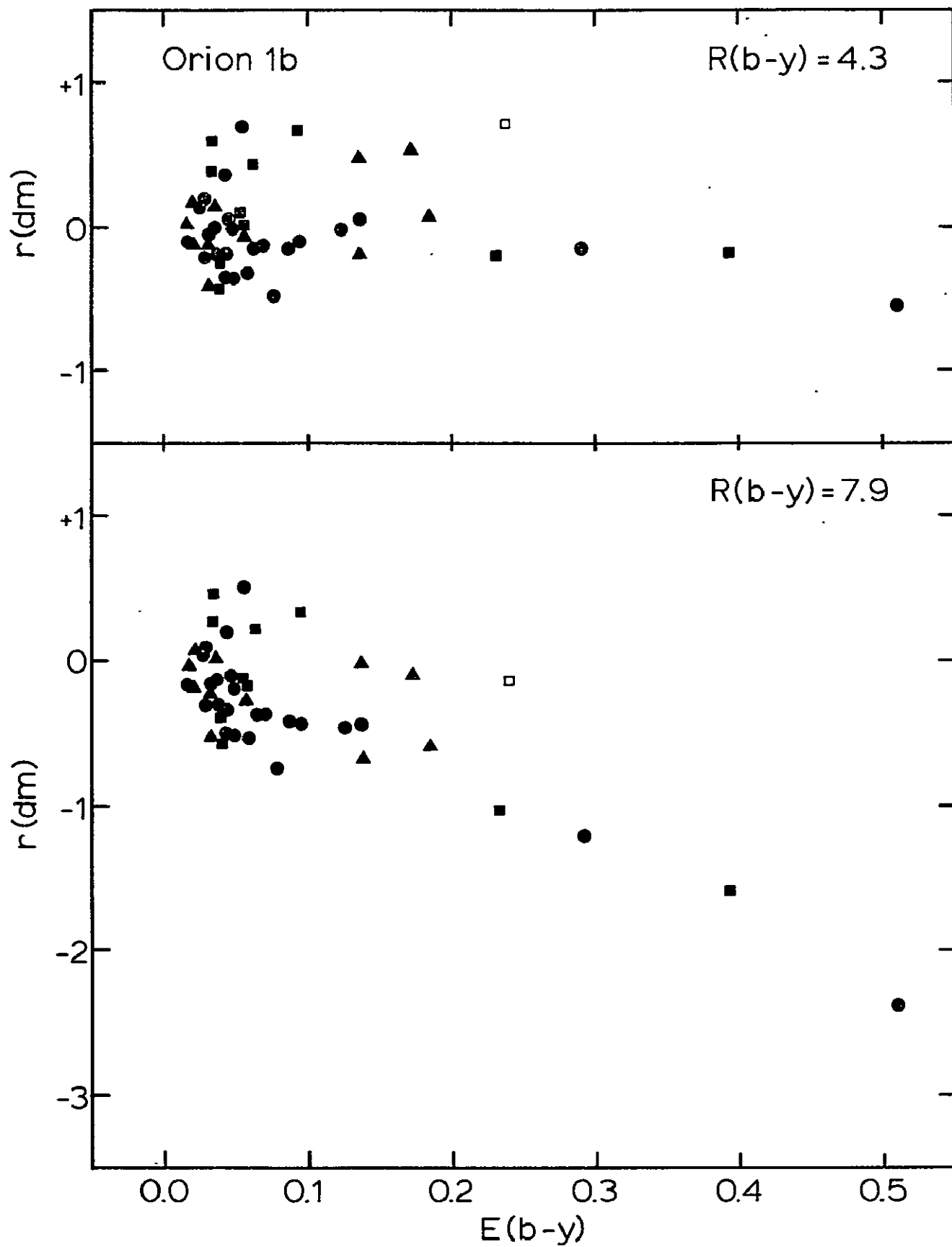


Figure 14

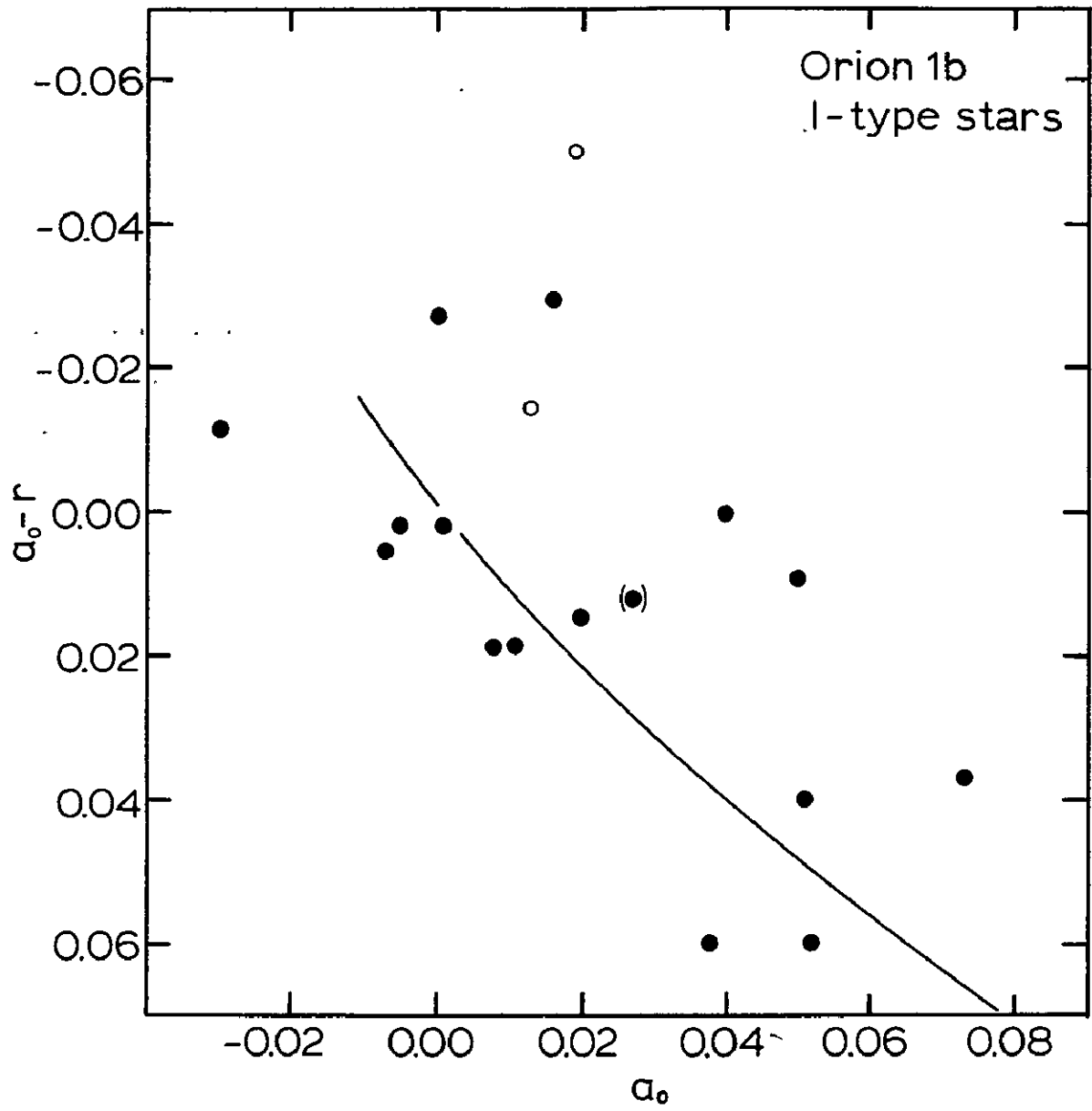


Figure 15

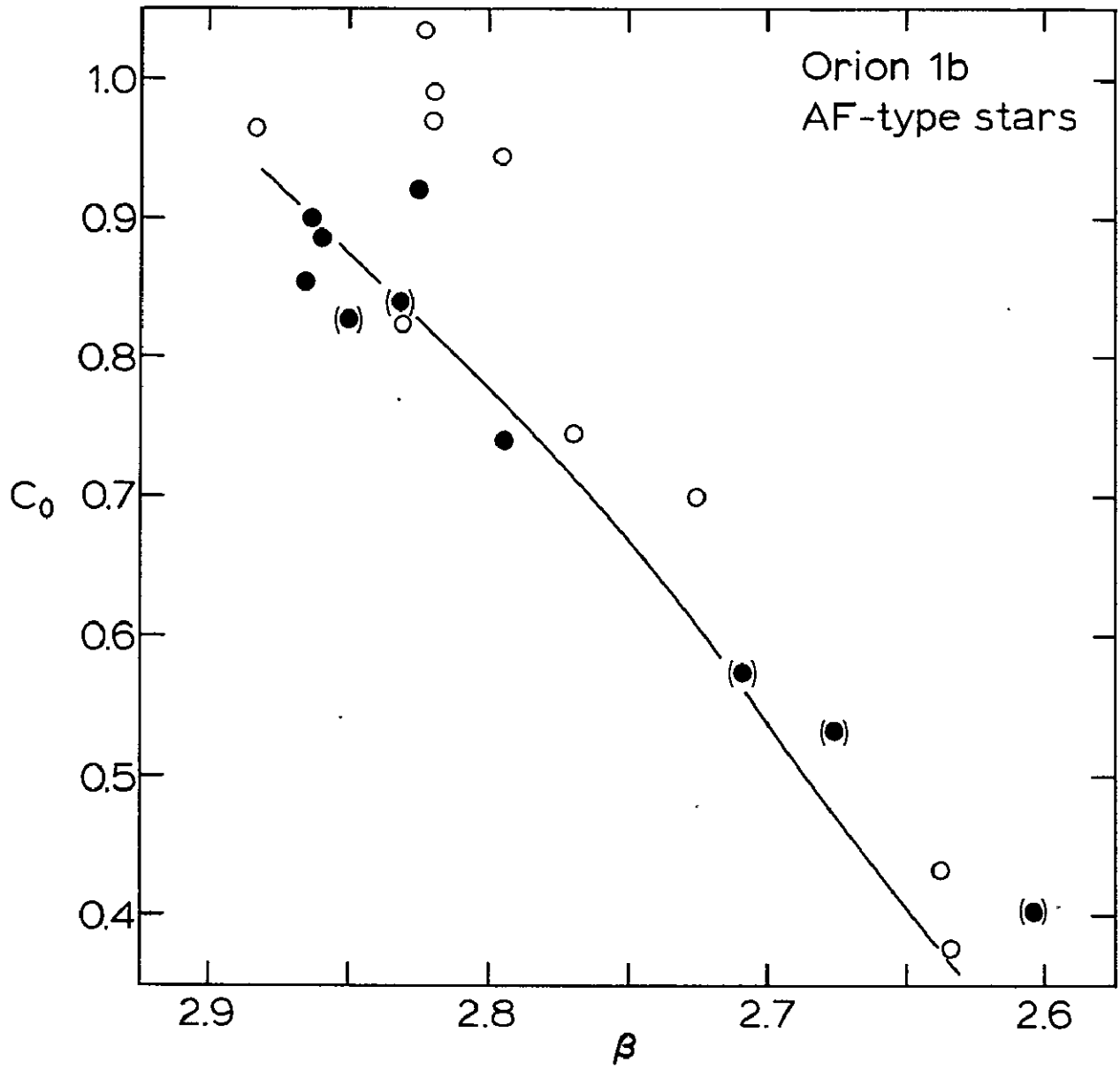


Figure 16

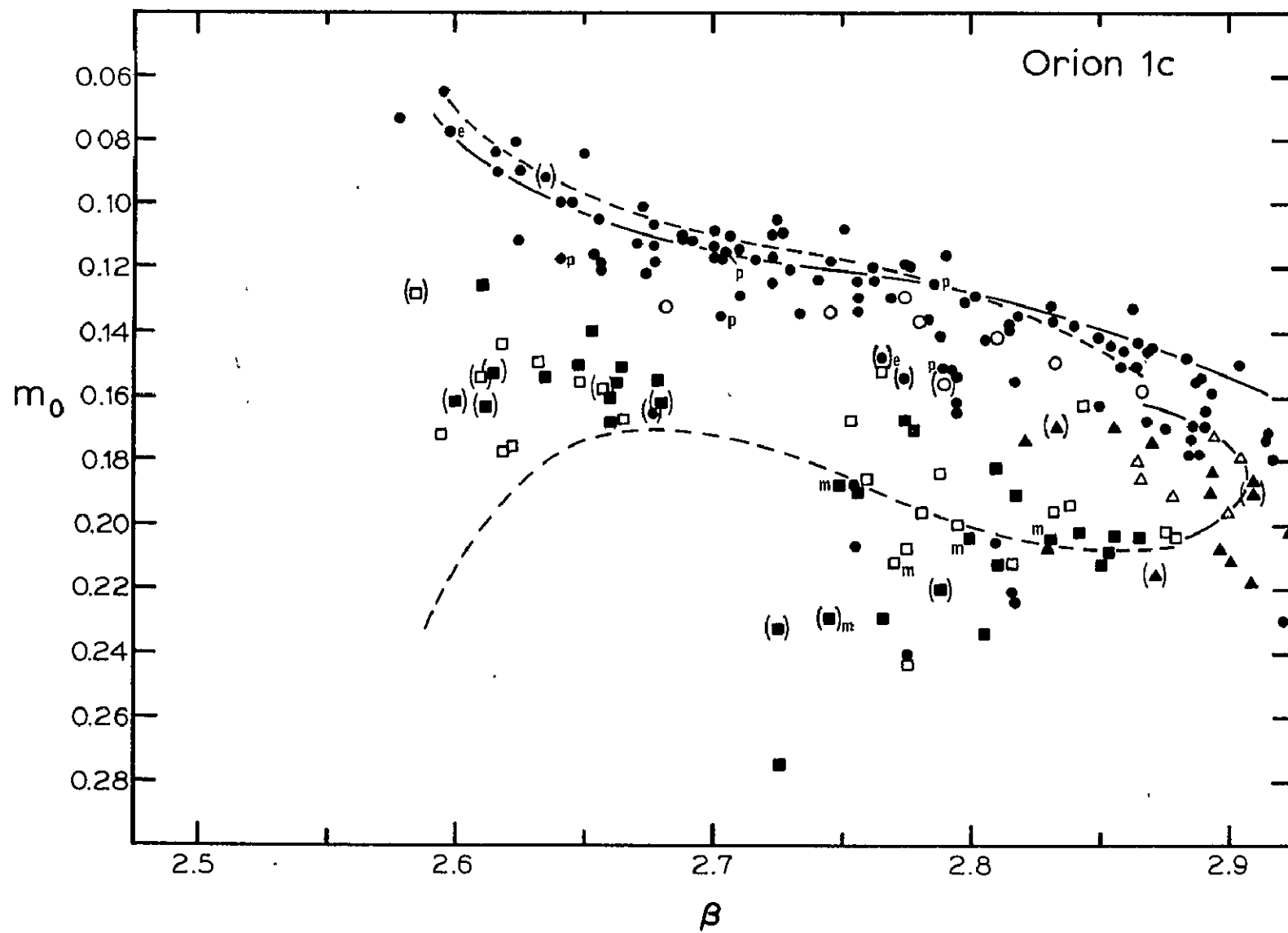


Figure 17

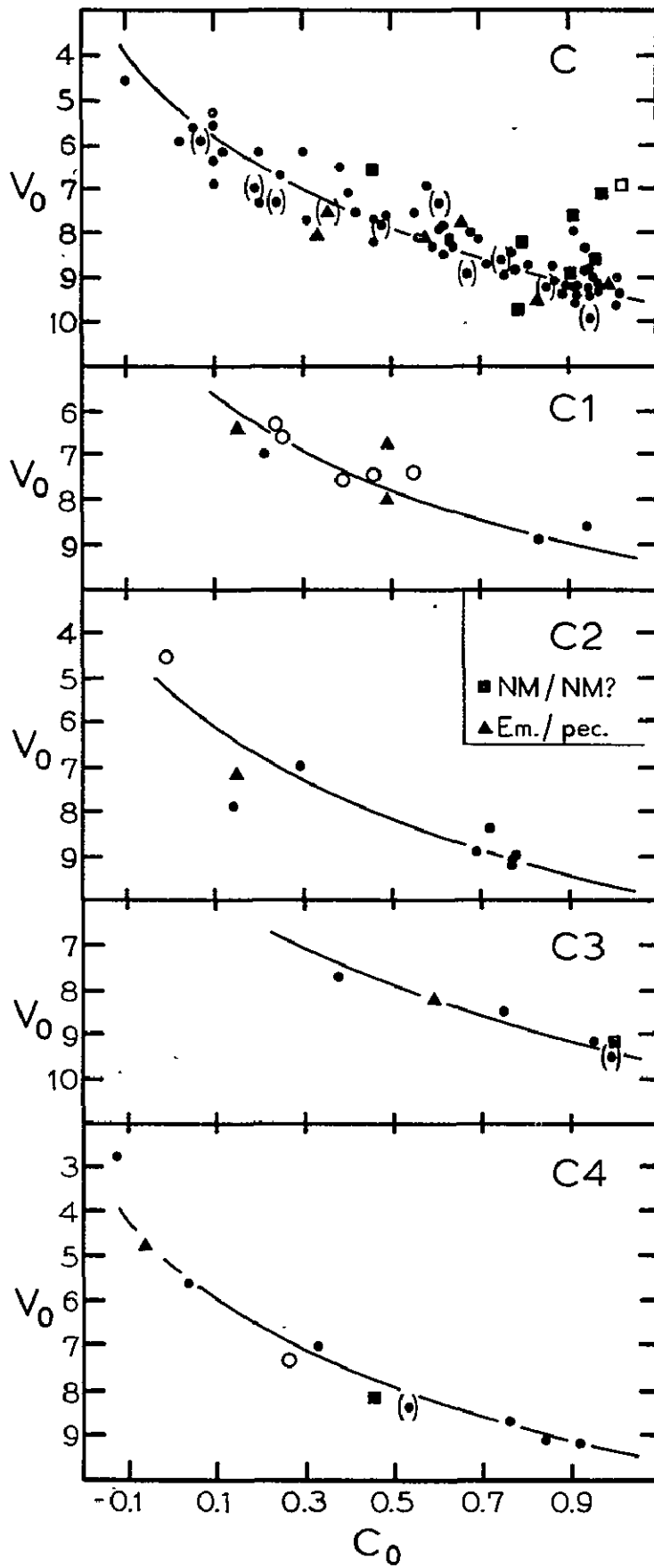


Figure 18

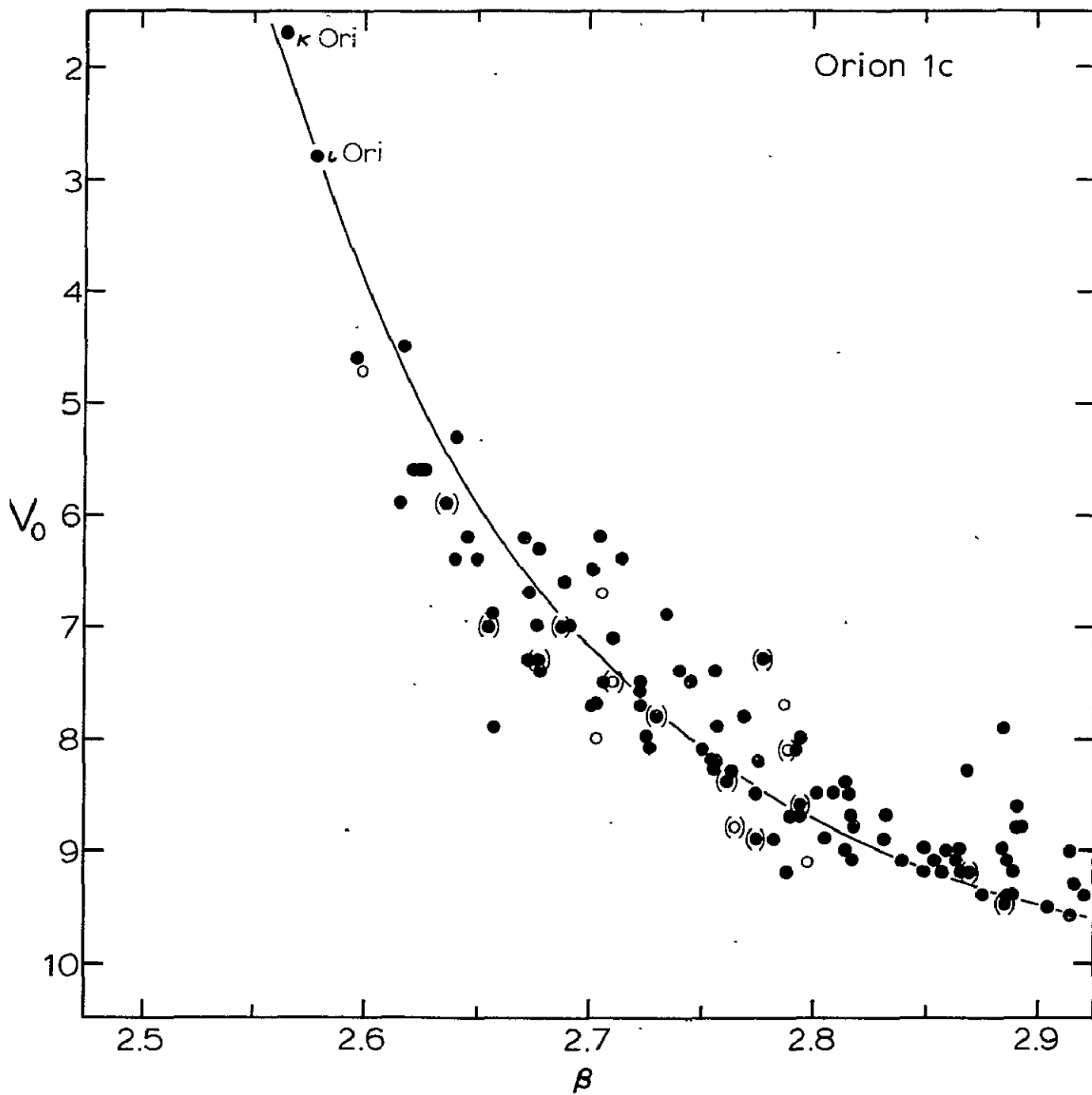


Figure 19

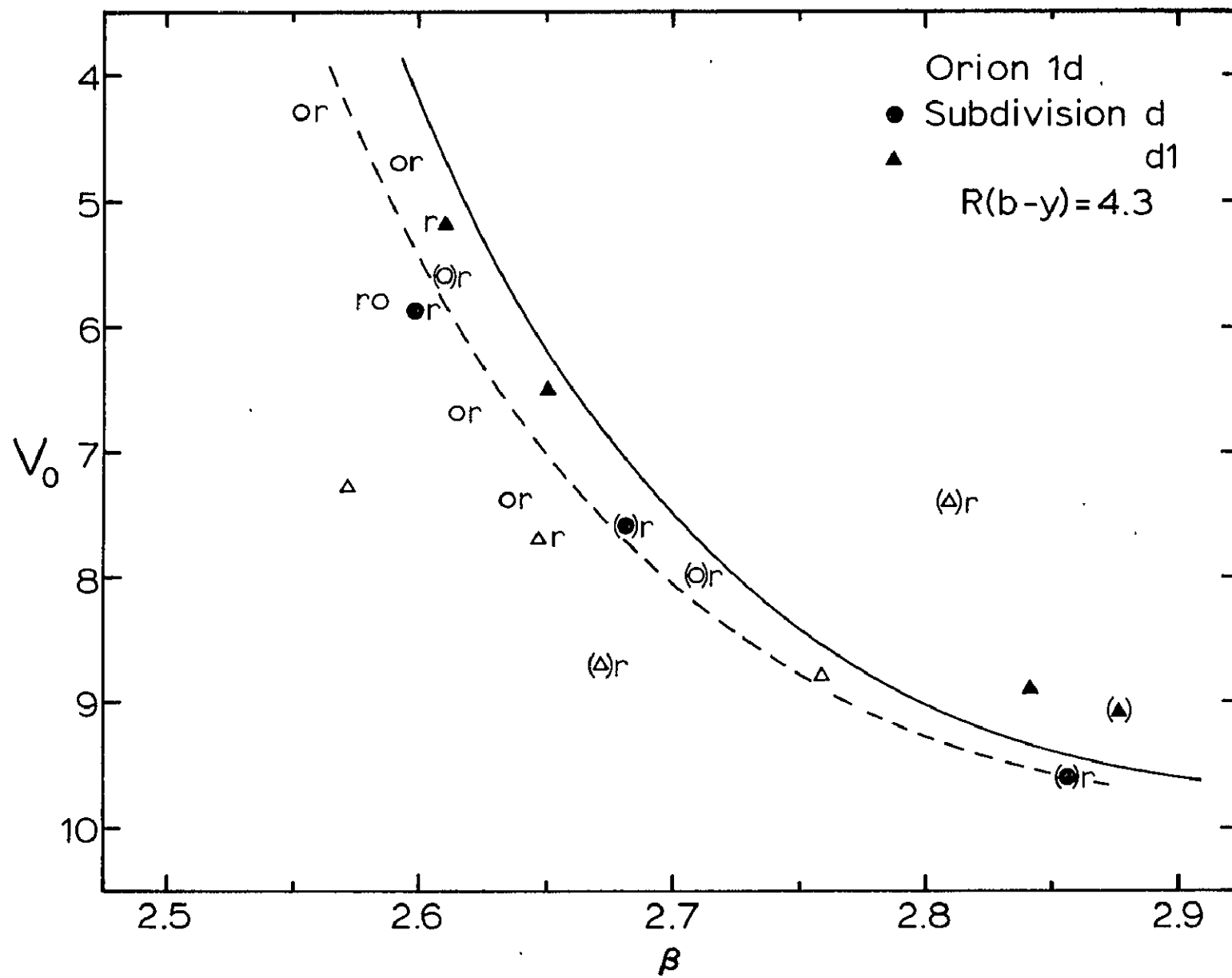


Figure 20

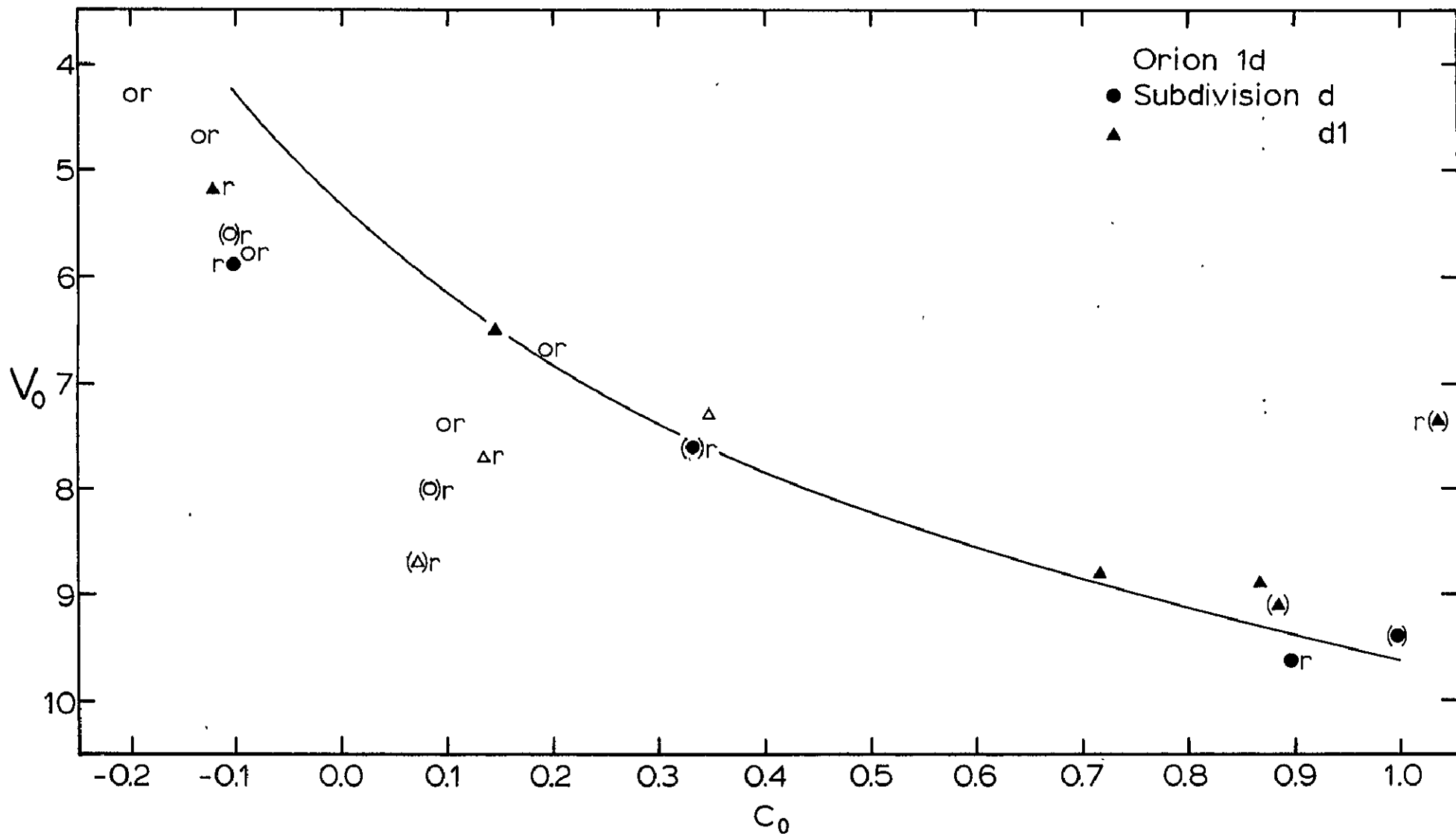


Figure 21

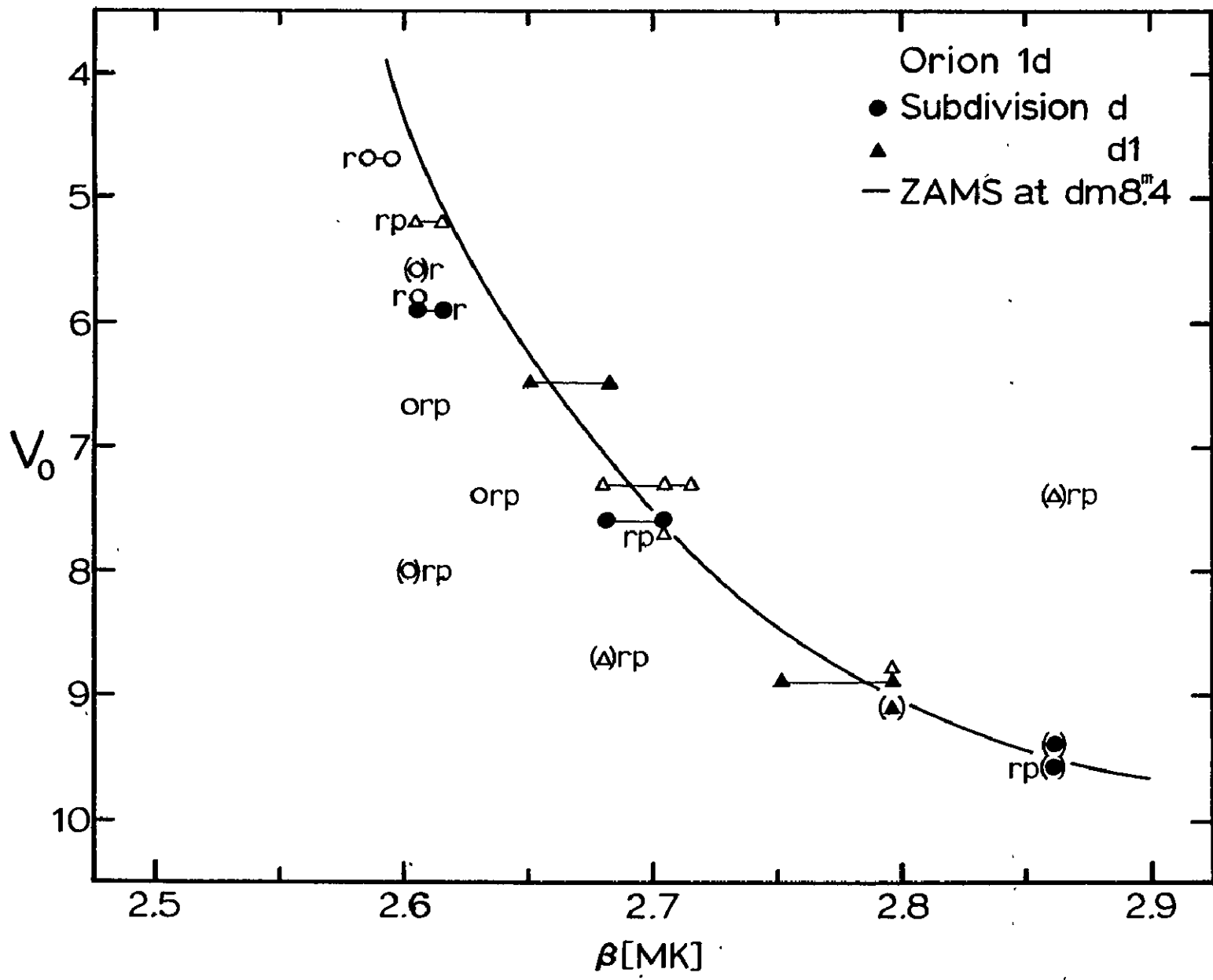


Figure 23

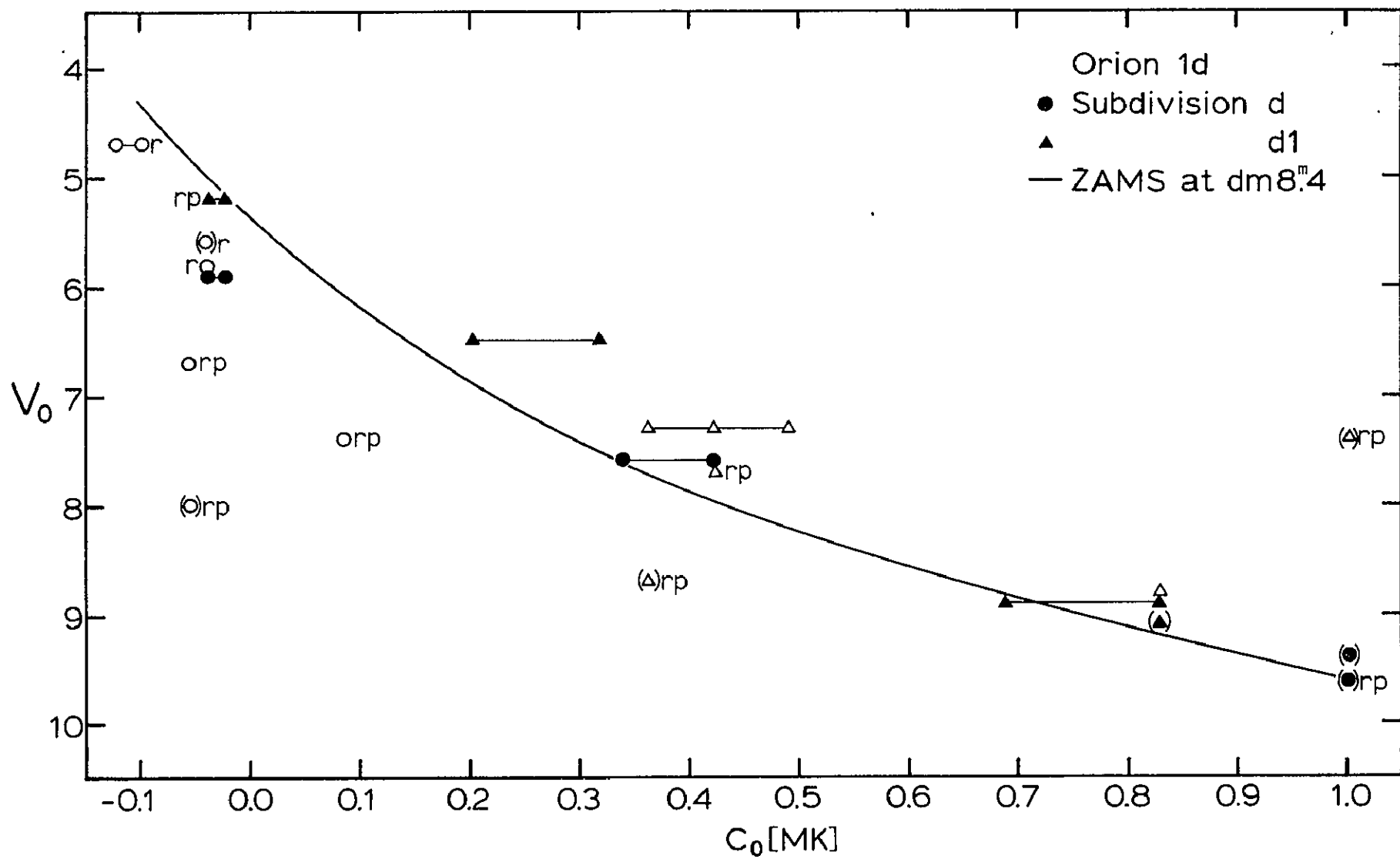


Figure 24

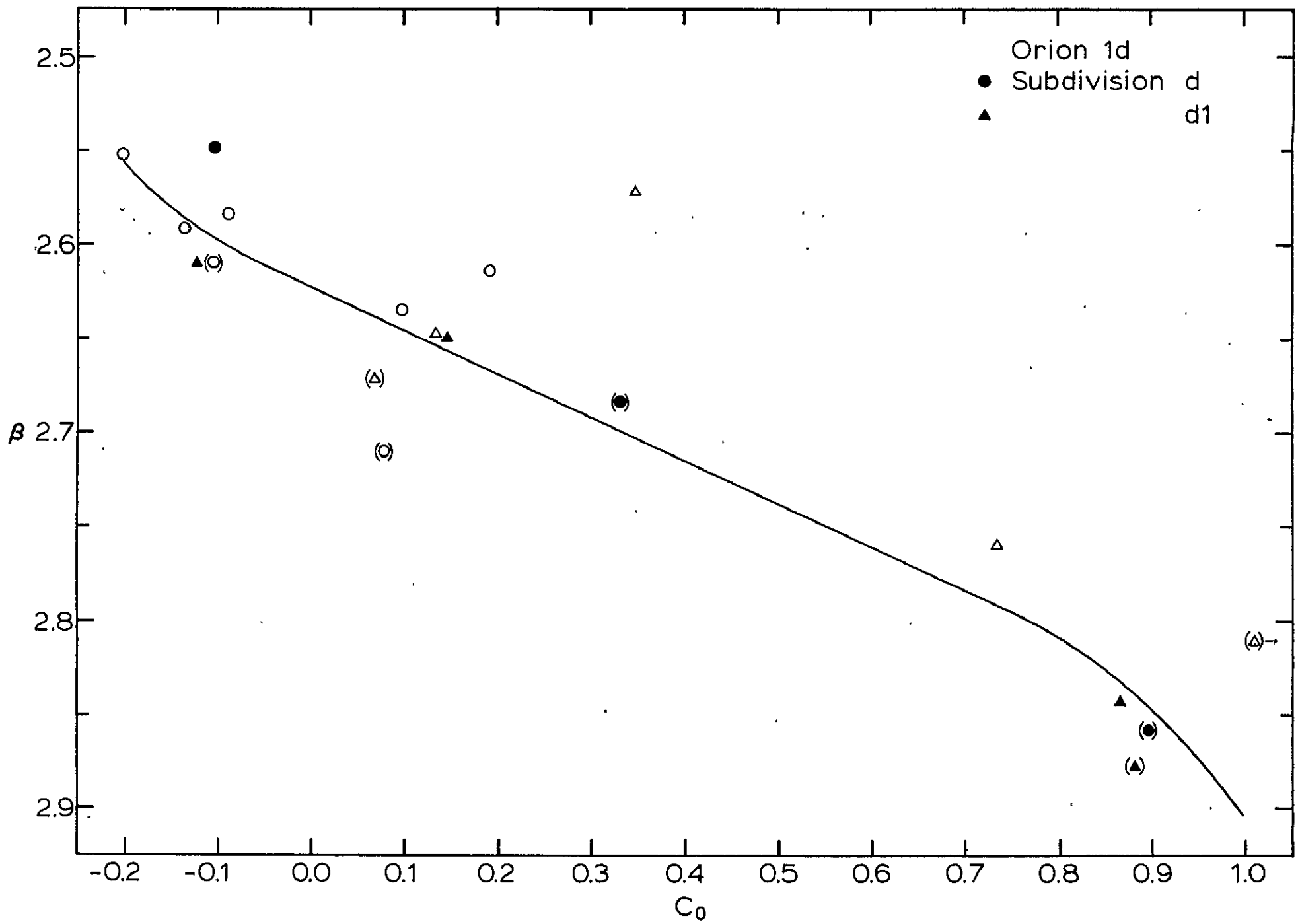


Figure 25

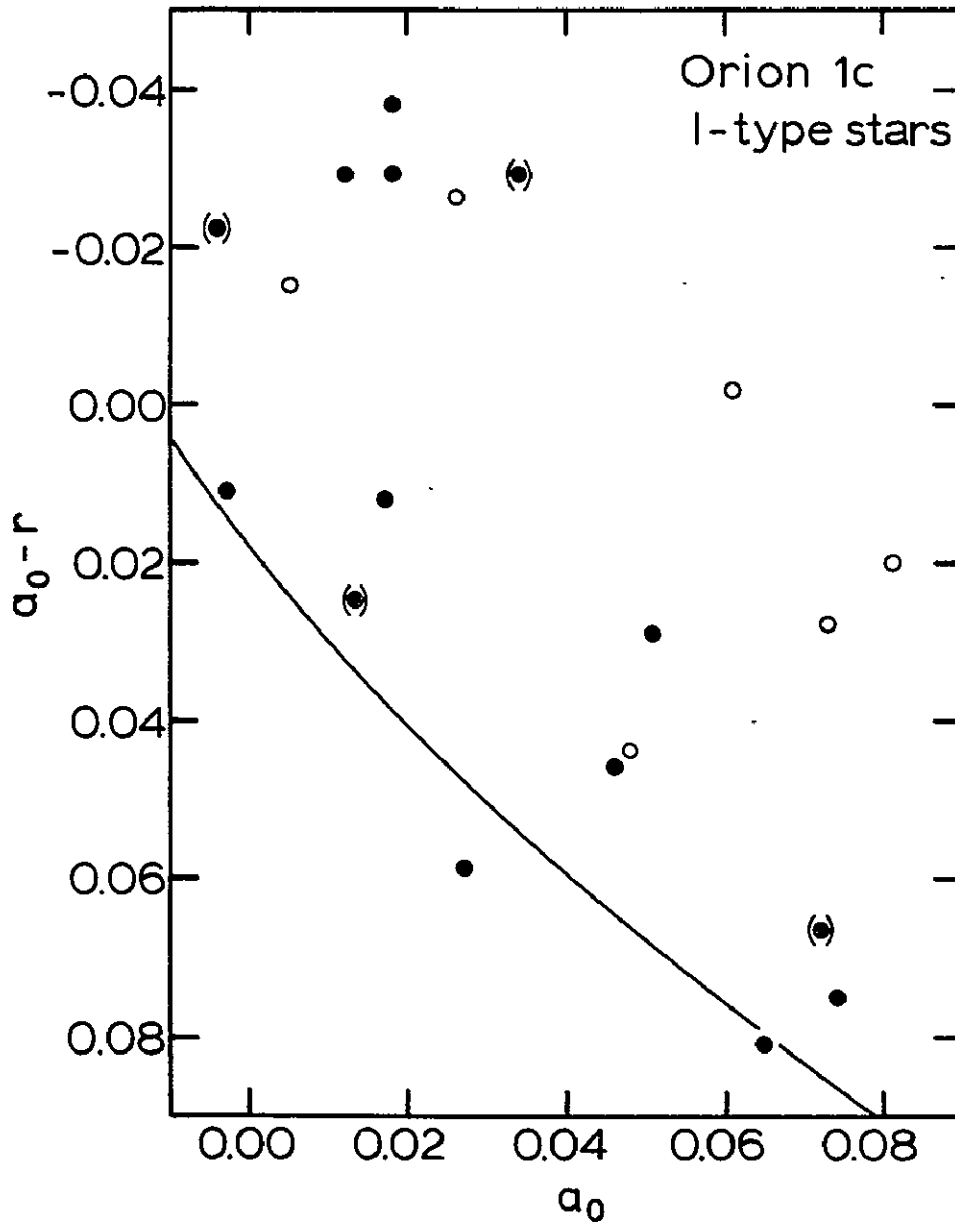


Figure 26

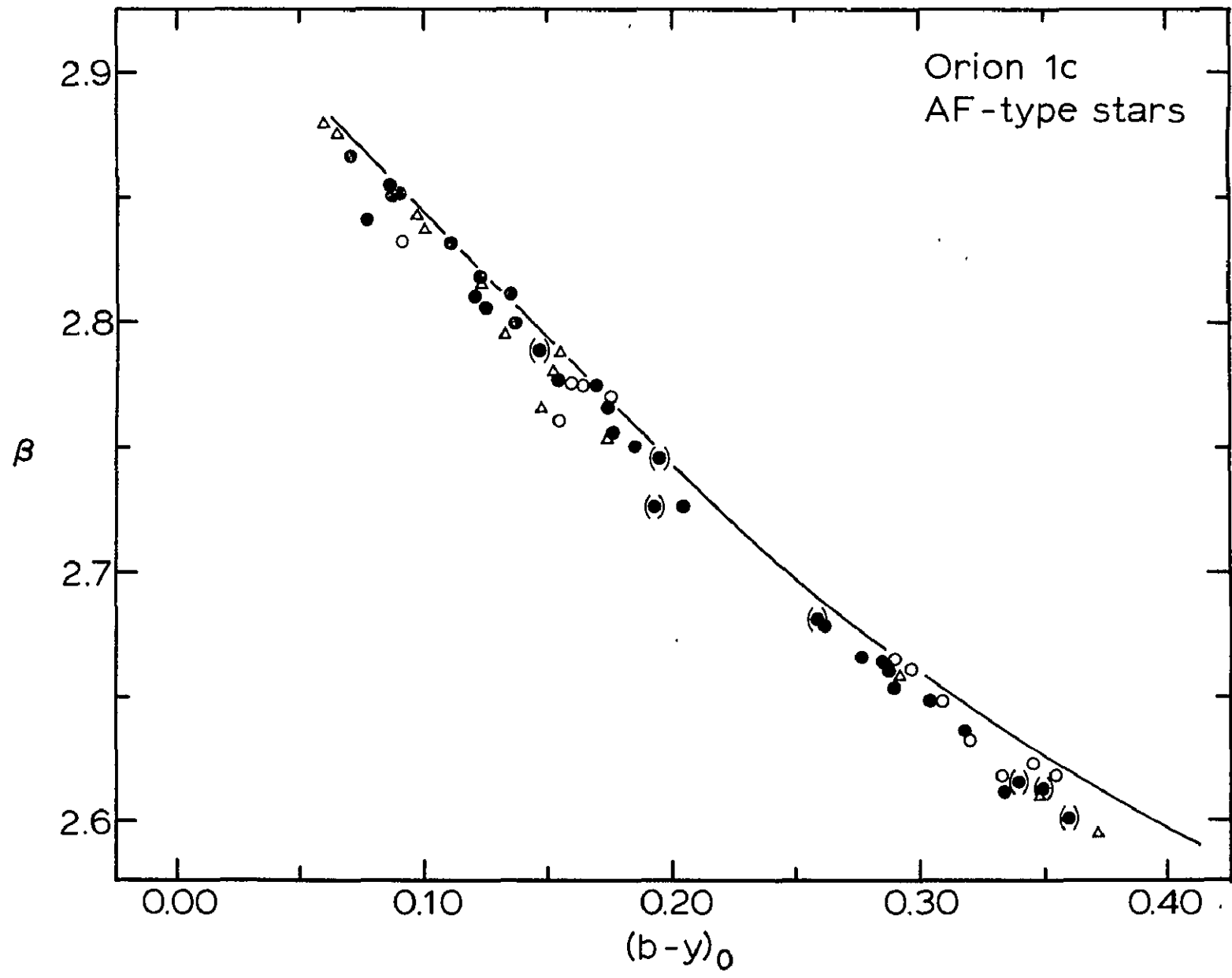


Figure 27

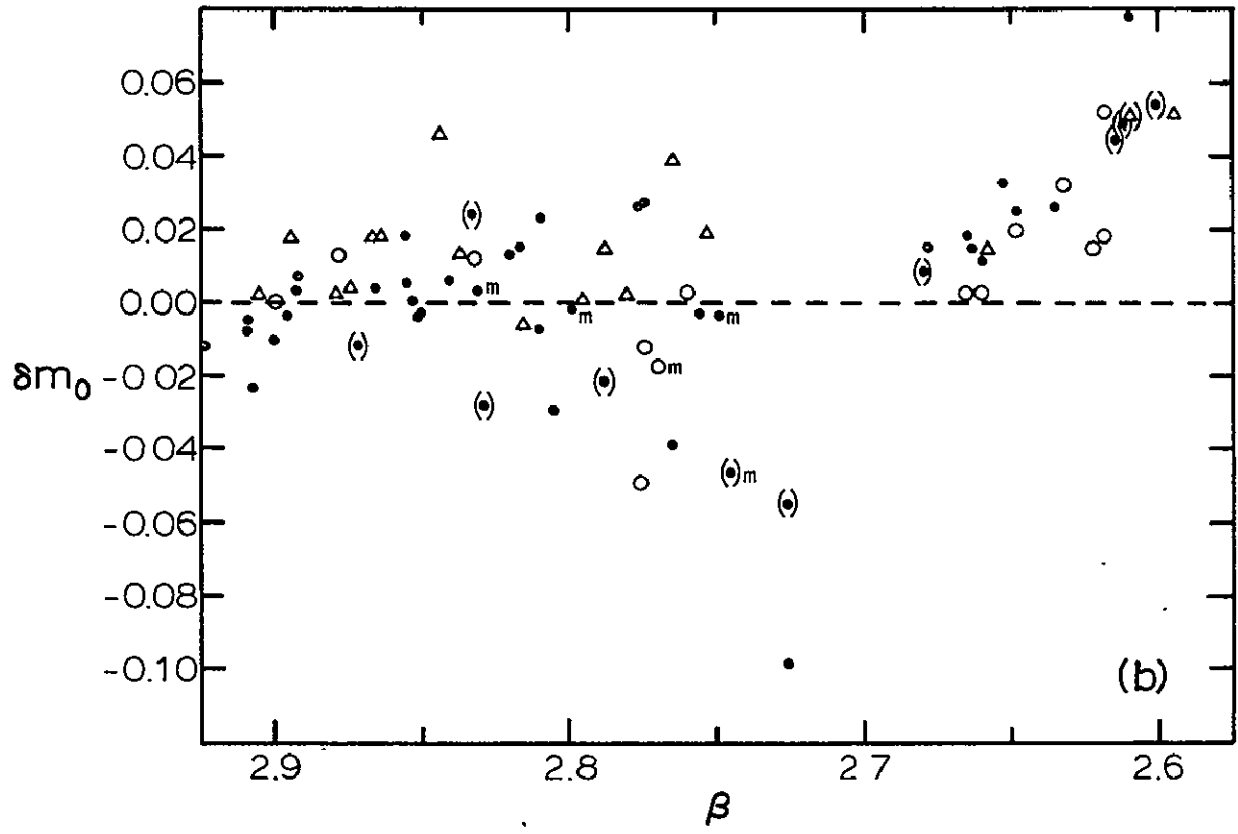
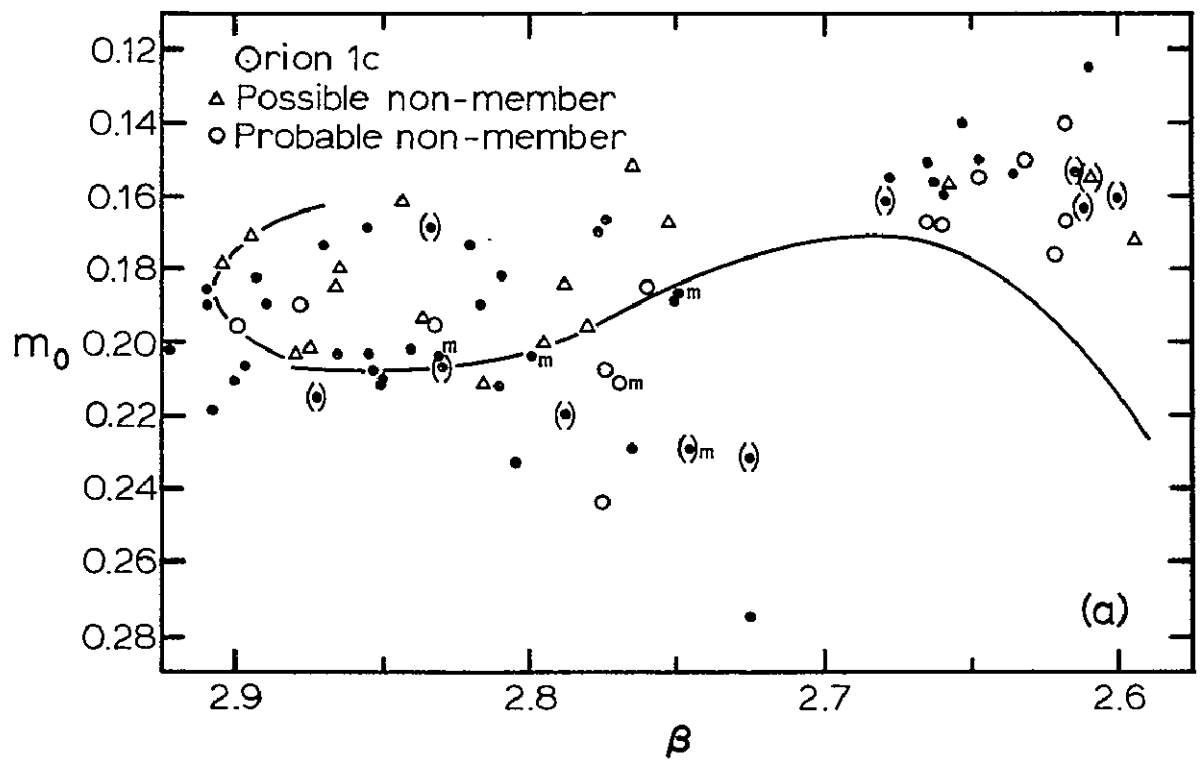


Figure 28

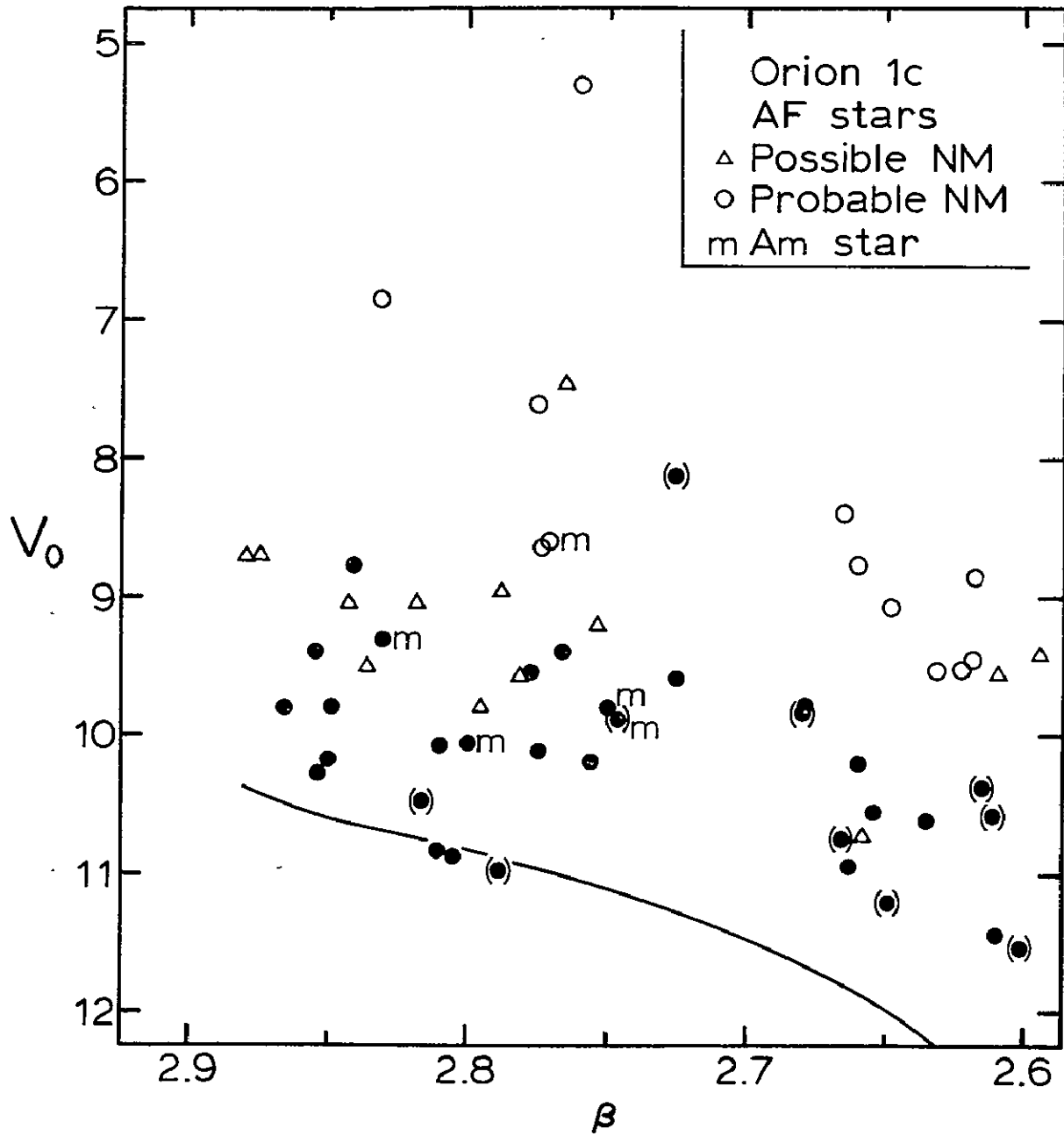


Figure 29

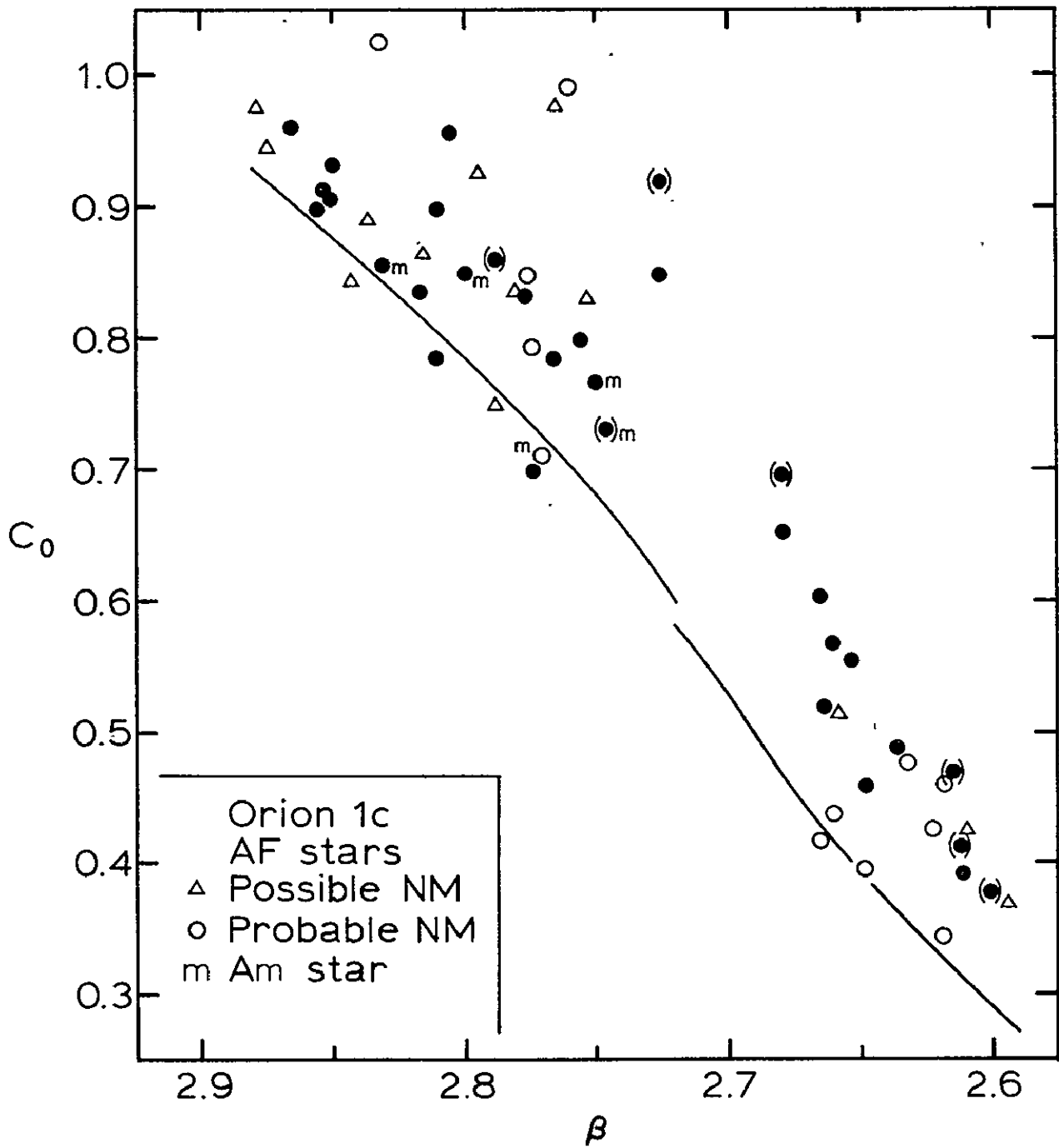


Figure 30

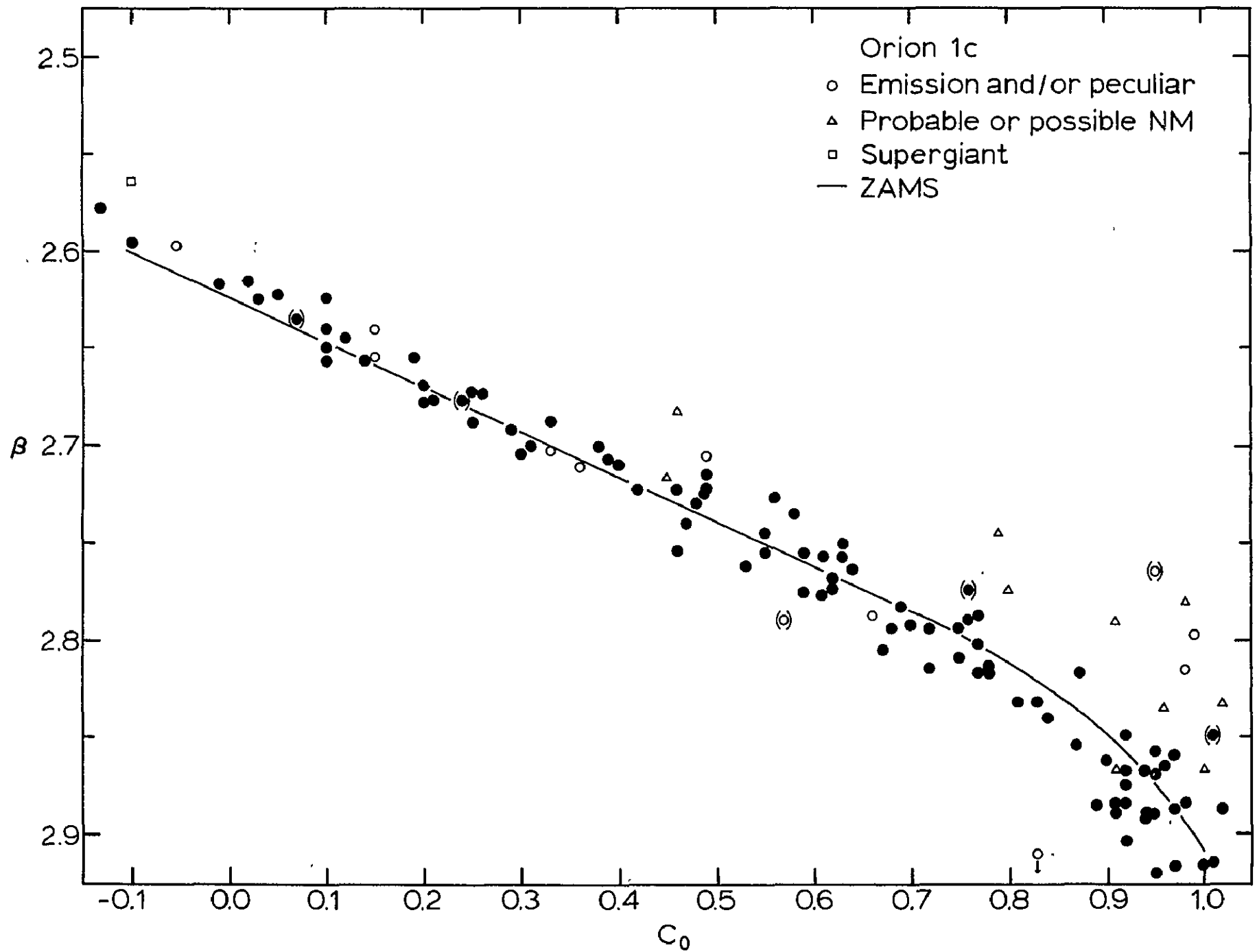


Figure 31

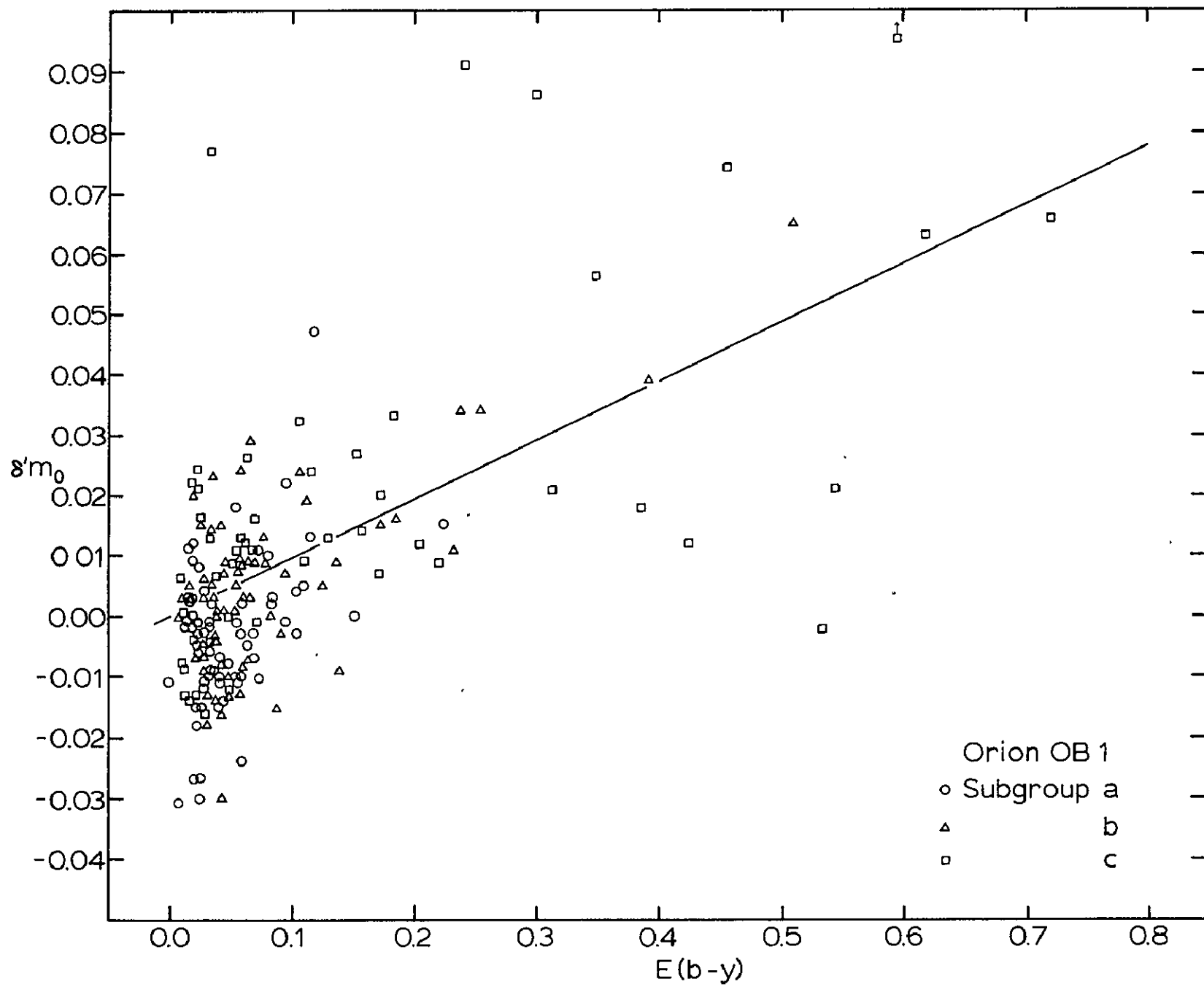


Figure 32

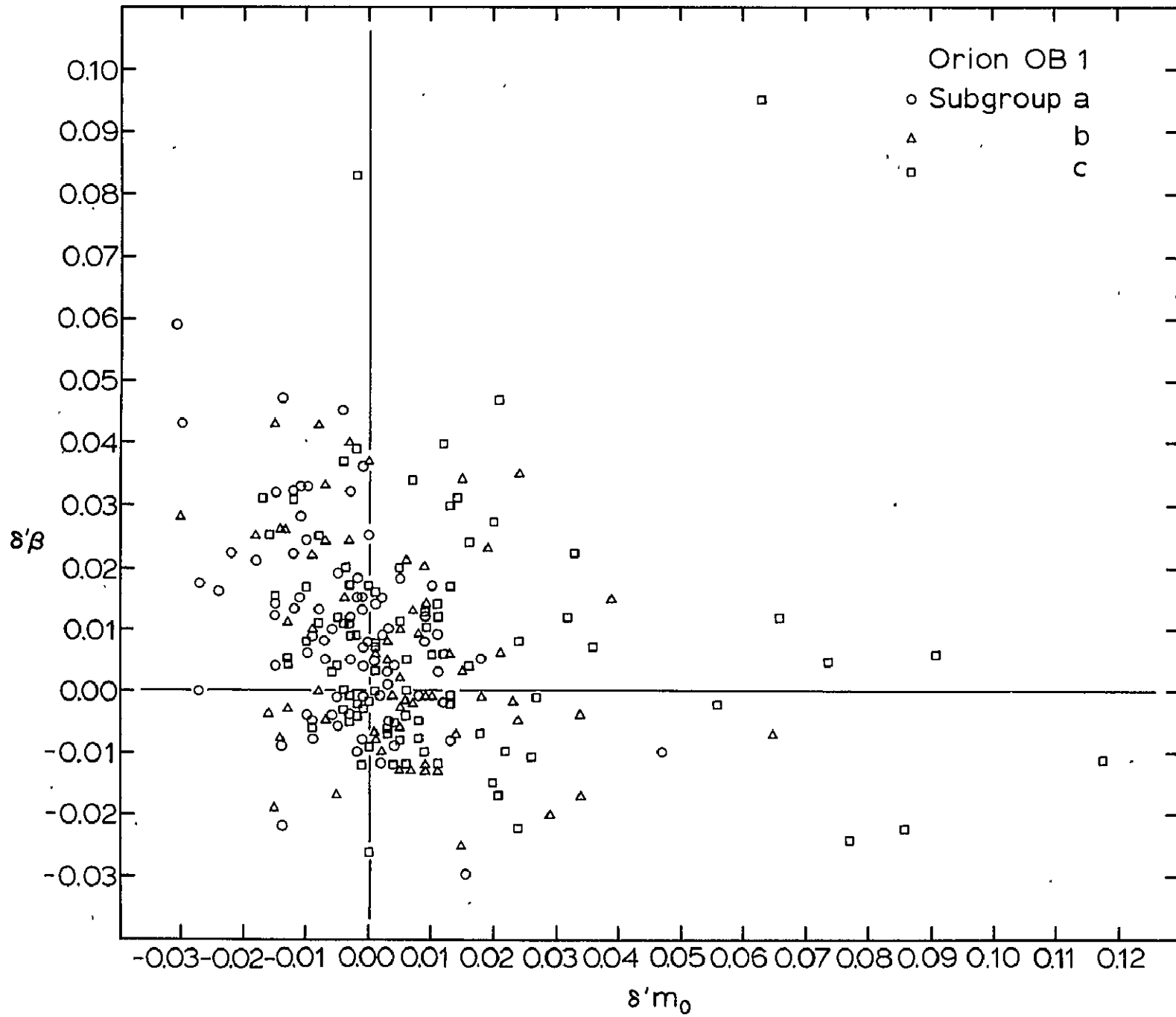


Figure 33

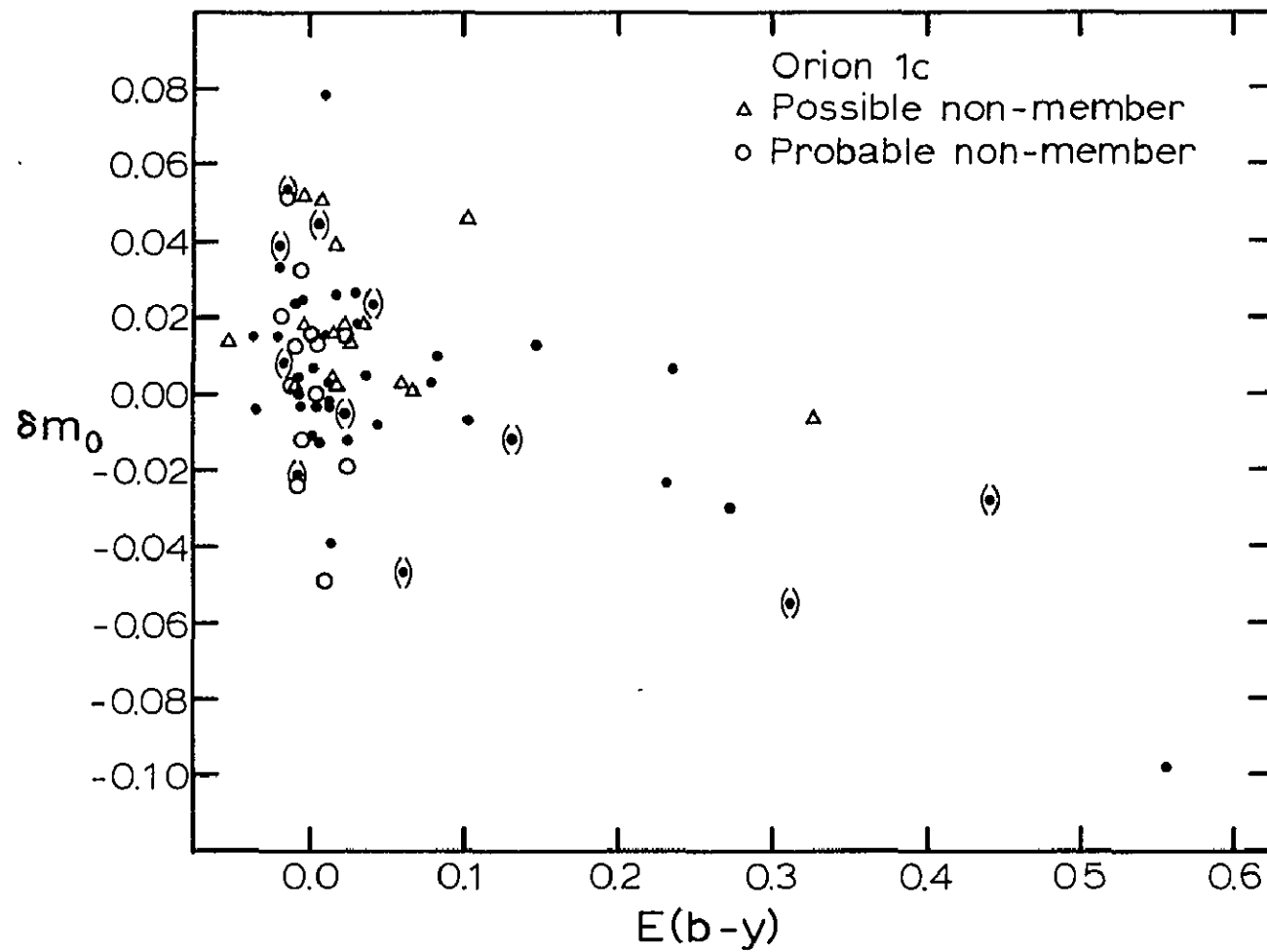


Figure 34

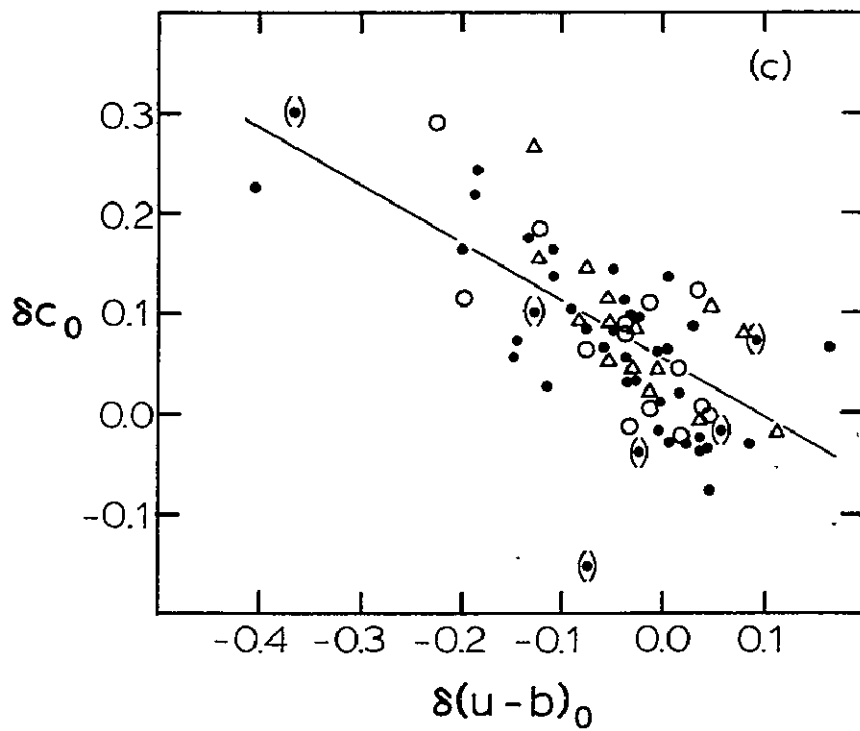
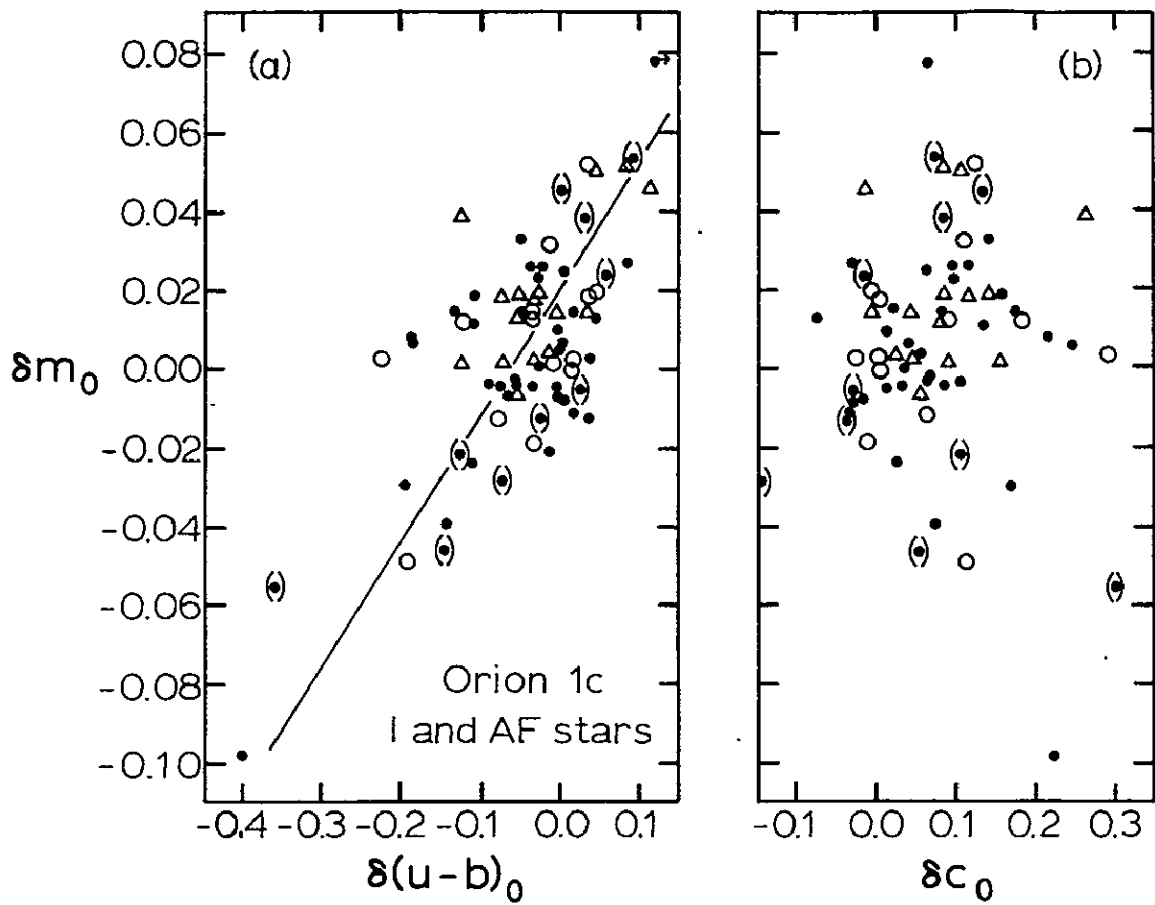


Figure 35

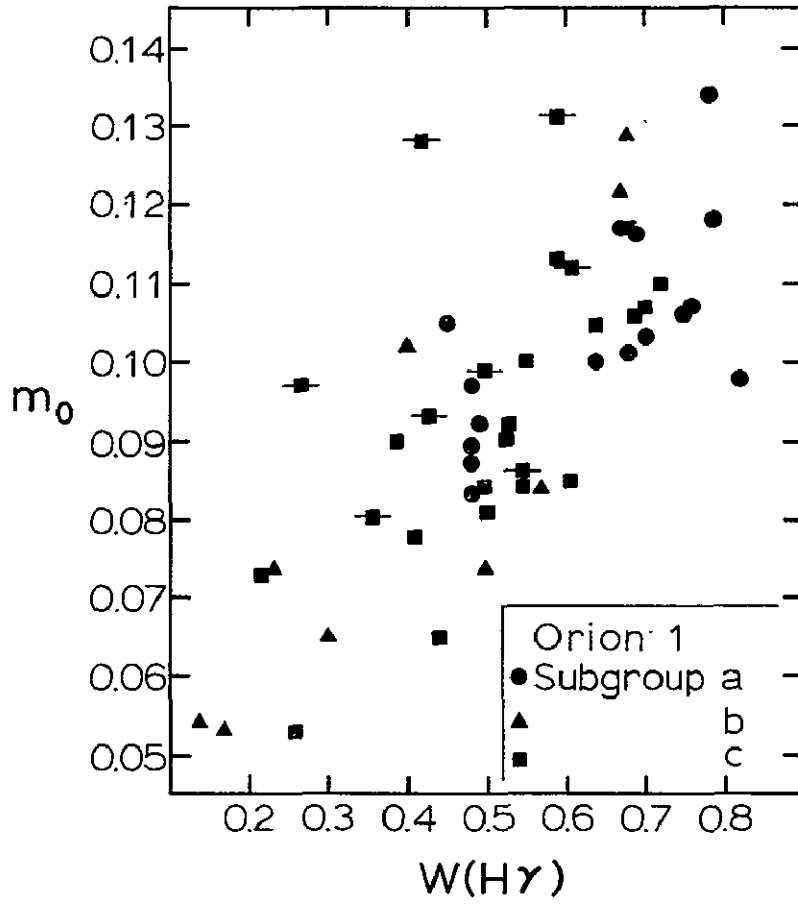


Figure 36

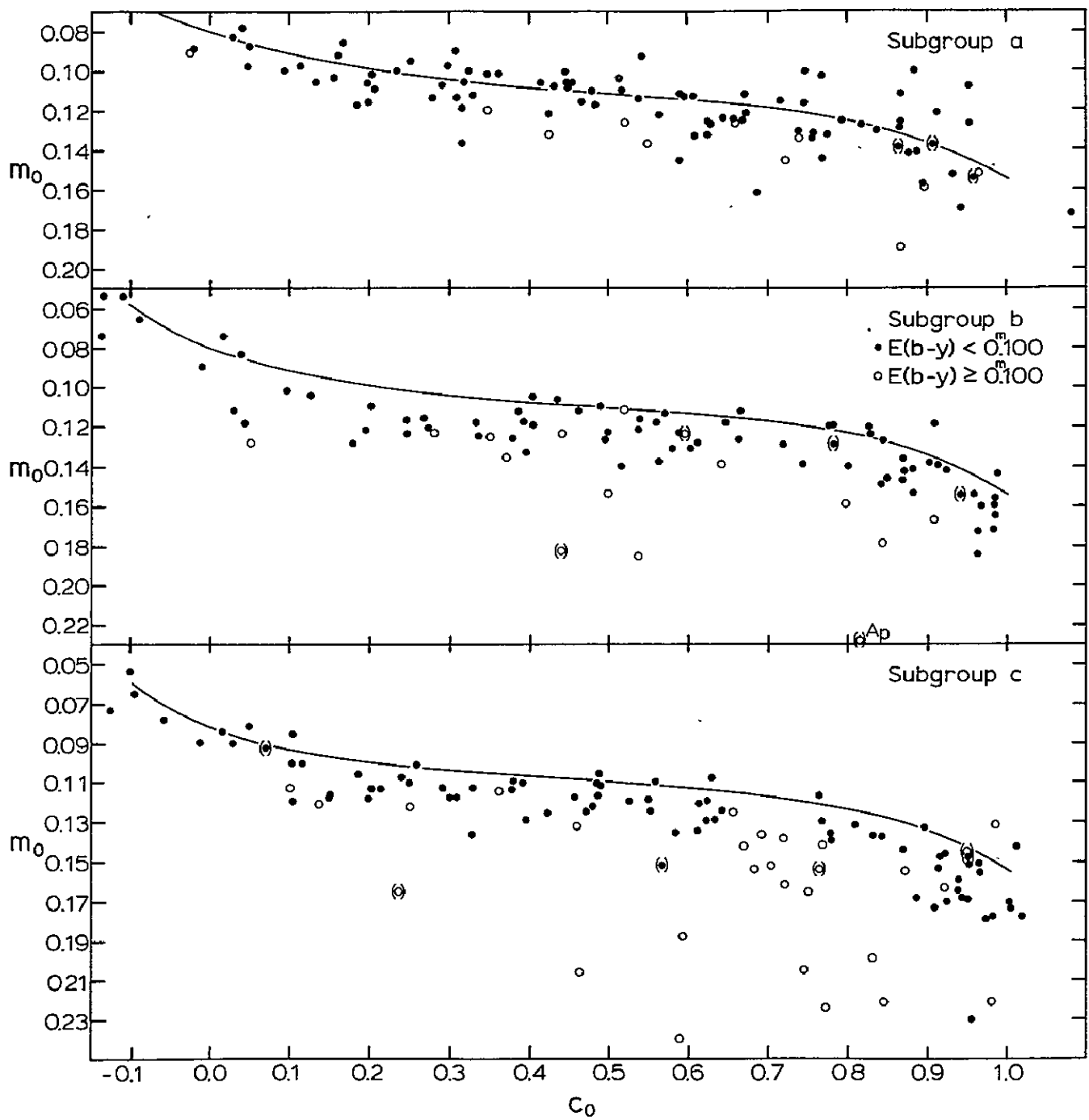


Figure 37

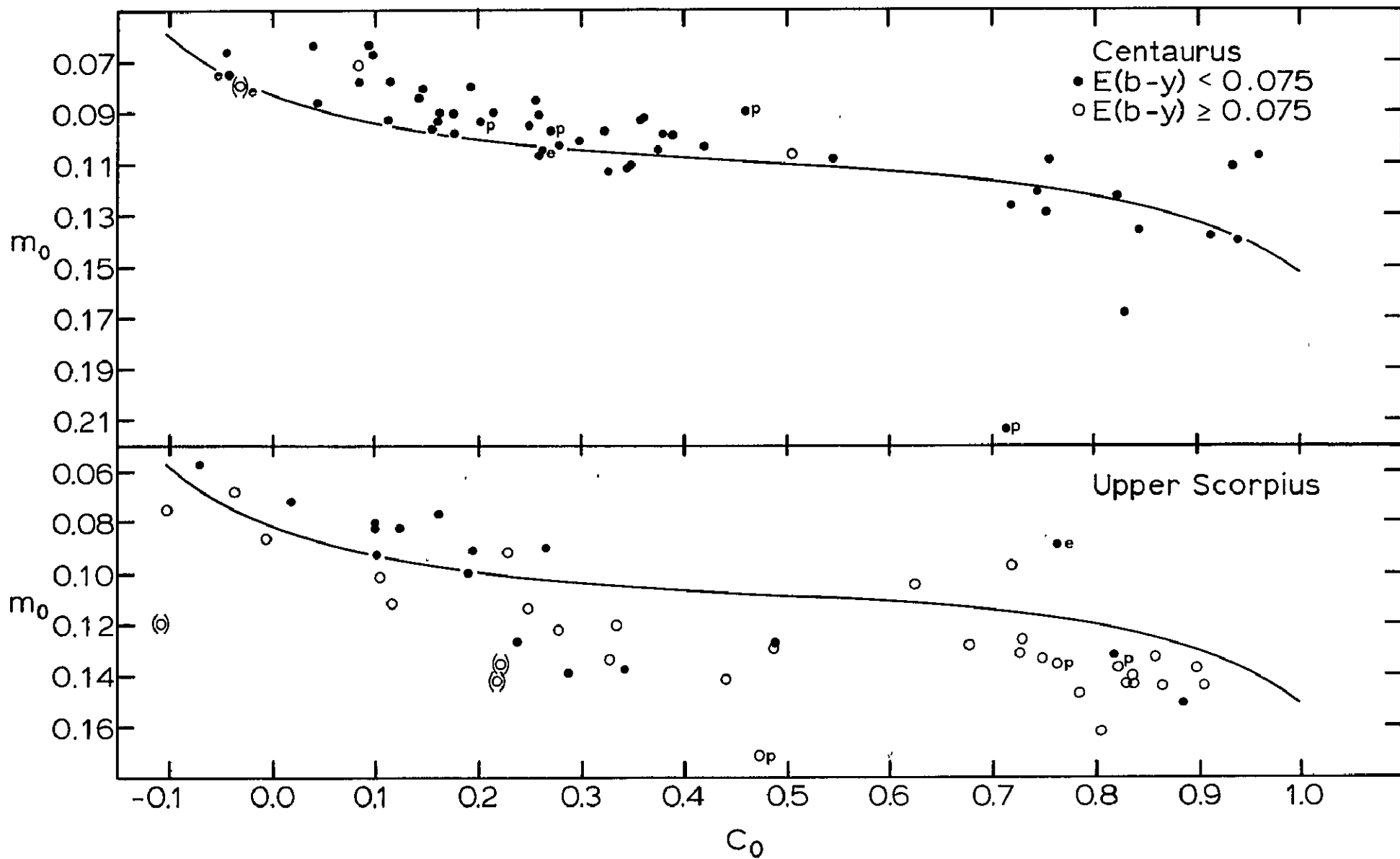


Figure 38

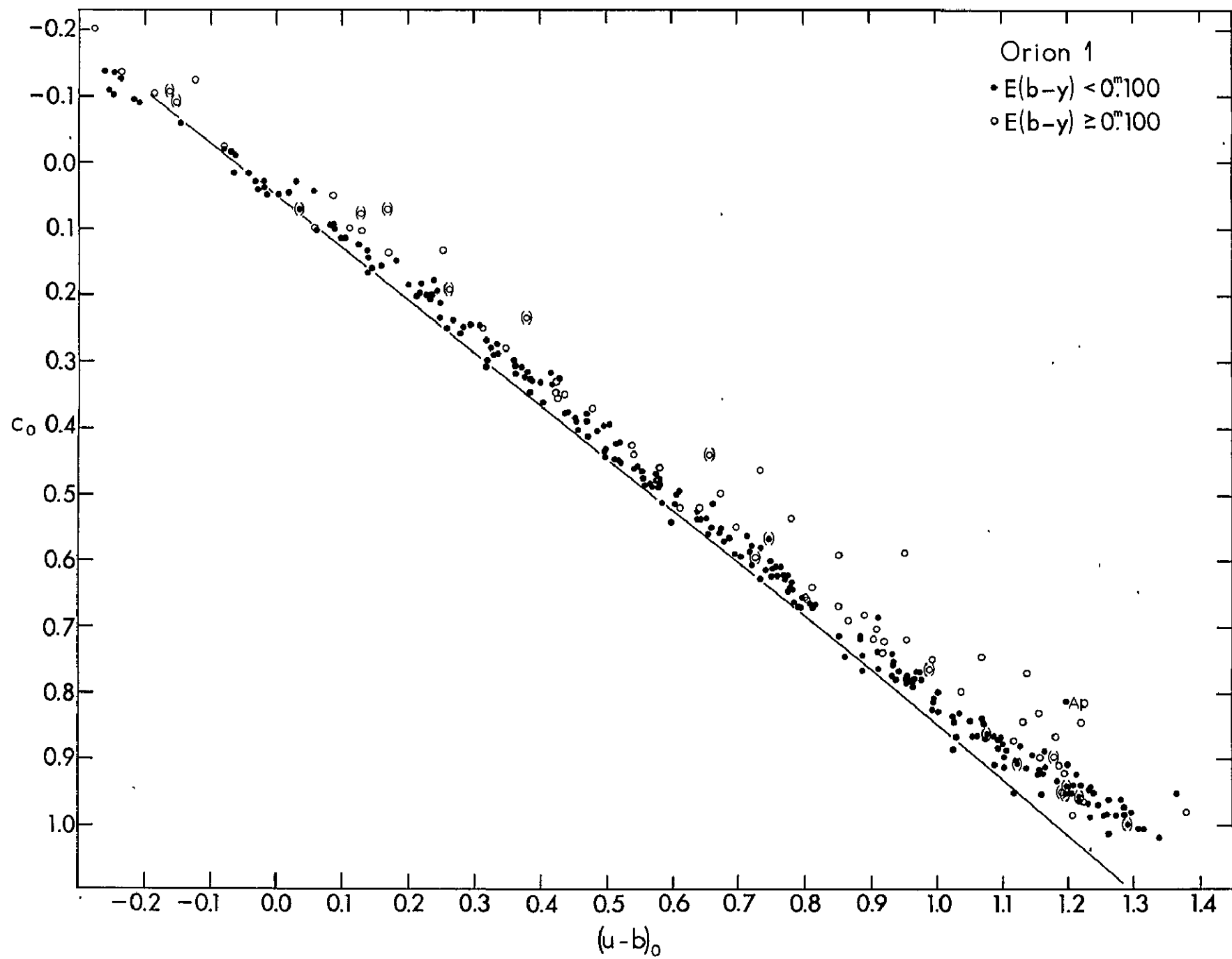


Figure 39

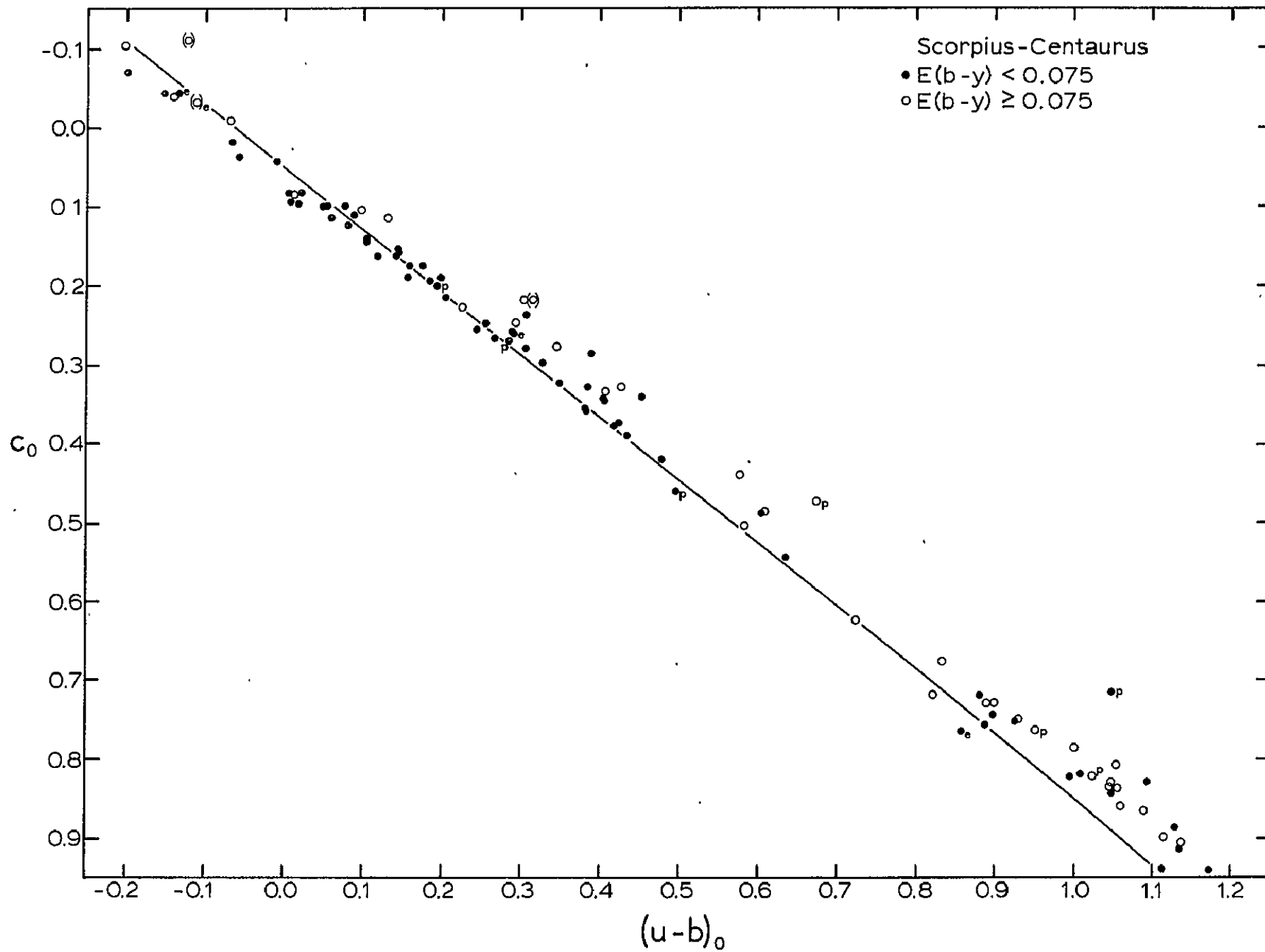


Figure 40

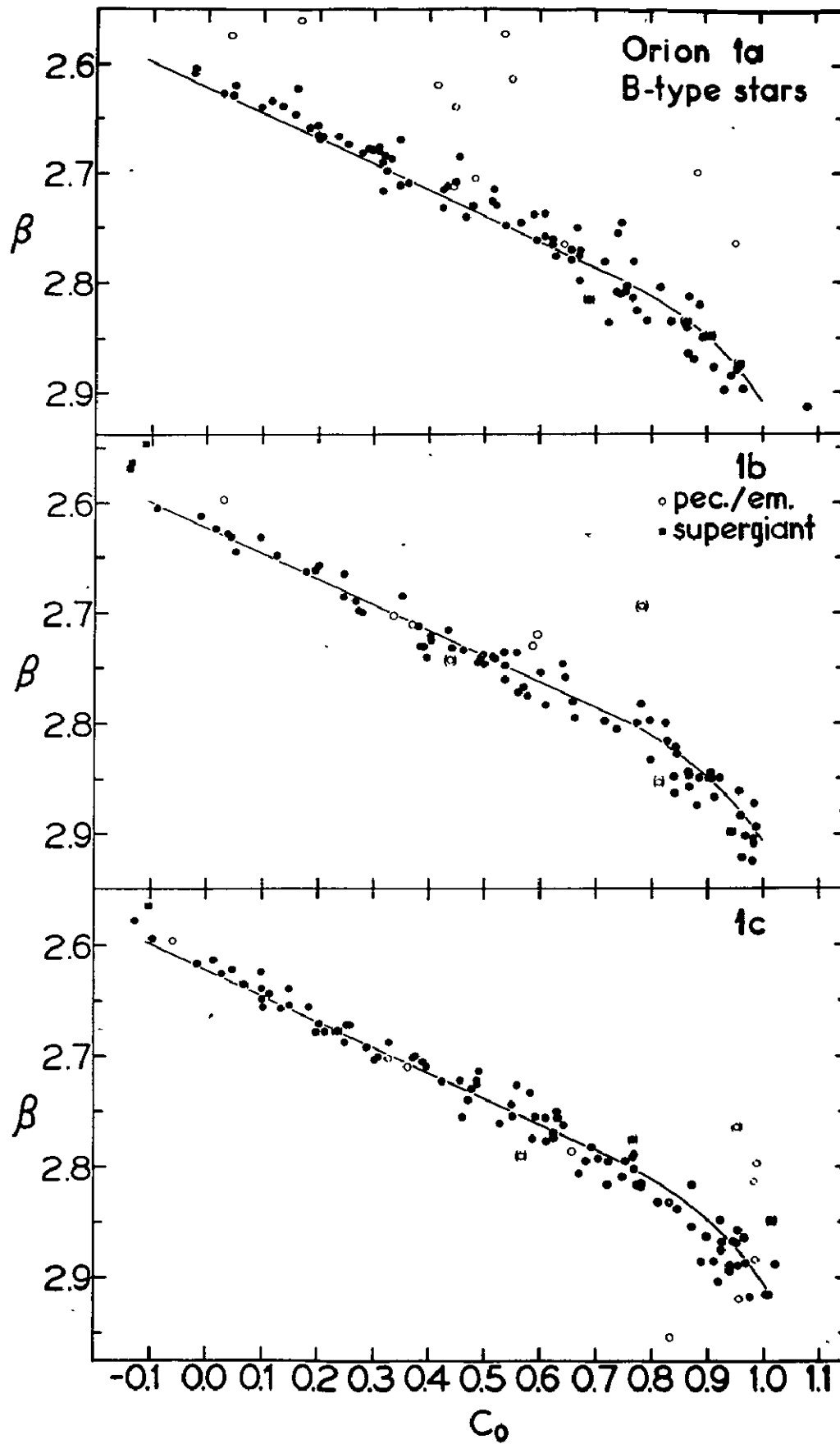


Figure 41

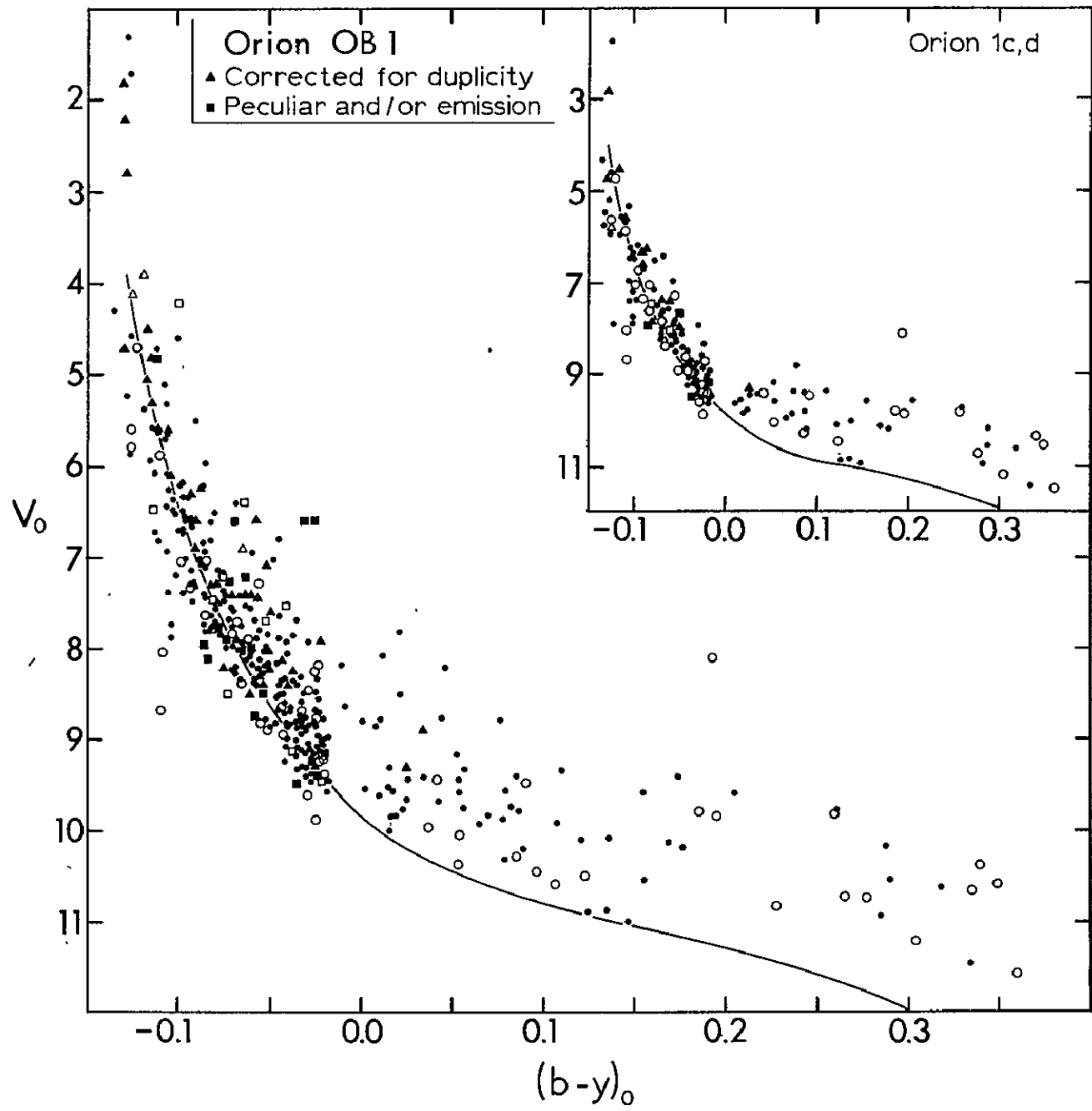


Figure 42

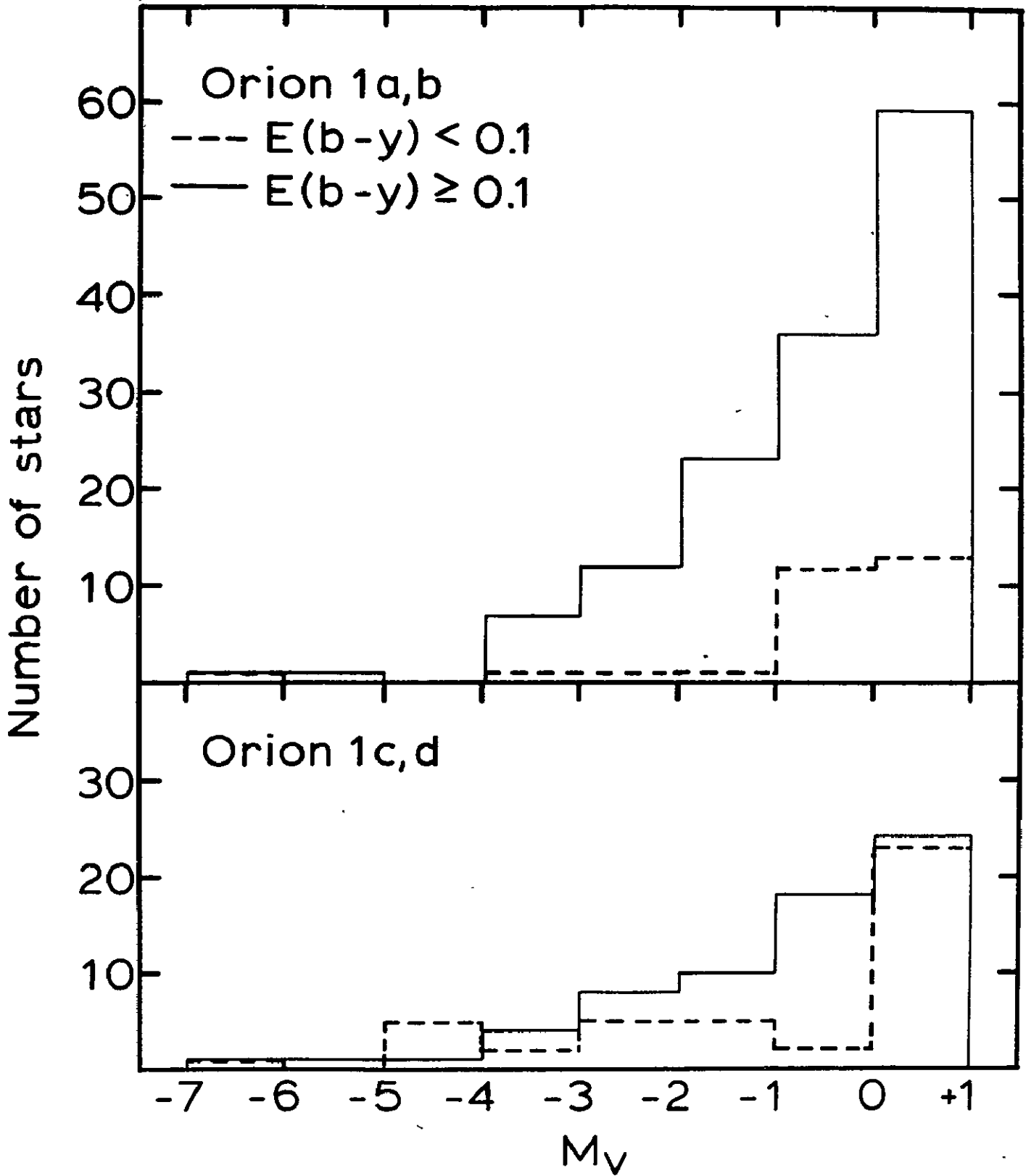


Figure 43

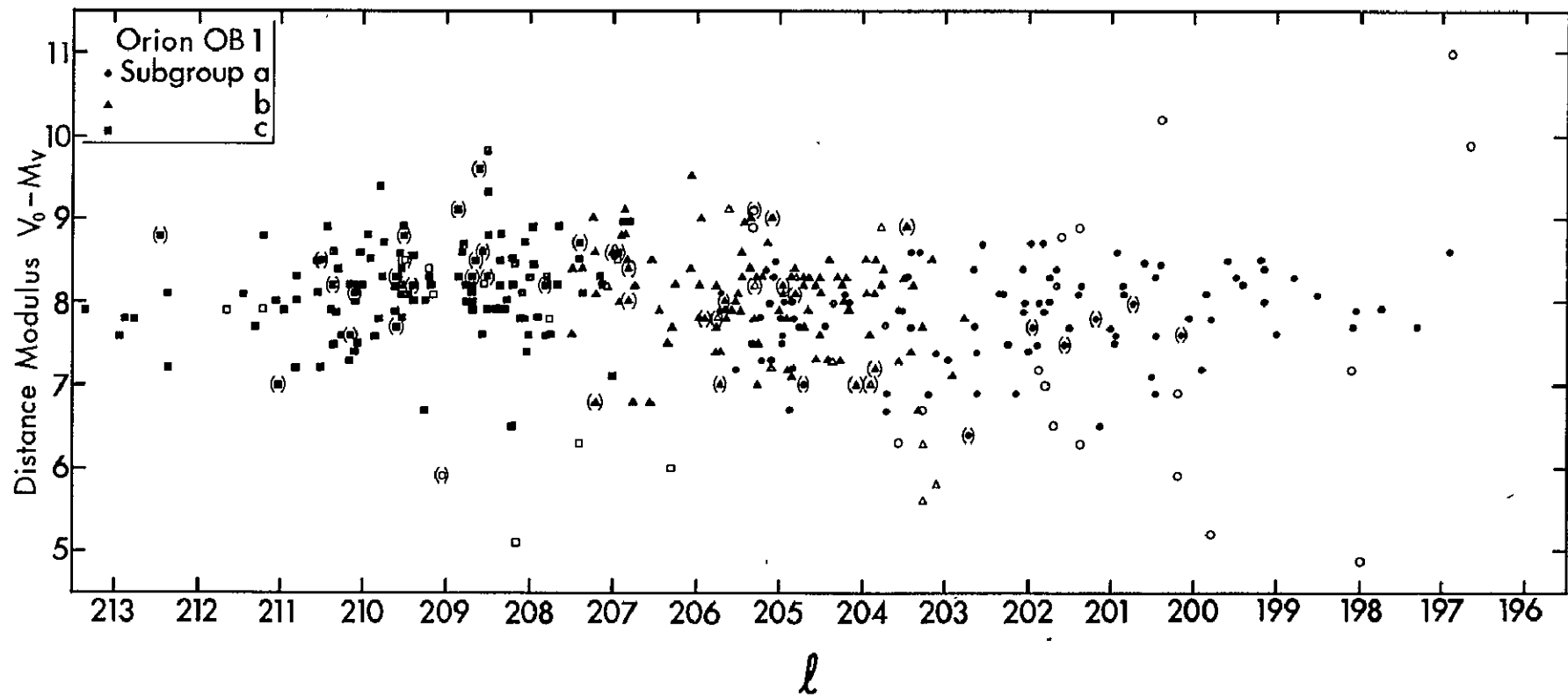


Figure 44